Investigation and Characterisation of Renin-Dependent Transgenic Rat Models of Hypertension and Left Ventricular Hypertrophy

Alisdair D. S. Ryding

PhD Thesis

University of Edinburgh

2005

Declaration

I hereby declare that the work presented in this thesis is the product of my own efforts, and has not been submitted in any previous application for a degree. The work on which this is based is my own except where stated in the text and in the acknowledgements section.

Alisdair Ryding

Non-Standard Abbreviations

Standard abbreviations and symbols recommended by the IUPAC-IUB Commission on Biochemical Nomenclature have been used. Standard abbreviations for nucleotides and three-letter abbreviations for amino acids have been used throughout the text. Non-standard abbreviations used are described in full in brackets after their first use in the text.

AAC	abdominal aortic constriction
AC	aortic constriction
ACE	angiotensin converting enzyme
AHC	aryl hydrocarbon
AHR	aryl hydrocarbon receptor
AKAP	A-kinase anchoring protein
Ang I	angiotensin I
Ang II	angiotensin II
ANOVA	analysis of variance
ANP	atrial natriuretic peptide
AR	adrenoreceptor
Arnt	aryl hydrocarbon nuclear translocator
ATP	adenosine-5'-triphospohate
ATPase	adenosine triphosphatase
AT_{1a}	angiotensin receptor type 1a
AT_2	angiotensin receptor type 2
A-V	arterio-venous
BLAST	basic local alignment search tool
BMI	body mass index
BNP	B-type natriuretic peptide
BP	blood pressure
BSA	bovine serum albumin

Ca^{2+}-ATPase	adenosine triphosphate-dependent calcium pump
Cain	calcineurin inhibitory protein
CAL	coronary artery ligation
cDNA	complemenatry DNA
CHP	calcineurin B homolgous protein
CnA	calcineurin A subunit
CsA	cyclosporin A
CSQ	calsequestrin
C_t	threshold cycle
CT	cardiotrophin
CYP	cytochrome P450
DBP	diastolic blood pressure
dNTP	deoxynucleotide triphosphate (dATP, dCTP, dGTP, dTTP).
ddH2O	double distilled water
DMSO	dimethylsulfoxide
DNA	2-deoxyribonucleic acid
dn	dominant negative
dNTP	deoxyribonucleotide-5'triphosphate
	N=A:adenine
	N=C:cytosine
	N=G:guanine
	N=T:thymine
DR	Dahl salt-resistant rat
DS	Dahl salt-sensitive rat
dsDNA	double stranded DNA
dt	deceleration time
DTT	1,4-dithiothreitol
E/A	E wave to A wave ratio (early and active phases of ventricular filling)
ECE	endothelin converting enzyme

ECG	electrocardiogram
ECL	enhanced chemiluminesence
ECM	extracellular matrix
EDTA	ethylenediaminetetraacetic acid
eFS	endocardial fractional shortening
EGF	epidermal growth factor
ERK	extracellular signal related kinase
EST	expressed sequence tag
ET	endothelin
$ET_{A/B}$	Type A or B endothelin receptor
F344	Fischer rat strain 344
FAC	focal adhesion complex
FAK	focal adhesion kinase
FCS	foetal calf serum
FGF	fibroblast growth factor
FK506	tacrolimus
FKBP	FK506 binding protein
FRNK	FAK C-terminal domain
GH	growth hormone
GSK-3β	glycogen synthase kinase 3 β
GST	glutathione S-transferase
GYT	glycerol yeast tryptone medium
h	hour(s)
HA	haemagglutinin
HEPES	N-2 hydroxyehylpiperazine-N'-2-ethanesulfonic acid
HMG CoA	hydroxymethylglutaryl Coenzyme A
HOCM	hypertrophic obstructive cardiomyopathy
HOPE	Heart Outcome Protection Evaluation study
hrp	horseradish peroxidase
HTS	high titre stock

I3C	indole-3 carbinol
IE	immediate early (gene)
IGF	insulin like growth factor
IL	interleukin
IMAC	immobilised metal affinity chromatography
I_{to}	transient outward current
IVC	independently ventilated cage
IVRT	isovolumic relaxation time
IVS	interventricular septum
JNK	c-jun-N-terminal kinase
JVS	juvenile visceral steatosis
kDa	kilodalton
kb	kilobase pairs
LB	Luria-Bertani
LIF	leukaemia inhibitory factor
lox	locus of recombination
LV	left ventricle
LVDd	left ventricular diameter in diastole
LVDs	left ventricular diameter in systole
LVH	left ventricular hypertrophy
LVMI	left ventricular mass index
LVOT	left ventricular outflow tract
M	molar (moles/litre)
M6PR	mannose-6-phosphate receptor
MAPK	mitogen activated protein kinase
MCIP	myocyte enriched calcineurin interacting protein
MEF	myocyte enhancer factor
MEKK1	MEK Kinase 1
mFS	midwall fractional shortening
MHC	myosin heavy chain

min	minute(s)
MKK	MAPK Kinase
MLC	myosin light chain
MLP	muscle-specific LIM protein
MMP	matrix metalloproteinase
MOI	mulitplicity of infection
MRI	magnetic resonance imaging
mRNA	messenger RNA
NADPH	reduced nicotinamide adenine dinucleotide phosphate
NFAT	nuclear factor of activated T cells
NFkB	nuclear factor kappa B
NHE	sodium hydrogen exchanger
NO	nitirc oxide
NPRC	natriuretic peptide receptor type C
OD_{600}	optical density at 600nm
PBS	phosphate buffered saline
PCR	polymerase chain reaction
PE	phenylephrine
pfu	plaque forming unit
PI3K	phosphoinositol-3 kinase
PKA	protein Kinase A
PKB	protein Kinase B
PKC	protein kinase C
PLB	phospholamban
PLC	phospholipase C
PMSF	phenylmethylsulfonylfluoride
PP2B	protein phosphatase 2B
PR	P-wave to R-wave interval
PWT	posterior wall thickness
QRS	Q-wave to S-wave interval

QT	Q-wave to T-wave interval
QTcB	QT interval corrected using Bazette's formula
RAS	renin-angiotensin system
Ren2	*Ren2*^{d} mouse renin
RNA	ribonucleic acid
RNase	ribonuclease
ROS	reactive oxygen species
rpm	revolutions per minute
RR	R wave to R wave interval
RTPCR	reverse transcriptase polymerase chain reaction
RWT	relative wall thickness
RYR	ryanodine receptor
s	second(s)
SAPK	stress activated protein kinase
SBP	systolic blood pressure
SD	Sprague Dawley
SDS	sodium dodecyl sulphate
SDS	sequence detection system
SERCA	sarco(endo)plasmic ATPase
Sf9	*Spodoptera frugiperda* cell line
SHR	spontaneously hypertensive rat
SR	sarcoplasmic reticulum
SSC	sodium chloride, sodium citrate solution
STAT	signal transducers and activators of transcription
SW	stroke work
TAC	thoracic aortic constriction
TAE	Tris EDTA acetic acid
TBS	Tris buffered saline
TE	Tris EDTA
TEMED	N,N,N'N'-tetramethylethylenediamine

TGF	transforming growth factor
TGR	transgenic rat
TIMP	tissue inhibitor of matrix metalloproteinase
T_m	melting temperature
TNF	tumour necrosis factor
TNM-FH	*Trichoplusia ni* Medium – Hink Formulation
Tris	Tris (hydroxymethyl) aminomethane
UV	ultraviolet
VTI	velocity time integral
v/vol	volume
w	weight
x *g*	times gravitational force
X-gal	5-bromo-4-chloro-3-indolyl-β-D-galactopyranoside

Standard prefixes were used

k	kilo (10^3)
m	milli (10^{-3})
μ	micro (10^{-6})
n	nano (10^{-9})
p	pico (10^{-12})

Acknowledgements

This work would not have been possible without the unstinting support of many people. In particular:

Prof John Mullins: for supervision, and the privilege of working in his labs.
Dr Martin Denvir: for supervision and stimulating discussion.
Dr Janice Paterson: for supervision and moral support.
Mrs Gillian Brooker: for assistance with animal studies, in particular radiotelemetry device implanation.
Dr Tara Collidge: for co-operation with experiments.
Dr Juliette Hadchouel: for assistance with histopathology.
Dr Joerg Peters: University of Greifsfeld, Germany, for plasma RAS measurements.
Dr Matt Sharp: for assistance with real time PCR.
Prof Stewart Fleming: University of Dundee, for histopathology advice.
Dr Julia Dornan: for assistance with ion exchange chromatography.
Dr Patrick Lawlor: for assistance with tissue culture.
Dr Gillian Gray: for assistance with invasive heart studies.
Dr Linda Mullins: for assistance in the lab.
Mrs Nina Koteletseva: for assistance in the lab.
Mrs Morag Meikle: for assistance in animal studies.
Ms Ailsa Travers: for assistance in animal studies.

The financial support of the Wellcome Trust through the Wellcome Trust Cardiovascular Research Initiative is gratefully acknowledged. The adminstrative support of the CVRI scientific advisory board, and secretaries is also greatly appreciated.

Dedication

For Christine

Table of Contents

Abstract

Left ventricular hypertrophy (LVH) complicates conditions in which there is an increase in cardiac workload, such as hypertension, valvular and ischaemic heart disease. Although haemodynamic load is a potent stimulus for LVH, humoral factors also contribute, and there is increasing evidence that selective inhibition of humoral signalling pathways can prevent hypertrophy despite persisting haemodynamic stress. Furthermore, inhibition of LVH without altering haemodynamic conditions appears to prevent the development of cardiac failure, a common complication of LVH. This situation is counterintuitive since in the absence of LVH cardiac wall stress is increased, which would be expected to lead to heart failure. Calcineurin, a calcium calmodulin-dependent phosphatase has been shown to be a key regulator of LVH, and inhibition of calcineurin-dependent signalling is associated with a favourable outcome in animal models of LVH. We hypothesised that increased wall stress may be tolerated if an increase in myocardial contractility occurs.

To investigate this further we studied cardiac function in a novel conditional transgenic rat model of hypertension, TGRcyp1a1ren2, during the development of LVH. In this model the transgene comprises mouse ren2^{d} cDNA under the transcriptional control of the cytochrome p450 promoter cyp1a1, rendering it inducible by dietary arylhydrocarbons such as indole-3 carbinol (I3C). Initial studies demonstrated that 0.15% I3C (w/w) induced a chronic hypertensive phenotype with concentric LVH. No change in LV function was detected by echocardiography or LV catheterisation. Telemetric ECG data demonstrated significant electrical remodelling, but only a minor increase in arrhythmias.

We next investigated the effect of FK506, a calcineurin inhibitor, on the cardiac hypertrophic response during short-term studies using 0.3% I3C (w/w). Contrary to all previous reports concerning the use of this drug in models of hypertension we found that FK506 treatment abolished hypertension, as well as inihibiting vascular injury and end organ damage. At present we are unable to explain the precise mechanism by which this occurs.

In separate studies we sought to investigate the mechanism by which prorenin contributes to cardiac hypertrophy in transgenic rats. Current evidence indicates that glycosylated prorenin can be imported and activated by cardiomyocytes, via the mannose-6 phosphate receptor. However this mechanism does not account for the observation that non-glycosylated mouse prorenin-2 is also taken up by cardiomyocytes in vitro and in rats transgenic for ren2^{d}. We hypothesised that separate pathways probably exist for glycosylated and non-glycosylated prorenins. To investigate this further we produced enzymatically active recombinant mouse ren2^{d} prorenin in a baculovirus expression system. Unfortunately further studies of prorenin/cardiomyocyte physiology were prevented by problems with recombinant protein yield and purity.

Chapter 1

Introduction

1.1 Defining Cardiac Hypertrophy

Cardiac hypertrophy is defined as an increase in cardiomyocyte volume without an increase in cell number.[1] In addition, hypertrophy may be accompanied by increases in non-myocyte numbers and extracellular matrix. At the level of the whole organ this is manifest as an increase in cardiac mass.

To all intents and purposes the adult cardiomyocyte is terminally differentiated, and hypertrophy is the only response to stress.[2] Whilst some reports have documented evidence of mitotic activity in terminally differentiated cardiomyocytes, as well as derivation of cardiomyocytes from multipotent stem cells, the incidence of this is probably very small, and hypertrophy is the only adaptive response available to the majority of terminally differentiated cardiomyocytes.[3]

Although hypertrophy is generally considered pathological it is physiological during post-natal development[4-8] and in response to sustained exercise training.[9] It is a recognised complication of many cardiovascular diseases, such as hypertension, myocardial infarction and valvular heart disease. Hypertrophy is therefore widely believed to represent a compensatory response that allows the heart to maintain output in the face of an increased workload. Influential observations published by Grossman et al. (1975)[10] and Sasayama et al. (1976)[11] popularised the concept that hypertrophy acts to normalise systolic wall stress.

Different patterns of hypertrophy have been recognised based on the gross remodelling of the heart and the relative change in myocyte dimensions.[12] Concentric hypertrophy

describes an increase in cardiac mass with an increase in relative wall thickness (ventricular wall thickness/internal ventricular dimension) due to an increase in myocyte width. Pressure overload is a common cause of this pattern. Eccentric hypertrophy describes an increase in cardiac mass with normal relative wall thickness due to myocyte elongation. This pattern is typically associated with volume overload. In both cases, ventricular mass is increased, which distinguishes a third category of concentric remodelling, in which left ventricular (LV) mass is normal with increased relative wall thickening.[12]

Hypertrophy can be measured by several criteria, the simplest being whole heart or LV mass. Usually this is expressed relative to body weight (Heart weight: body weight ratio, Left Ventricular Mass Index, LVMI) or another anthropomorphic measurement such as height. Alternatively, myocyte dimensions can be determined microscopically, either in fixed tissues or after dissociation from the heart by enzymatic digestion.[13,14] Isolated myocyte dimensions can also be assessed by Coulter counter methods that measure electrical resistance.[15] The gold standard is demonstration of increased electrical capacitance,[16] which, needless to say is rarely used. In vivo cardiac mass can be estimated by measuring ventricular dimensions, either by echocardiography, or magnetic resonance imaging (MRI).[17]

1.2 Epidemiology, Aetiology and Sequelae of Cardiac Hypertrophy

1.2.1 Population Studies

Left ventricular mass is a normally distributed variable in the human population, and definitions of abnormality are therefore statistical.[18] Epidemiological studies of the general population have estimated the prevalence of left ventricular hypertrophy (LVH) using echocardiographic criteria to be 8% in men under the age of 30 years, and 33% in men over 70.[19]

Population studies have been useful in establishing both the causes of left ventricular hypertrophy, and the determinants of variation within the normal population. Cardiac mass is influenced independently by lean body mass,[20] obesity,[21,22] age,[23] sex,[20,24-26] and ambulatory systolic blood pressure.[27-29] Unknown genetic factors also appear to have an influence.[30-34] States that impose a workload burden on the heart such as hypertension, valvular heart disease and myocardial infarction are commonly associated with LVH. The importance of blood pressure in hypertensive populations in determining cardiac mass would appear to be self-evident. However, the relationship is not particularly strong, and patients with similar degrees of hypertension vary widely in their cardiac masses.[23,35-38] It is now apparent that blood pressure in isolation is a poor estimate of haemodynamic load and that other parameters such as stroke volume,[29,39] stroke work,[20,40] cardiac contractility[39,40] and cardiac geometry[40] are much stronger predictors of cardiac mass. Furthermore, increased cardiac contractility can theoretically compensate for increased workload without the need for an increase in LV mass.[40] Whilst blood pressure per se may be relatively unimportant, non-haemodynamic factors related to hypertension (e.g. neuroendocrine mediators, genetic influences) may be more significant.

De Simone and colleagues have proposed a concept of inappropriate left ventricular hypertrophy, based on the assumption that LVH can be predicted by knowledge of cardiac loading (Systolic blood pressure and stroke volume), body size (height$^{2.7}$) and gender.[41] Subjects with LVMI exceeding their predicted value can be classified as having inappropriate LVH, and presumably have additional factors contributing to excessive LVH. Analysis of plasma insulin and insulin-like growth factor-1 in hypertensive cohorts with and without LVH has demonstrated that these hormones are elevated in subjects with inappropriate LVH.[28,42] In addition, such patients have impaired cardiac function and a worse cardiovascular prognosis compared to patients with appropriate LVH.[41,43]

1.2.2 Sequelae of Cardiac Hypertrophy

A longstanding tenet of cardiology has been that LVH represents an adaptive response to increased cardiac workload, and that increased muscle mass is required to maintain cardiac performance in the face of increased demand. However, many large-scale studies have established that LVH is associated with a significant increase in cardiovascular and all-cause mortality, independent of hypertension (reviewed Vakili et al., 2001[44]). Therefore LVH may be considered to be a maladaptive response. Human population studies estimate the relative risk of cardiovascular death to be 1.5 to 3.5 fold greater in those with LVH,[45-48] in proportion with the degree of hypertrophy,[48] and highest for those with concentric hypertrophy.[47-51] Regression of LVH appears to be associated with a reduction in relative risk,[52] though few studies have rigorously tested this. The increased risk of death is presumably explained by a greater incidence of angina,[46] myocardial infarction,[46] heart failure,[46] arrhythmias,[53,54] stroke[55] and sudden death[46,56] compared to patients without LVH who otherwise have comparable risk factors.

1.3 The Hypertrophic Phenotype

1.3.1 Hypertrophic Gene Expression Patterns

A characteristic pattern of changes in gene expression has been defined in studies of cardiomyocyte hypertrophy in vitro and in vivo.[57-59] The earliest changes, identifiable within minutes of a hypertrophic stimulus involve transient expression of immediate early genes (IE) such as c-jun,[58] c-fos,[58] jun-B,[60] c-myc,[61] egr-1,[59] GATA-4,[62] nkx2.5.[63] These transcription factors orchestrate induction of specific hypertrophy associated genes that are normally restricted to embryonic development, including atrial natriuretic peptide (ANP),[61] B-type natriuretic peptide (BNP),[64] α-skeletal actin,[61] smooth muscle actin[65] and beta-myosin heavy chain (β-MHC).[66,67] Induction of the "foetal gene programme" is used as a hallmark of pathological hypertrophy. It is likely that increased expression of natriuretic peptides is a protective mechanism that lowers blood pressure and exerts antihypertrophic/antifibrotic effects on cardiomyocytes and non-cardiomyocytes. Similarly, myosin heavy chain isoform switching may adapt the heart

to increased workload.[68] Other changes that have been documented include induction of angiotensin-converting enzyme (ACE),[69] transforming growth factor β (TGFβ),[70] collagen,[71,72] fibronectin, frizzled,[73] Nix [74] and downregulation of sarcoplasmic endoreticular calcium ATPase (SERCA), alpha-myosin heavy chain (αMHC) and natriuretic peptide receptor type C (NPRC).[64]

Since multiple hypertrophic stimuli appear to induce very similar changes in gene expression in many different models, it has been widely assumed that the hypertrophic phenotype stems from the induction of a co-ordinated genetic programme. Gene expression profiling using microarrays,[75,76] expressed sequence tag (EST) analysis[77] and subtractive hybridisation[78] techniques has identified a modest number of genes that are differentially regulated during the induction and regression of LVH in various animal models. These studies have found patterns of gene expression relating to transcription/translation/protein synthesis, structural/sarcomeric proteins, signalling, metabolism, apoptosis and stress responses. Many of the sequences identified so far are novel EST's, indicating that our current knowledge of LVH is rather limited. Whilst most studies have confirmed up regulation of archetypal hypertrophy markers such as ANP, there is relatively limited overlap between studies, suggesting that a highly conserved LVH pattern does not exist. Aronow et al, (2000)[76] compared four transgenic mouse models of pressure-independent LVH using commercial microarrays. They demonstrated that ANP was the only gene out of approximately 8,800 analysed that was upregulated in all four models. Further analysis revealed patterns of expression that were characteristic of individual models, suggesting that specific stimuli evoke particular molecular changes.[79] Similar findings have also been reported in comparisons of cardiac gene expression between $NOS1^{-/-}$ and $NOS3^{-/-}$ mice.[80] Whilst it could be argued that none of the models studied were physiologically relevant, this study highlights the disparity between different models, and the need to reassess our assumptions about LVH. Another criticism is that single time points were compared in models with different natural histories. There is little doubt that expression patterns in LVH probably change both quantitatively and qualitatively with time. Despite this it is

pertinent to note that comparison between hypertrophied and foetal hearts using subtractive hybridisation has demonstrated similarity in expression profiles.[78]

Recent data suggests that myocyte hypertrophy and foetal gene expression can be dissociated suggesting that the foetal gene expression patterns may be surrogate markers of hypertrophy without an integral role in the hypertrophic process itself. Therefore it is possible to demonstrate pathological LVH in PTEN$^{-/-}$ mice without upregulation of ANP/BNP,[81] and similar results have been demonstrated in other models.[82-86] In contrast, foetal markers are greatly upregulated in GSK-3β transgenic mice subjected to aortic constriction compared to wild type mice, despite complete absence of LVH by several other criteria.[87] Therefore, the notion that foetal gene reexpression is intrinsic to LVH is probably wrong. It is intriguing that haemodynamic unloading of the rat heart also induces foetal gene expression patterns very similar to those caused by aortic banding,[88] which implies that the foetal gene pattern may simply represent a response to haemodynamic change, in either direction.

Most attention has focussed on gene expression patterns, but it is well recognised that many critical events in LVH are regulated at a post-translational level. Most of the known signalling pathways mediating LVH comprise kinases and phosphatases.[89] Furthermore, many proteins involved in excitation-contraction coupling are regulated by phosphorylation, and may be altered in LVH.[90,91] So far proteomic analysis of LVH has not been reported.

1.3.2 Cardiac Function in Hypertrophy

1.3.2.1 Measurement of Cardiac Function

It is important to appreciate that assessment of cardiac function is not straight forward, particularly when using in vivo measurements in small rodents.[92] Cardiac function, or cardiac output is an integration of many factors both intrinsic to the myocardium and imposed on it by the loading conditions. Contractility is the ability of the heart to generate force and is influenced by inotropic agents. The function of the heart is not

fixed, but finely tuned to the prevailing haemodynamic conditions of preload and afterload, as described by Frank and Starling.[93] Therefore, comparisons should either be made under identical loading conditions, or using a functional parameter that is independent of loading. The majority of in vivo parameters measured using popular methods such as echocardiography and left ventricular catheterisation are heavily influenced by haemodynamic conditions,[94] and few studies take this in to account. This is not to say that their conclusions are not valid within the context of the study itself, but comparisons cannot be easily made between studies. One way to avoid such problems has been to measure cardiac function ex vivo using Langendorff and working heart preparations, or papillary muscle set ups, where conditions can be strictly controlled.

Some in vivo functional parameters are considered to be relatively independent of loading conditions, particularly derivation of end systolic/diastolic pressure-volume relations and end systolic stiffness from pressure-volume loops.[94] However, significant difficulties can be encountered even with these methods since anaesthesia is usually required.[95,96] Therefore, analysis of cardiac function is currently fraught with difficulty and no single test can be considered definitive.

1.3.2.2 Function of the Hypertrophied Ventricle

Hypertrophy is associated with normal,[11,97,98] subnormal,[99,100] or supranormal [101,102] cardiac function depending on the species, model, timepoint and method of study. Although the diversity of findings suggests confusion, certain conclusions can be drawn.

LVH is probably an evolving phenotype, rather than a static one, and alterations in gene expression and cardiac function are constantly changing.[11,103,104] For reasons that are not fully understood, cardiac function inevitably declines and decompensation in to heart failure occurs.[105-107] This is characterised by impaired systolic and diastolic function,[108] ventricular dilatation and increased wall stress.[10,109] It is not clear whether decompensation is due to specific events that occur late in the natural history of LVH, or if it is a consequence of very early adaptations during compensated hypertrophy. It is

likely that decompensation results from multiple causes with a minor impact on their own, but a profound effect in combination.

Although it is possible that decompensation is intrinsic to the hypertrophied myocyte, some decompensatory mechanisms are triggered by extracellular signals. Prime candidates appear to be upregulation of cardiac endothelin system activity[110-113] and cardiac RAS.[111,113-115] In some animal models endothelin antagonists and subpressor ACE or AT_{1a} blockers prevent functional decline and mortality, without affecting LVH per se.[110,114,116,117] Cardiomyocytes isolated from failing human hearts have a reduced ability to synthesise ET-1 and IGF-1 in response to Ang II.[118] Alterations in growth factors such as cardiotrophin and neuregulin, and their receptors gp130 and Erbb2/4 have been described in animal models and failing human hearts.[119-121]

1.3.3 Mechanisms of Myocardial Dysfunction in Cardiac Hypertrophy

Four main causes of myocardial dysfunction during cardiac hypertrophy probably exist: intrinsic myocyte dysfunction, myocyte loss, altered extracellular matrix, and altered bioenergetics.

1.3.3.1 Intrinsic Myocyte Dysfunction

Myocyte dysfunction appears to develop as a consequence of abnormal calcium homeostasis and altered sarcomeric properties. Seminal work by Sordahl et al. (1976)[122] demonstrated impaired sarcoplasmic reticular calcium uptake in failing rabbit myocardium. Gwathmey et al. (1985)[123] showed that this resulted in calcium transients of reduced amplitude and prolonged duration, caused by reduced SERCA expression/activity.[124-126] Such changes reduce the force of contraction, impair relaxation and limit contractile reserve.[127,128]

SERCA down-regulation is a marker of decompensation in rats with aortic constriction.[129,130] Mice heterozygous for functional SERCA2 develop accelerated heart failure in response to aortic constriction.[131] Furthermore, overexpression of SERCA

isoforms in myocytes via adenoviral transfer methods, or transgenic techniques leads to improved contractility[132-136] and resistance to the development of heart failure following aortic constriction.[137,138] However, in vitro studies suggest that an optimum level of SERCA replacement exists, with high levels being detrimental.[139]

SERCA activity is inhibited by phospholamban (PLB), an interaction that is regulated by PKA-mediated phosphorylation.[140] No consistent changes in phospholamban expression or phosphorylation have been found in studies of heart failure/LVH decompensation.[141] Even where PLB expression is altered, the stoichiometry of expression relative to SERCA is usually maintained, so that the effect may be negated. Mice deficient in phospholamban ($PLB^{-/-}$) demonstrate enhanced contractility[142] and when crossed to genetic models of heart failure (muscle-specific LIM protein, $MLP^{-/-}$ and calsequestrin overexpressing mice, CSQ_{OE}) maintain normal cardiac function.[143,144] Conversely, overexpression of a superinhibitory phospholamban in mice causes cardiac hypertrophy, heart failure and death by 6 months.[145,146] However, $PLB^{-/-}$ mice do not differ from wild type mice in their response to aortic constriction, and appear to have an earlier decline in LV function.[147] Therefore LV decompensation is probably more complex than reduced SERCA activity alone. Indeed, cardiomyocytes from transgenic mice overexpressing activated calcineurin have enhanced calcium handling properties due to changes in levels of SERCA/PLB, and enhanced contractility in vitro, yet they develop profound cardiac failure.[148]

Changes in expression of other proteins important for calcium homeostasis such as ryanodine receptor, calsequestrin and calreticulin are inconsistent between reports.[141] However, hyperphosphorylation of ryanodine receptors, and abnormal function has been described.[149] Transgenic overexpression of calsequestrin leads to LVH and heart failure,[83,150] confirming the role of calcium as a mechanism contributing to heart failure. In addition, downregulation or abnormal function of the Na^{+}-Ca^{2+} exchanger appears to contribute to diastolic dysfunction in heart failure.[151-153]

Contraction of cardiomyocytes is a consequence of cross-bridge cycling between actin and myosin filaments in the sarcomere. Altered sarcomeric function will obviously have a direct impact on contractility, but this area has received relatively little attention. Depressed myofibrillar ATPase activity has been described in hypertrophy,[154] which may be explained at least in part by reciprocal regulation of α and β-MHC isoforms.[155,156] Similar findings have been described in rodents.[68,157,158] The recent finding that gelsolin, a regulator of thin filament turnover, is upregulated in heart failure adds weight to the importance of altered sarcomeric function.[159]

1.3.3.2 Myocyte Loss

Loss of cardiomyocytes by necrosis or apoptosis reduces the availability of contractile units, and thereby decreases contractility. In situations such as myocardial infarction, cell death is very obvious, but the issue as to whether or not cellular loss contributes to the progression of LVH to heart failure is contentious, largely due to methodological problems.[160-163] However, there is no doubt that induction of apoptosis in cardiomyocytes by controlled overexpression of toxins/apoptotic mediators leads to ventricular remodelling and heart failure.[74,164,165]

Several investigators have examined the role of apoptosis in cardiac remodelling. There appears to be undetectable to very low levels of apoptosis in normal rat hearts,[166] which increases with age.[167,168] Cardiac hypertrophy in response to aortic constriction is accompanied by a discrete wave of apoptosis during the first 4 days.[166] As LVH decompensates later on, apoptotic rates increase, particularly in the LV free wall in the endo/mid-myocardium and areas of fibrosis,[169-171] which can be abrogated by captopril.[172]

Table 1.1 Cardiomyocyte Survival Pathways

Reference	Model	Pathway targeted	Stimulus	Response
Hirota et al., 1999[173]	gp130$^{-/-}$	CT-1/LIF/IL-6 signalling	AC	Dilated cardiomyopathy, apoptosis and death
Rogers et al., 1999[174]	RGS4	G-protein signalling	AC	Rapid decompensation and death
Brancaccio et al., 2003[175]	melusin$^{-/-}$	β1-integrin signalling	AC	Dilated cardiomyopathy Normal LVH with subpressor AngII/PE
Shai et al., 2002[176]	β1-integrin$^{-/-}$	β1-integrin signalling	AC	Dilated cardiomyopathy and death. Depressed baseline cardiac function
Crone et al., 2002[177]	Erbb2$^{-/-}$	neuregulin signalling	AC	Dilated cardiomyopathy, apoptosis and death Increased anthracycline sensitivity
Badorff et al., 2002[178]	lpr mutant	Fas (apoptosis signalling)	AC	Dilated cardiomyopathy and death
O'Connell et al., 2003[5]	$\alpha_{1a/c}^{-/-}/_{1b}^{-/-}$	adrenergic signalling	AC	Hypertrophy, heart failure and death (Basal heart size diminished by 40%)

AC: aortic constriction, CT-1: cardiotrophin, LIF: leukaemia inhibitory factor, IL-6: interleukin 6, Ang II: angiotensin II, PE: phenylephrine.

Neurohumeral factors may be responsible for the altered balance between pro- and anti-apoptotic factors. Cardiac specific overexpression of α_1-AR, TNFα, Gαq and Gsα in transgenic mice leads to LVH and heart failure associated with cell loss and apoptosis.[105,179-182] Since these G-proteins are involved in signal transduction for catecholamines, angiotensin II and endothelin, a role in decompensation for these factors is also implied. Furthermore, since these agents actually cause cardiac hypertrophy, it suggests that hypertrophic and apoptotic pathways may be activated simultaneously, and that under certain circumstances apoptosis prevails. This concept is supported by

evidence that specific proapoptotic genes, including Nix/Bnip3L are activated in several animal models and human hypertensive LVH.[74] Equally, Erbb2$^{-/-}$, Gp130$^{-/-}$ and FGF-2$^{-/-}$ knockout mice are prone to apoptosis and dilated cardiomyopathy in response to hypertrophic stimuli, indicating that they have an essential anti-apoptotic, or survival role during cardiac hypertrophy[173,177,183] (table 1.1). A similar case can be made for IGF-1.[184-188] In conditional Erbb2$^{-/-}$ mice, adenoviral overexpression of an antiapoptotic gene, bcl-xl delays cardiac failure.[177]

Myocyte stretch in vitro[189,190] and in vivo[169] also induces apoptosis via angiotensin II-mediated autocrine signalling.[191] Reactive oxygen species (ROS) may be another trigger for apoptosis in cardiac hypertrophy, activating redox-sensitive proteins[192] and causing structural damage.[193-195]

1.3.3.3 Extracellular Matrix Remodelling

Increasing evidence suggests that extracellular matrix (ECM) remodelling occurs in pathological LVH, and it may be a critical event in the transition from compensated hypertrophy to heart failure.[107,196] During both LVH[197,198] and ageing,[199] ECM components are changed in quantity and quality. An increase in fibronectin EIIIA isoform and collagen type I has been described in SHR at the onset of decompensation,[107] a process that may be controlled by TGFβ. Whilst increased fibrosis can account for increased myocardial stiffness,[200] and in particular diastolic dysfunction,[201] the situation must be more complex, as ultimately the main problem is one of ventricular dilatation, rather than restriction.

Several studies have documented an increase in the expression levels and activities of matrix-metalloproteinases (MMP's) and their inhibitory counterparts, tissue-inhibitors of matrix metalloproteinases (TIMP's) in various models of decompensation and heart failure.[202-206] Furthermore, chronic administration of broad-spectrum MMP inhibitors to heart-failure prone SHR,[207] or rats with volume overload due to aorto-caval fistula,[208]

prevented decompensation without affecting LVH, although not all aspects of myocardial function were rescued.

Woodiwiss et al., (2001)[209] found that collagen cross-linking was reduced in two rat models of decompensated LVH, even though collagen content was not even increased in one model. Taken together this suggests that decompensation is not simply due to excessive fibrosis, but relates more to the increased turnover and reduced integrity of ECM components. Newly synthesised collagen requires a series of postranslational modifications, including cross-linking, that allow formation of mature fibres. It has been suggested that compromised ECM structure allows LV dilatation via myocyte "slippage".[210] Regulators of MMP/TIMP balance include TGFβ and TNFα.[211] Chronic infusion of TNFα in rats causes cardiac dilatation and reduced collagen content, with reversible changes in myocardial contractility.[212] A similar phenotype is seen following transgenic overexpression of TNFα in mice.[213] Conversely, treatment of patients and various models of LVH/heart failure with TNFα or TGFβ inhibitors prevents ECM remodelling and in some cases arrests ventricular dilatation.[212,214-217]

1.3.3.4 Altered Bioenergetics

Myocardial force generation during systole depends on the conversion of chemical energy in to kinetic energy by the hydrolysis of ATP by myosin ATPase, permitting actin/myosin cross-bridge cycling and filament sliding. Therefore, anything that alters the availability of ATP will impact on the mechanical performance of the heart. In the heart the ATP reservoir is buffered by storing high-energy phosphates as phosphocreatine, which is readily converted to ATP and creatine in the presence of creatine kinase and ADP. Phosphocreatine also acts as a readily diffusible energy shuttle from mitochondria to sites of intense ATP usage, as ATP itself is less diffusible. The energy status of the heart can be assessed by measuring the phosphocreatine/ATP ratio by [^{31}P]-MR spectroscopy.[218] The development of heart failure is frequently associated with a decline in the availability of high-energy phosphates,[218] though this is not a universal finding,[219] suggesting that impaired ATP generation may be responsible for the

decompensation of LV function. Furthermore, similar energetic abnormalities predate decompensation in several animal models, lending credence to this hypothesis. However, the intracellular concentration of ATP remains above the Km for most ATPase enzymes, suggesting that ATP supply is rarely sufficiently limited to impair such processes. A range of evidence indicates that impaired phosphocreatine shuttling,[220] CK flux,[221] and reduced free energy liberation from ATP hydrolysis occur in the presence of elevated ADP levels.[222]

In addition to these abnormalities, myocardial substrate utilisation influences myocardial efficiency and contractility. Mice deficient in insulin-sensitive glucose transporters (GLUT4) develop severe LVH and contractile dysfunction,[219] whilst mice overexpressing GLUT1 in the heart resist pressure overload induced heart failure.[223]

Despite these changes myocardial efficiency, assessed as oxygen consumption in relation to work output, is often normal or increased during the transition to heart failure.[224-226]

1.4 Mechanisms of LVH

LVH occurs in response to haemodynamic stress, vasoactive peptides, cytokines, growth factors, reactive oxygen species, altered ECM coupling, sarcomeric defects and altered cardiomyocyte metabolism.[1] Broadly these can be considered as mechanical, neurohumeral and intrinsic signals. Despite this diversity of stimulatory factors the intracellular signalling pathways that are activated overlap significantly, resulting in a common outcome, namely LVH. A contentious issues remains as to what extent LVH is determined by mechanical load versus endocrine signals, and how these stimuli activate hypertrophic signalling pathways.

1.4.1 Mechanical Stress

Mechanical stress (haemodynamic load) leads to cell stretching. In vitro, stretched cardiomyocytes hypertrophy, with demonstrable increases in cell size and induction of

foetal genes such as ANP.[227-231] Therefore, mechanical stretch alone appears to be sufficient to cause hypertrophy. Langendorff perfused hearts and working heart models also show features of early hypertrophy in response to increased wall stress.[232-234] Demonstrating a pure mechanical effect in vivo is difficult due to activation of neurohumeral pathways in response to haemodynamic changes. For example, although thoracic aortic constriction is classically considered to be a model of pure pressure overload, it is associated with distinct patterns of cytokine activation with in the heart,[235] whilst abdominal aortic constriction leads to renal ischaemia and RAS activation.[236] Furthermore, even in vitro experiments are complicated by the fact that stretch activates autocrine and paracrine signalling in cardiomyocytes and non-cardiomyocytes[237-241] so that it is virtually impossible to study purely mechanical stimuli.

A mechanism must exist in myocytes that detects stretch and initiates hypertrophic responses. Several possible mechanotransducers have been described: integrins and the cytoskeleton, stretch-activated ion channels/membrane associated enzymes and autocrine/paracrine pathways.[242] The latter will be discussed in the section on neurohumeral mechanisms of LVH.

1.4.1.1 Integrin Signalling in the Heart

Integrins are a family of cell surface receptors that mediate adhesion to extracellular matrix. In effect they link the ECM to the cytoskeleton at focal adhesion sites, making them ideally placed to act as transducers of external forces imposed on the heart.[243] The cytoplasmic domains of integrin heterodimers recruit non-receptor signalling molecules, including focal adhesion kinase (FAK), Src, Grb2, Sos, Ras, Raf, phospholipase C (PLC γ), extracellular signal related kinases (ERK's) and stress activated protein kinases (SAPK's) forming focal adhesion complexes (FAC's) which mediate "outside-in" signalling in response to changes in ECM conditions and mechanical stretch (reviewed Ruhof 2000[242]). Tyrosine phosphorylation of FAK and activation of downstream signalling complexes can be detected within minutes of pressure overload in rats subjected to aortic constriction.[244] Overexpression of β1 integrins and FAK by gene

transfer techniques in cultured cardiomyocytes has demonstrated that these factors can directly induce cellular hypertrophy.[243,245] Disruption of cardiac β1-integrin function via gene targeting techniques leads to cardiac hypertrophy and failure.[176,246] Signalling via the cytoplasmic domain of β1-integrin requires interaction with a muscle-specific protein, melusin. Conditional cardiac melusin knockouts develop heart failure in response to aortic constriction, but hypertrophy normally in response to subpressor doses of AngII, thereby confirming the role of β1-integrin signalling in stress transduction.[175] Disruption of FAK signalling in vitro inhibits hypertrophic responses to phenylephrine and ET-1, suggesting that hypertrophy via humoral signalling is dependent on normal cell-matrix interactions.[247-249] FAK is inhibited by the PTEN tumour suppressor and an endogenous C-terminal FAK fragment (FRNK).[249,250] In keeping with this, cardiac restricted deletion of PTEN in mice leads to cardiac hypertrophy in the absence of hypertension.[81] Therefore, integrins and associated downstream signalling pathways appear to be good candidates for the cardiac mechanotransducer.

1.4.1.2 Stretch-Activated Ion Channels/Membrane Associated Enzymes

Membrane deformation by stretch has been postulated to lead to conformational changes in membrane associated enzymes and ion channel complexes.[227] Candidiates include phospholipase C/D (PLC and PLD), protein kinase C (PKC), small and heterotrimeric GTPases, sodium-hydrogen exchanger (NHE) and stretch-activated channel.[242] For most of these pathways there are multiple possible mechanisms for activation and evidence is contradictory as to whether they are directly activated by stretch, or secondarily activated by autocrine/paracrine signalling/FAC's.

NHE is a Na^+–H^+ antiporter that causes cellular alkalinisation. Increased pH in itself can stimulate hypertrophy of cardiomyocytes,[251] and NHE appears to be activated by stretch,[252] although this may also involve paracrine signalling.[253] NHE is a potential therapeutic target for inhibiting cardiac hypertrophy, post-myocardial infarction remodelling and ischaemia reperfusion injury.[254-258] Ca^{2+} influx via stretch-activated ion channels is a poorly defined mechanotransduction mechanism. As such this may lead to

activation of PKC and calmodulin-dependent enzymes such as cyclin-dependent kinase-2 (CDK-2) and calcineurin, causing hypertrophy.[242]

1.4.2 Neuroendocrine Signalling

Whilst there is ample evidence for load-induced cardiac hypertrophy, there is equally substantial data supporting a necessary and sufficent role for endocrine stimuli. Quite simply, overexpression of single endocrine components in the heart is sufficient to cause cardiac hypertrophy without any change in the prevailing haemodynamic conditions: such studies are summarised in table 1.2, and will be discussed in detail in the following sections.

1.4.2.1 Renin-Angiotensin System

The renin angiotensin system (RAS) is a cascade comprising the enzymes renin and angiotensin-converting enzyme (ACE) and the substrate angiotensinogen which is cleaved to form angiotensin I. Angiotensin II (Ang II) is the final effector molecule. Other angiotensin derivatives have been described, but will not be discussed here. The RAS is fundamental to the regulation of blood pressure via its effects on vascular tone and salt-water homeostasis. In addition it may have effects on cardiac hypertrophy, independent of haemodynamic effects.

1.4.2.2 Renin

Renin is a substrate-specific aspartyl protease,[259-261] which cleaves angiotensinogen to form angiotensin I. Human renin is a 43kDa polypeptide, with an active site residing in a cleft between two symmetrical lobes.[262-264] The initial mRNA translation product is pre-prorenin (45kDa), which includes a 20 amino acid signal sequence and a 43 amino acid pro-segment.[265] Post-translational modifications include the formation of disulphide bonds,[266] site-specific hydrolysis of the peptide chain,[265] and glycosylation at asparagine

Table 1.2 Transgenic Models of Pressure Independent LVH

Reference	Transgene	Pathway actiavted	Phenotype
Hein et al., 1997[267]	αMHC-AT_1R	AT_1 receptor	Myocyte hyperplasia and heart block
Paradis et al., 2000[268]	αMHC-AT_1R	AT_1 receptor	LVH progressing to HF
Milano et al, 1994[269]	αMHC-β_1AR*	β_1 adrenoreceptor	LVH
Engelhardt et al., 1999[105]	αMHC-β_1AR	β_1 adrenoreceptor	LVH progressing to HF
Zuscik et al., 2001[270]	α_{1B}AR	α_{1B} adrenoreceptor	LVH, hypotension
Adams et al., 1998[180]	αMHC-Gaq	AngII/ET-1/catecholamines	LVH progressing to HF due to apoptosis
Sakata et al., 1998[271]	αMHC-Gaq	AngII/ET-1/catecholamines	Eccentric LVH and HF in response to TAC
Mende et al., 1998[272]	αMHC-Gaq*	AngII/ET-1/catecholamines	LVH progressing to HF (transient expression)
Iwase et al., 1996[273]	αMHC-G_sa	β adrenoreceptors	LVH progressing to HF due to apoptosis
Hunter et al., 1995[274]	MLC_{2v}-ras*	ras	LVH with diastolic dysfunction
Sussman et al., 2000[275]	αMHC-rac1*	rac-1	LVH or dilated cardiomyopathy in different lines
Wakasaki et al., 1997[276]	PKCβII	PKCβ	LVH with systolic dysfunction
Bowman et al., 1997[277]	PKCβ	PKCβ	LVH in adult: lethal in neonate (inducible transgene)
Mochly-Rosen et al., 2000[85]	αMHC-ψεRACK	PKCε	Physiological LVH
Chen et al., 2001[278]	αMHC-ψδRACK	PKCδ	LVH
Takeishi et al., 2000[86]	PKCε	PKCε	LVH
Molkentin et al., 1998[82]	αMHC-CnA*	Calcineurin/NFAT	LVH
	CK-CnA*	Calcineurin/NFAT	LVH
	αMHC-NFAT3*	Calcineurin/NFAT	LVH
Gruver et al., 1993[279]	ANF-CaM	Calmodulin	LVH and cardiomyocyte hyperplasia
Passier et al., 2000[280]	αMHC-CaMKIV*	MEF2	LVH progressing to HF (synergy with NFAT)
Hirota et al., 1995[281]	gp130	CT-1/LIF/IL6	LVH
Kunisada et al., 2000[282]	STAT3	Jak/STAT	LVH
DeLaughter et al., 1999[283]	IGF-1	IGF-1	LVH with progressive dysfunction
Bueno et al., 2000[284]	αMHC-MEK1*	ERK MAPK	LVH with enhanced LV function: resist apoptosis
Shioi et al., 2000[7]	αMHC-p110a*	PI3-K / Akt	Physiological LVH
Matsui et al., 2002[285]	αMHC-Akt*	Akt	Spectrum: dilated – concentric LVH: resist apoptosis
Zhang et al., 2000[286]	αMHC-TAK1-DN*	p38 MAPK	LVH rapidly progressing to HF
Zhang et al., 2001[287]	αMHC-SRF	Transcription factor	LVH and heart failure
Veniant et al., 1996[288]	α1ATrat renin	RAS	LVH and vascular injury, normotensive
Shioi et al., 2000[7]	FAK*	Integrin signalling	LVH
Sato et al., 1998[83]	αMHC-CSQ	Calsequestrin	Mild LVH, contractile Depression
Diwan et al. 2004[213]	αMHC-mTNF∝	TNF∝	LVH
Depre et al., 2002[289]	αMHC-H11K	H11 Kinase	LVH

* activated mutant, WT: wild type, αMHC alpha-myosin heavy chain promoter, CK: creatinine kinase promoter, ANF: atrial natriuretic peptide promoter, α1AT: alpha-1 antitrypsin promoter. LVH: left ventricular hypertrophy, HF: heart failure.

residues in some species.[290] The cleavage of angiotensinogen is the rate-limiting step of the RAS. In humans the availability of active renin governs the rate of this reaction,[291] whilst in mice it is dependent on angiotensinogen concentration.[292] The optimal in vitro pH is 6.0 for human renin, though this varies with species.[293] Species specificity is also exhibited with regard to angiotensinogen cleavage, particularly amongst murine renins.[294,295]Renin is a zymogen:[296,297] electrostatic and hydrophobic interactions between specific amino acids in the P10-20 region of the prosegment appear to be important for both enzyme inhibition and prorenin expression.[298-300] It is thought that the prosegment sterically hinders the active site, and under normal conditions has to be proteolytically removed to allow enzymatic activity. Proteolysis occurs at a conserved site, Arg-43P Leu-1, but the identity of the enzyme responsible is not known.[301] Candidates based on appropriate in vitro cleavage include kallikrein,[302] cathepsin B,[303,304] proconvertases[305-307] and epidermal growth factor (EGF)-binding protein type-B.[308] However, studies of prorenin activation kinetics,[309] prosegment binding[310] and active site trapping[299] experiments suggest that proteolytic removal of the prosegment is not mandatory for enzymatic activity. Conformational changes induced by changes in temperature, pH, specific antibodies or mutation are sufficient to allow enzymatic activity.[298,311,312] Although short term infusion studies in rats[313,314] and monkeys[315-317] do not support a physiological role for prorenin, transgenic mice expressing prorenin with non-cleavable prosegments demonstrate evidence of enzymatic activity in vivo.[318,319] Furthermore, elevated prorenin levels in diabetics are predictive of microvascular complications, adding further weight to this argument.[320-322]

The juxtaglomerular apparatus is the major site of renin expression,[323,324] but other sites are important, including submaxillary gland in mice, placenta, heart, aorta, brain, adrenal, testis, adipose and eye in many species.[324-337] In juxtaglomerular cells prorenin secretion is constitutive whilst active renin secretion is regulated.[338-340] Plasma levels of prorenin usually exceed those of renin,[341] with a significant contribution from extrarenal sites.[342,343]

1.4.2.3 Renin-Angiotensin Aldosterone System and Cardiac Hypertrophy

At the most simple level, AngII can stimulate hypertrophy of purified cardiomyocytes isolated from chicks, and neonatal rats.[344-346] However, this effect is weak compared to other hypertrophic stimuli, possibly owing to the low density of AT_1 receptors on cardiomyocytes and the putative antihypertrophic effect mediated by AT_2 receptors.[347,348] In addition it should be noted that some of the effects of AngII are mediated in part by paracrine secretion of endothelin, TGFβ-1 and interleukin-6 family cytokines from non-myocytes,[70,239,240,349] and that stretch of isolated cardiomyocytes induces autocrine AngII secretion.[237] However the conclusions of such studies may not be completely robust since most have used neonatal rat cardiomyocyte preparations, which may not be directly comparable to the adult situation. In particular, such cells undergo physiological hypertrophy in vivo in the neonatal period[4] and may therefore be predisposed to hypertrophy. In addition, contamination by cardiac fibroblasts and other cell types cannot be completely avoided with this approach, thereby complicating interpretation.

Infusion of angiotensin II in rats and mice causes cardiac hypertrophy via AT_1 mediated pathways.[350] Subpressor doses of AngII, which are insufficient to raise blood pressure suggest that AngII has a direct effect on cardiomyocytes.[351] However, relatively minor degrees of hypertension can cause LVH in mice, and no studies have actually demonstrated continuous normotension via radiotelemetry, thereby leaving open the question as to whether the effect is truly blood pressure-independent.

Support for a load-independent hypertrophic role for AngII is provided by several transgenic studies. Overexpression of the AT_1 receptor in mice in a cardiomyocyte restricted distribution leads to hypertrophy and heart failure without any change in blood pressure.[267,268] This suggests that AngII can directly induce cardiomyocyte hypertrophy if sufficient AT_1 receptors are present. However, it does not necessarily indicate that this occurs in normal mice. Similarly, mice with cardiac overexpression of angiotensinogen, or doubly transgenic for human renin and cardiac-restricted human

angiotensinogen, develop hypertrophy in the absence of hypertension.[352,353] Cardiac overexpression of AT_1 receptor in transgenic rats leads to exaggerated cardiac hypertrophy in response to volume and pressure stimuli, but not in the basal state.[354] Rats overexpressing rat prorenin also develop cardiac hypertrophy despite normal blood pressure.[288] These studies provide more conclusive evidence that local AngII is hypertrophic, but they do not distinguish between a direct or paracrine effect.

Contradictory evidence regarding the importance of AngII in LVH comes from other studies. Van Kats et al. (2001)[355] recently demonstrated that cardiomyocyte specific overexpression of AngII in transgenic mice (via a ubiquitously cleaved fusion protein) is not sufficient to cause myocyte hypertrophy, but only mild interstitial fibrosis. Furthermore, in some studies, AT_1 receptor blockade/deficiency has failed to prevent hypertrophy after aortic/pulmonary constriction.[356-358] In addition, the homeostatic activation of the RAS in response to dietary manipulation does not cause cardiac pathology in rats.[359] These studies therefore suggest that the hypertrophic effect of AngII is load-dependent, and that AngII is not an obligatory pathway in load-induced hypertrophy.

Which angiotensin receptor mediates LVH has become a contentious issue in the light of recent reports. Most pharmacological studies have suggested a dominant role of the AT_1 receptor in LVH development, whilst AT_2 signalling has antihypertrophic effects.[360,361] Indeed, AT_1 antisense delivered to the heart by a retroviral vector protects TGRmren2-27 from cardiac hypertrophy in a blood pressure independent manner.[362] Similarly, mice deficient for $p91^{phox}$ (a component of NADPH oxidase), are protected from the hypertrophic effects of subpressor doses of AngII,[351] implicating a role for AT_1 signalling. However, recent studies have indicated that AngII mediated hypertrophy may be AT_2 receptor dependent. $AT_2^{-/y}$ receptor mice resist the development of LVH and fibrosis in response to aortic banding and pressor doses of AngII[363,364] whilst $AT_{1a}^{-/-}$ are susceptible.[356-358] Equally, neonatal cardiomyocytes from $AT_{1a}^{-/-}$ mice hypertrophy in response to stretch via activation of tyrosine kinase pathways,[365] despite the previously

reported AT_1 dependence of this process.[366] This data suggests that AT_1 signalling is dispensable in several models of LVH, and that AT_2 signalling may be essential. A major caveat is that another $AT_2^{-/-}$ model was not protected from LVH, suggesting that strain-dependent or vector-dependent effects may be important.[367,368] Furthermore, cardiac overexpression of AT_2 in mice attenuates the development of perivascular fibrosis in response to AngII via kinin/NO-dependent mechanisms, without an increase in LVH.[369] Therefore, the exact roles of AT_1/ AT_2 in LVH are complex and await clarification.

Overall a reasonable interpretation of these conflicting studies is that AngII has weak direct effects on cardiomyocytes, mainly due to low levels of AT_1 receptors. Indirect effects of AngII, either by activation of paracrine pathways, or load-induced stretch may be more potent stimuli. Signalling via AT_2 receptor appears as important, if not more important than the AT_{1a} receptor. Although activation of the RAS stimulates cardiac hypertrophy, it is not absolutely pivotal.

The role of aldosterone in cardiac hypertrophy has been less intensively studied. In vitro, aldosterone has hypertrophic effects on neonatal rat cardiomyocytes,[370] whilst antagonism of the mineralocorticoid receptor prevents LVH in young SHR,[371] and reduces LVH in humans.[372] Whether aldosterone is synthesised de novo within the heart is a matter of controversy. The essential enzymes for aldosterone synthesis cyp11b1 and cyp11b2 are detectable in rat myocardium,[373] and appear to be upregulated post-myocardial infarction,[374] but overall, the contribution of myocardial aldosterone synthesis appears to be small.[375] Furthermore, the accepted paradigm that aldosterone stimulates cardiac hypertrophy and fibrosis is called in to question by recent transgenic experiments. Hundred-fold overexpression of aldosterone synthase within cardiomyocytes in transgenic mice does not cause LVH or fibrosis, but induces coronary endothelial dysfunction.[376] Conversely, conditional transgenic expression of mineralocorticoid receptor antisense RNA selectively in the heart induces reversible cardiac fibrosis and heart failure in mice.[196]

1.4.2.4 Cardiac Renin-Angiotensin System

Increasing evidence supports the concept of tissue-based RAS's in which the constituent parts of the RAS are present, and exert a physiological effect on a particular tissue, independently of the plasma-based RAS.[335,336]

The existence of a cardiac-based RAS is supported by many studies, though no single experiment has provided indisputable proof. In the heart, expression of most of the components of the renin-angiotensin system has been demonstrated conclusively,[333,377,378] including a truncated prorenin transcript lacking the normal signal peptide which may be imported in to mitochondria.[379,380] AngII accumulation can be demonstrated in cardiomyocytes suggesting either uptake via AT receptor internalisation or intracellular generation.[381] Active generation of AngII occurs in porcine and human hearts in vivo [382,383] and rat hearts perfused with renin / angiotensinogen ex vivo.[384,385] Furthermore, mechanical stress/disease appears to upregulate all the key components of the RAS, including renin, ACE and angiotensinogen.[69,115,118,241,386-390] Indeed the activity of the cardiac RAS correlates directly with end systolic wall stress in humans.[118] These results indicate that an active local RAS exists and may be important in mediating and sustaining disease states.[118,386]

In most studies cardiac renin expression is extremely low if present at all.[391] Despite this, renin activity is readily detectable in cardiac extracts, correlating with and exceeding levels in the plasma.[392,393] In addition, this activity disappears after nephrectomy, suggesting that renal-derived renin is taken up and accumulated by the heart.[394-397] This evidence is supported by other studies which show that cultured rat cardiomyocytes and human endothelial cells bind and take up recombinant human (pro)renin via the cation-independent mannose-6-phosphate receptor / Insulin-like growth factor type 2 receptor (M6PR/IGF2R).[398-401] Although prorenin taken up by this mechanism can be shown to be activated to renin, generation of AngI in the presence of angiotensinogen could not be demonstrated.[399,400] Furthermore, prorenin binding to M6PR does not lead to any intracellular signalling events, despite the fact that it couples

with G-proteins, nor is there any evidence that prorenin binding in the presence of angiotensinogen leads to intracellular AngII formation.[402] For these reasons it is possible that this pathway simply mediates clearance of (pro)renin, as is suggested by studies in which prorenin was infused into rats[403] and monkeys.[317,404] This would be in keeping with the role of M6PR in the clearance and inactivation of numerous hormones (IGFII, leukaemia inhibitory factor, proliferin, thyroglobulin) and proteolytic enzymes.[405] An exception is the uptake and activation of latent TGFβ by M6PR.[406] Several studies clearly show that exogenous renin participates in the generation of cardiac AngII, [353,382,384,385] but none have identified the mechanism of uptake. Therefore it is reasonable to conclude that (pro)renin uptake is more than a clearance mechanism, suggesting that another uptake mechanism may exist.

Another reason to question the role of M6PR-mediated renin uptake is that in general this receptor recognises proteins containing M6P moieties (IGFII is an exception). Cardiomyocyte uptake of non-glycosylated forms of renin (eg mouse ren-2) have been demonstrated in transgenic rats and in vitro, suggesting that a glycosylation-independent mechanism may be involved.[407,408]

Renin binding protein was previously identified in rats,[409] but appears to function as a carbohydrate epimerase,[410] so renin binding activity is probably co-incidental. Other tissue renin-binding sites have been described, but the molecule(s) involved have not been identified.[411]

A recent development in this field is the identification of a novel renin/prorenin receptor by expression cloning a human mesangial cell cDNA library with iodinated human recombinant renin.[412] This receptor comprises a 350 amino-acid protein with a single predicted transmembrane domain. Expression studies have demonstrated localisation of the putative renin receptor to mesangial cells and vascular smooth muscle cells in the subendothelium of renal and coronary arteries. In vitro studies demonstrated that the receptor binds (pro)renin with high affinity, and that it enhances the catalytic activity of

both renin and prorenin leading to local generation of AngII. In addition, binding by renin and prorenin activates ERK1/2 signalling pathways independently of AngII. Notably, the renin receptor does not mediate (pro)renin uptake, nor does it appear to be expressed on cardiomyocytes, so that another receptor may explain the results of Peters et al., (2002).[407]

In summary, there is substantial evidence for tissue and cellular uptake of circulating renin/prorenin, and activation of the local RAS. It seems likely that this may be mediated in part by a renin receptor, whilst the M6PR may act as a clearance mechanism for circulating renin. It is also worth noting that intracellular angiotensin II may mediate physiological effects via intracellular AT_1 receptors, the so-called intracrine RAS.[413] Iontophoretic experiments using physiological concentrations of angiotensin II demonstrate roles in intercellular signalling and inward calcium ion currents.[381,413]

1.4.3 Other Neurohumeral Pathways in LVH

Several humeral signalling pathways have direct hypertrophic effects, which are at least as important as those of the RAS.

1.4.3.1 Adrenergic Signalling

α-adrenergic receptor stimulation is pro-hypertrophic in neonatal cardiomyocyte cultures, using selective agents such as phenylephrine.[414] Not surprisingly, transgenic α_{1B}-adrenergic receptor overexpression in the murine heart leads to cardiac hypertrophy,[269,270] and cardiac failure.[179]

Stimulation of cardiomyocyte β-adrenergic receptors in vitro and in vivo also leads to myocyte hypertrophy, often with evidence of myocardial necrosis,[62] whilst transgenic cardiac over expression of β_1-adrenoreceptors in mice causes substantial cardiac hypertrophy leading to heart failure.[105,415] Mice lacking endogenous catecholamines due to dopamine β-hydroxylase deficiency ($Dbh^{-/-}$) resist cardiac hypertrophy development following transverse aortic constriction.[416,417]

1.4.3.2 Endothelin

There is little doubt that endothelin is a potent stimulus for cardiac hypertrophy in vitro.[418] Direct in vivo evidence is restricted to pharmacological studies[419] due to the embryonic lethal phenotype of endothelin/endothelin receptor knockouts.[420-422] However there is substantial evidence that the downstream signalling pathways activated by endothelin, such as G-protein signalling molecules, are required for cardiac hypertrophy. Gαq couples to endothelin, angiotensin II and α_1-adrenergic receptors: experiments in which activated mutants of Gαq have been overexpressed in a cardiac selective manner demonstrate a hypertrophic effect as well as activation of apoptosis, leading to heart failure.[84,180,271] Conversely, dominant-negative Gαq mutants resist TAC,[423] whilst $G\alpha q^{-/-}$ /$G\alpha 11^{-/-}$ cardiac-specific conditional double knockouts display a similar phenotype.[424]

1.4.3.3 Cardiotrophin

Seminal work by Pennica et al (1995) using expression cloning with an embryonic stem cell-based model of cardiogenesis[347] identified cardiotrophin 1 (CT-1) as a hypertrophic stimulus. This is a member of the Leukaemia Inhibitor Factor/IL-6 cytokine family, which signal via gp130 tyrosine kinase receptors. Whilst other members of this family demonstrate weak hypertrophic effects, CT-1 potently induces cardiomyocyte elongation and hypertrophy in vitro.[347,425] Constitutive activation of cardiac gp130 receptors causes eccentric hypertrophy in vivo.[281] CT-1 is crucial for normal cardiac development and physiological hypertrophy, in that $gp130^{-/-}$ mice have hypoplastic ventricles.[426] Cardiac selective deletion of gp130 in adult mice leads to dilated cardiomyopathy and heart failure in response to pressure overload,[173] whereas cardiac specific expression of a dominant negative form of gp130 prevents pressure-induced cardiac hypertrophy.[427] Therefore the role of gp130/CT-1 in cardiac hypertrophy is complex and model-dependent.

1.4.3.4 Insulin, Growth Hormone and IGF 1

Given the pleiotropic roles of insulin, growth hormone (GH) and IGF-1 in cell growth and metabolism, a role in cardiac hypertrophy is likely. Cardiac selective deletion of the

insulin receptor during postnatal development inhibits physiological cardiac hypertrophy, with a 25% reduction in heart weight to body weight ratio.[6] The requirement for insulin signaling in pathological hypertrophy has not been tested.

Left ventricular hypertrophy is a recognised complication of acromegaly,[428] indicating a possible effect of GH/IGF-1 excess on cardiac mass. Certainly IGF-1 has direct in vitro hypertrophic effects,[429] and studies in rats, pigs and humans have demonstrated increased expression of IGF-1 during the development of pressure and volume overload cardiac hypertrophy.[430-432] Treatment of rats with recombinant GH or IGF-1 leads to eccentric LVH,[433] whilst IGF-$1^{+/-}$ mice demonstrate impaired cardiac hypertrophy after myocardial infarction.[186] Constitutive overexpression of IGF in the heart enhances cardiac performance.[434]

1.5 Signalling in Cardiac Hypertrophy

1.5.1 Intracellular Signaling Cascades and LVH

Stimulation of diverse cell surface receptors and mechanical stress can lead to LVH, via activation of intracellular signaling cascades.[89,242] Whilst the patterns of signaling overlap between different stimuli, they are non the less distinctive. Using transgenic techniques it has been possible to demonstrate that activation of a single receptor type, or down stream signalling molecule is often sufficient to induce cardiac hypertrophy in mice. Furthermore, knockout studies have suggested that certain molecules are indispenible for cardiac hypertrophy to proceed at all, whilst other molecules appear to be negative regulators of hypertrophy (table 1.3) or cardiomyocyte survival factors (table 1.1). Amongst the most intensively studied hypertrophic regulators is calcineurin.

Table 1.3. Antihypertrophic Pathways

Reference	Knockout	Pathway targeted	Stimulus	Response
Knowles et al., 2001[435]	$Npr1^{-/-}$	ANP/BNP	AC	Exaggerated LVH and failure
Vega et al., 2003[436]	$MCIP1^{-/-}$	Calcineurin/NFAT	CnA*	Exaggerated LVH and failure
Crackower et al., 2002[81]	$PTEN^{-/-}$	PTEN/PI3K	-	LVH without foetal gene induction. Impaired systolic function
Asakawa et al., 2002[437]	$PPAR\gamma^{-/-}$	Energy metabolism	AC	Exaggerated LVH
Abel et al, 1999[438]	$G4H^{-/-}$	Insulin induced glucose uptake	-	LVH with preserved contractility
Kong et al., 2001[439]	$FHL2^{-/-}$	transcription	Iso	Exaggerated LVH
Xin et al., 2002[440]	$FKBP12.6^{-/-}$	SR Ca^{2+} release	-	LVH
Ichinose et al., 2004[441]	$NOS3^{-/-}$	NO production	AC	Exaggerated LVH and failure

Npr: natriuretic peptide receptor, MCIP1: myocyte enhanced calcineurin inhibitory protein, PPAR: peroxisome proliferative A receptor, FKBP: FK506 binding protein, ANP: atrial natriuretic peptide, BNP: B-type natriuretic peptide, NFAT: nuclear factor of activated T cells, AC: aortic constriction, CnA*,: activated calcineurin mutant, Iso: isoprenaline, PI3K: phosphoinositol-3 kinase SR: sarcoplasmic reticulum.

1.5.2 Calcineurin-NFAT Signalling in Cardiac Hypertrophy

In a seminal paper Molkentin et al. (1998)[82] identified a role for the calcineurin-NFAT signalling pathway in the development of cardiac hypertrophy. Using a yeast two-hybrid system to isolate cofactors interacting with the cardiac specific transcription factor GATA-4, they identified NFATc4 (NFAT3) a transcription factor belonging to the nuclear factor of activated T-cells (NFAT) family. Identification of binding sites for NFATc4/GATA4 in the promoter of BNP suggested a direct regulatory role for this pathway in cardiac hypertrophy. In addition, translocation of NFAT's from the cytoplasm to the nucleus was known to require calcineurin phosphatase activity in lymphocytes. They demonstrated that activated mutants of NFATc4 and calcineurin caused hypertrophy of neonatal rat cardiomyocytes in vitro, and transgenic mice over expressing similar constructs in the heart developed profound cardiac hypertrophy and heart failure. Furthermore, pharmacological inhibition of calcineurin with ciclosporin

(CsA) prevented the development of hypertrophy in activated calcineurin transgenic mice, but not NFAT transgenics, giving credence to the proposed signalling pathway.

1.5.2.1 Calcineurin Biology

Calcineurin (Protein Phosphatase 2B (PP2B)) is a heterodimeric calcium-calmodulin-dependent serine-threonine phosphatase, comprising calcineurin A (CnA) and B (CnB) subunits.[442] The 58-59kDa CnA-subunit exists in 3 isoforms (α, β, γ), for which multiple splice variants have been described. It contains the active site, an autoinhibitory domain, calmodulin-binding domain and a CnB binding domain. CnA isoforms share 81% sequence homology in the catalytic domain, and the CnAα and β genes share 99% amino acid sequence homology between mouse and human species. Expression of CnAα and β is almost ubiquitous, whilst that of CnAγ is restricted to the testis.(reviewed Crabtree 1999[442]) In the heart CnAα is probably responsible for most of the known effects on cardiac hypertrophy.[443,444] Surprisingly CnAα knockouts develop normally, though they have subtle alterations in neuronal architecture and T-cell function.[445] Both CnAα and β-null mice demonstrate abnormalities of skeletal muscle fibre type switching.[446] CnB is a 19kDa subunit containing a calcium-binding domain. Two isoforms have been identified (α and β).[447] Calcineurin regulates the activity and cellular localisation of several transcription factors including NFAT members,[448] myocyte enhancer factor 2 (MEF2),[280] elk-1[449,450] and IκB/NFκB.[451] Therefore it may have profound effects on gene expression.

Calcineurin is activated through binding calcium and calmodulin. Multiple stimuli are known to raise calcium and calmodulin levels in cardiomyocytes, such as humoral factors (AII, ET-1, LIF, PE) and mechanical strain. It is thought that calcineurin is sensitive to sustained alterations in the calcium concentration mediated via "capacitative calcium entry", as opposed to the short-term changes that occur with each cardiac cycle.[452] Precisely how this is sensed is unclear, but it may depend on the compartmentalisation of calcium within the myocyte. The distribution of calcineurin

with in the cardiomyocyte appears to be regulated by specialised anchoring proteins. Frey et al. (2000)[453] have identified a novel family of calcineurin-interacting proteins, "calsarcins" that tether calcineurin to α-actinin at the z-line of skeletal and cardiac myocytes. This suggests that calcineurin is directly exposed to the fluctuating calcium concentration of the sarcomere, rather than protected from it. In addition it also raises the possibility that calcineurin may also have roles in the sensing / transduction of mechanical strain and the regulation of sarcomeric contractility. Other anchoring proteins described below appear to direct localisation to the sarcoplasmic reticulum and the nucleus.

Calcineurin activity appears to be highly regulated. Modulatory calcineurin interacting proteins also known as myocyte-enriched calcineurin interacting proteins (MCIP1, 2 and 3) bind and inhibit CnA in striated muscle.[454] In the heart transcription of MCIP1 is potently induced by calcineurin signalling as well as mechanical strain and LIF,[455] thereby providing a negative feedback loop on this pathway. This effect has been confirmed in MCIP1$^{-/-}$ mice crossed to MCK-CnA* transgenics, which develop exaggerated LVH.[456] However, the function of MCIP's may be more complex, and there is experimental evidence that MCIP's may have a permissive role on CnA activity in certain conditions, and inhibitory functions in others.[456]

Cain (calcineurin inhibitory protein, also known as cabin) is a 240kDa scaffolding protein that binds multiple proteins including calcineurin.[457,458] CHP (calcineurin B homolgous protein) is homologous to CnB and competes for binding the CnA subunit.[459] AKAP79 (A-kinase anchoring protein 79) is a scaffolding protein expressed in neurones that binds protein kinases A and C in addition to inhibiting calcineurin.[460] Finally, cyclophilin and FK506 binding protein (FKBP) bind and inhibit calcineurin in the presence of the immunosuppressants ciclosporin A and FK506 respectively.[461-463]

1.5.2.2 NFAT Biology

Although several transcription factors are regulated by calcineurin the best charcterised target is the NFAT family of transcription factors.[464] There are five known members designated NFATc1 (NFATc or NFAT2), NFATc2 (NFATp or NFAT1), NFATc3 (NFAT4 of NFATx), NFATc4 (NFAT3), and NFAT5.[448] NFAT5 resides exclusively in the nucleus, whilst the others are cytoplasmic (hence NFATc designations). Calcineurin-mediated dephosphorylation of serine residues within SP repeats exposes nuclear localisation signals allowing translocation in to the nucleus.[465] The mechanism of nuclear export is not fully understood and probably differs for each NFATc. Kinases such as glycogen synthase kinase-3β,[87,466] p38 MAPK,[467-469] JNK,[467,470] MEKK1 and casein kinase 1a[471] all probably rephosphorylate NFAT's leading to nuclear export. Thus activity of NFAT's appears to be regulated mainly through spatial localisation, with continual shuttling between cytoplasm and nucleus. They bind a consensus DNA sequence GGAAAAT via a rel (NFκB) homology domain as monomers or dimers.[448] Target genes containing this sequence include IL-2 in lymphocytes, BNP[82] adenylosuccinate synthetase[472] and MCIP1 in the heart.[473] All NFAT types are expressed in human heart.[474] Expression is otherwise restricted to T-cells and skeletal muscle, except NFATc4 which is widely expressed.[475] Other transcription factors cooperate with NFATc members in DNA binding, and are collectively known as NFATn: these include AP-1, c-MAF and GATA4, depending on the tissue.[448] NFATc4 and GATA4 synergistically activate the BNP promoter within cultured cardiomyocytes.[82]

NFAT's appear to be critical in cardiovascular and immune development. Homozygous NFATc1 knockout mice fail to develop cardiac semi-lunar valves and are embryonic lethal.[476,477] Knockout mice deficient in both NFATc3 and NFATc4 are defective in angiogenesis and vascular patterning, a phenotype that can be replicated by an inactivating mutation of the calcineurin B gene.[478] NFATc1, NFATc2 and NFATc3 knockouts demonstrate immune dysfunction,[479-483] whilst NFATc2 and c3 null mice also have skeletal muscle abnormalities.[484,485]

1.5.2.3 Pharmacological Inhibitors of Calcineurin

Two calcineurin inhibiting drugs, ciclosporin (CsA) and FK506 are currently available and are used to maintain immunosuppression in patients receiving allografts. CsA is a lipophilic 11 amino acid cyclic polypeptide derived from Tolypocladium inflatum Gams.[486] It is metabolised by hepatic cytochrome P-450IIIA enzymes to approximately 30 derivatives that are only weakly active. FK506 is a macrolide antibiotic obtained from Streptomyces tsukubaensis.[487] It is 100 times more potent than ciclosporin,[488] and it is extensively metabolised by hepatic cytochrome P-450IIIA1.[489] Both agents depend on accessory molecules for their inhibitory effect on calcineurin. Cyclophilin A-D and FK506 binding protein-12 (FKBP12) are ubiquitous cytosolic peptidyl-propyl isomerases that bind CsA and FK506 respectively.[461-463] These complexes bind and inhibit calcineurin phosphatase activity. The isomerase activities of cyclophilin and FKBP-12 are also inhibited, though this has no bearing on the immunosuppressant effect.

Although the effect of these drugs is attributed to their inhibitory effect on NFAT dephosphorylation / nuclear translocation, other calcineurin-independent effects have been proposed which contribute to their mode of action and side effects. CsA induces TGFβ, and inhibits members of the mitogen activated protein kinase (MAPK) pathway, both of which could add to the immunosuppressant effect.[490] Whether these are direct actions is not established. In addition, CsA alters properties of the ryanodine release channel(RYR)[491] and the L-type calcium channel,[492] both of which could impact on myocardial function.

FK506 has several activities that impinge on myocardial calcium regulation, and might therefore be expected to alter contractile function. In cardiomyocytes FKBP12.6 is associated with the ryanodine receptor whilst FKBP12 is cytosolic. The ryanodine receptor is a sarcoplasmic reticular calcium release channel responsible for the regulated release of calcium stores essential for excitation-contraction coupling. FKBP12.6 regulates the gating of the RYR channel[493] whilst FK506 induces dissociation of

FKBP12.6 from the channel. Male FKBP12.6$^{-/-}$ mice develop LVH,[440] whilst FKBP12$^{-/-}$ mice develop cardiac failure and ventricular septal defects. [494] Calcineurin has also been hypothesised to regulate RYR function by dephosphorylation via an FKBP-dependent interaction.[494]

1.5.3 Inhibition of Left Ventricular Hypertrophy using Pharmacological Inhibitors of Calcineurin

Considerable attention has focussed in recent years on the use of calcineurin inhibitors to prevent / reverse LVH. The main studies published to date are summarised in table 1.4, and it can be seen that numerous models have been studied using both CsA and FK506 in various dosing regimens, in both rats and mice. The overwhelming majority of published studies support a role for calcineurin signalling in cardiac hypertrophy, although apparently identical experiments have produced disparate results. The results of these studies have been extensively reviewed,[486,495,496] and the salient points will be summarised here.

1.5.3.1 Aortic Constriction

Eleven studies have examined the effect of calcineurin inhibition in aortic constriction models of cardiac hypertrophy in both rats and mice.[142,497-505] Whilst the majority of studies demonstrated a benefit, this was not universally the case, and in some studies there are real concerns about the methodology used, or the interpretation applied. For example, many made no assessment of the haemodynamic gradient across the constriction.[497,500,503] This is very important because meticulous studies by Zhang et al. (1999)[498] demonstrated a reduction in the trans-stenotic gradient in drug treated groups, which negated an apparently beneficial effect of drug treatment on LVH. In addition, few studies took into account the general toxic effects of drug treatment, in particular weight loss. To address this issue Lim et al. (2000)[500] fed sham-operated and banded rats a very low calorie diet to induce a similar degree of weight loss as drug treatment. These control groups maintained identical cardiac mass indexes to their counterparts on normal diet, suggesting that additional changes seen in drug treated groups were

genuine. Sussman et al (1998)[497] claimed complete inhibition of LVH, but more than half of the treated rats died perioperatively of heart failure. High levels of mortality have also been seen in other studies using both CsA and FK506.[498,506] Some of this may be operator-dependent, as well as related to drug dosage, strain background and possibly even infection. It is known that different rat strains may vary markedly in their tolerance to drug dosage, with Wistar rats tolerating ten fold higher doses of FK506 than Dahl-Iwai rats.[502,507] Whether strain differences impact on LVH potential and calcineurin-dependence is not known. It is also likely that the site of aortic constriction (thoracic vs abdominal) may be important. Abdominal aortic constriction is associated with substantial activation of the RAS, and this appears to be reflected in a different pattern of hypertrophy marker gene induction.[236] Therefore different forms of hypertrophy may be being studied. Furthermore, although AC is frequently referred to as a "physiological" model of hypertrophy, it is difficult to see how this can be justified. Recent studies by Baumgarten et al. (2001 and 2002)[235,508] examined cytokine expression after transverse aortic constriction in mice and demonstrated a rapid but transient rise in IL-1β, IL-6 and TNFα within hours of constriction. Expression was localised to both endothelial cells and myocytes.

Although the importance of this early inflammatory signalling to the development of hypertrophy was not examined, it is tempting to speculate that calcineurin inhibition may down regulate cytokine signalling in cardiomyocytes, in a manner analogous to T-lymphocytes, and this may alter LVH development. Lim and Molkentin (1999)[523] have suggested that the importance of calcineurin signalling may be time-dependent in response to AC: an effect with CsA was noted 6 days after constriction, but not after 21 days. This implies that calcineurin inhibition simply retards the onset of LVH without affecting the final outcome. However, other studies have shown that late treatment can reduce established hypertrophy.[500]

Table 1.4 Drug Inhibition Studies of Calcineurin

Study	Species	Model	Treatment (mg/kg/day)	% red[n] LVH	Comments
Aortic Constriction					
Sussman, 1998[497]	Rat	AAC	CsA 20, 8 days	100%	High mortality
Luo, 1998[506]	Rat	AAC	CsA 20 and 40, 14 days	no effect	Disputed interpretation
	Rat	AAC	FK506 2, 14 days	no effect	
Muller, 1998[509]	Mouse	TAC	CsA 50, 3 weeks	no effect	
Zhang, 1999[498]	Rat	AAC	CsA 10 and 20, 2/4 weeks	no effect	Reduced BP gradient
	Rat	AAC	FK506 0.3, 4 weeks	no effect	in treated animals
Ding. 1999[504]	Mouse	TAC	CsA 50, 4 weeks	no effect	
Meguro. 1999[499]	Mouse	TAC	CsA 25, 3 weeks	32%	Increased CHF / mortality
Shimoyama, 1999[502]	Rat	AAC	FK506 1, 3 weeks	100%	Preserved EF%
Eto, 2000[503]	Rat	TAC	CsA 40, 4 weeks	58%	
Lim, 2000[500]	Rat	AAC	CsA 20, 14 days	87%	
			CsA 8, 14 days	34%	
			CsA 20, 14 days late intervention	62%	Reversal of LVH
Wang, 2001[505]	Mouse	TAC	CsA 50. 3 weeks	66%	
Hill, 2000[501]	Mouse	TAC	CsA 50, 5 weeks	100%	Preserved Function
Cardiomyopathy					
Molkentin, 1998[82]	Mouse	αMHC-CnA*	CsA 50, 7 days	>95%	
Sussman, 1998[497]	Mouse	Tropomodulin	CsA 30, 15 days	100%	Impaired FS%
			FK506 6, 15 days	100%	
	Mouse	MLC2v mutant	CsA 30, 6 weeks	100%	
	Mouse	β-tropomyosin	CsA 30, 8 days	100%	Dilation inhibited
	Mouse	Activated RARα	CsA 30,	no effect	
Mende, 1998[272]	Mouse	αMHC-Gα_q *	CsA 30, 28 days	ambiguous§	
Lim, 2000[510]	Mouse	αMHC-CnA*	CsA 30, 13 or 26 days	90%	Improved FS%
		αMHC-CnA*	CsA 30, 14 reversal	29%	Fibrosis unchanged
		β-tropomyosin	CsA 30, 8 days	100%	
Fatkin, 2000[511]	Mouse	αMHC$^{403/-}$	CsA 30, <35 days	worse	Altered intracellular Ca^{2+}
			FK506 6, <35 days		and increased mortality
Hypertension (Non-Aortic Constriction)					
Mervaala, 1997[512]	Rat	SHR	CsA 5, 6 weeks	no effect	Not primary aim of study
Zhang, 1999[498]	Rat	SHR	CsA 5, 6 weeks	no effect	Increased mortality
Lassila, 2000[513]	Rat	SHR	CsA 5, 6 weeks	no effect	
Mervaala, 2000[514]	Rat	dTGR	CsA 5, 3 weeks	50%	Reduced BP
Murat, 2000[515]	Mouse	2K1C	CsA 50, 4 weeks	100%	
Hayashida, 2000[516]	Rat	Dahl	CsA 10, 4/6 weeks	no effect	
Shimoyama, 2000[507]	Rat	Dahl	FK506 0.02 and 0.2, 6 week	≈50%§	>50% mortality
			FK506 0.02 and 0.2, late 4 weeks	≈25%§	Preserved EF% Partial reversal
Sakata, 2000[517]	Rat	Dahl	FK506 1, 12 weeks	48%	Fibrosis unchanged
			FK506 1, late intervention 4 weeks	no effect	Increased wall stress
Nagata, 2002[518]	Rat	Dahl	FK506 0.1, 6 weeks	87.5%	Rescued FS%. Dilated LV Reduced fibrosis
Goldspink, 2001[519]	Rat	Angiotensin II	CsA 50, 7 days	100%	
Takeda, 2002[520]	Rat	Mineralocorticoid	FK506 0.5, 6 weeks	70%	
			CsA 10, 6 weeks	62.5%	

Table 1.4 (continued)

Study	Species	Model	Treatment (mg/kg/day)	% red^{n} LVH	Comments
Miscellaneous					
Øie, 2000[521]	Rat	CAL	CsA 50, 2 weeks	14%	Worse CHF
Eto, 2000[503]	Rat	Exercise	CsA 40, 10 weeks	100%	
Kamiya, 2001[522]	Mouse	JVS	FK506 0.5 or 1, 4 weeks	partial	

SHR: spontaneously hypertensive rat. αMHC: alpha myosin heavy chain promoter. CnA*: constitutively active calcineurin A mutant. MLC2v: myosin light chain 2v. RARα: retinoic acid receptor alpha. AAC: abdominal aortic constriction. TAC: thoracic aortic constriction. $G\alpha_q$ *: G-protein alpha-q constitutively active mutant. dTGR: double transgenic rat (human renin and human angiotensinogen). CAL: coronary artery ligation. 2K1C: 2 kidney one clip model of hypertension. JVS: juvenile visceral steatosis model (systemic carnitine deficiency). CsA : ciclosporine A. FK506: Tacrolimus. FS%: fractional shortening. EF% : ejection fraction. CHF: congestive heart failure. § significant effect only if left ventricular mass normalised to tibial length.

1.5.3.2 Murine Models of Cardiomyopathy

It is well recognised that cardiac hypertrophy can develop in the absence of hypertension, and many hereditary forms of dilated and hypertrophic cardiomyopathy are described in which mutations of sarcomeric components are present. These diseases have been replicated in transgenic mice, and calcineurin inhibition has been shown to effectively prevent/reverse pathology in several studies.[82,497,510] Two exceptions are a transgenic model of constitutively active retinoic acid receptor (RAR) over expression,[497] and a model of hypertrophic cardiomyopathy caused by MHC mutation.[511] In the later case, calcineurin inhibition exacerbated hypertrophy and increased mortality. In addition, Mende et al. (1998)[272] described a model of sustained and progressive cardiac hypertrophy due to transient over expression of a constitutively active $G\alpha_q$ mutant in the heart. They found that hypertrophy could be attenuated using CsA, but the result was ambiguous because an effect was apparent only when LV mass was normalised to tibial length, as opposed to body weight.

1.5.3.3 Models of Hypertension

Both CsA and FK506 are known to cause hypertension, as discussed above. Indeed, CsA has been used as a means of inducing hypertension in rats for many years.[524,525]

Therefore the fact that these drugs might blunt the effect of hypertension on the heart is paradoxical. The effects of these calcineurin inhibitors appear to be dependent on the model of hypertension studied. In SHR strains LVH appears to be resistant to the effects of CsA, though this observation was not the primary aim of two of these studies, so a subtle effect may have been missed.[498,512,513] In distinct contrast, FK506 appears to strongly inhibit cardiac hypertrophy in Dahl salt sensitive (DS) rats,[507,517,518] and doses differing by ten fold appeared to be equally efficacious. Early treatment appeared to preserve cardiac function, whilst late treatment led to an increase in wall stress,[507] and declining efficacy once LVH was established.[507,517] However, careful analysis of the data by Shimoyama et al. (2000)[507] reveals that the antihypertrophic effect is not seen if LV mass is normalised to body weight, and the effect reported by Nagata et al. (2002)[518] is less. Hayashida et al. (2000)[516] found that CsA had no effect in DS rats. Using a transgenic rat model of hypertension based on over expression of human angiotensinogen and human renin Mervaala et al. (2000)[514] found that CsA attenuated LVH by 50%. However, CsA also reduced systolic blood pressure by about 35mmHg, which may have accounted for at least some of this effect. Positive results have also been reported using CsA or FK506 in Wistar rats treated with angiotensin II infusion,[519] uninephrectomised Wistar rats treated with aldosterone[520] and a murine model of renovascular hypertension (two kidney one clip).[515]

This data therefore lends support to the notion that calcineurin inhibition is important in the development of LVH in response to hypertension. The studies of LVH regression also suggest that the maintenance of hypertrophy may be partly calcineurin-dependent. The lack of effect in SHR cannot be easily explained except that LVH in this model may be calcineurin-independent, or that they are particularly susceptible to CsA-induced hypertension, which negates any antihypertrophic effect. It has been suggested that models of hypertension/hypertrophy that are RAS-dependent are particularly susceptible to calcineurin inhibition. Although the mechanisms of hypertension operating in SHR and Dahl rats are incompletely understood, there is evidence to support a role of the cardiac RAS in the development of LVH in both models.[526,527]

1.5.3.4 Miscellaneous Studies

Several studies have been published which do not fall in to any of the above categories, but warrant discussion. Øie et al. (1999)[521] demonstrated that CsA inhibited post-MI cardiac hypertrophy in rats, but at the expense of cardiac function. However, their analysis was flawed in that the result was only significant if LV mass was normalised to tibial length: if body weight was used there was an apparent increase in LVMI. Furthermore, they found very little difference in hypertrophy gene marker expression, adding weight to the argument that this study was actually negative.

Eto et al. (2000)[503] have demonstrated that exercise-induced hypertrophy in Wistar rats, is calcineurin-dependent and Kamiya et al. (2001)[522] demonstrated attenuated LVH in a murine model of hypertrophy due to systemic carnitine deficiency (Juvenile Visceral Steatosis).

1.5.3.5 Conclusions Regarding Pharmacological Inhibition of Calcineurin

Overall there is substantial evidence to support a role for calcineurin signalling in the development and maintenance of many forms of cardiac hypertrophy. However, this is not universal, and the reasons for the discrepancies between studies are not clear. Several general points warrant further discussion in this regard. An important aspect of many of these studies is the effect of the drug on the general health of the animals, as substantial weight loss is frequently reported. This complicates the interpretation of whether or not LVH has regressed due to a direct effect of the drug, or simply as a consequence of a general catabolic state. Only one study has actually assessed the effect of weight loss induced by dietary restriction,[500] and this demonstrated that heart mass was reduced in proportion to body weight, so that LVMI remained constant despite an absolute reduction in LV mass. This is concordant with many other studies investigating the effects of starvation diets on rats,[528,529] rabbits,[530] dogs,[531] and humans.[532] In contrast, Cicogna et al (2000)[529] observed that cardiac hypertrophy was reduced in SHR fed a restricted diet compared to those on a normal diet despite similar blood pressures.

Although the mechanism is not clear, the catabolic state of starvation reduces cardiac protein synthesis and shortens the half-life of proteins, leading to cardiac atrophy.[530]

Other calcineurin-independent effects of the drugs probably have an effect on cardiac function. Therefore pharmacological inhibition of calcineurin is a less than ideal method for assessing its contribution to cardiac hypertrophy.

1.5.4 Transgenic Models of Calcineurin Inhibition

Since pharmacological inhibition of calcineurin has many drawbacks, several groups have developed transgenic models of calcineurin inhibition, listed in table 1.5, either using the endogenous calcineurin inhibitors discussed above, or gene targeting methods. These studies unanimously support a role for calcineurin in the development of cardiac hypertrophy.

De Windt et al. (2001)[533] used cardiac-specific transgenic mice expressing deletion mutants of either Cain or AKAP79 to inhibit calcineurin. They found that mice expressing high levels of inhibitor had an LVMI apporximately 10% less than wild type littermates at baseline, suggesting that calcineurin is important in physiological hypertrophy during normal growth.

In addition they demonstrated a marked reduction in LVH in response to isoprenaline infusion or abdominal aortic constriction. Furthermore, adenoviral transfer of Cain in aortic-banded rats also attenuated hypertrophy. In each case there was diminished induction of hypertrophy-related marker genes. However, one transgenic founder died prematurely of dilated cardiomyopathy, suggesting that very high levels of expression of the inhibitor may have been detrimental to normal cardiac function. Furthermore, although there was a favourable reduction in hypertrophy, cardiac function was not studied.

Table 1.5. Transgenic Studies of Calcineurin Inhibition

Study	Species	Model	Hypertrophic stimulus	% inhibition of LVH	Comments
De Windt et al. 2001[533]	Mouse	αMHC-ΔCain	Iso 14 days	50%	Low baseline LVMI in high expressors
			AAC 14 days	68-79%	
	Mouse	αMHC-ΔAKAP79	Iso 14 day	50%	Low baseline LVMI in high expressors
			AAC 14 days	25-38%	
	Rat	Adenoviral-ΔCain	TAC 14 days	40%	
Zou et al. 2001[534]	Mouse	αMHC-dnCnA	AAC 3 weeks	56%	
Rothermel et al. 2001[456]	Mouse	αMHC-hMCIP1	αMHC-CnA*	72%	5-10% baseline reduction in LVMI. Preserved FS
			Iso 7 days	59%	
			Exercise 28 days	58%	
Hill et al. 2002[535]	Mouse	αMHC-hMCIP1	TAC 3 weeks	27%	Preserved FS at 3 months Augmented ANF induction
			TAC 3 months	27%	
Bueno et al. 2002[536]	Mouse	CnAβ$^{-/-}$	AAC 14 days	67%	12% baseline reduction in LVMI
			Iso 14 days	75%	
			AII 14 days	46%	
Wilkins et al., 2002[474]	Mouse	NFATc3$^{-/-}$	aMHC-CnA*	20-44%	Little effect on foetal gene expression
			AAC 14 days	100%	
			AII	100%	
	Mouse	NFATc4$^{-/-}$	αMHC-CnA*	0%	
			AAC 14 days	0%	
			AII	0%	

αMHC: alpha myosin heavy chain promoter. ΔCain: calcineurin inhibitory domain of Cain. ΔAKAP79: calcineurin inhibitory domain of A-kinase-anchoring-protein 79. dnCnA: dominant negative calcineurin mutant. hMCIP1: human myocyte-enriched calcineurin interacting protein 1. CnAβ$^{-/-}$: calcineurin Aβ subunit knockout. Iso: isoprenaline osmotic minipump infusion. AAC: abdominal aortic constriction. TAC: thoracic aortic constriction. CnA*: constitutively activated calcineurin A mutant. AII: angiotensin II osmotic minipump infusion. LVMI: left ventricular mass index.

Zou et al. (2001)[534] used a dominant-negative approach to inhibit cardiac calcineurin. They generated a transgenic mouse expressing mutant calcineurin lacking the calmodulin-binding and autoinhibitory domains. Basal LVMI was normal, as was basal calcineurin activity. However, in response to abdominal aortic constriction, hypertrophy, fibrosis, calcineurin activation and foetal gene expression were blunted. Although echocardiography was performed, cardiac function was not reported.

Rothermel et al. (2001)[456] created transgenic mice overexpressing hMCIP1 in the heart. This strategy has the advantage that MCIP1 is probably the natural calcineurin inhibitor in the heart. These mice had a reduced LVMI at baseline, concurring with DeWindt et

al. (2001).[533] Additionally they were resistant to hypertrophy induction by isoprenaline infusion, and exercise. Crossing the mice to activated CnA (CnA*) transgenics partially inhibited the development of hypertrophy, and suppressed reprogramming of gene expression. Using the same model, Hill et al. (2002)[535] demonstrated an impaired hypertrophic response to thoracic aortic banding, with preserved LV function, as assessed by echocardiography. However, there was a paradoxical increase in ANF and BNP expression, and the decrease in LVH was relatively small (30%). Given the proposed role of MCIP1 as an inhibitor of calcineurin, Vega et al., (2003)[436] investigated the hypertrophic response of MCIP1$^{-/-}$ mice. Whilst CnA* mediated hypertrophy was exaggerated as predicted, they unexpectedly found that MCIP1 deficiency prevented hypertrophy in response to aortic constriction and isoprenaline infusion.[436] Therefore, the role of MCIP's in relation to calcineurin regulation is complex.

Bueno et al. (2002)[536] used a knockout approach in mice to examine the role of CnAβ. This is the predominant form of CnA expressed in the heart, accounting for 80% of calcineurin activity in the basal state in this study. Knockout mice were overtly normal except for a 12% reduction in basal heart size compared to wild type littermates. Knockout mice had severely impaired hypertrophic responses to abdominal aortic constriction, isoprenaline infusion and angiotensin II infusion. Presumably the residual hypertrophic capacity reflects activation of non-calcineurin dependent pathways. Surprisingly the effect of CnAβ deletion on hypertrophy-related gene expression was relatively minor, and fibrosis was not inhibited. Again, assessment of cardiac function wasnot performed.

Although over expression of NFATc4 in the heart causes profound cardiac hypertrophy,[82] NFATc4$^{-/-}$ mice remain susceptible to hypertrophy induction by aortic constriction, activated calcineuirn and angiotensin II infusion.[474] In contrast NFATc3$^{-/-}$ mice demonstrate an attenuated hypertrophic response to these stimuli,[474] though the effect is partial. Whilst this suggests a prime role for NFATc3, it would appear that other NFAT's are sufficient for hypertrophic responses, and that there is a degree of

redundancy in the NFAT signalling pathway in the heart. Inhibition of all NFATs by cardiomyocyte overexpression of GSK3β causes a more profound impairment of pressure overload induced hypertrophy though this is still incomplete.[87]

These studies provide compelling evidence for the importance of calcineurin in physiological and pathological hypertrophy. All studies demonstrate a significant effect in response to a variety of stimuli, though importantly, there was rarely complete abolition of hypertrophy, either at an anatomical or molecular level.

1.5.5 Role of Calcineurin in Human Hypertrophy/Heart Failure

Given the evidence presented above, the question remains does calcineurin signalling have a role in human cardiac hypertrophy, and if so does inhibition lead to clinical benefit? Limited data are available in this regard, due to the difficulty of obtaining human tissue. Early studies examined calcineurin protein expression, rather than activity, and found conflicting results in end-stage heart failure patients.[523,537] Haq et al. (2001)[444] obtained samples of failing and normal hearts at transplant, and cardiac hypertrophy samples from donor hearts that were unsuitable for transplant by virtue of significant hypertrophy. They found that CnA protein levels were elevated 1.82 fold in cardiac hypertrophy, and 1.5 fold in heart failure. CnA activity normalised to CnA expression increased in hypertrophy but not in heart failure. Therefore, there appears to be over expression in both conditions, with an increase in specific activity in hypertrophy. Ritter et al. (2002)[538] obtained samples from patients with hypertrophic obstructive cardiomyopathy (HOCM) undergoing transaortic subvalvular myotomy-myectomy and samples of cardiac hypertrophy secondary to aortic stenosis from patients under going valve replacement. They found increased CnA expression in both conditions, with increased enzyme activity, associated with NF-AT dephosphorylation. Furthermore, they detected an apparent decrease in expression of the C-terminal autoinhibtory domain, suggesting that proteolytic activation of calcineurin may be occurring, analogous to constitutively active CnA mutants described by Molkentin et al. (1998).[82]

Since calcineurin appears to have a role in human cardiac hypertrophy one might expect evidence of benefit from the use of calcineurin inhibitors in organ transplantation studies. On the contrary, CsA has been associated with induction of hypertrophy via blood pressure-dependent mechanisms.[539,540] Therefore, if calcineurin is ever deemed to be a desirable therapeutic target for cardiac hypertrophy, it is unlikely that current inhibitors will be used.

1.5.6 Signalling Pathway Cross Talk

Calcineurin-NFAT signalling does not occur in isolation to other signalling pathways, and there is mounting evidence for important interactions that potentiate or counterbalance each other. In particular there are multiple interactions, or points of "cross-talk" between Calcineurin-NFAT, Mitogen Activated Protein Kinase (MAPK) signalling and Glycogen synthase kinase-3β in the heart.

There is evidence that p38 MAPK antagonises NFAT by direct phosphorylation,[467-469] which would be expected to be antihypertrophic. This is surprising because p38 and other MAPK pathways are considered prohypertrophic.[284,286,541-544] However, the role of MAPK signalling is probably complex, because inhibition of the p38 MAPK pathway in the heart using transgenic dominant-negative species of MAPK Kinase 3 (MKK3), MKK6 and p38 MAPK actually leads to cardiac hypertrophy, and exaggerated responses to haemodynamic stress. This indicates that the antihypertrophic effect of p38 MAPK on NFAT signalling predominates over any putative prohypertrophic effects.[545] A corollary of this is the regulation of elk-1 transcription factor phosphorylation mediated by p38 MAPK, ERK1/2 versus dephosphorylation by calcineurin.[450] In addition, calcineurin enhances MCP-1 expression, leading to p38 MAPK inactivation.[546] Therefore, somewhat surprisingly, MAPK and calcineurin pathways appear to counteract rather than co-operate with each other.

Some studies have indicated a poorly defined co-operative effect between calcineurin and MAPK signalling. For example, Murat et al. 2000[515] found that treatment of

cardiomyocytes or mice with CsA inhibited activation of not only calcineurin, but also PKC isoforms, and MAPK, and similar evidence has been presented by de Windt et al., 2000.[547] However, pharmacological inhibitor studies such as these may be confounded by diverse non-specific effects, and should be interpreted with caution.

Other pathways also impinge on calcineurin-NFAT. Glycogen synthase kinase-3β (GSK-3β) exerts a constitutive constraint on hypertrophy via dephosphophorylation of NFAT and GATA4, amongst other transcription factors.[548-552] This is potently demonstrated by the resistance of transgenic mice over expressing activated GSK-3β in the heart to several hypertophic stimuli.[87] In fact GSK-3β is inactivated by virtually all known hypertrophic stimuli,[548] and therefore, it seems plausible to suggest that most hypertrophic signals potentiate calcineurin-NFAT signalling. In particular this appears to apply to Fas receptor signalling,[553] insulin PI3K/PKB/akt,[554] endothelin, angiotensin and β-catecholamines.[466]

1.6 Pressure Independent Inhibition of Cardiac Hypertrophy

Many of the genes required for humoral signalling (Dbh, $G\alpha q/G_{11}$, CnA, $Agtr_2$) appear to be indispensable for a normal hypertrophic response,[364,417,424,536,555] and knockout animals demonstrate resistance to LVH after aortic constriction: this is termed pressure–independent inhibition of LVH (Table 1.6). Such studies provide powerful proof that humoral signalling pathways are necessary for mechanical load sensing and activation of the hypertrophic phenotype. If the concept that LVH normalises wall stress is valid, one would anticipate that failure to adequately hypertrophy would have deleterious consequences. However it appears that the converse is true, and that these animals maintain normal cardiac function and have a survival advantage compared to wild type animals that develop LVH. This implies that LVH is maladaptive and that normalisation of wall stress is a flawed concept.

The original observations of Grossman[10] measured end systolic and end diastolic meridional wall stress in patients with pressure overload, volume overload, and normal controls. Whilst wall stress was normalised by concentric hypertrophy in pressure-overloaded patients, this was not the case for the volume overload group. Therefore, compensation does not necessarily require wall stress to be normalised and other mechanisms may have a role. Futhermore, the concept of wall stress only takes in to account the thickness of the myocardium at the instant that it is measured. Of course this neglects the contractile properties of the myocardium and other qualities, such as elasticity, which must also contribute to maintaining the integrity of the ventricle.

An elegant study by Esposito et al., (2002)[417] examined the stress-strain relationship of wild type, G-protein inhibitor transgenic mice (Gαqi) and catecholamine deficient mice ($Dbh^{-/-}$) using sonomicrometric implants after aortic constriction. Wild type animals hypertrophied and normalised wall stress, but succumbed to heart failure later on.

In contrast Gαqi mice were shown to have a blunted hypertrophic response resulting in increased end systolic wall stress, but preserved cardiac function for many months. Although not specifically commented on in the paper, the end systolic pressure volume relationship (ESPVR) of the Gαqi mice was increased relative to controls, suggesting that they adapted by increasing their myocardial contractility.

In other words, increased contractility may be compensating for increased wall stress and mitigate the requirement for LVH. Indeed, there is theoretical evidence for this in humans. [40,556] Exactly how contractility is increased in this model has not been reported. It is also interesting to note that contractility in $Dbh^{-/-}$ mice is increased at baseline,[416] so that this mechanism may not be generally applicable to other models. For example, Wettschureck et al 2002[424] reported that $G\alpha q/G_{11}{}^{-/-}$ mice subjected to aortic constriction have normalwall stress and contractility (end systolic elastance) despite complete inhibition of LVH. Potential mechanisms for increased contractility could involve enhanced Ca2+ handling by the sarcoplasmic reticulum, altered myosin isoforms (or

altered regulation), or enhanced metabolic efficiency. There is experimental evidence that altered expression of SERCA, phospholamban or GLUT1 are possible mechanisms by which this may occur.[132-138,223,557] However, whether such mechanisms occur naturally has not yet been investigated.

Table 1.6. Pressure Independent Inhibition of LVH in Response to Aortic Constriction

Reference	Knockout / transgene	% inhibition of LVH	Pathway targeted	Comments
Bueno et al., 2002[536]	CnAβ$^{-/-}$	66%	Calcineurin/NFAT	Reduced LVMI at birth ANF not attenuated
Wilkins et al., 2002[474]	NFATc3$^{-/-}$	100%	Calcineurin/NFAT	Complete inhibition of foetal gene expression
Antos et al., 2002[87]	GSK-3β	60%	NFAT	Enhanced ANP/BNP expression
Vega et al., 2003[436]	MCIP1$^{-/-}$	45%	Calcineurin/NFAT	Reduced LVMI at birth. Stimulus- dependent effect: exaggerated hypertrophy to CnA*
Wettshureck et al., 2002[424]	Gαq/G$_{11}$$^{-/-}$	100%	AngII/ET-1/catechols	Complete inhibition of foetal gene expression Normal wall stress. No increase in contractility
Esposito et al., 2002[417]	GαqI	≈50%	AngII/ET-1/catechols	Enhanced wall stress. Prolonged survival
Akhter et al., 1998[423]	GαqI	61%	AngII/ET-1/catechols	Preserved LV function
Senbonmatsu et al., 2000[364]	Agtr2^{-}/Y	≈80%	Angiotensin	Echo-based LVMI data
Esposito et al., 2002[417]	Dbh$^{-/-}$	≈50%	Catecholamines	Prolonged survival, preserved LV function.
Rapacciuolo et al., 2001[416]	Dbh$^{-/-}$	60%	Catecholamines	
Rogers et al., 1999[174]	RGS4	50%	G-protein signalling	Rapid decompensation and death
Bueno et al., 2001[543]	MKP-1	90%	MAPK	Impaired developmental hypertrophy with mild LV dilatation
Uozumi et al., 2001[427]	gp130 dn	63%	CT-1/LIF/IL-6	

$^{-/-}$ homozygous null, CnAβ: calcimeurin A β, NFAT: nuclear factor of activated T cells, GSK-3β: glycogen synthase kinase, MCIP1: myocyte enriched calcineurin interacting protein , GαqI: inhibitory mutant of Gαq, Agtr2: angiotensin receptor type II, Dbh: dobutamine β-hydroxylase, RGS4, MKP-1: MAPK phosphatase, dn: dominant negative, AngII: angiotensin II, ET-1: endothelin I, catechols: catecholamines, MAPK: mitogen activated protein kinase, CT-1: cardiotrophin, LIF: leukaemia inhibitory factor, IL-6, interleukin 6, LVMI: left ventricular mass index, CnA*: activated calcineurin mutant.

1.7 Conclusions Regarding the Regulation of Cardiac Hypertrophy

It appears that many genes and signalling pathways have an essential role in LVH development. Since this applies to multiple pathways, it is difficult to reconcile the fact that many single genes can be both sufficient and necessary for LVH. First of all, careful scrutiny of papers reveals that few models are 100% resistant to LVH, and there is usually a relative reduction in LV mass. Secondly, supraphysiological stimulation of a pathway by transgenic methods may be sufficient to overwhelm counter-regulatory mechanisms, and therefore be sufficient to cause LVH alone, whilst in normal physiology the concerted activation of several pathways may be necessary to achieve the same effect. In other words, multiple signalling pathways may have a co-operative or permissive effect on each other. If this is the case, it would explain why targeted deletion of one gene may have a profound disabling effect on the hypertrophic response.

Finally, the responses of individual models may be misleading, particularly where only one hypertrophic stimulus has been examined. For instance, MEKK1$^{-/-}$ mice are susceptible to LVH induced by aortic constriction,[558] but not Gαq overexpression.[541] Similarly gp130$^{-/-}$ mice develop cardiac failure after aortic banding,[173] but mice expressing a dominant negative inhibitor of gp130 have attenuated hypertrophic responses without development of failure.[427] This implies that different hypertrophic stimuli require different signalling pathways and that similar mouse models may not be equivalent.

1.8 Prorenin (ren2)-Dependent Models of Hypertension and Cardiac Hypertrophy

Several transgenic models of hypertension exist that rely on overexpression of mouse prorenin ($ren2^d$). Some of these form an integral part of this thesis, and are therefore described in detail. Other transgenic models of hypertension based on renin-angiotensinogen transgenes have been described, but are not discussed here.[559-561]

1.8.1 TGRmRen2-27

TGRmRen2-27 is the prototypical transgenic rat model of hypertension. The transgene comprises mouse DBA/2J ren2 genomic DNA, including flanking regulatory elements.[562] It is characterised by severe hypertension developing within weeks of weaning, but the precise phenotype is strongly influenced by gender, zygosity, and background strain.[563-565]

Although the genetic basis of hypertension in this model is well defined, the precise mechanism is not. Early studies demonstrated elevated plasma prorenin levels, reduced active renin and angiotensin II, with suppression of hypertension by angiotensin-converting enzyme inhibition.[562] Transgene expression is predominantly adrenal,[562,566] though this is probably not relevant to the development of hypertension.[567-569] More importantly, tissue angiotensin II levels are increased in a wide range of organs,[562,567,570] and expression in the vasculature and brain is also implicated in driving hypertension.[571-576] Development of lethal maligant hypertension in this model is strain-dependent,[563,564] and linkage studies have mapped the putative modifier loci to chromosomal regions close to ACE and At1 loci.[563]

Cardiac transgene expression is detectable, and may contribute to the development of left ventricular hypertrophy:[563,565] evidence of hypertrophy has been found as early as age 16 days, well before hypertension occurs.[362] Pharmacological and gene therapy data indicate that hypertrophy is driven by angiotensin II, independently of

hypertension.[362,577,578] However other studies support a prime role for hypertension in the development of LVH[579] and cardiac fibrosis.[580]

1.8.2 TGR α1ATren2

TGR α1ATren2 was generated by Dr D Ogg in the Mullins lab.[408] The transgene comprises the ren2^{d} cDNA under the transcriptional control of the human alpha-1-antitrypsin promoter, directing expression to the liver. The line is maintained on an inbred F344 background. TGRα1ATren2 was developed to investigate the dependence of hypertension in TGRmren2-27 on the site of ren2^{d} expression. Of 16 TGRα1ATren2 founders, 9 demonstrated evidence of hypertension, which in some was rapidly lethal without angiotensin-converting enzyme inhibition. Only one line, TG 12, has been maintained. Analysis of this line demonstrated that transgene expression, by radionucleotide protection assay was exclusively hepatic. Transgene-derived plasma prorenin levels are in 10-fold excess at 4 weeks of age, rising to 400-fold by 5 weeks, without excess plasma renin, angI or angII. Prorenin levels were higher in males than females. TG12 males demonstrated impaired growth compared to non-transgenic littermates, and died with 100% penetrance by 7 weeks of age. SBP measured by tail cuff plethysmography in lightly anaesthetised male animals was elevated at 4 weeks, and continued to rise to 7 weeks, reaching approximately 170mmHg.

Interestingly heart weight to body weight ratios were increased by 22% at 2 weeks of age, before significant hypertension had occurred, reaching 52% at 7 weeks. Histopathological analysis demonstrated cardiomyocyte hypertrophy and microscopic myocardial infarcts. In addition there was evidence of remodelling in interlobular arteries, glomerular ischaemia and occasional fibrinoid necrosis, consistent with malignant phase hypertension.

1.8.3 TGRcyp1a1ren2

The timing of malignant hypertension in TGRmRen2-27 is unpredictable, and can only be clinically identified at a late stage. Therefore to develop a controlled model of

malignant phase hypertension a conditional transgenic strategy was adopted, in which a ren2^{d} cDNA transgene was placed under the regulatory control of the promoter of cytochrome p450 cyp1a1.[581] This promoter is intrinsically inactive,[582] but transcription can be induced by arylhydrocarbon compounds (AHC) in the presence of the arylhydrocarbon receptor (AHR) and the aryl hydrocarbon nuclear translocator (arnt), which form a heterodimer-ligand transcription complex.[582-586] Therefore, in the absence of AHC the cyp1a1ren2 transgene is not expressed, whilst administration of AHC to TGRcyp1a1ren2 rats induces transgene expression. Transgene expression is predominantly in the liver, but also in the spleen.[587] More widespread expression has been described using this promoter, reflecting the tissue distribution of AHR and Arnt.[588-590] Background expression levels are undetectable in non-induced rats.[581] Blood pressure is dose-dependent and, in short term studies reversible, making this an extremely flexible model for studying hypertension, vascular injury and repair.[581]

Indole-3-carbinol (I3C) is a naturally occurring AHC found in brassicae. I3C itself is a weak inducer of cyp1a1 but derivatives formed in the stomach are much more potent: up to 24 different active metabolites have been found in rats fed I3C.[591] Since it is readily absorbed and metabolised, induction of cyp1a1 occurs within hours.[591] It also induces other members of the aryl hydrocarbon battery including CYP1A2, CYP2B1/2 and CYP3A1/2, and inhibits both the activity and expression of flavin monooxygenase 1:[592] thus, metabolism of other xenobiotics is undoubtedly affected and this may interfere with pharmacological studies.

0.3%(w/w) I3C reproducibly induces malignant phase hypertension in TGRcyp1a1ren2 over a 14 day period.[581] Severe hypertension is induced by 7 days of induction, and this is sustained until day 14. It is accompanied by a more than 200-fold increase in plasma prorenin level, whilst plasma renin, angiotensin II and aldosterone rise only slightly. A key finding of recent studies using this model is that an organ specific pattern of vascular susceptibility to endothelial damage and fibrinoid necrosis appears to be present. Fibrinoid necrosis is first identifiable in the vasculature of the heart and

mesentery on day seven of induction. On day 14 the renal vasculature succumbs to malignant injury, but the brain appears to be protected. The exact reasons for this phenomenon are not known, but may relate to the ability of the kidneys and brain to autoregulate perfusion pressure in the face of severe hypertension.

Peters et al., (2002)[407] have presented data to support the hypothesis that transgene-derived prorenin (ren2) is taken up by the heart and activated to renin in this model. This is also likely to contribute to pathogenesis of vascular damage and cardac hypertrophy.

1.9 Aims

This thesis concentrates on the mechanisms of LVH in transgenic rats conditionally overexpressing mouse ren2^{d} (TGRcyp1a1ren2). Earlier work in this model has demonstrated that 0.3% I3C (w/w) causes malignant hypertension over 14 days, with evidence of transgene-derived ren-2 uptake in cardiac tissue.[407,581] However the severity of hypertension in response to this dose of inducing agent limits the usefulness of the model for studies of cardiac hypertrophy. Chapter 3 describes experiments that characterise the development of cardiac hypertrophy in response to a lower dose of inducing agent, to determine if this represents a valid model of pressure overload cardiac hypertrophy. Given the variability of cardiac functional changes in different models of LVH we also measured the functional consequences of LVH at serial time points. In particular it was of interest to establish if chronic pressure overload led to heart failure or other adverse consequence of LVH such as arrhythmia.

Previous discussion has highlighted that inhibition of LVH by disruption of calcineurin signalling can abrogate progression to heart failure. We hypothesised that pressure-independent inhibition of cardiac hypertrophy in TGRcyp1a1ren2 by the calcineurin inhibitor FK506 would lead to compensatory changes in cardiac function that negate the negative effect of increased wall stress. These experiments are documented in chapter 4.

Overexpression of mouse ren2^{d} in rats is a potent stimulus for hypertension and cardiac hypertrophy, yet there are no known extra-renal sites for activation of prorenin to renin, suggesting that the mechanism by which ren2 exerts its effects is novel. Substantial evidence has accumulated to support the uptake of physiologically relevant quantities of human renin/prorenin by cardiomyocytes via the mannose-6 phosphate receptor, but this mechanism could not explain the uptake of non-glycosylated mouse prorenin-2 seen TGRcyp1a1ren2. Therefore we hypothesised that a mechanism distinct from the mannose-6 phosphate pathway mediates prorenin uptake. Chapter 5 describes the production of recombinant mouse ren2^{d} in a baculovirus expression system for investigation of renin uptake by cardiomyocytes.

Chapter 2

Materials and Methods

2.1 Materials

2.1.1 Chemicals and Solutions

Analytical grade chemicals, solvents, acids and alcohols were obtained from Sigma (Sigma-Aldrich Ltd, Poole, Dorset, UK) or BDH Laboratory Supplies (Poole, Dorset, UK), unless otherwise stated. Phenol was obtained redistilled, and buffered with Tris-HCL from BDH. Agarose was supplied by FMC Bioproducts (Flowgen, Sittingbourne, UK). Acrylamide monomer solution was supplied by National Diagnostics (Atlanta, Florida, USA). Radioisotopes were supplied by Amersham Pharmacia Biotech (Little Chalfont, UK). Oligodeoxynucleotide primers were synthesised by MWG Biotech (Ebersberg, Germany). Kodak XOMAT XAR-5 film was supplied by BDH. Kits for DNA plasmid Maxi preparation and RNA isolation (RNAeasy) were obtained from Qiagen (Crawley, UK).

All solutions were prepared with Milli-Q synthesis water (Millipore, Molsheim, France) and, where appropriate were autoclaved prior to use. RNAse free water (BDH) was used for RNA work.

2.1.2 Enzymes

Restriction endonucleases were supplied by Roche (Roche Diagnostics GmbH, Mannheim, Germany), Promega (Southampton, UK) or New England Biolabs (Hitchin, UK) and used according to manufacturer's recommendations. *Pfu* DNA polymerase was purchased from Stratagene (Amsterdam, Netherlands) and Taq polymerase was supplied by Qiagen. Superscript II reverse transcriptase was supplied by Invitrogen (Paisley, UK). DNase-free RNase A and proteinase K were supplied by Sigma.

2.1.3 Bacterial Strains

Escherichia coli (E. coli) strains TOP 10 One Shot and PIR1 were supplied by Invitrogen (Paisley, UK).

2.1.4 Antibiotics

Antibiotics were purchased from Sigma and used as indicated in table 2.2.

Table 2.2 Antibiotic Selection Concentrations

Antibiotic	Selection of plasmids	Stock solution
Ampicillin	100µg/ml	100mg/ml in dH_2O
Kanamycin	25 µg/ml	25mg/ml in dH_2O

2.1.5 Antibodies

Antibodies were used for Western blotting, immunoprecipitation and immunaffinity purification were supplied and used at the optimised dilutions, as indicated in table 2.3.

Table 2.3 Antibodies and Dilutions

Antibody	Type	Clonal Designation	Working dilution	Application	Supplier
αHA	MM	F-7	1:1000	WB	Santa Cruz SC-7392
αHA	MM	F-7	-	IP (agarose-conjugated)	Santa Cruz SC-7392AC
αHA	RM	3F10	-	IA (resin)	Roche 1815016
αrenin	RP	-	1:10000	WB	-
αR-hrp	GP	-	1:2000	WB	Dako P0448
αM-hrp	RP	-	1:1000	WB	SBST

MM: Mouse monoclonal, RM: rat monoclonal, hrp: horseradish peroxidase conjugated. αR: anti-rabbit Ig, αM: anti-mouse Ig, GP: goat polyclonal, RP, rabbit polyclonal, SBST: Scottish Blood Transfusion Service, IA: immunoaffinity, IP: immunoprecipitation, WB: Western blotting.

2.1.6 Reagents and Chemicals

Table 2.4 Common Reagents and Buffers

Reagent or Buffer	Composition	Comments
Alkaline lysis P1 Buffer	50mMTris, 10mM Na_2 EDTA, RNAse A 100mg/ml, pH8.0	Plasmid DNA miniprep
Alkaline lysis P2 Buffer	0.2M NaOH, 1% SDS	Plasmid DNA miniprep
Alkaline lysis P3 Buffer	5.0M Potassium Acetate, adjusted to pH5.5 with glacial acetic acid.	Plasmid DNA miniprep
Ampicillin LB Plates	LB agar, 100mg/ml Ampicillin	Selective E. coli growth plate
100x Denhardt's Solution	2% (w/v) Ficoll 400 (Pharmacia), 2% (w/v), Bovine serum albumin (Fraction V, Sigma), 2% (w/v) polyvinyl-pyrrolidone	Constituent of Southern blotting hybridisation solution
DNA Loading Buffer (6x)	0.25% Bromophenol Blue, 0.25% Xylene Cyanol FF, 30% Glycerol	DNA gel electrophoresis
Ethidium Bromide Stock	10mg/ml Ethidium Bromide	DNA gel electrophoresis
GYT Medium	10% (v/v) Glycerol, 0.125% yeast extract, 0.25% (w/v) tryptone	E. coli growth and storage Medium
Heparin (unfractionated)	20U/ml final concentration in whole blood	Plasma for electrolyte measurment
Immobilsed metal affinity chromatography (IMAC) resin	Talon resin (Nickel) (Clontech)	IMAC
IMAC wash buffer (1x)	50mM Na Phosphate 300mM NaCl	IMAC
IMAC elution buffer (1x)	50mM Na Phosphate 300mM NaCl 150mM Imidazole (Clontech)	IMAC
Immunoaffinity Lysis Buffer	50mM Tris pH7.5, 150mM NaCl 0.1% Nonidet P40, Complete Protease Inhibitor Cocktail (Roche)	Lysis buffer compatible with immunoaffinity column
Immunoaffinity Equilibration Buffer	20mM Tris pH7.5, 0.1M NaCl, 0.1mM EDTA	Immunoaffinity column buffer

Table 2.4 (continued)

Immunoaffinity Wash Buffer	20mM Tris pH7.5, 0.1M NaCl, 0.1mM EDTA, 0.05% Tween-20	Immunoaffinity column wash buffer
Immunoaffinity Elution Buffer	1 mg/ml HA peptide reconstituted in equilibration buffer.	Elution of HA-tagged protein from HA-immunaffinity column
Immunoaffinity Column Storage Buffer	20mM Tris pH7.5, 0.1M NaCl, 0.1mM EDTA, 0.09% sodium azide	Prevention of fungal growth
Immunoaffinity Column Regeneration Buffer	0.1M glycine pH2.0	Removal of HA peptide from immunoaffinity column
Immunoprecipitation Lysis Buffer	1% (w/v) Triton X-100, 50mM Tris.Cl pH 7.4, 300mM Na Cl, 5mM EDTA, 0.02% (w/v) Sodium Azide, 10mM iodoacetamide, 1mM PMSF 2mg/ml Leupeptin	Immunoprecipitation
Immunoprecipitation Wash Buffer	0.1% (w/v) Triton X-100, 50mM Tris.Cl pH7.4, 300mM NaCl, 5mM EDTA, 0.02% sodium azide	Immunoprecipitation
Ion Exchange Lysis Buffer	20mM Tris pH7.5, 150mM NaCl, 2mM EDTA, 1% Triton X-100	Insect cell lysis buffer for recombinant protein purification
Ion Exchange Buffer A	50mM Tris pH7.5: filtered (0.22µm) and degassed.	Ion exchange column wash buffer
Ion Exchange Buffer B	50mM Tris pH7.5, 1M NaCl: filtered (0.22µm) and degassed.	Ion exchange elution buffer
2xLaemmli Buffer	0.125M Tris-Cl pH6.8, 4% SDS, 20%v/v Glycerol, 0.2M DTT, 0.02% Bromophenol Blue	Protein loading buffer for SDS-PAGE
LB (Luria-Bertani) Medium	1.0% Tryptone, 0.5% Yeast Extract, 1.0% NaCl, pH7.0	E. coli growth medium

Table 2.4 (continued)

LB Plates	LB medium, 1.5% agar	E. coli growth plate
Plasma	6.25mM EDTA	Plasma collection for renin and prorenin samples (final concentration in whole blood)
Plasma inhibitor mix	6.25mM EDTA pH8.0, 0.625mg/ml 1,10-Ω-phenanthraline, 1.0 mg/ml pepstatin A, 14.33mM β-mercaptoethanol, 4.0 mg/ml captopril, 0.1 mM PMSF	Plasma inhibitor cocktail for angiotensin samples (final concentrations in whole blood)
Protein Extraction Buffer (Animal Tissues)	150mM NaCl, 0.25% Na deoxycholic acid, 1% NP40 1mM Na_3VO_4, 1mM NaF 1mM EDTA, 1mM PMSF, 1mg/ml aprotinin, 1mg/ml pepstatin A, 1mg/ml leupeptin	Tissue lysis buffer for protein analysis
Protein Extraction Buffer (Sf9 cells)	250mM Na Phosphate, 1.5M NaCl, EDTA-free Mini-Protease Inihibitor (Roche), 100mg/ml PMSF, pH 7.0	Lysis buffer for Sf9 cells
SDS-PAGE Tank Buffer	0.025M Tris pH8.3, 0.192M Glycine, 0.1% SDS	Protein electrophoresis
SDS-PAGE 4X Running Gel Buffer	1.5M Tris-Cl pH8.8	Protein electrophoresis
SDS-PAGE 4x Stacking Gel Buffer	0.5M Tris-Cl pH6.8	Protein electrophoresis
SDS-PAGE Water Saturated Butanol	50 ml n-butanol, 5 ml deionised water	Protein electrophoresis
SDS-PAGE Acrylamide Monomer solution (National Diagnostics)	30%(w/v) acrylamide: 0.8% (w/v) bis-acrylamide stock solution, 37.5:1	Protein electrophoresis

Table 2.4 (continued)

SDS-PAGE 10xTris Buffered Saline	0.2M Tris-Cl pH 7.4 1.5M NaCl	Protein electrophoresis
Silver staining fixative solution	50% (v/v) Methanol, 10% (v/v) Acetic acid, 10% (v/v) Fixative enhancer concentrate (Biorad), 30% (v/v) ddH_2O	Protein detection after polyacrylamide gel electrophoresis
Silver staining and development solution (Biorad)	50% (v/v) Development accelerator solution, 5% (v/v) Silver complex solution, 5% (v/v) Reduction moderator solution, 5% (v/v) Image development reagent, 35% (v/v) ddH_2O	Protein detection after polyacrylamide gel electrophoresis
SOB Medium	2% (w/v) Tryptone, 0.5% (w/v) Yeast extract, 0.05% (w/v) NaCl, 2.5 mM KCl, pH 7.0 adjusted with 5N NaOH. $MgCl_2$ added to final concentration of 10mM before use.	SOC precursor
SOC Medium	SOC + 20mM Glucose	E. coli recovery medium following electroporation
Southern blotting denaturing solution	0.5M NaOH, 1.5M NaCl	DNA gel denaturation
Southern blotting acid hydrolysis solution	0.125M HCl	DNA blotting
Southern blotting hybridisation Buffer	5x SSC, 5x Denhardt's, 0.5% SDS	DNA blotting
Southern blotting neutralising Solution	1.5M Tris-Cl, 1.5M NaCl, 1mM EDTA, pH7.2	DNA blotting
Southern hybridisation wash solution	2xSSC/ 0.1%SDS	Standard stringency wash solution for Southern hybridisation
Southern hybridisation stripping solution	1% (w/v) SDS, 0.1xSSC, 40mM Tris, pH 7.6	Probe removal from Southern blots

Table 2.4 (continued)

20xSSC	3M NaCl, 0.3M Na Citrate, pH 7.0	DNA transfer buffer in Southern blotting
0.8% 1xTAE Agarose Gel	Agarose 3.2g , ddH_2O 392ml, 50xTAE 8ml, Ethidium bromide stock 20µl	DNA electrophoresis
50xTAE	2M Tris, 0.87M Acetic Acid, 0.05M Na_2 EDTA pH8	DNA electreophoresis buffer
Tail Digestion Buffer	50mM Tris HCl pH8.0, 0.1M EDTA, 0.1M NaCl, 1% SDS	Buffer for isolation of genomic DNA from rat tail biopsy
TE	10mM Tris pH8.0, 1mM EDTA pH8	DNA buffer
Tris Buffered Saline (TBS) x 10	0.2M Tris base, 1.5M NaCl, pH 7.4	Protein buffer
Western Blotting Blocking Solution	5% non-fat milk powder, 1xTBS, 0.1% Tween 20	Protein blotting
Western Blotting Transfer Buffer (Towbin)	0.0479M Tris, 0.0384M Glycine, 0.037% SDS, 20% Methanol	Protein blotting
Western Blotting Incubation/Wash Buffer	1xTBS, 0.1% Tween-20	Protein blotting
Western blotting stripping solution	100mMβ-mercaptoethanol, 2% SDS, 62.5mM Tris-HCl pH6.7	Antibody stripping

2.1.7 Cloning Vectors

Plasmids puniV5HisTOPO® and pBlueBac4.5E were supplied by Invitrogen whilst pGEM T-Easy was from Promega.

2.1.8 Tissue Culture

Tissue culture plastic was supplied by Iwaki (Aberbargoed, Mid-Glamorgan, UK) and Corning (Jencons, UK). Low passage Sf9 cells (clonal isolate of IPLBSF21-AE) were obtained from Invitrogen. All media were obtained from Gibco (Paisley UK). Cells were

cultured in Grace's Insect Medium (supplemented with yeastolate, lactalbumin hydrolysate and glutamine) (TNM-FH) with 10% insect qualified Foetal Calf Serum (FCS) (Gibco), Gentamicin 10μg/ml (Sigma) and 1% Pluronic F-68 (Gibco). Washes were performed with Grace's Insect Medium (without supplements). DMSO was supplied by Sigma.

Sf9 monolayers were maintained in a humidified environment of filtered air at 27°C in a Hera Cell Incubator (Heraeus Instruments GmbH, Hanau, Germany). Manipulations were carried out in a laminar flow hood (Jouan, France). All surfaces were cleansed with 70% (v/v) ethanol prior to use. Sf9 suspension cultures were carried out in 500ml Erlenmeyer flasks (Corning) using a digitally controlled shaker (Ika Werke, KS 130) in a cooled incubator at 27°C (LTE Scientific). SeaPlaque GTG Agarose (FMC Bioproducts) was used for baculoviral plaque assays.

2.1.9 Animals

All animal experiments were carried out in accordance with the Animal (Scientific Procedures) Act 1986 at the Biomedical Resource Facility, University of Edinburgh. Transgenic rats were bred in-house in individually ventilated cages (IVC) to specific pathogen free standards, and transferred to standard cages at weaning. Control Fischer F344 males were obtained from Harlan (Bicester, Oxon, UK) at 10 – 12 weeks of age. Ambient temperature was maintained between 18 and 22°C with 45-55% humidity, on a 12 hour light-dark cycle (07.00am – 07.00pm). Rats were fed standard rat chow (Special Diet Services, Witham, Essex) containing 0.32% NaCl, in either pellet or powder form. Free access to food and water was allowed at all times. Rats were housed in groups of 2-6 animals, except during telemetry experiments when they were housed individually. Only male rats were studied.

2.1.9.1 TGRcyp1a1ren2

In-bred TGRcyp1a1ren2 on a Fischer F344 background were studied from around 12 weeks of age (weighing 200-300g). Hypertension was induced using indole-3 carbinol

(Sigma) in powdered standard rat chow (Special Diet Services, Witham, Essex, UK), at either 0.15% or 0.3% (w/w). Age and weight matched Fischer F344 male rats were used as control animals and were fed an identical diet.

2.1.9.2 TGRα1ATren2

TGRα1ATren2 were on an in-bred Fischer F344 background as heterozygotes. Litters were bred from transgenic females maintained on captopril (10mg/kg) in drinking water. At weaning males were selected and maintained on normal drinking water. Tail biopsies were only taken after death in study animals to avoid the effects of tail trauma on tail cuff plethysmography. Experiments were therefore performed blinded to the genotype of animals.

2.1.10 Drugs and Anaesthetics

Table 2.5 Drugs and Anaesthetics

Drug	Dose	Supplier	Comments
Amiodarone	1 mg/ml in drinking water	Sanofi-Synthelabo	Antiarrhythmic
Captopril	10mg/kg, administered in drinking water at 0.5mg/ml	Sigma	ACE inhibitor
FK506	1mg/kg intraperitoneal in suspension in ddH_2O, daily	Fujisawa	Calcineurin inhibitor, immunosuppressant
Halothane	1-5% in Oxygen.	Merial	Gaseous anaesthetic
Indole-3 carbinol	0.3 or 0.15% (w/w) in powdered diet	Sigma	Aryl hydrocarbon
Ketamine	100mg/kg intraperitoneal	Pharmacia-UpJohn	Injectable anaesthetic used in combination with xylazine.
Nifedipine	0.5% (w/w) in powdered diet	Sigma	Dihydropyridine calcium channel blocker
Xylazine	5mg/kg intraperitoneal	Bayer	See ketamine

2.1.11 Animal Physiology

All radiotelemetry equipment was supplied by Data Sciences International (St Paul, MN, USA). TL11M2-PXT radiotelemetry devices were used and radiotelemetry signals were received using PhysioTel RPC-1 receiver plates and stored on a personal computer. Data was analysed using Dataquest ART 2.1 and Physiostat ECG 3.1 software. Animals were housed on a custom-built rack in indiviual cages separated by aluminium shields.

Tail cuff plethysmographic blood pressure was measured using a photometric cuff (Harvard Instruments, USA) and a customised computer detection system.

Echocardiographic studies were performed using a custom-built digital echocardiography machine with a 16MHz linear array probe at 300 frames per second with 2 focus lines (Dynamic Imaging, Livingston UK). Analysis was performed using a custom designed image analysis programme (Image Analyser). Doppler studies were performed using a VingMed Vivid 5 (General Electric) digital echocardiography machine with a 10 MHz probe at 196 frames per second using a single focus line. Analysis was performed off-line using the Echopac digital analysis programme (VingMed, General Electric).

A 2F high fidelity micromanometer catheter (Millar, Texas, USA) was used to measure left ventricular pressures. Data was acquired using a PowerLab 4_{SP} acquisition system (ADInstruments Ltd, Chalgrove, UK) and analysed using Chart v5.0.1 (ADInstruments).

2.2 Methods

General methods of nucleic acid manipulation were as described in Sambrook et al. (1989)[593] and Ausubel et al. (2003).[594] Restriction endonucleases and other DNA modifying enzymes were used according to the manufacturers' instructions. Protein methods of were as described in Coligan et al. (2001),[595] whilst insect cell culture and baculoviral methods were as described by the supplier.[596,597]

2.2.1 Plasmid DNA Preparation

2.2.1.1Alkaline Lysis Miniprep

Small-scale preparations of plasmid DNA for screening purposes were performed by a modification of the method of Birnboim and Doly.[598] Single bacterial colonies were picked using aseptic technique and transferred to 50ml sterile tubes (Corning) containing 3-5 ml of LB and appropriate antibiotic. These were cultured overnight at 37°C and shaken at 225rpm (Innova 4000 Incubator Shaker, New Brunswick Scientific). 1 ml of bacterial culture was removed and centrifuged at 13000rpm for 30 seconds (Biofuge Pico, Heraeus). The supernatant was removed and the bacterial pellet resuspended in 100 ml of ice-cold P1 buffer, vortexed for 10 seconds and allowed to stand on ice for 5 minutes.

200 ml of P2 buffer was added, and the tube inverted 6 times to ensure complete mixing. After no more than 5 minutes 150 ml of ice cold P3 was added and the tube inverted 6 times again. Cell debris was removed by centrifugation at 13000 rpm for 5 minutes. The supernatant was transferred to a fresh tube and 0.7 volumes of isopropanol added to precipitate DNA. DNA was recovered by centrifugation at 13000 rpm for 5 minutes. The supernatant was discarded, and the pellet washed twice with 70% ethanol. After allowing the pellet to air dry it was resuspended in 50 ml of TE containing RNAse (20mg/ml) and stored at -20°C.

2.2.1.2 DNA Maxi-Preps

Large-scale plasmid preparation was carried out using Qiagen Maxi-prep kit, according to the protocol for high copy plasmids. 3ml pre-cultures containing appropriate antibiotic were inoculated with single bacterial colonies and incubated for 8 hours at 37°C/225rpm. Of this 0.1-0.2ml was transferred to a conical flask containing 500ml of LB/antibiotic and incubated overnight at 37°C/225rpm in an orbital shaker (Series 25 Incubator Shaker, New Brunswick Scientific). DNA was prepared according to the manufacturer's instructions.

2.2.2 Genomic DNA Preparation From Tail Biopsy

1cm of tail tip was cut from rats at weaning (day 21) and frozen at –20°C until analysed. Tissue was digested for 8-16 hours in 600µl of tail buffer with 30µl proteinase K (10mg/ml) at 55°C whilst rotated gently in a hybridisation oven. 10µl of 10mg/ml DNase-free RNase A (Sigma) was added and incubated at 37°C for one hour.

Phenol-chloroform extraction was performed to remove contaminating protein: one volume of phenol (equilibrated with Tris HCl) was added with 37.5µl of 2M β-mercaptoethanol, and mixed for 15 minutes on a vertical rotator. Phases were separated by centrifugation at 13000rpm for 3 minutes. The upper aqueous phase was transferred to a fresh microcentrifuge tube using cell saver tips to avoid shearing the DNA. 0.5 volumes of phenol, and 0.5 volumes of chloroform/isoamyl alcohol (24:1) were added. After mixing for 5 minutes on a vertical rotator, the sample was centrifuged as before, and the aqueous phase transferred to another tube. One volume of chloroform/isoamyl alcohol was added, mixed by gentle rotation for 5 minutes and separated by centrifugation. The aqueous phase was removed and DNA precipitated by addition of one volume of isopropanol and mixing by inversion. The DNA was pelleted by centrifugation at 13000rpm for 3 minutes. The supernatant was discarded and the pellet dissolved in 200ml of TE at 4°C overnight, or at 37°C for 30 minutes. DNA was precipitated again with 0.5 volumes of 6M-ammonium acetate and 2 volumes of

isopropanol. The DNA was pelleted by centrifugation at 13000rpm for 3 minutes, and supernatant removed. Salt was removed from the pellet by washing with 70% ethanol and centrifugation. This was repeated and the pellet air-dried at room temperature. Once the DNA was opaque 100ml of TE was added, and allowed to solubilise overnight at 4°C.

2.2.3 Agarose Gel Electrophoresis

Plasmid DNA molecules were separated on 1% (w/v) agarose gels (Seakem LE), whilist genomic DNA was separated on 0.8% (w/v) agarose gels. Gels were prepared using electrophoresis grade agarose in 1x TAE buffer with 0.5µg/ml ethidium bromide. Electrophoresis was performed using Flowgen electrophoresis apparatus (Ashby de-la Zouch, UK) and an Electrophoresis Power Supply EPS-301 (Amersham Pharmacia Biotech) in 1x TAE at 1-3 V/cm. Samples were run in conjunction with standard size markers, usually Hind III digested lambda phage DNA. (Promega). Electrophoresed DNA was visualised under UV light (302 nm, UVP Transilluminator TM36, UVP Inc, San Gabriel, California, USA) and photographed with Kodak EDAS 290 digital camera system (Eastman Kodak Company, Rochester, New York, USA) with Kodak 1D 3.5.3-USB Scientific Imaging System software.

2.2.4 Quantitation of Nucleic Acids

DNA and RNA were quantitated by spectrophotometric analysis at wavelengths of 260nm and 280nm (UV 1201, Shimadzu) in a quartz cuvette. Plasmid preparations were diluted at 1 in 200 in TE to a final volume of 200µl. A TE blank was used to zero readings, and the cuvette was rinsed with ddH_2O between measurements. DNA concentration was automatically calculated from the A260 reading by the spectrophotometer. RNA concentration was calculated on the basis that 40µg/µl RNA gives an A260 reading of 1.0. DNA/RNA purity was estimated by the A260:A280 ratio. At pH 7.5 pure RNA has a ratio of 1.9-2.1, whilst DNA has a ratio of 1.7-1.9.

2.2.5 Gel Purification of DNA Fragments

DNA was electrophoresed, then visualised under UV light for the minimal time possible to allow appropriate bands to be cut from the gel using a clean razor blade. DNA was extracted using Qiagen Qiaquick Gel Extraction Kit according to the manufacturer's instructions. Purified DNA was eluted using 10mM Tris pH8.0.

2.2.6 DNA Precipitation

DNA was precipitated from solution by addition of 0.1 volume of 3M sodium acetate and 2.5 volumes of 100% ethanol. The solution was mixed well by tube inversion 10-12 times, stored at –20°C for 30 minutes, then pelleted by microcentrifugation at 13,000rpm for 10 minutes. Pellets were washed with 70% ethanol and respun for 5 minutes. Ethanol was aspirated by pipette and the pellet allowed to air-dry for 5 – 10 minutes before resuspension in TE. tRNA (1µg) was added to the initial sample if small yields of DNA were anticipated to aid visualisation of the pellet.

2.2.7 Restriction Digestion of DNA

In general DNA was digested using restriction endonucleases supplied by Roche or Promega, with supplied buffers and BSA (0.1mg/ml) where appropriate. DNA was digested at a concentration of 0.1-0.5 µg/µl with less than 10% (v/v) enzyme. Digestions were performed at 37°C for 8-16 hours, dependening on the quantity and type of DNA. Double digests were performed either in a single reaction with a compatible buffer, or else sequentially after precipitation and phenol-chloroform extraction of DNA.

2.2.8 TA Cloning of PCR Products

Two TA cloning vectors were used, puniV5HisTOPO® (Invitrogen) and pGEM T-Easy (Promega), depending on the application. Pfu generated PCR products were incubated with 1 unit of Taq at 72°C for 10 minutes to allow addition of 5' adenosines. It was not necessary to gel purify PCR products. Approximately 1µl of PCR product was incubated with 1 µl of vector in ligation buffer according to the manufacturers'

instructions. 2µl of ligation mix was used to transform TOP10 E.coli. Appropriate control reactions were performed.

2.2.9 Preparation of Electrocompetent *E. coli*

10ml cultures of *E.coli* without antibiotic selection were grown overnight. A new 100 –500ml culture was set up, using the overnight culture diluted 1:1000. Bacterial growth was monitored intermittently by measuring the OD_{600}. At mid-log phase (OD_{600} 0.6) cells were chilled on ice for 15 minutes harvested, then centrifuged for 10 minutes at 4°C at 2500 g in a bench top centrifuge (Megafuge 3.0R Heaeus) in prechilled 50ml Corning tubes. The supernatant was removed and the cell pellet resuspended in 1 volume of ice-cold ddH_2O (Milli-Q quality) by vortexing. Centrifugation and resuspension were repeated once more. After this, cells were resuspended in 0.2 volumes of ice-cold GYT. Cells were again centrifuged for 10 minutes at 4°C at 2500 g, the supernatant discarded, and the pellet resuspended in the liquid remaining in the tube. This suspension was transferred to cold 1.5ml microcentrifuge tube and the volume made up to 1.5 ml with ice-cold GYT. This was centrifuged at 13000 g at 4°C, the supernatant removed and the pellet resuspended in 1 ml GYT. The suspension was divided into 50ml aliquots on ice and frozen immediately at –80°C. Competence was assessed by transfection of plasmid at limiting dilutions and counting the number of colonies formed.

2.2.10 Transformation of Electrocompetent *E. coli*

Electrocompetent bacteria were transfected using an Easyject Plus Electroporation System (Equibio, Broughton Monchelsea, UK) electroporation apparatus. 1-2 µl of plasmid DNA was added to a fresh 50µl aliquot of electrocompetent *E. coli* on ice, without mixing by pipette. This was transferred to a chilled 2mm electroporation cuvette and electroporated at 2300V and 25µF. Bacteria were immediately placed on ice, transferred to 200 µl of SOC at room temperature and incubated at 37°C/225rpm for 45 minutes. 20 - 50 µl of the culture was then plated out on antibiotic selection plates.

2.2.11 Cre recombination reactions

Homologous recombination between plasmid vectors containing lox P sites was carried out using Cre recombinase according to the supplier's instructions (Invitrogen).

2.2.12 DNA sequencing

Plasmid sequencing was performed by the Centre for Inflammation Research core facility using an ABI Prism 377 DNA sequencing machine (Applied Biosystems, Warrington, UK). 200 – 250ng of maxiprep DNA was used per reaction, with 3.2 pmol primer (0.8pmol/µl) and 8 µl of ABI BigDye Terminator Ready Mix (Applied Biosystems), in a total reaction volime of 20µl. PCR conditions were performed on a GeneAmp 9700 PCR machine (Applied Biosystems), under the conditions specified in table 2.6. Sequencing was performed according to the principle of the dideoxynucleoside chain termination reaction.[599]

Table 2.6 Sequencing PCR Conditions

Step	Conditions
1	Rapid thermal ramp to 96°C 96°C for 10 seconds Rapid thermal ramp to 50°C 50°C for 5 sec Rapid thermal ramp to 60°C 60°C for 4 min 25 cycles
2	Rapid thermal ramp to 4°C: held until ready to purify

DNA was precipitated and pelleted as described in section 2.2.6. Pellets were stored at –20°C until sequenced. Sequences were analysed using ABI EditView 1.0.1, ABI sequence editor (Applied Biosystems) and BLAST2 (www.ncbi.nlm.nih.gov).[600] Plasmid maps were constructed using Vector NTI (InforMax Inc, Bethesda, USA).

2.2.13 Polymerase Chain Reaction (PCR)

Polymerase chain reaction was carried out using a DNA Engine PTC-200 (MJ Reasearch). Primers were designed using Vector NTI software, and annealing

temperatures were calculated from the melting temperature (T_m) of a primer pair. In general a T_m between 55°C and 65°C was acceptable. Typical reaction conditions for Taq and Pfu are indicated in table 2.7. Variation from these conditions is indicated in the text. Optimum reaction conditions were found empirically by varying the Mg^{2+} concentration (usually 1.5 mM), and using a temperature gradient. Typically reactions were carried out in 20µl with 500mM dNTP, 0.375 mM primers, 5 U enzyme. A 50:50 mixture of Taq/Pfu was used.

Table 2.7 PCR Conditions for Taq and Pfu Polymerase

Step	Conditions for Taq	Conditions for *Pfu*/Taq
1	Rapid thermal ramp to 94°C and hold for 2 minutes	Rapid thermal ramp to 94°C and hold for 2 minutes
2	Rapid thermal ramp to 94°C 94°C for 10 sec Rapid thermal ramp to 55°C 55°C for 30 sec Rapid thermal ramp to 68°C 68°C for 1 minute/kb (25 – 30 cycles)	Rapid thermal ramp to 94°C 94°C for 50 sec Rapid thermal ramp to 55°C 55°C for 50 sec Rapid thermal ramp to 68°C 68°C for 2 minute/kb (25 cycles)
3	68°C for 10 minutes	68°C for 15 minutes
4	Rapid thermal ramp to 4°C and hold	Rapid thermal ramp to 4°C and hold

2.2.14 Reverse Transcription-PCR (RT-PCR)

Reverse transcription from RNA was carried out using Superscript II RNAse H^- reverse transcriptase (Invitrogen) according to the manufacturer's protocol for random octamer primers.

2.2.15 Southern Blotting

5-10µg of genomic DNA was digested overnight with an appropriate restriction enzyme at 37°C, and electrophoresed in a 0.8% agarose gel in 1xTAE overnight. Samples were always included from known transgene positive and negative animals. Gels were photographed under UV light with a transparent ruler to allow band size to be determined. Capillary transfer was used to transfer nucleic acid to nitrocellulose

membrane, based on the method of Southern (1975).[601] Briefly, gels were then depurinated in acid hydrolysis solution for 10 minutes with constant rocking. After washing in ddH_2O, the gel was treated with denaturing solution for 30 minutes, rinsed in ddH_2O and then treated with neutralising solution twice, each for 20 minutes. The gel was placed on 3MM Whatman paper presoaked in 20x SSC, on a standard blotting apparatus. The gel was covered by a piece of nylon-supported nitrocellulose membrane (Schleicher and Schuell) presoaked in 10x SSC, and 2 sheets of 3MM paper soaked in 20x SSC. DNA was allowed to transfer overnight using a paper towel stack as a wick. The membrane was baked for two hours at 80°C between Whatmann 3M paper and stored at room temperature until required.

2.2.16 DNA hybridisation Probe Radiolabelling

Random priming and incorporation of α^{32}P-dCTP was performed using the Ready-To-Go DNA labelling beads (Amersham Pharmacia Biotech) according to the manufacturer's instructions, based on the method of Feinberg and Vogelstein (1983).[602] Probes for genotyping TGRα1ATren2 were isolated from pBSα1ATren2 (JJM4) by sequential digestion with Sac1 and HindIII, which generated a 1.2kb fragment containing full-length $ren2^d$ cDNA. This was isolated by electrophoresis and gel purification.

2.2.17 Southern Hybridisation analysis

The nitrocellulose blot was rehydrated in 5xSSC at room temperature and prehybridised at 65°C for a minimum of 30 minutes. A radioactive probe was prepared, denatured at 100°C for 3 minutes and added to the prehybridisation buffer to achieve a final concentration of 2ng/ml. After a minimum of 16 hours hybridisation, the blot was washed three times with standard stringency Southern hybridisation wash solution prewarmed to 65°C. If excessive radioactive signal remained on the blot after the standard washes, further high stringency washes were carried out using 0.5x SSC, 0.1% SDS. After the final wash excess liquid was removed from the filter by placing it on 3MM paper. The filter was covered in Saran wrap, exposed to Kodak X-Omat AR film

in a film cassette with an intensifier screen at –80°C, and developed after 24 to 48 hours in a Konica SRX-101 Developer.

2.2.18 RNA Extraction

Total RNA was isolated from animal tissues using Qiagen RNeasy kits according to the manufacturer's instructions. Frozen tissues were rapidly weighed prior to homogenisation to ensure recommended buffer volumes were used. Tissues were maintained on dry ice until homogenised in buffer using an Ultra-Turrax T8 homgeniser (Ika Werke, Germany) in a 15ml Falcon tube. Between samples the homogeniser was cleaned with 3% hydrogen peroxide and two washes in ddH_2O. Homogenised heart tissue was diluted with two volumes of ddH_2O and incubated with proteinase K (0.65 mg/ml) at 55°C for 20 minutes to aid disruption and improve RNA yield. Bound RNA was eluted from the column with RNAse-free water and recovered by centrifugation.

RNA was DNAse-treated (Ambion) and then precipitated with 0.5 volumes of 7.5M ammonium acetate and 2.5 volumes of ethanol (-20°C). Samples were centrifuged at 13000 rpm for 20 minutes at room temperature. The supernatant was discarded, and the pellet of RNA washed twice in 80% ethanol (-20°C). After the final wash the pellet was air-dried and dissolved in RNAse free water. RNA integrity checked by 0.8% agarose gel electrophoresis. RNA was stored at –80°C until analysed.

2.2.19 Semiquantative Real-Time PCR

Real-time PCR was carried out using probes and primers developed with Primer Express 1.5 (Applied Biosystems) according to standard criteria recommended by the manufacturer. Primers were chosen that spanned intron-exon boundaries to increase specificity of amplification. Details of probes and primers are given in appendix A1. PCR reactions were performed and monitored using an ABI Prism 7000 Sequence Detection System (Applied Biosystems) according to the standard conditions recommended by the manufacturer (table 2.8).

Assays were set up in a class II tissue culture hood to avoid contamination. cDNA was prepared from total RNA as described in sections 2.2.14 and 2.2.18. RNA samples that had not been reverse transcribed were used as controls to detect genomic contamination. All reactions and controls were performed in thin walled 96 well optical plates (Applied Biosystems) sealed with optical covers (Applied Biosystems) in 19µl volumes.

Quantitation was normalised to 18S ribosomal RNA, and therefore every assay included standard curves for 18S ribosomal RNA and the gene of interest using a standard pool of reverse transcribed RNA (calibrator). The same reverse transcribed RNA pool was used for standard curves for all plates that were to be compared. Each experimental sample was analysed in triplicate for 18S ribosomal RNA, the gene of interest, as well and no reverse transcriptase control. In addition, a no template control was included on each plate for each gene.

Table 2.8. PCR conditions for real-time PCR

Step	Conditions
1	Rapid thermal ramp to 50°C and hold for 2 minutes
2	Rapid thermal ramp to 95°C and hold for 10 minutes
3	Rapid thermal ramp to 95°C 95°C for 15 sec Rapid thermal ramp to 60°C 60°C for 1 minute } 40 cycles
4 (SYBR green assays)	Slow thermal ramp to 90°C over 10 minutes

2.2.20 Protein Extraction

Animal tissues were kept frozen at –80°C until required for analysis. Tissues were homogenised in chilled protein extraction buffer using an Ultra-Turrax T8 (Ika Werke, Germany). Depending on the tissue, 1ml of buffer was used per 0.5g of tissue. Homogenates were kept on ice, and centrifuged at 1000rpm /4°C for 2 minutes to remove partially homogenised debris. Supernatants were stored at –80°C until analysed.

2.2.21 Determination of Protein Concentration

Protein concentration was determined using the bicinchonic acid method (BCA kit: Pierce) in 96 well format in duplicate, according to the manufacturer's instructions. Samples were incubated in the reaction mixture for 30 minutes at 37°C, cooled on ice and immediately analysed on a plate reader (MRX, Dynex Technologies) at 570nm. A standard curve was generated using a bovine serum albumin standard (Pierce), and protein concentration was derived from this. Samples were diluted to 1-4 mg/ml with extraction buffer, depending on the tissue and intended use.

2.2.22 SDS-Polyacrylamide Gel Electrophoresis (SDS-PAGE)

SDS-PAGE was performed using Mini-Protean apparatus (Bio-Rad). A 10% running gel was prepared and immediately poured between the gel plates, leaving approximately 3.0 cm clear from the top of the plates. This was immediately covered with water-saturated butan-1-ol: this was poured off once the gel had set. A 4% stacking gel was then poured on top and a gel comb placed between the plates and allowed to set. 10-50 ng protein samples (7.5 µl maximum) were denatured in 2xLaemmli buffer at 95°C for 3 minutes, snap cooled on ice and spun down. Samples and rainbow molecular weight marker (Amersham Pharmacia) were loaded in to wells and electrophoresed in tank buffer at 50mA (constant) for 60 to 90 minutes depending on the resolution required.

Table 2.9. 10% SDS-PAGE Running Gel Recipe

Constituent	Volume
30% acrylamide/bis-acrylamide (29:1)	3.35 ml
4x running gel buffer	2.5 ml
dH_2O	4.0 ml
20% SDS	50 µl
EDTA (100mM)	100 µl
10% ammonium persulphate	100 µl
TEMED	10 µl

Table 2.10. 4% SDS-PAGE Stacking Gel Recipe

Constituent	Volume
30% acrylamide/bis-acrylamide (29:1)	0.67 ml
4x running gel buffer	1.25 ml
dH_2O	2.95 ml
20% SDS	25 µl
EDTA (100mM)	50 µl
10% ammonium persulphate	50 µl
TEMED	5 µl

2.2.21 Western Blotting

Gels were separated from the gel plates and allowed to equilibrate with transfer buffer chilled at 4°C for 10 minutes. Proteins were transferred to Hybond-P membrane (Amersham Pharmacia) (presoaked in methanol, then transfer buffer) at 100V for 60 minutes using the Bio-Rad Trans-Blot Cell, and the quality of transfer was assessed by the intensity of rainbow marker.

2.2.22 Antibody Detection by Enhanced Chemiluminesence

Antibodies and their working concentrations are listed in table 2.3. Membranes were blocked in 5ml 5% non-fat milk in TBS/0.1%Tween 20 in a 50ml tube (Corning) for 1 hour 4°C. Membranes were then washed in TBS/Tween three times (20ml each) and incubated overnight at 4°C with primary antibody at the appropriate concentration in blocking solution. A further five washes in TBS/Tween (20ml each) were performed before incubation with horseradish peroxidase-conjugated secondary antibody in blocking solution for an hour at room temperature. A final series of five washes were performed before incubation in ECL+plus (Amersham Pharmacia Biotech) according to the manufacturer's instructions. Signal was detected with either Kodak X-Omat AR film, or using a phosphoimager (Storm 860) set to blue-yellow fluorescence. Bands were quantitated using ImageQuant 5.0 software (Storm).

2.2.23 Silver Staining

SDS-PAGE gels were silver stained using Silver Stain Plus (Bio-Rad) according to the manufacturer's instructions. Gels were soaked in ddH_2O prior to vacuum-drying at 80°C for 60 minutes.

2.2.24 Tissue Culture

Sf9 cells were grown in monolayer, or in suspension under the following conditions at 27°C in humdified air in an incubator (LTE), according to the supplier's recommendations and general references [596,597,603,604].

Table 2.11 Tissue Culture Conditions for Sf9 Cells

Type of culture	Medium	Special Conditions
Monolayer	TNM-FH + 10% (v/v) FCS	-
Suspension	TNM-FH + 10% (v/v) FCS + 0.1% (v/v) F68 Pluronic	130 rpm horizontal shaker 1.0 - 3.5 x 10^6 cells / ml

TNM-FH: trichoplusia ni medium – Hink formulation, FCS: foetal calf serum

2.2.25 Maintenance and Passage of Sf9 Cells

2.2.25.1 Monolayer Culture

At confluence medium was replaced with 4 ml of fresh warmed medium and cells were disrupted by "spritzing" with a sterile Pasteur pipette. Cells were split 1:4, or transferred to an 80cm^2 flask containing 12ml of TNM-FH. Cells were checked daily for growth and signs of infection. Typically Sf9 cells doubled over 18-24 hours.

2.2.25.2 Suspension Cell Culture

To initiate a 100ml suspension culture approximately 8 –10 80cm^2 monolayer cultures were required. Cells were passaged by spritzing and transferred to a disposable 500 ml Erlenmeyer flask. Cell density was estimated using an improved Neubauer Haemocytometer and trypan blue staining, to allow identification and exclusion of non-viable cells from the counts. Two counts were made for each sample and averaged. Cell

density was adjusted to 1.8 – 2.0x10^6/ml with TNM-FH/Pluronic medium. Cell viability and densities were checked daily. Under these conditions, the doubling time was 24-36 hours. Log phase growth was maintained by keeping the cell density between 1.0 and 3.5 x 10^6/ml. Suspension cultures could be maintained in a healthy state for more than a month. Every 4 weeks suspension cultures were centrifuged at 600g for 5 minutes and resuspended in fresh medium to remove cell debris.

2.2.26 Freezing and Thawing Sf9 Cells

Log phase early passage cells were spritzed and cell density counted. Cells were centrifuged at 400-600g for 10 minutes at room temperature and the supernatant removed. The cell pellet was resuspended in freezing medium (60% Grace's medium, 30% FCS, 10% DMSO) to achieve a density of 1x10^7 cells /ml and transferred to sterile cryovials. These were placed in an isopropanol filled freezing chamber and allowed to cool to –80°C at approximately 1°C per hour. After 5 days cryovials were transferred to liquid nitrogen. To initiate monolayer cultures from frozen stocks 1x10^7 log phase Sf9 cells were rapidly defrosted from liquid nitrogen storage and transferred to a 25cm^2 tissue culture flask containing 4 ml of TNM-FH warmed to 27°C. Cells were allowed to attach for 20 minutes after which the medium was changed to remove DMSO.

2.2.27 Baculoviral Transfection of Sf9 Cells

2x10^6 Sf9 cells were plated evenly in 60mm dishes in complete TNM-FH, and allowed to attach over 15 minutes. 4 µl of plasmid vector (1µg/µl) (pBlueBac) containing the gene of interest was mixed with 4 µl of Bsu 36 I deletant baculovirus (Invitrogen) in1ml of Grace's insect medium (without supplements or FCS) and 20µl of Lipofectin liposomes (Invitrogen). Control transfections of vector DNA or viral DNA alone were carried out. The mixture was vortexed for 10 seconds and incubated at room temperature for 15 minutes. Medium was removed from the plated cells and replaced with 2 ml of Grace's medium without supplements or FCS. This was removed and replaced with the transfection mixture by distributing drops evenly across the monolayer using a pipette. The plates were sealed in sterile plastic bags and rocked very gently (2 per minute) at

room temperature for 4 hours. 1ml of TNM-FH was added, the plate sealed again in plastic and the cells incubated at 27°C for 72 hours. At this time point cytotoxic effects could be observed within the monolayer, characterised by cell enlargement, granulation and lysis. Supernatant was harvested and stored at 4°C.

2.2.28 Baculoviral Plaque Assay

Dilutions of the transfection viral stock were made, ranging from 10^{-2} to 10^{-4}. Eight or more 100mm plates were seeded with $5x10^6$ cells to achieve 50% confluence: 2 plates were used for each dilution, and 2 plates were used for control. Cells were allowed to attach at room temperature over 30 minutes whilst being rocked gently to ensure even distribution. All but 2 ml of medium was removed and 1 ml of the appropriate viral dilution added by distributing drops over the entire monolayer. Plates were then sealed in plastic and incubated at room temperature for 1 hour with gentle rocking.

After one hour monolayers were covered in 10 ml agarose-TNM-FH mixture (5 ml 2.5% sterilised Seaplaque agarose at 47°C mixed with 5ml TNM-FH/X-gal (150mg/ml) at room temperature). The agarose mixture was added against the side of the dish under sterile conditions, and allowed to set at room temperature. Plates were sealed in plastic bags containing paper towels soaked in 5mM EDTA to maintain humidity and prevent fungal growth. These were incubated at 27°C for 5-6 days, and then inspected for recombinant plaques.

2.2.29 Isolation of Recombinant Plaques: Generation of P1 Stocks

Recombinant plaques were identified on the basis of blue-green colouration of agarose, which could be seen with the naked eye. At the microscopic level, plaques were characterised by a central area of cell clearing due to cell lysis and surrounding cytopathic effects. Plaques were "picked" using sterile Pasteur pipettes to penetrate the agarose and aspirate the underlying cells. In general, plaques were isolated from the plates with the lowest density of plaques to minimise the risk of cross-contamination. Aspirates/agarose plugs were transferred to a 12 well plate seeded with $5x10^5$ Sf9 cells

per well in 2ml TNM-FH. This was repeated for each plaque. Plates were sealed with parafilm and incubated at 27°C for 4-7 days. The supernatant was collected and stored at 4°C: this represents the P1 viral stock.

2.2.30 Generation of High Titre Stocks (HTS)

High titre stocks were generated by a two-step process. P2 stocks were made by infecting two 25cm^2 flasks (2x10^6 log-phase Sf9 cells) with 20µl of P1 stock, and incubating for 10 days i.e. until all cells were lysed. Half this stock was frozen at –80°C, and the remainder was stored at 4°C. P3 stock was generated by infecting a 100ml suspension culture of Sf9 cells (1.8-2.2x10^6 cells/ml) with 1ml of P2 viral stock. Several flasks were infected and co-incubated for 7-10 days (complete cell lysis). The stock was purified by centrifugation at 1000g for 20 minutes, and the supernatant stored at 4°C.

2.2.31 Determination of Viral Titres

Viral titres of the HTS were determined by limiting dilution plaque assays, as described above. However, since the titre of the P3 stock should be many orders of magnitude higher than the transfection stock, viral dilution of 10^{-6}-10^{-8} were used on duplicate plates. Viral titre was calculated from the number of plaques visible on a plate multiplied by the dilution factor.

2.2.32 Sf9 Cell Lysis for Recombinant Protein Purification

100ml suspension of baculoviral infected Sf9 cells (MOI 1) were harvested after 72 hours by centrifugation at 1000g for 15 minutes at 4 °C. The cell pellet was resuspended in approximately 2 ml of chilled protein extraction buffer containing protease inhibitors. The suspension was mixed with 10g alumina (Sigma) in a chilled mortar and pestle and ground for 2 minutes to lyse cells. The lysate was diluted with 20 ml of extraction buffer and centrifuged at 10,000rpm in a HB6 rotor (Becton-Dickinson) for 30 minutes at 4°C.

2.2.33 Protein purification by Immobilised Metal Affinity Chromatography

5ml of Talon metal affinity resin (Clontech) (bed volume 2.5ml) was mixed 45 ml of extraction buffer, centrifuged at 800 rpm for 3 minutes, and the wash step repeated twice. The cleared lysate was mixed with the equilibrated resin and incubated at room temperature for 20 minutes on a vertical rotator. The sample was centrifuged at 700g for 5 minutes at 4°C, the supernatant discarded and replaced with 45 ml of extraction buffer. This was incubated at room temperature for another 10 minutes and then centrifuged again. The wash step was repeated. The resin pellet was transferred to a 10ml elution column and allowed to settle. A 10ml wash with extraction buffer was performed and then the bound protein was eluted with 5 bed volumes of elution buffer and collected in 1ml fractions. At each stage of the purification process 100µl samples were taken for quality control. Resins were regenerated by cleaning in 6M guanidium (pH5.0)/1%NP40, washing with ddH2O, 20mM morphoethanolsulphonic acid/0.1M NaCl and stored in 20% ethanol/0.1% azide until reused.

Fractions were examined by Western blotting and silver staining to assess recombinant protein content and purity. Suitable samples were pooled and the elution buffer replaced with physiological buffer (150mM NaCl, 50mM Tris, pH 7.45) by dialysis in 1000 times the sample volume overnight at 4°C. Samples were concentrated using Amicon filters (YM30). Recombinant proteins were stored at 4°C as freezing was found to inactivate enzymatic activity.

2.2.34 Immunoaffinity Protein Purification

10ml of bacculoviral infected Sf9 cells in suspension ($1x10^9$/ml) were pelleted and washed repeatedly as described above, except that PBS was substituted for extraction buffer. Cells were lysed in immunoaffinity lysis buffer on ice for 30 minutes. The lysate was clarified by centrifugation at 10,000rpm in a HB6 rotor for 30 minutes. The immunoaffinity column containing 1ml of resin was equilibrated using 10 bed volumes of equilibration buffer, taking care to avoid dehydration. 4 ml of clarified protein solution was added (<5mg protein) and allowed to drain. The column was washed with

20 bed-volumes of wash buffer at room temperature to remove non-specifically bound protein. One bed volume of elution buffer was added and incubated at 37°C for 15 minutes, and the eluate collected and stored at 4°C until analysed. Additional elution buffer was added, incubated and collected. The column was regenerated by stripping with 20 bed volumes of regeneration buffer. Column storage buffer was added and the resin stored at 4°C.

2.2.35 Immunoprecipitation

0.5 ml of clarified lysate from Sf9 suspension culture was mixed with 1µg of agarose-conjugated anti-HA antibody, and mixed at 4°C on a vertical rotator for 60 minutes. Suspensions were microcentrifuged at 13,000rpm for 5 seconds and the supernatant aspirated and discarded. The pellet was resuspended with 1ml lysis buffer, pelleted by centrifugation and finally washed 3 times with wash buffer.

2.2.36 Ion Exchange Chromatography

All solutions prepared for ion exchange chromatography were chilled to 4°C prior to adjusting pH, filtered (0.22µm) and thoroughly degassed. An Äkta FPLC system was used (Amersham Pharmacia Biotech) fitted with a MonoQ anion exchange resin (Amersham Pharmacia Biotech). Prior to use the chromatography equipment was purged of contaminating proteins by perfusing with buffer B at 5ml/min for 30 minutes. The column was then flushed with buffer A and allowed to equilibrate. Clarified lysate (30ml) was prepared from 1 litre of baculovirally infected Sf9 cells using ion exchange lysis buffer, and filtered (0.22µm) prior to injection in to the chromatography system. A280 was measured continuously to monitor protein elution and10ml samples were collected automatically. The column was perfused with Buffer A at 5 ml/min until the elution A280 reading had returned to baseline, indicating that unbound protein had been washed from the resin. Protein was eluted using a linear salt gradient from 0-50% buffer B over 90 minutes, created by controlled mixing of buffers A and B. Eluted samples were collected in 5ml aliquots and stored at 4°C until analysed. Samples identified as

containing recombinant prorenin by Western blotting were pooled and repurified using a further round of ion exchange chromatography.

2.2.37 Collection of Blood, Tissue and Urine

Animals were sacrificed by CO_2 inhalation, or cervical dislocation under anaesthetic. Blood was collected by direct cardiac puncture in to pre-chilled tubes on ice, then microfuged at 10,000rpm for 5 minutes at room temperature. Plasma was stored at –80°C until analysed.

As soon as possible after sacrifice tissues were dissected and either snap frozen on dry ice, or transferred to 10% buffered formal saline. Excess blood was removed from the heart by blotting dry on tissue paper. The heart was weighed after removal of the aortic root and other mediastinal structures. The left ventricular free wall and septum were dissected from the right ventricle and atria, and weighed separately, then frozen immediately on dry ice. Tibial length was measured between the tibial plateau and the intercondylar groove using a sliding micrometer caliper, accurate to 0.1mm.

Urine was collected from individual rats over 24 hours using metabolic cages. Urine was centrifuged at 10 000 rpm for 5minutes to remove debris, then frozen at –80°C until analysed. Water intake was measured by weighing water bottles before and after the experiment.

2.2.38 Histological Analysis

Tissues were routinely fixed in 10% buffered formal saline (Sigma) overnight, or longer if necessary. Samples were then transferred to 70% ethanol, until processed. A Citadel 2000 (Shandon Southern Products Ltd, Cheshire, UK) tissue processor was used to process tissues through serial dehydration steps in graded ethanol concentrations (70%, 80%, 90% and 3x 100%), followed by dealcoholisation with a clearing agent, Histoclear (National Diagnostics, Atlanta, Florida, USA) 3 times, and paraffin wax (Histoplast, Thermo Shandon) immersion twice at 60°C. Tissues were embedded in paraffin wax

using a Blockmaster III (Raymond Lamb) wax embedding apparatus. Sections were cut on a microtome (Bright 5040) and floated on a water bath at 50°C (Electrothermal). For heart 6μm sections were used, whereas 4 μm sections were cut for all other tissues. Tissue sections were transferred to poly-lysine coated slides (BDH, Poole, UK) and baked at 56°C for 2 hours. Slides were stored at 4°C until used.

2.2.38.1 Haematoxylin and Eosin Staining

Tissue slides were dewaxed in xylene and rehydrated in decreasing concentrations of alcohol (100%, 90%, 70%) and stained in haematoxylin for 5 minutes. Slides were rinsed in tap water and stained in eosin for 5 seconds, briefly rinsed in tap water again and rapidly dehydrated in alcohol (70%, 90%, 100%). Slides were cleared in xylene and a cover slip mounted over the tissue using pertex (National Diagnostics).

2.2.38.2 Picrosirius Red Staining [605]

Paraffin sections were dewaxed and rehydrated as before, then immersed briefly in haematoxylin to stain nuclei. Sections were washed in running tap water for 10 minutes, then stained in solution A (Sirius Red F3B 0.5g, Picric Acid (saturated aqueous solution) 500ml) for 1- 5 minutes. Slides were washed in two changes of solution B (0.5% Acetic Acid). Excess water was remoned by vigorous shaking, followed by dehyration through graded alcohols (70%, 90%, 100%). Slides were cleared in xylene and mounted in pertex.

2.2.38.3 Tissue Photomicrography

Bright field histology was photographed using an Axiovert S100 inverted microscope using Open Lab 3.0 software for image capture and processing.

2.2.38.4 Quantification of Left Ventricular Fibrosis

Picrosirius red stained left ventricular sections were examined at high power (X100), and 10 fields within the left ventricular free wall were randomly selected and photographed, as above. Captured images were imported in to Adobe Photoshop 7.0

and 96 point grid applied. Areas of fibrosis (red) underlying grid points were counted for each section, and the average calculated for each animal.[606]

2.2.39 Analysis of Blood

2.2.39.1 Renin Angiotensin System Radioimmunoassays

Renin, prorenin, angiotensin I and angiotensin II assays were performed by Dr J Peters (University of Greifswald, Germany). For active and inactive renin concentrations plasma samples were pretreated with buffer or trypsin (400units/ml) and incubated with lyophilised renin substrate (80μg/μl) for 1 hour at 37°C. The concentration of angiotensin I generated was determined by radioimmunoassay.[566,607] For plasma renin concentration the samples were incubated directly with substrate. Angiotenin II samples were processed by Sep-Pak elution prior to radioimmunoassay.

2.2.39.2 Plasma Potassium

Plasma potassium concentrations were measured using a Hitachi 911 analyser (Roche) by the Department of Biochemistry, Royal Hospital for Sick Children, Edinburgh.

2.2.40 Anaesthesia

Animals were anaesthetised either by intraperitoneal injection of inhalation of Ketamine (100mg/kg) (Pharmacia-UpJohn) and Xylazine (5mg/kg),[249] or by inhalation of Halothane 1-5% (Merial, UK) in pure oxygen. Anaesthetised animals were kept warm with a heat pad set to 37°C. The level of anaesthesia was assessed by hindlimb responses to pain. For echocardiography a "light" anaesthetic was given, in which prompt withdrawal responses were elicited, without other signs of consciousness. For operative procedures a deeper level of anaesthesia was maintained in which no hindlimb responses could be elicited.

2.2.41 Tail Cuff Plethysmography

Systolic blood pressure (SBP) was measured by tail cuff plethysmography[608] in conscious restrained animals. The equipment was calibrated manually using a

sphygmomanometer. Measurements were made daily between 09:00 and 11:00 after at least 5 days of training. Systolic blood pressure was defined as the deflation pressure at which arterial blood flow was first detected. Vasodilation of the tail was induced by warming the rats in a Thermocage heater set at 38°C for 15 minutes before the procedure. Vasodilation was maintained during recordings by placing rats on a pad heated to 38°C. A minimum of three recordings were obtained for each animal at each time point and averaged.

2.2.42 Left Ventricular Catheterisation

Left ventricular pressures were measured using a 2F high fidelity micromanometer catheter (Millar, Texas, USA) via a right carotid artery approach in anaesthetised rats. The catheter was advanced retrogradely across the aortic valve in to the left ventricle. Prior to use the catheter was zeroed to ambient atmospheric pressure. Data was acquired using a PowerLab 4_{SP} acquisition system (ADInstruments Ltd, Chalgrove, UK) and Chart v5.0.1 (ADInstruments) at a rate of 200Hz and analysed off line. Left ventricular end diastolic pressure was taken as the pressure recorded just prior to the systolic upstroke. At least five consecutive beats were averaged for each measurement. The following parameters were routinely analysed: aortic systolic and diastolic pressure (mmHg), left ventricular peak developed pressure (mmHg), left ventricular end diastolic pressure (mmHg), +dP/dt max (mmHg/s), -dP/dt min (mmHg/s), and heart rate (bpm).

2.2.43 B and M-mode Echocardiography

Anaesthetised rats were examined in a left lateral position on a heat pad (38°C) after the chest had been shaved. Warmed ultrasonography gel was applied sparingly and left parasternal long and short axis B mode views were obtained. The recommendations of the American Society of Echocardiography[609] were followed with regard to cursor placement, using the "leading edge" method. M-mode images were obtained using B mode guidance from the parasternal long axis. The cursor was positioned at the tips of the mitral valve leaflets, so that it transected the septum and posterior ventricular wall perpendicularly. Ventricular dimensions were measured from m-mode recordings

wherever possible. This methodology is widely used and has been validated in rat post-mortem studies[610] Measurements were made from 3-5 consecutive beats to minimise the effect of respiration on dimensions.

2.2.44 Doppler Echocardiography

Pulse wave Doppler was used in the apical four and five chamber views to assess transmitral filling and aortic outflow respectively. Sample volume was reduced to the minimum possible.

2.2.44.1 Transmitral Flow Velocities

Mitral inflow is biphasic, with an early rapid phase of filling, which is passive and occurs immediately after mitral valve opening (E wave), followed by a later phase of active filling, caused by atrial contraction (A wave). The peak velocity of the E and A waves were measured in 5-6 consecutive beats, as well as the deceleration time (dt) and the rate of deceleration of the early filling phase.

2.2.44.2 Isovolumic Relaxation Time

Isovolumic relaxation time (IVRT) was measured by positioning the pulse wave Doppler sampling volume between aortic and mitral flows to obtain both mitral and aortic signals. IVRT was measured from the closure of the aortic valve, represented by a small "click" in the Doppler spectra coincident with the end of aortic flow, to the onset of transmitral flow.

2.2.44.3 Aortic Doppler Velocities and Cardiac Output

Aortic Doppler signals were detected in the five-chamber view, with the pulse wave sampling volume positioned in the left ventricular outflow tract, allowing measurement of left ventricular outflow tract (LVOT) peak velocity. Velocity time integral (VTI) was determined by tracing round the Doppler signal.

2.2.45 Echocardiographic Formulae

Left ventricular mass

Left ventricular mass was estimated using the uncorrected cubed formula, derived and validated in humans by Devereux and Reichek.[611]

$$LV\ mass = 1.04\{(IVS_d + LVD_d + PWT_d)^3 - (LVD_d)^3\} \qquad \text{Equation 1}$$

where IVS_d is end diastolic interventricular septum thickness, LVD_d is end diastolic left ventricular diameter and PWT_d is the posterior wall thickness in diastole. This assumes that the heart comprises a prolate ellipsoid with a specific gravity of 1.04 g/cm^3, with the long axis dimension being twice that of the short axis. Although such an assumption may not be valid, particularly in pathological situations, the formula has been validated in hypertensive rats.[612] Other formulae are available for LVM estimation,[613] but they require adequate B-mode (2 dimensional) images which are not always obtainable in rats.

Endocardial Fractional Shortening (eFS)

$$eFS\% = 100\ X\ \frac{(LVD_d - LVD_s)}{LVD_d} \qquad \text{Equation 2}$$

Midwall Fractional Shortening (mFS)

$$mFS\% = 100X\frac{\{(LVD_d + PWT_d) - (LVD_s + 2a)\}}{(LVD_d + PWT_d)} \qquad \text{Equation 3}$$

where a is the distance from the posterior wall endocardium of a theoretical midwall fibre at end systole.[614] "a" can be solved from the following equation, derived from the assumption that the volume of the ventricular muscle remains constant throughout the cardiac cycle.

$$\frac{(0.5LVD_d+0.5PWT_d)^2-(0.5LVD_d)^2}{(0.5LVD_d+PWT_d)^2-(0.5LVD)} = \frac{(0.5LVD_s+a)^2-(0.5LVD_s)^2}{(0.5LVD_s+PWT_s)^2-(0.5LVD_s)} \quad \text{Equation 4}$$

Cardiac output

Cardiac output was estimated using the following formula.[103]

$$\text{Cardiac Output (CO)} = VTI \times \{\pi(LVOT/2)^2\} \times \text{heart rate} \quad \text{Equation 5}$$

where VTI is the velocity time integral, and LVOT is left ventricular outflow tract diameter.

2.2.46 Radiotelemetry Device Implantation

Radiotelemetry devices capable of monitoring blood pressure and ECG data were implanted in the abdomen of mature rats (weight 250-350g) under halothane anaesthesia by Mrs Gillian Brooker. The blood pressure cannula was introduced in to the abdominal aorta below the renal arteries, and fixed with tissue glue. The two electrodes were implanted subcutaneously in the lead II configuration, with the negative lead at the right forelimb and the positive lead at the left hind limb. The device was fixed to the anterior abdominal wall with silk sutures, and the wound closed with surgical clips. Animals were allowed to recover for at least 14 days before studies were commenced.

2.2.47 Radiotelemetry Blood Pressure Analysis

Data was collected using Dataquest ART 2.1 software (Data Sciences). The frequency of recordings varied depending on the duration and purpose of the study. Usually recordings were taken from each animal for 10s every 20 minutes. Data quality was assessed from the appearance of the blood pressure waveform in real time (continuous mode), and overall appearance of readings for the recording period. The development of catheter thrombi was recognised by poor quality "damped" waveforms and artificially high or low blood pressures. Data was not collected from these animals. Raw blood

pressure data was exported as ASCI files and analysed in Microsoft Excel (2001). Systolic and diastolic blood pressures were obtained for each animal, and a moving average was applied to the whole group to smooth out variations where indicated.

2.2.48 Radiotelemetry ECG Data Analysis

ECG waveform data was analysed using Physiostat ECG software 3.1 (Data Sciences International) set to the default parameters for rats. The "end fit" method was used for detection of the end of T wave, as opposed to the threshold method. Traces were reviewed manually for each time point for each rat, to assess alterations in cardiac rhythm and recording quality. Parameters for each screen of ECG data (representing one 10s recording period) were automatically analysed and averaged by the software to generate an average or "reference" complex. This data was exported and analysed in Microsoft Excel 2001. For each parameter, a daily average was calculated for each animal, which was used to calculate group averages for that day. Data from unsatisfactory recordings due to movement artefact was discarded. The following parameters were routinely measured: Heart rate (bpm), P wave: duration, amplitude (s) (mV), PR and PQ interval (s), R wave amplitude (mV), QRS duration (s), S wave amplitude (mV), T wave amplitude (mV).

QT interval was analysed Bazett's Formula [615]

$$QTcB\ (s) = \frac{QT\ interval}{\sqrt{RR\ interval}} \qquad \text{Equation 6}$$

2.2.49 Radiotelemetry Arrhythmia Analysis

All ECG recordings were scrutinised for evidence of arrhythmias. Ventricular arrhythmias were graded according to the Lown classification.[616] This method has been applied to both human and animal populations and grades ventricular premature beats as follows: no ventricular ectopic beats (grade 0), occasional isolated ventricular premature beats (grade1), frequent ventricular premature beats (>1/min or >30/h) (grade 2), multiform ventricular premature beats (grade 3), couplets (grade 4a), salvos of

ventricular premature beats (grade 4b) and early ventricular premature beats (R on T) (grade 5).

2.2.50 Statistics

All animal experiments were carried out with 6 animals per group, unless otherwise stated. Data is represented as the group mean, plus/minus the standard error of the mean. Microsoft Excel (Office 2001) was used for data handling and analysis. GraphPad Prism 4.0a software was used for statistical analysis. $p<0.05$ was considered significant, and two-sided tests were used. Comparison of single groups at single time points was made using Student's t-test. Comparisons between multiple groups were made using one-way ANOVA, followed by Tukey's post-hoc test for significance. Two-way ANOVA was used to test for interactions between 2 or more variables, followed by Bonferroni's post-hoc test. When repeated measurements were made during longitudinal follow up studies, statistical analysis was by repeated measures ANOVA.

Chapter 3

Low Dose Induction Experiments in TGRcyp1a1Ren2

3.1 Introduction

Short term experiments in TGRcyp1a1ren2 demonstrated that there is a dose-dependent effect between I3C and RAS activation, and that 0.3% I3C (w/w) induces malignant hypertension over a 14 day period.[581,587] However it is not clear whether the dose of inducing agent is critical to the phenotype of this model in long-term experiments. This issue is complicated, because the relationship between prorenin level, hypertension, vascular remodelling and vascular injury is not known, and may be dependent on many kinetic variables relating to I3C metabolism, transgene induction, transgene clearance, substrate availability,[617] and vascular structural remodelling, not to mention mechanisms of compensation and repair. Experiments in rats transgenic for human angiotensinogen found a non-linear relationship between the dose of osmotic minipump delivered human recombinant renin and blood pressure,[618] suggesting that a lower level of prorenin induction in TGRcyp1a1ren2 may have dramatically less effect on blood pressure.

Other renin-based transgenic models of hypertension such as TGRmren2-27,[562] TGRα1ATren2[408] and dTGR[619] appear to develop cardiac hypertrophy, but succumb to malignant hypertension (MH) before the development of heart failure. In contrast, models such as the spontaneously hypertensive rat (SHR) develop compensated LVH before progressing to heart failure after 18-24 months,[106] whilst certain SHR sub-strains are prone to heart failure within 12 months.[620] Dahl salt sensitive rats (DS) have an accelerated progression from compensated LVH to heart failure, occurring over just a few months.[108,114] Such differences do not appear to be related to the severity of

hypertension, which is similar between all models, so it is possible that RAS activation either predisposes to MH, which is rapidly fatal, or else RAS activation is not sufficient alone to stimulate progression to cardiac decompensation.

Given that 0.3 % I3C induces a severe phenotype that is potentially fatal, we chose to explore the effect of a lower dose of inducer to assess the possible consequences of chronic hypertension on cardiovascular pathophysiology. In particular we sought to establish whether chronic hypertension would lead to hypertensive heart disease, cardiac failure and fatal arrhythmias, as is seen in essential hypertension in humans.[44] TGRcyp1a1ren2 may be an ideal monogenic model of hypertension in which to explore manipulations that accelerate or ameliorate LVH and progression to heart failure. Furthermore, TGRcyp1a1ren2 also allows the reversibility of LVH and cardiac dysfunction to be studied by simply removing the inducing agent from the diet.

We therefore characterised the effect of chronic hypertension induced by dietary 0.15% I3C (w/w) on cardiovascular function in cohorts of TGRcyp1a1ren2 and F344 controls. One group of animals was monitored using chronically implanted radiotelemetry devices to accurately determine haemodynamic and ECG variables. This group also underwent serial echocardiographic assessment of cardiac function. Other groups were studied at different time points in a standard manner to assess cardiac function by left ventricular catheterisation, as well as to obtain samples for left ventricular BNP expression, cardiac histology and plasma RAS parameters. In addition, the reversibility of all these parameters was assessed in a group that were returned to standard rat chow after 42 days of I3C.

3.2 Plasma Renin-Angiotensin System Parameters.

3.2.1 Plasma Prorenin

Prior to dietary I3C exposure, plasma prorenin levels were not significantly different between TGRcyp1a1ren2 compared to F344 control animals (figure 3.1a). As expected, I3C had no effect on plasma prorenin levels in F344 animals at any time point, but led to

a progressive and substantial increase in TGRcyp1a1ren2 animals over a 140-day period. At days 42, 84 and 140, prorenin levels were elevated 130, 270 and 1225 times respectively, compared to F344 controls ($p<0.001$). Removal of I3C from the diet at day 42 resulted in almost complete resolution of plasma prorenin levels to pre-induction levels within 7 days.

3.2.2 Plasma Renin

The pattern of plasma renin levels differed to that of prorenin in both magnitude and timing. At baseline and day 42, plasma renin activities were identical between transgenic and control animals, despite the elevated prorenin levels at these time points (figure 3.1b). By day 84, renin levels were 4-fold higher in transgenics, reaching only 5.7 fold at day 140. Therefore, in contrast to prorenin, active plasma renin levels are only modestly elevated, and this is only seen at later time points. After withdrawal of dietary I3C plasma renin levels were within the normal range by day 7.

3.2.3 Plasma Angiotensin II

Plasma angiotensin II levels were not significantly different between groups at baseline or day 42 (figure 3.1c). Ang II levels were non-significantly elevated at later time points by approximately 2-3 fold.

3.3 Blood Pressure Response

To define the chronic effect of 0.15% I3C on blood pressure, animals were studied with radiotelemetry devices implanted in the abdominal aorta. This allowed continuous monitoring of blood pressure on a beat-to-beat basis in conscious free moving animals over several months. Recordings were started one month after device implantation due to technical problems with telemetry receivers. This delay also avoided the effects of surgery/anaesthesia on cardiovascular function,[621] To simplify analysis a twenty-four hour moving average was applied to blood pressure data. Baseline parameters were obtained over a 3-day period prior to dietary I3C exposure, and were indistinguishable between TGRcyp1a1ren2 and F344 rats (figure 3.2).

Figure 3.1 Renin-Angiotensin System in TGRcyp1a1ren2 in Response to 0.15% I3C

a)

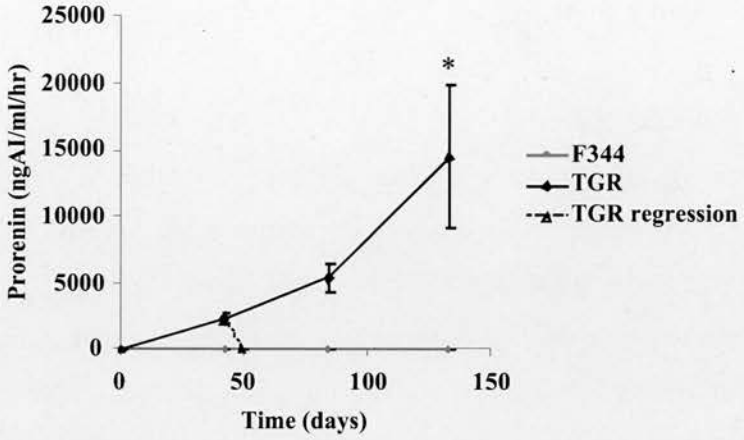

b)

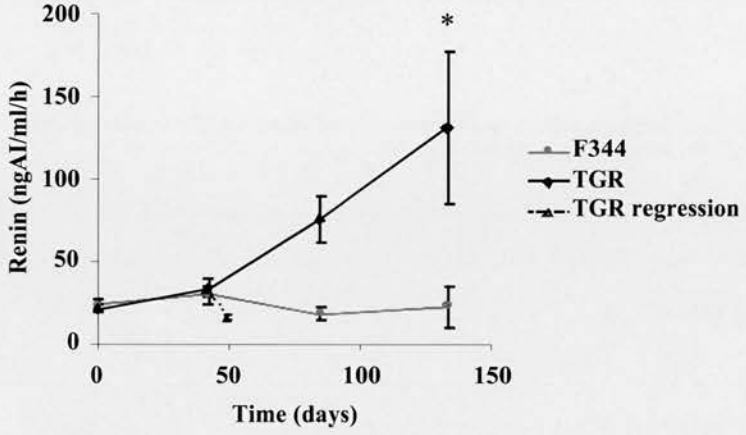

c)

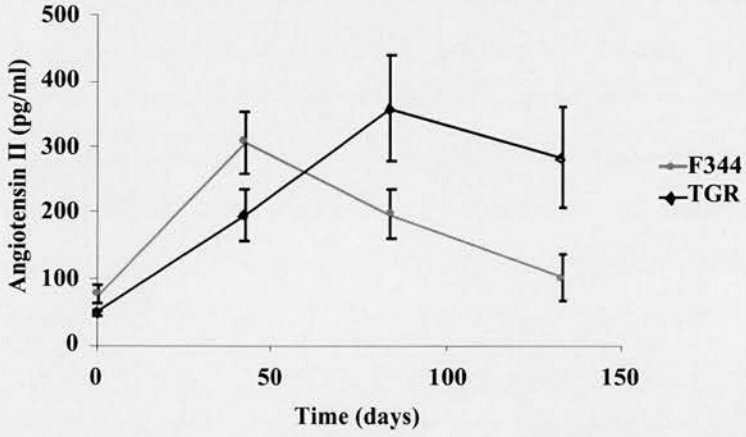

TGRcyp1a1ren2 and F344 controls were fed 0.15% I3C (w/w) over 140 days **a)**. Plasma prorenin. **b)**. Plasma active renin. **c)**. Plasma angiotensin II. n=6 per group, mean ± SEM. * $p<0.001$ TGR *vs* F344. TGR:TGRcyp1a1ren2, F344: Fischer 344 control. Two-way ANOVA, Bonferroni's test.

Figure 3.2. Blood Pressure Response of TGRcyp1a1ren2 to 0.15% Indole 3-Carbinol.

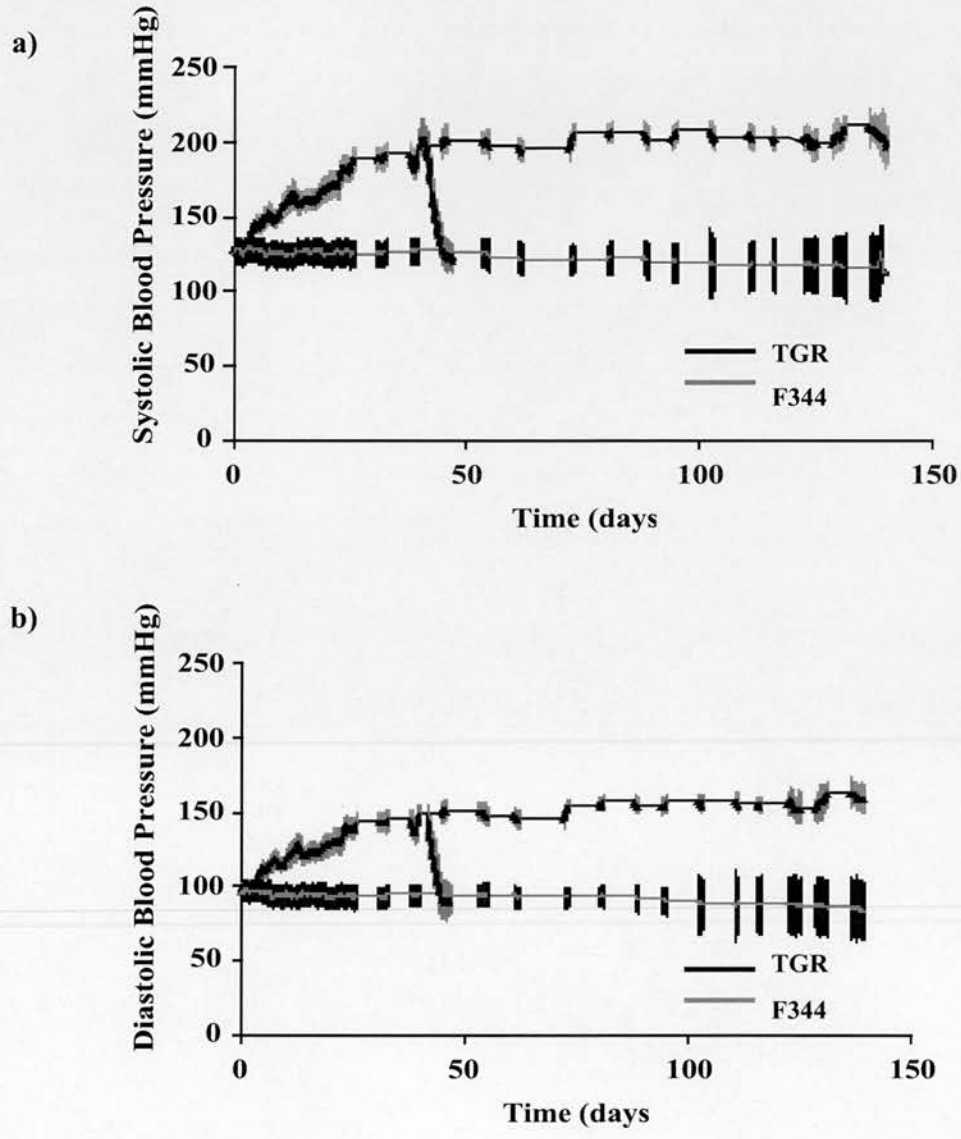

24-hour averaged telemetric blood pressure of TGRcyp1a1ren2 and F344 animals. Rats were fed 0.15% I3C from day 3 onwards for 140 days. Dietary I3C was omitted in 4 TGR after 42 days to study the reversibility of blood pressure changes. Data was collected continuously for the first month and then at weekly intervals for 24 hours. Data between recordings is interpolated. **a)**. Systolic blood pressure. **b)**. Diastolic. TGR: transgenic (n= 8 and 4), F344: Fischer 344 control (n= 6). Mean ± SEM.

I3C 0.15% w/w induced a sustained rise in systolic and diastolic blood pressures in TGRcyp1a1ren2 but not F344 controls (figure 3.2). Blood pressure stabilised at 189±7/144±6 mmHg after 30 days, and remained elevated until day 140, at which time the study was terminated. In the regression group, blood pressure was not significantly different from control animals within 4 days of stopping I3C (figure 3.2).

3.4 Heart Rate and Heart Rate Variability

Radiotelemetric ECG recordings were analysed for heart rate and RR interval variability. Baseline heart rate was similar between groups, but there was significant variability in heart rate within groups from week to week. However, linear regression analysis demonstrated an increase in heart rate in the transgenic group over the study period (fig 3.3), whilst overall, the heart rate did not change significantly for the control group.

Figure 3.3 Average Heart Rate During Induction of TGRcyp1a1ren2 with 0.15% I3C (w/w)

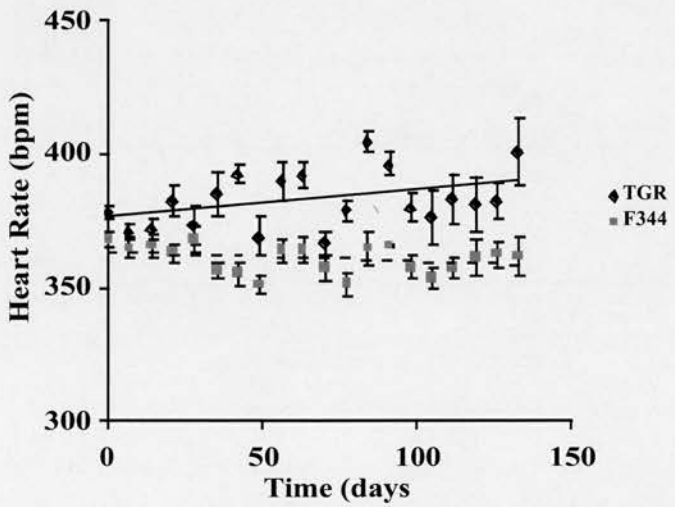

Linear regression analysis demonstrated a significant difference in the heart rate of transgenic and control animals over the course of the study. p =0.018 TGR vs F344 (TGR y=0.6707x+376.6, F344 y=-0.2572x+363.1: p=0.018). TGR: transgenic (n=8), F344: Fischer 344 control (n=6).

Heart rate variability was measured as the standard deviation of the RR interval, and again there was substantial intra-group variability with time. Linear regression demonstrated a significant decline in heart rate variability in the transgenic group compared to controls (figure 3.4).

Figure 3.4 Heart Rate Variability During Induction of TGRcyp1a1ren2 with 0.15% I3C (w/w)

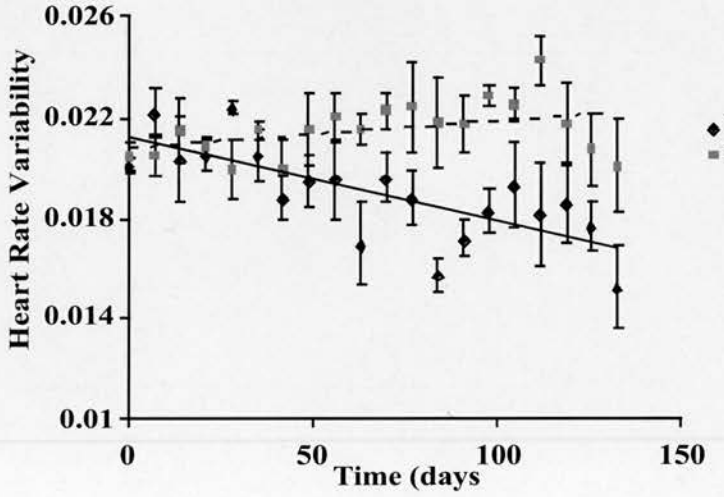

Heart rate variability was determined as the standard deviation of the RR interval. Whilst F344 animals retained heart rate variability throughout the study, transgenic animals demonstrated a steady decline. Statistical analysis was by linear regression (TGR $y=-2.328x10^{-4}$ x + 0.02119, F344 $y=6.0x10^{-4}$ x +0.02100: $p<0.0001$). Mean ± SEM. 95% confidence intervals are shown for regression lines. TGR: transgenic (n=8), F344: Fischer 344 control (n=6).

3.5 Left ventricular hypertrophy

Since TGRcyp1a1ren2 develop chronic hypertension in response to an activated RAS, evidence of left ventricular hypertrophy was sought. This was measured gravimetrically relative to body weight as the left ventricular mass index (LVMI). As expected, LVMI was identical in TGRcyp1a1ren2 and F334 animals prior to induction of hypertension

(figure 3.5). After 42 days of induction the LVMI of transgenic animals was increased by 25% compared to controls, increasing to 77% by day 140. LVH at 6 weeks was reversible, with the regression group demonstrating a 75% reduction 7 days after cessation of I3C, and complete regression by 42 days (figure 3.5). Therefore, LVH appeared to be rapidly reversible in response to restoration of normal haemodynamic and neurohumeral parameters.

Figure 3.5 Changes in Gravimetric Left Ventricular Mass Index.

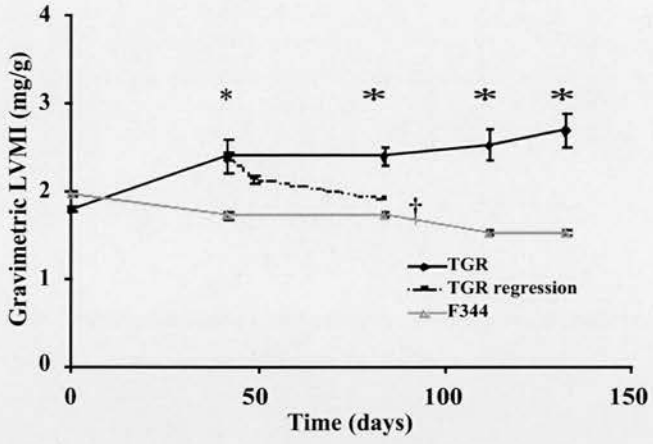

LVMI was measured at serial time points before, during and after induction of hypertension with I3C. n=6 per group, mean ± SEM. * $p<0.001$ TGR vs F344, † $p>0.05$ TGR regression vs F344. TGR n= 8, TGR regression n=4, F344 n=6. TGR: transgenic, F344: Fischer 344 control. 2-way ANOVA, Bonferroni's test.

LVH is characterised by a typical pattern of gene expression changes, including the increased expression of BNP.[64] To demonstrate that TGRcyp1a1ren2 develops typical LVH, left ventricular BNP expression was determined by a SYBR green Real Time PCR assay. Primers were designed using Primer Express software with reference to the published rat BNP genomic sequence:[622] primers JJM504/505 span the intron 2/exon 3 junction (figure 3.6), and were found to meet the criteria for Real Time PCR. Experiments to optimise the primer concentrations were performed (figure 3.7), and

cloned PCR product was sequenced to confirm the fidelity of amplification. BNP expression relative to 18S ribosomal RNA was increased by 70% at day 42 of induction ($p<0.01$), and suppressed by 35% after regression, relative to F344 controls (p=ns) (figures 3.8, A2.1, A2.2, tables A2.1 and A2.2). This data indicates that the increases in LVMI are associated with induction of the foetal programme of gene expression, and that LVH is reversible both in terms of LV mass and patterns of gene expression.

Figure 3.6 Rat BNP Real-Time PCR Primer Design

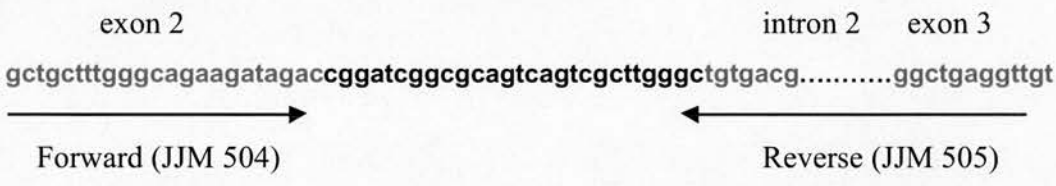

Rat BNP sequence 5'-3'. BNP specific primers (red) were design to comply with Real Time PCR parameters using Primer Express software. In addition, primers were designed to span intron 2, thereby reducing the risk of genomic DNA amplification. BLAST analysis of primers indicated that they had no homology with other rat sequences.

Figure 3.7 Primer Optimisation for BNP Real Time PCR Assay

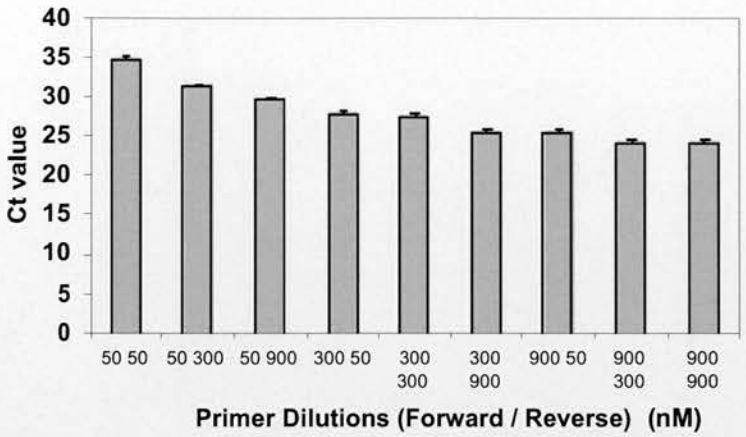

A single left ventricular cDNA sample was amplified in quadruplicate using BNP primers at the concentrations (nM) indicated. The optimal primer concentrations were considered to be 300nM forward, 900nM reverse. Ct: threshold cycle. Mean ± SEM.

Figure 3.8 Left Ventricular BNP Expression

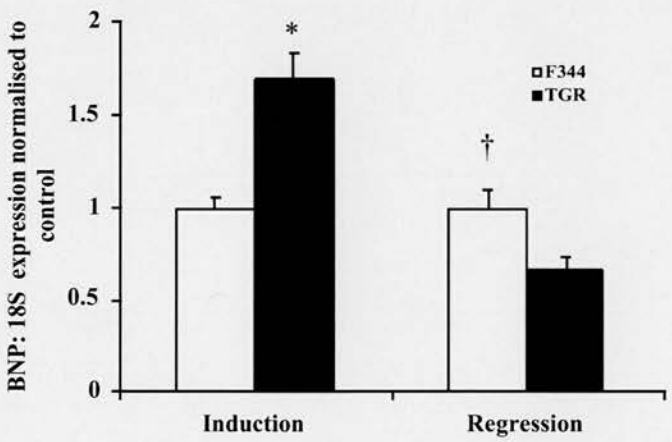

Left ventricular BNP was measured in two separate groups after 42 days of 0.15% (w/w) I3C, and after 42 days of regression. Results are relative to a calibrator sample and normalised to 18S expression. BNP was elevated 1.7-fold after 42 days of induction. Conversely after regression, BNP was suppressed. Mean ± SEM. *$p<0.01$, † p=ns TGR vs F344. TGR: transgenic, n=5, F344: Fischer 344 control, n=4. 2-way ANOVA, Bonferroni's test.

3.6 Cardiac Function During LVH Development

3.6.1 Echocardiography

Echocardiography was performed to estimate cardiac function and mass non-invasively during the development of hypertension. To establish the reliability of echocardiographic measurements, and the degree of intraobserver variability, digital echocardiographic recordings from one group of animals were analysed on two separate occasions 2 days apart by the same observer. Estimates of intraobserver variability are given in table 3.1, and in general this was low except for posterior wall thickness during diastole. Similar values have been reported in the literature, suggesting that such variability is acceptable, though not ideal.[623]

Table 3.1 M-mode Echocardiographic Intraobserver Variation

Parameter	% difference	Standard Error	p value
IVSd	7.12	2.95	NS
LVDd	1.31	0.84	NS
PWTd	8.25	1.77	p=0.004
IVSs	2.92	1.29	NS
LVDs	2.17	1.71	NS
PWTs	3.41	1.64	NS

Measurements from M-mode digital recordings of 6 TGRcyp1a1ren2 rats were made on two separate occasions 2 days apart. Averages for each parameter were compared, and the percentage difference calculated. (Mean ± SEM). IVS: interventricular septum, LVD: left ventricular internal dimension, PWT: posterior wall thickness, d: diastole, s: systole. Repeated measures ANOVA, Bonferroni test.

Echocardiography demonstrated that LVH was concentric, in that there was a progressive increase in septal and posterior wall thicknesses, and a significant reduction in relative wall thickness in the transgenic group compared to controls (table 3.2, fig 3.9 & 3.10). Echocardiographically determined LVMI mirrored the gravimetric measurements, but absolute values were significantly different (fig 3.9). There was no significant change in endocardial or midwall fractional shortening over the duration of the study (table 3.2). Although there was a decline in fractional shortening in the transgenic group by day 140, this was not statistically significant (two-way ANOVA) (table 3.2). Therefore, there was no evidence of heart failure in the transgenic group.

Figure 3.9 Echocardiographic Changes in Left Ventricular Mass Index

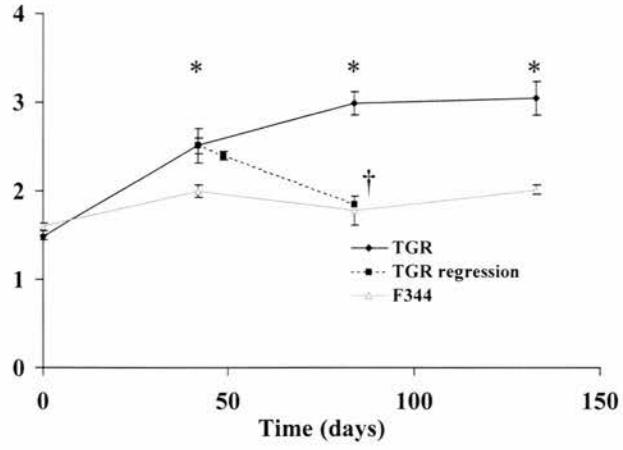

Echocardiography was performed before, during and after induction of hypertension with 0.15% I3C. LV mass was calculated using the cubed formula[611] (section 2.2.45) and used to calculate LVMI. n=6 per group, mean ± SEM. * $p<0.001$ TGR vs F344, † $p>0.05$ TGR regression vs F344. TGR n= 8, TGR regression n=4, F344 n=6. TGR: transgenic, F344: Fischer 344 control. 2-way ANOVA, Bonferroni test.

Figure 3.10 Echocardiography in TGRcyp1a1ren2 and F344 Rats

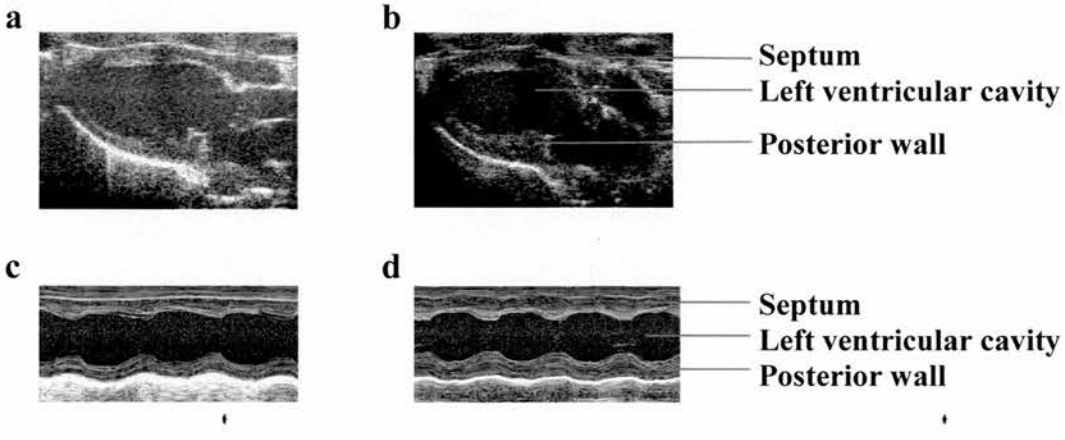

Standard parasternal long axis (a and b) m-mode (c and d) echocardiographic views of F344 (a, c) and TGR (b, d), demonstrating concentric LVH after 140 days of induction with 0.15% (w/w) I3C.

Table 3.2 Serial Echocardiography During the Development of Hypertension and LVH

	Day 42		Day 84		Day 133	
	TGR	**F344**	**TGR**	**F344**	**TGR**	**F344**
IVS_d (mm)	2.08 ^{C} ±0.03	1.69 ±0.12	2.27 ^{C} ±0.04	1.62 ±0.04	2.30 ^{C} ±0.11	1.72 ±0.04
$LVID_d$ (mm)	7.55 ±0.11	7.91 ±0.20	7.29 ^{A} ±0.16	7.73 ±0.11	7.45 ^{B} ±0.15	8.114 ±0.13
PWT_d (mm)	1.50 ±0.09	1.18 ±0.05	1.94 ^{C} ±0.13	1.34 ±0.11	1.812 ^{A} ±0.08	1.33 ±0.02
RWT	2.56 ^{B} ±0.14	3.38 ±0.17	1.93 ^{c} ±0.14	2.99 ±0.18	2.07 ^{B} ±0.09	3.04 ±0.08
LVMI (mg/g)	2.51 ^{C} ±0.08	2.00 ±0.07	2.99 ^{C} ±0.13	1.78 ±0.17	3.05 ^{C} ±0.19	2.02 ±0.05
eFS (%)	24.3 ±2.01	26.5 ±1.1	24.1 ±2.1	24.7 ±1.8	19.3 ±3.3	26.5 ±2.5
mFS (%)	14.2 ±1.4	14.7 ±1.3	12.3 ±1.23	14.93 ±1.4	12.4 ±0.5	16.1 ±1.1

2-way ANOVA, Bonferroni's test. ^{A} $p<0.05$, ^{B} $p<0.01$, ^{C} $p<0.001$ vs F344. Mean ± SEM. n=8. TGR, n=6 F344. eFS: endocardial fractional shortening, mFS: mid-wall fractional shortening, IVS: interventricular septum, LVID: left ventricular internal dimension, PWT: posterior wall thickness, RWT: relative wall thickness, d: diastole, s: systole.

3.6.2 Left Ventricular Catheterisation

Left ventricular catheterisation on day 140 demonstrated that left ventricular end diastolic pressure, maximal and minimal rates of LV pressure change ($dP/dt_{max/min}$), and maximal and minimal rates of LV pressure change corrected for pressure ($(dP/dT_{max/min})/P$) were not significantly different between groups at any time point (Table 3.3). It should be noted that the maximal developed LV pressures and aortic pressures were substantially lower than arterial pressures measured by radiotelemetry, suggesting that anaesthesia and surgery had a significant impact on haemodynamics and cardiac function.

Table 3.3 Day 140: Left Ventricular Catheter Data

	LVEDP mmHg	dP/dt_{max} mmHg/s	dP/dt_{min} mmHg/s	$(dP/dT_{max})/P$ /s	$(dP/dT_{min})/P$ /s
TGR	16.7 ±2.2	5349 ±462	4665 ±537	68.7 ±3.8	58.3 ±2.6
F344	16.0 ±1.6	4632 ±139	4375 ±176	67.3 ±6.1	57.4 ±4.3

TGRcyp1a1ren2 and F344 animals underwent LV catheterisation at day 140. N=6 per group. Mean ± SEM. No significant differences between groups (1-way ANOVA). LVEDP: left ventricular end diastolic pressure, $dP/dt_{max}/_{min}$: maximal and minimal rates of pressure change, $(dP/dT_{max/min})/P$: maximal and minimal rates of pressure change corrected for instantaneous pressure.

3.7 Electrical Remodelling

Electrophysiological changes in hypertrophied cardiomyocytes are reported to predispose to ventricular arrhythmias.[54,624] It was therefore of interest to determine whether such changes could be detected in TGRcyp1a1ren2, and whether arrhythmias contributed to premature mortality. Telemetric ECG recordings were made for 12 TGRcyp1a1ren2 and 6 F344 rats over 140 days. These were analysed for changes in ECG morphology and cardiac rhythm.

3.7.1 Changes in ECG Morphology

Several distinct and significant changes in ECG morphology developed over time as hypertension and LVH developed. These included significant prolongation of QRS duration, PR and QT intervals, and increased amplitude of the R and T waves. In all cases, regression of hypertrophy after 42 days resulted in complete resolution of ECG morphology to baseline.

3.7.2 QT Interval and QRS Duration

QT interval was measured using the threshold method to identify the end of T waves. To validate QT interval measurement using this software 2 transgenic and 2 F344 rats were treated with amiodarone (1mg/ml in drinking water), a drug known to prolong QT interval. Over 10 days this resulted in an increase in QTcB of 8% compared to baseline (167± 1 to 181± 1 ms, $p<0.05$), indicating the validity of this approach (figure 3.11). The changes in QT interval followed the same pattern regardless of the method used to correct for differences in heart rate. Data presented here was analysed using Bazette's formula, which is widely used in human and some rodent studies.[625]

QT interval was identical between groups at baseline, but began to rise after 14 days of I3C induction in the transgenic group (figure 3.12). This rise was progressive and sustained throughout the entire study. By day 140, QTcB was increased by 44% compared to the starting value ($p<0.001$). There was a minor increase in QT interval in the control group (p=ns). Regression of LVH after 42 days resulted in restoration of QT interval to normal in a matter of days, despite continued LVH beyond this time. This indicates that the changes causing QT prolongation are probably driven by either the prevailing haemodynamic conditions or RAS activation, rather than being integral to LVH itself. Since QT interval is influenced by serum potassium concentration this was analysed in a cohort of rats at day 84, at time point at which QT interval is significantly prolonged. No significant difference was found between groups (F344 5.14 ± 0.13mM vs TGR 5.06 ± 0.15mM, $p>0.05$), suggesting that QT changes were due to intrinsic changes in hypertrophied hearts.

Figure 3.11 Effect of Amiodarone on QTc Interval

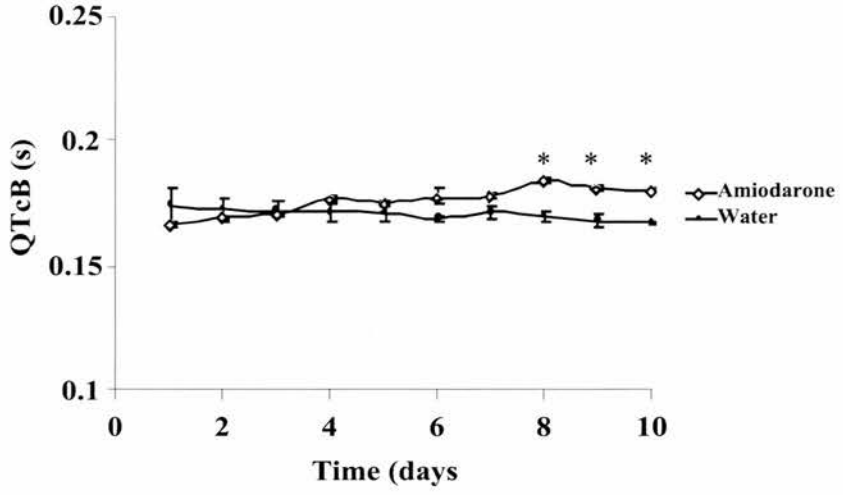

Drinking water was supplemented with amiodarone (1mg/ml) for 2 rats, and left unsupplemented for 2 others. ECG monitoring was carried out using chronically implanted radiotelemetry devices. QT interval corrected by Bazette's formula was measured for each group and averaged for each day. Mean ± SEM. *p<0.05 Amiodarone vs Water: 2-way ANOVA, Bonferroni's test.

Figure 3.12 Corrected QT Interval During the Development and Regression of LVH

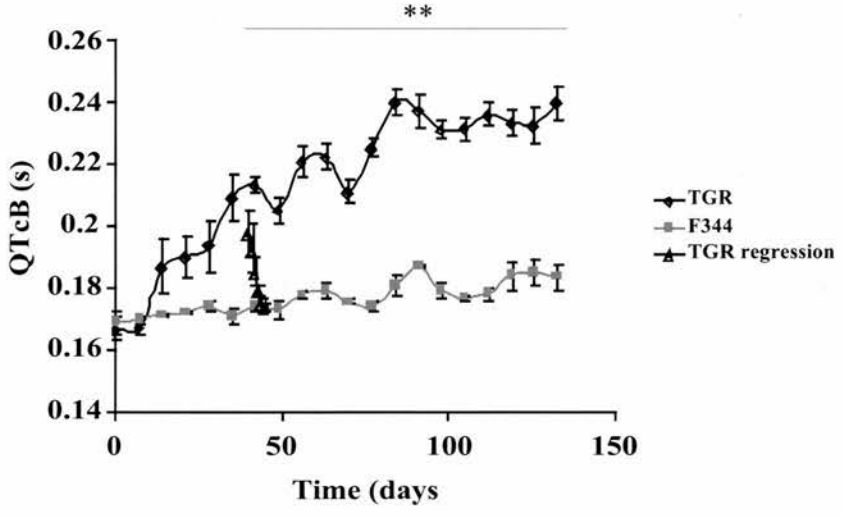

QT interval corrected by Bazette's formula was measured for all ECG recordings for each group and averaged for each week. TGR n= 8 and 4, F344 n= 6, mean ± SEM. *p<0.001 TGRvs F344: two-way ANOVA, Bonferroni's t test. TGR: transgenic, F344: Fischer 344 control.

Figure 3.13 QRS Duration During the Development of LVH

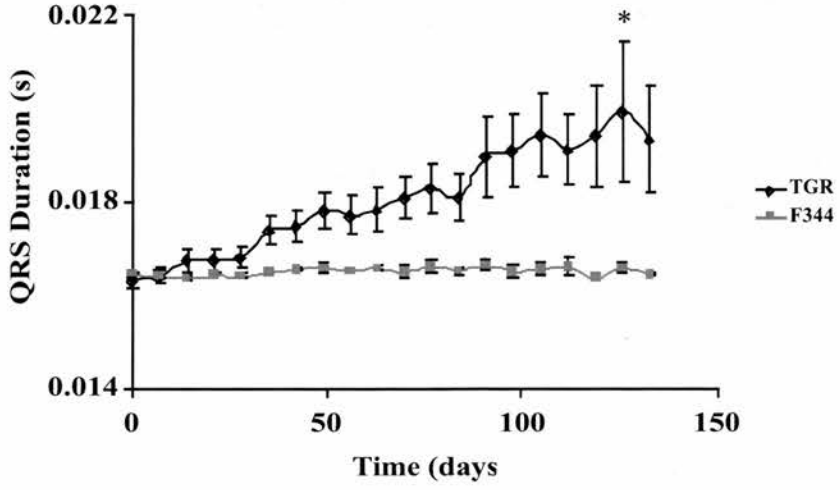

QRS duration was measured for all ECG recordings for each group and averaged for each week. TGR n= 8, F344 n= 6, mean ± SEM. * $p<0.05$ TGRvs F344. Two-way ANOVA, Bonferoni's test. TGR: transgenic, F344: Fischer 344 control.

QRS duration was initially identical between groups at baseline, and remained so until 42 days (figure 3.13). However, after this, QRS prolongation occurred, increasing by 18% by the end of the study ($p<0.05$). No evidence of bundle branch block was seen.

3.7.3 R and T wave Amplitude

In humans LVH typically gives rise to increased R wave voltages, and this was demonstrated in this study. Amplitudes were similar between groups prior to induction (figure 3.14).

Figure 3.14 R Wave Amplitude During the Development and Regression of LVH

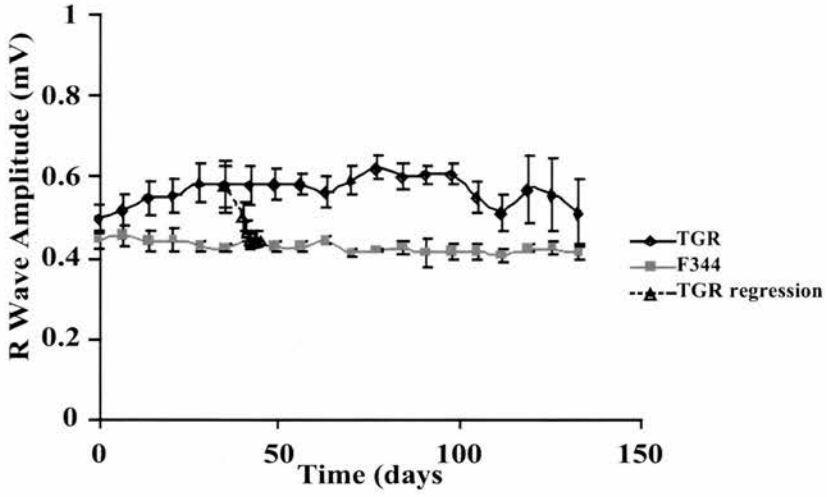

R wave amplitude was measured from radiotelemetric ECG recordings. Each point represents the mean ± SEM of all recordings for each week for each group. Although the differences between groups did not reach statistical significance at any time point, the interaction between genotypes was highly significant ($p<0.0001$, 2- way ANOVA). The decline in R wave amplitude and increased variability at later time points in TGR represents the onset of R wave alternans in this group. TGR: transgenic, F344: Fischer 344 control. TGR n= 8 and 4, F344 n= 6, mean ± SEM.

Induction caused a prompt increase in R wave amplitude, which progressed with the development of LVH, reaching a maximum increase of 26% at day 77. The differences between groups did not reach statistical significance by two-way ANOVA at any time point, although the interaction between genotypes was highly significant ($p<0.0001$). After day 77, R wave variability increased due to the development of R wave alternans in 4 of 8 of the transgenic animals. This phenomenon likely accounts for the apparent decline in R wave amplitude towards the end of the study. Interestingly the animals that developed R wave alternans did not develop evidence of echocardiographic heart failure, nor were they predisposed to premature death. Withdrawal of inducer and regression of hypertension led to a rapid decline in R wave amplitude, despite persistence of LVH at

this time point, suggesting that hypertension or RAS activation, rather than LVH are responsible for the observed increase in R wave amplitude.

Figure 3.15 T Wave Amplitude During the Development of LVH

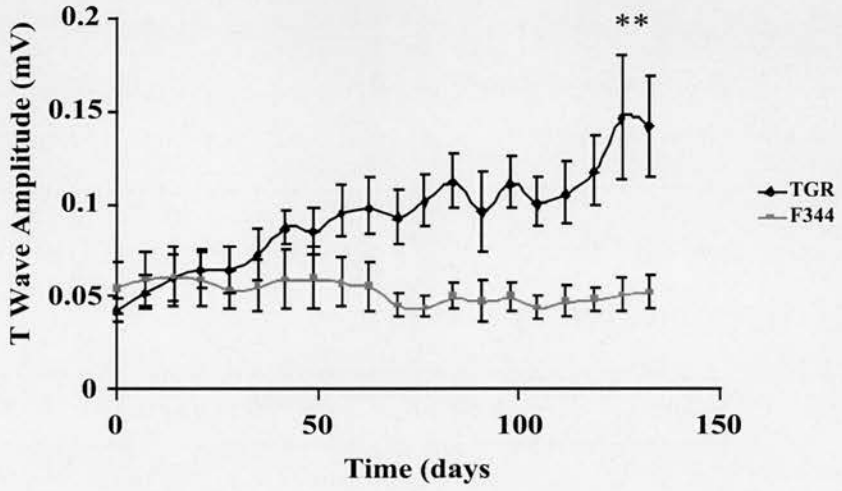

The overall interaction between genotype and T wave amplitude was highly significant ($p<0.0001$), with evidence of a progressive increase in amplitude in the transgenic group compared to controls. TGR n= 8, F344 n= 6, mean ± SEM. * $p<0.05$ TGRvs Con. TGR: transgenic, F344: Fischer 344 control. 2-way ANOVA

Compared to baseline, T wave amplitude increased to a maximum of 0.146 mV by day 126, representing a 342% increase ($p<0.05$) (figure 3.15). Variability within the transgenic group was high.

3.7.4 Arrhythmias

ECG recordings for each animal were examined for evidence of arrhythmia, summarised below.

3.7.4.1 Ventricular Ectopy and Ventricular Tachycardia

All ECG data was reviewed and ventricular ectopy was graded according to the Lown classification.[616] Overall, the incidence of ventricular arrhythmias was low in both

groups. Ventricular ectopy (Lown Grade II) was statistically more frequent in the transgenic group (1.9 vs 0.0 per animal p=0.026). Other ventricular arrhythmias failed to reach statistical significance, and there was no evidence of sustained ventricular tachycardia (Table 3.4), even in animals that died in the final week of the study.

3.7.4.2 Bradyarrhythmias and Heart Block

One transgenic animal developed 2:1 heart block after 13 weeks: this was almost permanent, though periods of normal sinus rhythm were noted. Transient episodes of 2:1 heart block were detected in all other animals, both transgenic and control.

Table 3.4 Incidence of Ventricular Ectopy During Development of Hypertension

	Lown Grade of Ventricular Ectopy				
Genotype	**I**	**II**	**III**	**IVa**	**IVb**
	(Total incidence per animal over duration of study)				
TGR	5.6 ±2.82	1.9[a] ±0.67	0.0 ±0.0	1.0 ±0.63	1.4 ±0.91
F344	3.0 ±1.15	0.0 ±0.0	0.0 ±0.0	0.0 ±0.0	0.25 ±0.25

Results are presented as mean ± SEM. I – IVb: Lown Grade of Ventricular Ectopy. TGR n=8, F344 n=6.

[a] p=0.026 vs F344. 1-way ANOVA, Tuckey's test.

Figure 3.16 Examples of Arrhythmias Detected by Radiotelemetry

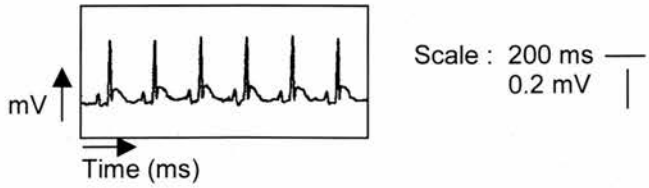

a)

b)

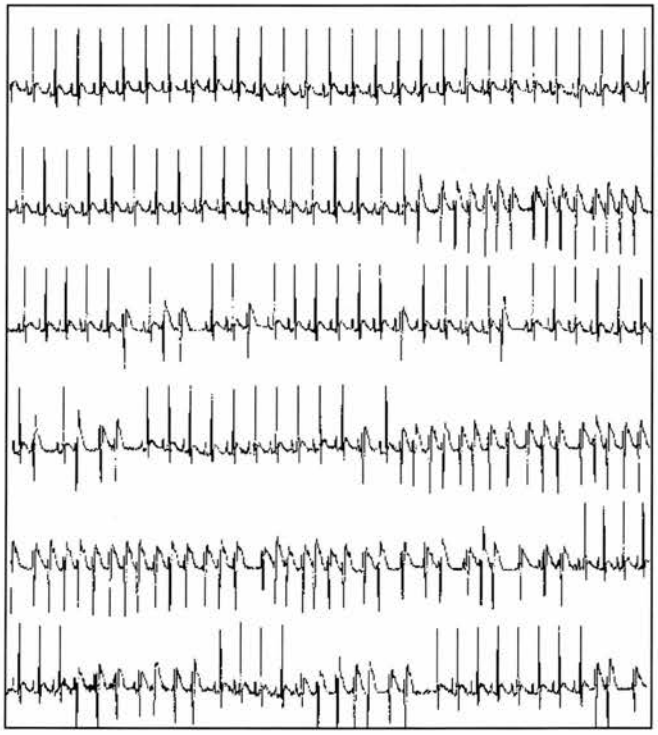

c)

Radiotelemetric ECG recordings from TGRcyp1a1ren2 fed 0.15% (w/w) I3C. a) Normal sinus rhythm. b) Ventricular bigeminy. c) Salvos of non-sustained ventricular tachycardia.

3.8 Cause of Death

Telemetered animals were studied for 140 days at which point the study was terminated following the unexpected death of 3 animals over a 2-day period. 2 animals had witnessed generalised seizures prior to death, and the third was noted to have brief focal seizures on the day prior to death. Analysis of telemetric ECG recordings at the time of death in these animals did not reveal any specific arrhythmia to account for the seizures, nor was there a significant rise in blood pressure to suggest the development of malignant hypertension.

Figure 3.17 Renal and Cardiac Histology at Day 140

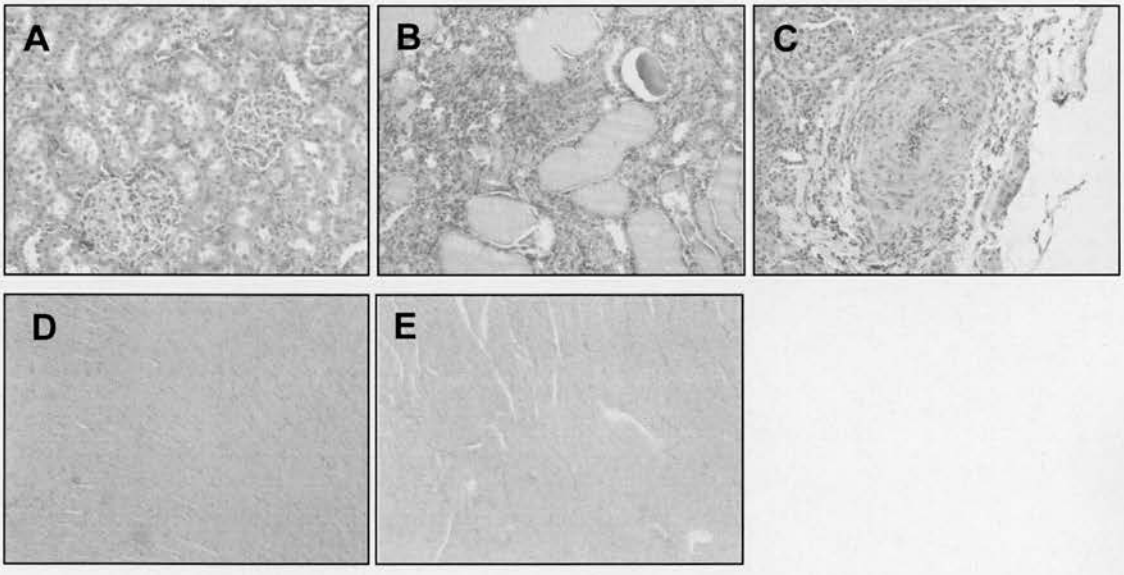

Haematoxylin and eosin stained kidney sections from Fischer F344 (A) TGRcyp1a1ren2 (B-C) B: hyaline tubular cast formation (h). C: severe arteriolosclerosis (a). Picrosirius red stained cardiac sections from F344 (D) and TGR (E) demonstrating mild interstitial fibrosis.

oedema to account for the seizures. Cardiac histology did not suggest recent or previous myocardial infarction nor was there a significant difference in interstitial fibrosis (figures 3.16 and 3.18). Renal histology revealed changes consistent with severe ischaemia secondary to hypertensive arteriolosclerosis (figure 3.16). It therefore seems likely that the rats suffered from renal impairment, causing metabolic disturbance and seizures.

Figure 3.18 Left Ventricular Fibrosis at Day 140

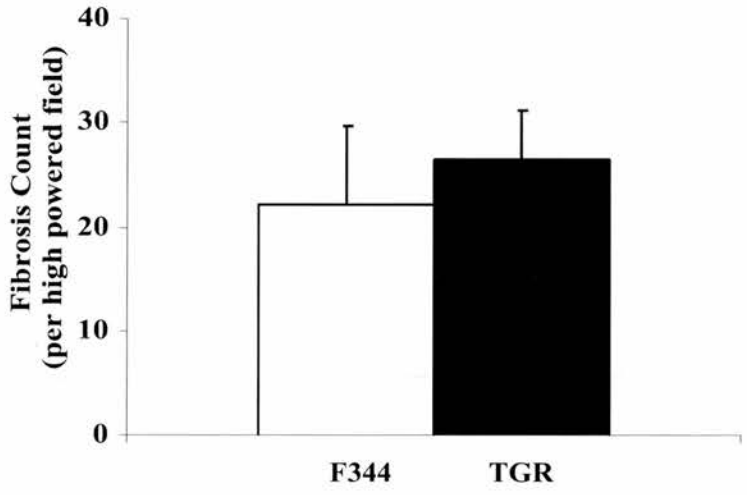

Fibrosis was quantified (arbitrary units) from high-powered photomicrographs of picrosirius red stained left ventricular sections using a grid method. TGR n= 4, F344 n= 4, mean ± SEM. p = ns, TGRvs F344. TGR: transgenic, F344: Fischer 344 control. 1-way ANOVA, Tuckey's test.

3.9 Discussion

3.9.1 Dose-Dependent Phenotypes

This study has demonstrated that TGRcyp1a1ren2 develops chronic sustained hypertension when transgene expression is induced with 0.15% (w/w) I3C. This is in distinct contrast to induction with the higher dose, 0.3% (w/w) I3C, which causes malignant hypertension.[581] The explanation for this profound difference in phenotype probably relates to both the rate of blood pressure rise and the level of RAS activation. Similar levels of blood pressure are reached with both drug doses, but the onset of hypertension is more rapid with the higher dose. Presumably an acute rise in blood pressure leads to endothelial injury, whereas a gradual increase is better tolerated with more time for compensatory and repair processes to act. Another difference is the rate and level of plasma prorenin increase. In response to 0.15% (w/w) I3C this rises more slowly and peaks at values a quarter of those seen with 0.3% (w/w) I3C.[581] Therefore the combination of acute severe hypertension, and excessive prorenin may be required for malignant vascular injury to occur.

Extensive studies in TGRmren2-27 suggest that hypertension is mediated by a tissue RAS,[574,626] and that the development of malignant hypertension is primarily determined by RAS factors rather than hypertension per se. For example subpressor doses of ACE inhibitors or angiotensin receptor antagonists can inhibit vascular injury without significantly affecting blood pressure.[627,628] Similar results have been reported for the 2 kidney one clip model of MH and dTGR, in which RAS activation also occurs.[629,630] Furthermore, crosses of TGRmren2-27 on to a Sprague-Dawley (Edinburgh) genetic background previously demonstrated that susceptibility to MH is independent of blood pressure,[564,631] whilst rats transgenic for rat renin demonstrate vascular injury in the absence of hypertension.[288] Genome wide mapping studies of TGRmren2-27 crossed to Fischer or Lewis backgrounds identified two loci, on chromosomes 10 and 17, which contribute to the lethal MH phenotype. These loci are close to the ACE and At1 genes and plasma ACE activity was significantly different between these backgrounds.[631] Therefore, it seems plausible that differences in RAS activity, perhaps at the tissue level,

contribute to the development of MH. Human studies have identified an association of the ACE D-allele with MH.[632,633] Given the weight of this evidence it seems that the phenotypes observed with different doses of I3C relate to differences in RAS activation, rather than the kinetics of blood pressure change. Although there is a clear dose-dependent effect, the relationship between I3C dose, prorenin expression and hypertension is non-linear. This is consistent with previous work which demonstrated a logarithmic relationship between human plasma renin level and hypertension in short term studies in another transgenic rat model.[618]

3.9.2 Plasma Renin Angiotensin System

Analysis of plasma prorenin and renin at intervals during induction of hypertension demonstrated a curvilinear increase with time. Prorenin elevation was much greater than renin compared to controls, whilst plasma angiotenin II did not differ statistically from control at any time point. In these respects TGRcyp1a1ren2 is similar to the other prorenin-based transgenic rat models of hypertension, TGRren2-27, TGRα1AT$_r$renin and TGRα1ATren2.[288,408,562] Previous work points to an effect of prorenin at the level of the tissue RAS in mediating hypertension and end organ damage in these models,[567,574,626,627] and there is evidence to support this in TGRcyp1a1ren2 as well.[407,581] It is likely that prorenin levels have to be substantially elevated to mediate this effect, as short-term infusion studies using recombinant prorenin in monkeys, stroke prone SHR or rats transgenic for human angiotensinogen, do not demonstrate any effect on blood pressure.[313-316] Emerging evidence of a possible receptor for renin/prorenin may explain some of the putative direct effects of prorenin,[412,634] but these are likely to be small since conventional RAS inhibitors are effective antihypertensives in rats transgenic for prorenin.[408,577,587,627,635]

Angiotensin II levels were higher in F344 animals than previously reported,[581] and this may have obscured any increase in the transgenic group. Possible explanations include activation of the RAS by anaesthesia or during sample processing.

3.9.3 Haemodynamic Characterisation

Hypertension was induced in TGRcyp1a1ren2 within days of exposure to 0.15% I3C (w/w), leading to a progressive rise in blood pressure over a month, followed by a prolonged period of sustained hypertension, with little further change in blood pressure. In particular there was no evidence of a conversion to malignant hypertension at the end of the study. The degree of hypertension observed was similar to many other rat models of hypertension, in particular TGRcyp1a1ren2 fed 0.3% I3C (w/w). This indicates that a dose intermediate between 0.15 – 0.3% would not have any effect on maximal blood pressure, but simply modify the pattern of vascular damage. Whether an additional increment in blood pressure would be achieved by salt-loading is not clear, as this may simply accelerate end organ damage.

The plateauing of blood pressure occurred despite a continued increase in plasma prorenin and renin, suggesting that compensatory mechanisms develop to counteract RAS activation. Possibilities include down regulation of AT_1 receptors, or upregulation of vasodilatory/natriuretic pathways such as NO, EDRF, bradykinin and ANP/BNP. For example, upregulation of renal, cardiac and vascular NOS has been demonstrated in hypertensive rats.[636,637]

Complete analysis of heart rate variability and circadian rhythms of blood pressure requires power spectral analysis,[638] which was not possible with available software. Nevertheless, analysis of basic parameters such as standard deviation of the RR interval demonstrated a progressive increase in heart rate and reduction in heart rate variability in TGRcyp1a1ren2. Such changes are likely to represent alterations in autonomic control, as has been observed in studies of hypertensive subjects.[639,640] The severity of autonomic dysfunction correlates with hypertension severity [641] and appears to be regulated at least in part by the brain RAS.[642,643]

3.9.4 Reversibilty of Hypertension and Transgene Expression

In contrast to previous studies with TGRcyp1a1ren2 we studied the reversibility of transgene induction and hypertension after prolonged induction. The consequences of sustained hypertension include vascular smooth muscle hypertrophy, reduced vascular compliance, endothelial dysfunction, altered neural control of blood pressure and renal damage.[644] It is conceivable that such changes may be sufficient to prevent complete normalisation of blood pressure after removal of the hypertensive stimulus. Indeed, correction of renal artery stenosis in human patients with hypertension does not necessarily lead to improvement in blood pressure control, despite evidence of procedural success.[645] Similarly withdrawal of high salt diet from the Dahl salt-sensitive rat (DS) does not completely reverse changes in blood pressure 7 weeks later.[646]

In this study blood pressure was completely normalised within 4 days of I3C cessation at day 42. Although we did not formally assess vascular remodelling, other evidence of end organ damage, such as cardiac hypertrophy was apparent at the time of I3C cessation, suggesting that vascular remodelling was also present. It would be interesting to assess the reversibility of hypertension and transgene expression after more prolonged induction. Prorenin/renin levels were indistinguishable from controls when measured at 1 week after I3C cessation. This data suggests that sustained induction of the cyp1a1 promoter does not lead to chronic independent activity.

Only one other conditional transgenic model of hypertension has been described to date,[647] in which rat vascular chymase is over expressed in vascular smooth muscle cells under the control of the tetracycline-regulatory system. However, to our knowledge the reversibility of hypertension and transgene expression has not been reported.

3.9.5 Induction of LVH

Concentric LVH was a prominent phenotype of this model using 0.15% (w/w) I3C. The maximum increase in LVMI was 77% at day 140, which is within the range observed in similar rat models of hypertension such as SHR (260% increase at 12 months),[625] dTGR

(80% at 7 weeks),[648] TGRα1ATren2 (52% at 7 weeks),[408] DS rats (50% at 12 weeks),[649] and TGRmren2-27 (30% at 12 weeks).[650] Since these models develop similar degrees of hypertension the explanation for the large differences in LVH probably lies in the different strain backgrounds. However both TGRα1ATren2 and TGRcyp1a1ren2 are on a F344 in-bred background, and can be considered to be congenic. Presumably the large difference in LVMI between these models reflects the different ages at which hypertension develops and differences in levels of transgene expression. Cross breeding studies in rats have identified a variety of QTL's associated with variation in LV mass, including a possible contribution of NppA (ANF) promoter polymorphisms influencing LVH in WKY/SHR/WKHA/WKHT strains.[651,652] Selective cross breeding of SHR on a F344 background produced a normotensive strain with substantial cardiac hypertrophy, again suggesting a strong role for genetic determination of LVH in SHR independent of hypertension.[653] Studies in humans have identified a number of candidate gene polymorphisms that may influence susceptibility to LVH, including ACE,[654] angiotensinogen,[654] aldosterone synthase,[655] α-adducin,[656] PPARα,[657] G-protein β-3 subunit,[658] and HLA type,[659] although some associations have been disputed.[660,661] Congenic strains of TGRcyp1a1ren2 on Fischer and Lewis backgrounds which differ reciprocally for MH lethality susceptibility QTL's on chromosomes 10 and 17 have been generated in the Mullins laboratory. Since these QTL's included the ACE and At1 loci it would be interesting to investigate their effect on hypertension and LVH susceptibility in response to 0.15% (w/w) I3C.

3.9.6 Echocardiographic and Catheterisation Studies

Although the absolute values for LVMI assessed by echocardiography and those measured gravimetrically are not entirely concordant, this is exacerbated by the fact that serial echocardiographic measurements were made in a single cohort of animals, whilst different animal cohorts were sacrificed at the specified time points for gravimetric measurement. Hence some discrepancy is to be expected. Furthermore, the assessment of LV mass by echocardiography is notoriously inaccurate,[17] especially using single plane measurements, such as the Devereux method.[611] Firstly the formula assumes the

heart is a prolate elipsoid, which is an over simplification of the geometry of the rat heart. Furthermore, measurements are made in only one dimension and cubed to estimate volume, thereby amplifying any error in measurement. Whilst the method has been validated in mice and rats,[612,662] the limitations of the method are generally accepted. More accurate assessment would require biplane or three-dimensional methods.[613,663] Within this context the values obtained in this study are probably acceptable within the limits of the method.[613,662,664]

Assessment of LV function by echocardiography in animals is prone to error due to the need for anaesthesia. The effects of different anaesthetics on cardiovascular function vary between agents, with time and between animals and strain. All adversely affect blood pressure, myocardial contractility, and heart rate to some degree.[96,665,666] The consistency of meaurements within the control group, in terms of LVMI and FS over the course of the study was relatively good, suggesting that the confounding effect of anaesthesia was consistent at different time points.

Evidence from echocardiography and left ventricular catheter studies in TGRcyp1a1ren2 suggest that LVH is compensated. In other words, there was no evidence of heart failure, though serial echocardiographic analysis demonstrated a non-significant decline in mid-wall and endocardial fractional shortening. Similar changes in cardiac function have been demonstrated in human hypertensive patients and other animal models of hypertension.[667-672] However, the methods employed predominantly examine the function of radially arranged cardiac fibres. It is increasingly recognised that subendocardial myocardial fibres are arranged longitudinally and contribute significantly to contraction in that dimension.[673,674] Furthermore, the effects of hypertension and LVH impact initially on subendocardial myocardium, so that an early decline in longitudinal systolic function is often observed before any effect on radial function.[675] Increased radial function is frequently observed in LVH in a variety of species,[104,676-679] and it is not until late in the hypertrophic process that this is impaired. It is not clear exactly whether the increase is a true compensatory mechanism, or an

artefact of hypertrophied myocardium.[667] More sophisticated echocardiographic techniques that examine myocardial velocities in vivo, such as Doppler tissue imaging,[680,681] have also provided convincing evidence that pathological LVH is associated with subtle abnormalities of contraction and myocardial strain at an early stage that simply cannot be appreciated with conventional techniques. In addition, such tecniques provide evidence that the functional effects of LVH are spatially heterogeneous, and that single site measurements are probably inadequate to decribe overall LV systolic function.

LV catheterisation data demonstrated no significant difference in LV systolic or diastolic performance using a variety of parameters. Again, anaesthetic effects are likely to have been significant since aortic pressure was significantly less than telemetric recordings at this time point. Almost all methods used to evaluate LV systolic function are heart rate and load-dependent, in that they vary with the prevailing haemodynamic conditions of the heart due to the Frank-Starling mechanism.[94,682] If loading conditions are identical between groups, this would be less of an issue, however since one group is hypertensive this must be important. A gold standard, load-independent assessment of global LV systolic function is end systolic stress (Ees) derived from pressure volume loops obtained under variable loading conditions.[94] A variety of methods are available to obtain pressure volume loops, including microconductance catheters,[683-686] sonomicrometric crystal implants,[417,687] or simply monitoring LV dimensions by echocardiography whilst measuring LV pressure.[688-690] However, in animals all these methods require anaesthesia and manipulation of loading conditions either surgically or pharmacologically so that many new confounding variables are introduced.

Whether extended induction, beyond 5 months, would eventually lead to heart failure can only be a matter of speculation at present. The occurrence of sudden death in 3 of 8 animals at this time point suggests that any study aiming to address this question would require a large number of TGRcyp1a1ren2 so that attrition due to fatal complications

could be tolerated, without diminishing the statistical power of the study. Perhaps salt-loading would also accelerate LV dysfunction.

3.9.7 Left Ventricular Fibrosis

At a gross histological level left ventricular fibrosis did not develop, though more definitive experiments are required to determine if extracellular matrix composition changes, or if turnover is altered. Histological stains are an imprecise method for determining fibrosis, but are likely to detect a large difference. In addition analysis of fibrosis localisation, (eg perivascular, subendocardial) may reveal specific sites of fibrosis. Ventricular fibrosis is generally held to be stimulated by RAS activation [196,355,363,374,518,691] via autocrine/paracrine effects on non-myocytes,[692] and would therefore be expected to be observed in this model. Ventricular fibrosis is well documented in similar models of hypertension/LVH such as TGRmren2-27[217,580] and SHR[693] though it is disputed whether the main stimulus is haemodynamic or endocrine. Since the rats used in this study were mature, the effects of RAS activation/LVH on ventricular fibrosis may have been masked by ageing.[199,694] Fibrosis is counteracted by upregulation of BNP[695] and kinin/NO,[369] so it is plausible that such mechanisms could protect the heart from fibrosis in this study. Furthermore, fibrosis is not an inevitable consequence of RAS activation, as mice expressing angiotensinogen in the heart develop LVH without fibrosis.[352]

3.9.8 Cardiac Electrical Remodelling

Further evidence of adaptation to hypertension was demonstrated by progressive changes in ECG parameters such as R wave amplitude, QT interval, QRS duration, heart rate and heart rate variability. It was notable that many of these parameters continued to change even after blood pressure and LVH had plateaued, for reasons that are unknown. This emphasises the dynamic nature of LVH.

QT interval prolongation is well recognised in LVH,[696] and is thought to be largely due to reduced voltage-gated K^+ channel expression.[697,698] Altered membrane currents,

sarcoplasmic calcium load,[699] increased muscle mass and fibrosis[700] predispose to arrhythmias and sudden death.[56,701] However, little evidence of proarrhythmia was seen in this study, and cardiac arrhythmia was excluded as a cause of death. Continuous collection and analysis of radiotelemetric data was not possible due to the constraints of the telemetry system and data handling limitations. Therefore arrhythmic events are likely to have been underestimated. Despite this, the relative difference between transgenic and F344 rats remains surprisingly small. It is possible that spontaneous ventricular arrhythmias in rats with this degree of LVH are rare,[702] and that the proarrythmic effects of LVH may only be manifest with physical or biochemical stress.[703] Another explanation may be the lack of ventricular fibrosis in this model, which is generally considered to be pro-arrhythmic.[697]

Interestingly, intermittent R-wave alternans developed in 4 of 8 transgenic animals after 100 days. Altered intracellular calcium handling appears to underlie this phenomenon,[704,705] leading to altered mechanical performance and predisposition to ventricular arrhythmias. The significance of this observation is unclear at present, but may indicate imminent ventricular decompensation.

All ECG parameters normalised upon withdrawal of I3C from the diet. It was notable that regression of electrical remodelling was coincident with changes in blood pressure and RAS parameters, whilst LVH regression appeared to lag behind. This suggests that electrical changes were induced by neuroendocrine and haemodynamic alterations rather than LVH per se. Echocardiographic regression of LVH in humans is associated with reduction in R wave amplitude,[706] and QT interval,[707] leading to improved prognosis.[708,709] Baillard et al. (2000)[625] have previously shown that QT interval correlates with LVH in SHR, and reduction of blood pressure/LVH by ACE inhibition leads to reversal of QT interval prolongation. However studies in a guinea pig model of aortic constriction have demonstrated a failure of action potential duration to correct with regression of LVH.[710] Therefore, the reversal of ECG abnormalities with regression of LVH is not inevitable.

3.9.9 Regression of LVH

Previous studies of regression of LVH in rats, mice, guinea pigs, rabbits and sheep,[62,75,606,625,710-721] have demonstrated rapid and substantial regression, including normalisation of altered gene expression. An advantage of TGRcyp1a1ren2 over other models is the ability to investigate the regression of hypertrophy and vascular remodelling without recourse to pharmacological agents or surgical intervention.

Although regression of hypertrophy after cessation of the stimulus would appear to be inevitable, there are documented instances where this does not occur.[272,722] In particular, human studies of LVH regression with antihypertensive therapy generally show only small decreases in LVMI.[723] Similarly, whilst it is logical that regression of LVH is associated with diminished expression of hypertrophy associated genes, this is not always the case in many studies of LVH inhibition,[536] or even studies of true LVH regression.[75] Indeed, haemodynamic unloading of normal hearts (ie not hypertrophied) can lead to induction of foetal gene expression.[88] In this study, BNP expression was suppressed, even weeks after removal of the hypertrophic stimulus for reasons that are not entirely clear. This suggests that recovery from LVH is an orchestrated and prolonged phenomenon. Regression is not simply the reversal of hypertrophic changes. A limited number of studies have suggested that regression is transiently associated with increased apoptosis, particularly in the subepicardium, as assessed by terminal deoxynucleotidyl transferase, oligonucleosomal DNA fragmentation or morphometry.[716,717] The identity of the cells has not been established, but it seems likely that this phenomenon only involves non-cardiomyocytes, otherwise it is likely to lead to premature heart failure.

Chapter 4

Studies of FK506 in TGRcyp1a1ren2 and TGRα1ATren2

4.1 Introduction

In chapter 3 it was demonstrated that TGRcyp1a1ren2 develops chronic hypertension and left ventricular hypertrophy in response to 0.15% (w/w) I3C. It was of interest to establish whether LVH could be inhibited independently of blood pressure in TGRcyp1a1ren2 via calcineurin blockade, as this would provide a convenient model in which to study the possible mechanisms of non-hypertrophic compensation. FK506 is a macrolide antibiotic obtained from Streptomyces tsukubaensis[487] that inhibits calcineurin phosphatase activity in combination with FK506 binding protein-12 (FKBP-12).[461,462] It has previously been shown to be efficacious in preventing LVH in other models of hypertension,[497,502,507,517,518,520] though not universally.[498,506,511] In clinical practice it is used as an immunosuppressant in organ transplant recipients, and is 100 times more potent than ciclosporin A.[488] It is extensively metabolised by hepatic cytochrome P-450IIIA1.[511]

Although the weight of evidence supports an effect of FK506 on LVH in animal models, there are several theoretical drawbacks to its use in this context. In particular FK506 may interfere with sarcoplasmic calcium release and therefore alter excitation contraction coupling.[724] This is mediated via an effect on the ryanodine receptor (RYR) regulation. In cardiomyocytes FKBP12.6 is associated with the ryanodine receptor whilst FKBP12 is cytosolic.[725] FKBP12.6 regulates the gating of the RYR channel[493] whilst FK506 induces dissociation of FKBP12.6 from the channel.[725] This situation may be analogous to heart failure where there is hyperphosphorylation/ dissociation of FKBP and a reduced ratio of FKBP to RYR,[726,727] leading to abnormal channel regulation and an impaired response to β-agonists.[149] Calcineurin has also been hypothesised to

regulate RYR function by direct dephosphorylation via an FKBP-dependent interaction.[727,728]

In clinical practice FK506 causes hypertension in 60% of patients.[729] This appears to be mediated partly by nephrotoxicity, though it can occur with normal renal function. Studies in Wistar-Kyoto rats treated with immunosuppressive doses of FK506 (5mg/kg/day) demonstrated a 50 mmHg rise in systolic blood pressure over a 4 week period which appears to be due to increased vascular ET-1 synthesis and decreased endothelial NO synthesis.[525] Lower doses of FK506 (0.5 mg/kg/day) had no effect on blood pressure. In SHR toxic doses of FK506 induce renal failure, increased renin mRNA expression, and increased plasma renin activity.[730]

Another potential problem is FK506-induced weight loss, which may be severe and potentially confound interpretation of changes in LV mass.[500] Despite these concerns it was felt the evidence for a beneficial effect on LVH in other models of hypertension justified further investigation in short term experiments in which toxicity could be minimised. Therefore the effect of FK506 on LVH was studied in TGRcyp1a1ren2 induced with 0.3% I3C over 14 days. This protocol is known to induce malignant phase hypertension with mild-moderate degrees of LVH.[581] A dose of 1mg/kg/day administered by intraperitoneal injection was chosen as this has been shown to be effective in other studies of LVH inhibition in rats.[502,517]

4.2 Systemic Effects of Malignant Hypertension and FK506

In the rat FK506 is predominantly metabolised by cytochrome p450 3A2 (P450 3A2),[489] whilst I3C is metabolised by a distinct enzyme, P450 1A1.[591] However, since I3C can induce expression of cyp3a1/2,[592] there is a possibility of metabolic interactions between FK506 and I3C, which might confound experiments. This was explored in a pilot study by administering FK506 1mg/kg/day to 2 TGRcyp1a1ren2 over 7 days, one of which received 0.3% I3C. Blood levels of FK506 were measured (Department of

Biochemistry, Royal Infirmary of Edinburgh) and found to be identical in both animals, suggesting no significant interaction had occurred (data not shown).

In initial experiments TGRcyp1a1ren2 and F344 rats were treated daily with FK506 i.p. (1mg/kg) or vehicle, commencing 3 days prior to induction with I3C 0.3%(w/w), and continuing for the whole 14 day induction period. The rationale for pre-treatment was to ensure therapeutic levels were established before hypertension was induced. Induction of malignant hypertension in TGRcyp1a1ren2 over 14 days led to a decrease in body weight of 12-16% compared to a weight gain of around 8% in F344 animals fed I3C diet (Table 4.1)($p<0.001$ TGR vs F344). The cause of this profound weight loss is unknown, but most likely includes fluid loss due to polyuria, as well as anorexia and a catabolic state due to systemic illness. FK506 had no additional effect on body mass in the transgenic groups, but in the controls FK506 reduced weight gain to about 0-4%, though this was not significantly different to water treated controls (Table 4.1, group A). Therefore, both malignant hypertension and FK506 appeared to cause severe systemic disturbance. Because of the significant weight loss drug doses were adjusted twice weekly.

Table 4.1 Effect of FK506 on Body Weight and Left Ventricular Mass in TGRcyp1a1ren2

Group	Treatment		End Body Weight (g)	Change in BW (%)	LV mass (g)	LVMI (mg/g)	LV mass/tibial length (mg/mm)
A	TGR	FK	219.5	-23.1 [A]	0.498	2.27	13.75
			±4	±2.2	±0.016	±0.10	±0.41
		H_2O	236	-16.9 [A]	0.625 [A]	2.66 [A]	16.5
			±9	±1.0	±0.010	±0.06	±0.59
	F344	FK	227	+3.1 [A]	0.467	2.06	12.09
			±8	±1.6	±0.019	±0.09	±0.8
		H_2O	237	+19.2	0.498	2.11	14.30
			±5	±1.1	±0.009	±0.03	±0.36
B	TGR	FK	228.2	-9.8 [A]	0.553	2.42	14.26
			±5	±1.8	±0.009	±0.04	±0.19
		H_2O	240	-14.1 [A]	0.630 [A]	2.60 [A]	16.32 [B]
			±5	±1.3	±0.012	±0.02	0.60
	F344	FK	230	+3.2 [A]	0.426 [B]	1.85	14.76
			±7	±2.2	±0.012	±0.02	±0.22
		H_2O	238	+8.0	0.500	2.10	15.10
			±4	±1.2	±0.013	±0.03	±0.41
C	TGR	FK	260	-12.8 [A]	0.565	2.18	14.17
			±7	±1.0	±0.016	±0.04	±0.39
		H_2O	267	-12.2 [A]	0.638 [B]	2.40	16.11 [B]
			±9	±3.0	±0.023	±0.17	±0.61
	F344	FK	222 [B]	0.0 [B]	0.451 [A]	2.03	12.17 [A]
			±5	±2.7	±0.006	±0.04	±0.20
		H_2O	253	+8.8	0.544	2.15	14.9
			±16	±1.2	±0.01	±0.03	±0.17
D	TGR	FK	247 [A]	-13.98 [A]	0.599	2.46 [A]	15.14
			±10	±3.28	±0.026	±0.03	±0.65
		H_2O	244 [A]	-14.99 [A]	0.674 [A]	2.78 [A]	17.21 [B]
			±4	±3.30	±0.009	±0.03	±0.65
	F344	FK	287	+3.56	0.58	2.01	14.69
			±8	±1.67	±0.019	±0.05	±0.41
		H_2O	296	+8.01	0.601	1.99	15.16
			±10	±5.00	±0.023	±0.07	±0.56

Statistical analyses were performed within experimental groups. One-way ANOVA, Dunnett's post hoc test. [A] $p< 0.01$, [B] $p<0.05$ vs experimental group water treated control. BW: body weight, LVMI: left ventricular mass index, FK:FK506 treatment, H_2O:water treatment. TGR: transgenic, F344: Fischer F344 control. Change in body weight was calculated from body weights at start and end of study period. Mean ± SEM. n=6 per group. Group A: treatment from day –3 to day 14 of induction, Group B: treatment from day 3 - 14, Group C: treatment from day 7 - 14, Group D: treatment from day 14-21.

Table 4.2. Plasma Renin-Angiotensin Assays in FK506-treated TGRcyp1a1ren2

Group		Treatment	Prorenin (ngAI/ml/h)	Renin (ngAI/ml/h)	AngII (pg/ml)
A	TGR	FK	**21914** [AC] ±1846	**119.6** [AC] ±10	**227.4** ±40
		H_2O	**7235**[C] ±2545	**26.6** ±9	**125.2** ±19
	F344	FK	**65** ±7	**31.5** ±6	**178.4** ±57
		H_2O	**22** ±7	**31.5** ±6	**175.4** ±22
B	TGR	FK	**13917** [AC] ±4866	**266.7** [A B] ±81	**388.9** ±62
		H_2O	**6086**[C] ±1755	**69.6** ±16	**189.8** ±47
	F344	FK	**65** ±4	**79.9** ±26	**303.8** ±61
		H_2O	**22** ±4	**50.7** ±4	**184.2** ±27
C	TGR	FK	**6274** ±5031	**147.5** ±74	**193.0** ±32
		H_2O	**6222** ±1622	**69.6** ±16	**190.0** ±37
	F344	FK	**40** ±13	**50.6** ±4	**181.6** ±29
		H_2O	**22** ±4	**52.4** ±3	**185.0** ±28
D	TGR	FK	**10734**[C] ±6227	**151.8**[B] ±41	**435.7**[B] ±85
		H_2O	**19432**[C] ±6200	**193.2**[B] ±65	**569.4**[B] ±127
	F344	FK	**53** ±14	**57.6** ±17	**296.8** ±55
		H_2O	**31** ±8	**21.0** ±3	**133.5** ±23

Statistcal analysis was performed within experimental groups: 1-way ANOVA, Dunnett's post hoc test. [A] $p<0.05$ vs water-treated transgenics. [B] $p < 0.05$ vs water-treated controls [C] $p<0.001$ vs water-treated controls. TG: transgenic, F344: Fischer F344 control. FK: FK506. H_2O: water treatment. n=6 per group. Mean ± SEM. Group A: treatment from day –3 to day 14 of induction, Group B: treatment from day 3 - 14, Group C: treatment from day 7 - 14, Group D: treatment from day 14-21.

4.3 Effect of FK506 on Hypertension in TGRcyp1a1ren2

LVH is probably induced predominantly by haemodynamic load in TGRcyp1a1ren2, so that any effect of FK506 on LVH must be in the absence of any blood pressure reduction. Systolic blood pressure was measured by tailcuff plethysmography after a 5 day period of training. Since this method has several potential limitations, particularly the need for restraint, a pilot study was undertaken in two groups of TGRcyp1a1ren2 and F344 rats to assess the accuracy of plethysmographic measurements against the gold standard, radiotelemetry. Two groups were trained to undergo tail cuff plethysmography, whilst the other two were monitored by radiotelemetry: all groups were fed identical I3C 0.3%(w/w) diet simulatneously. Figure 4.1 demonstrates that the agreement between methods was extremely high, suggesting that in our hands tail cuff plethysmography provides an accurate assessment of systolic blood pressure.

Figure 4.1 Comparison of Tail Cuff Plethysmography and Radiotelemetric Blood Pressure Measurement

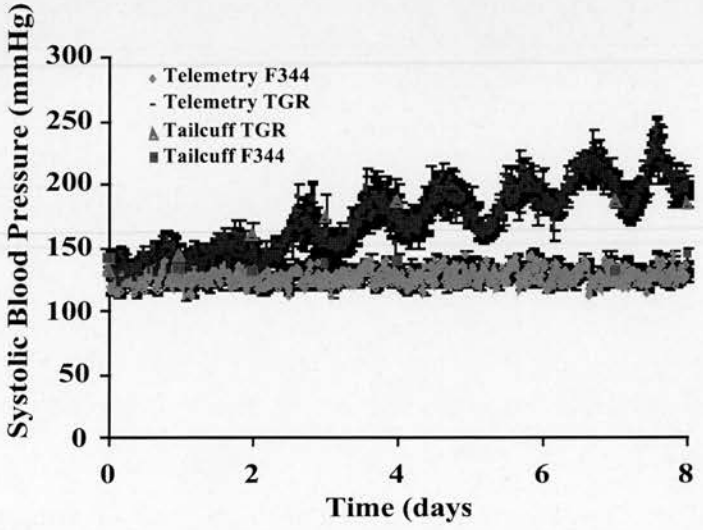

Cohorts of F344 and TGRcyp1a1ren2 were fed 0.3% I3C (w/w) for 7 days, whilst systolic blood pressure was measured by either tail cuff plethysmography or radiotelemetry. Agreement between the methods was found to be excellent. n=4 per telemetry group. n=6 per tail cuff plethysmography group.

As previously described,[581,587] 0.3% I3C (w/w) induced a rapid rise in blood pressure in water treated TGRcyp1a1ren2. Whilst the blood pressure of F344 animals was not altered by I3C or FK506, there was a significant reduction in blood pressure in transgenic animals treated with FK506 compared to those treated with vehicle (figure 4.1). After day 5 the blood pressure of FK506-treated transgenics was not significantly different from the F344 groups (figure 4.2). Therefore, unexpectedly, FK506 appeared to exert an antihypertensive effect.

Figure 4.2 Effect of FK506 on Hypertension in TGRcyp1a1ren2

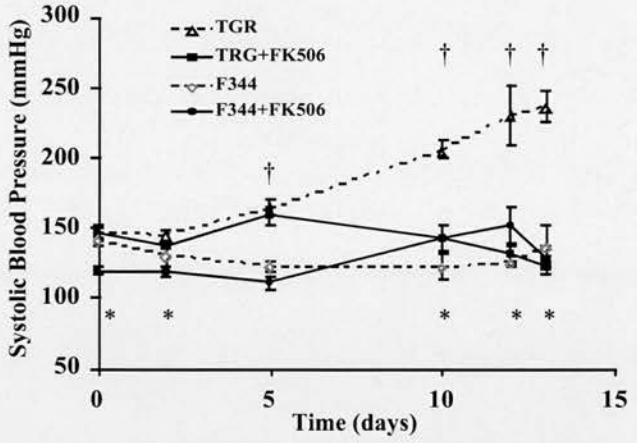

Water-treated TGRcyp1a1ren2 animals developed hypertension in response to 0.3% I3C, whilst administration of FK506 from day –3 of induction inhibited hypertension. Mean ±SEM (n= 5).* TGR + FK506 vs F344 p=NS. † TGR vs F344 p<0.001. 2-way ANOVA, Bonferroni's post-hoc test.

Although the pilot study had suggested that FK506 metabolism is not affected by I3C, the converse had not been examined. It was therefore important to establish whether or not transgene induction by I3C was inhibited by FK506. Measurement of plasma prorenin, renin and angiotensin II demonstrated that transgene induction and RAS activation occurred in both FK506 and vehicle-treated TGRcyp1a1ren2 animals (table 4.2, groupA). In fact, prorenin levels were significantly greater in the FK506 group, suggesting that transgene expression was enhanced ($p<0.05$, TGR FK506 vs TGR water). Measurement of hepatic renin expression by Real Time PCR confirmed that

transgene expression was increased 13-fold in the FK506-treated group relative to the vehicle group (0.066±0.0004 units water treated vs 0.897±0.1995 units FK506 treated, $p<0.001$) (figures 4.3 and A2.4, tables A2.5, A2.6). Therefore, FK506 appeared to inhibit the development of hypertension despite excessive induction of transgene expression.

Figure 4.3 Hepatic ren2^d Transgene Expression in Group A

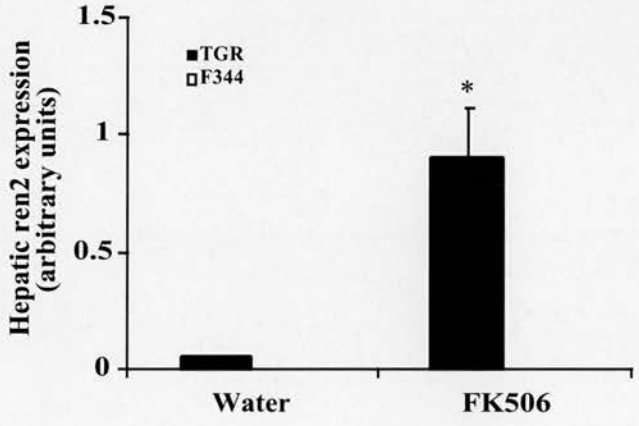

Hepatic expression of transgene-derived ren2^d mRNA was quantitated relative to ribosomal 18S RNA expression by real time PCR. In keeping with plasma prorenin levels there was significantly more expression in FK506-treated TGRcyp1a1ren2. There was no detectable ren2 mRNA in F344./ (n=3 per group, means ± SEM). * $p<0.001$, TGR + FK506 vs TGR + water. 2-way ANOVA, Bonferroni's post-hoc test.

4.4 Effect of Late Treatment with FK506

To further define the effect of FK506 on hypertension a series of experiments were performed in which the administration of FK506 was delayed until after the establishment of hypertension. Previous work has demonstrated that vascular damage follows a predictable time and organ-dependent course in this model.[581,587] Therefore the rationale was to identify a time point at which FK506 failed to inhibit hypertension, and correlate this with pathology. The time points chosen were days 3, 7 and 14 of induction.

At day 3, hypertension is established but no vascular damage is identifiable by routine histology. Day 7 is characterised by fibrinoid necrosis in the mesenteric and cardiac circulations, whilst day 14 is marked by the onset of renal fibrinoid necrosis. To simplify terminology, the different intervention time points will be referred to as summarised in figure 4.4. Group A: FK506 treatment commenced 3 days prior to induction of hypertension for 14 days (described above). Groups B and C: FK506 treatment commenced on day 3 or day 7 of hypertension induction respectively, until the experiment was terminated at day 14. Group D: FK506 treatment commenced on day 14 until day 21.

Figure 4.4 Design of FK506 Experiments in TGRcyp1a1ren2

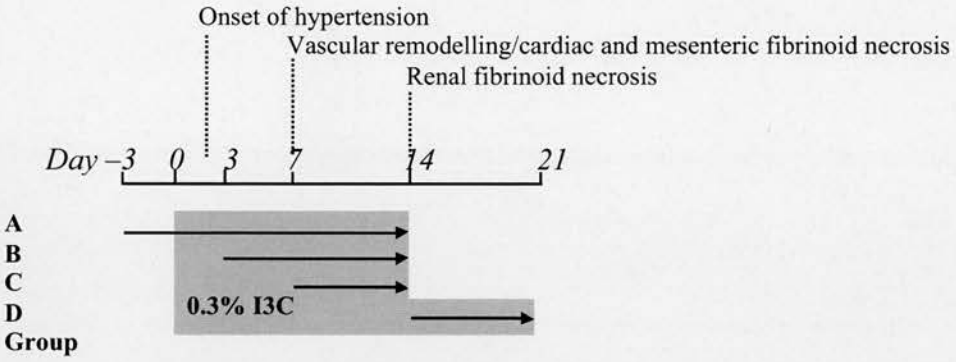

Experimental groups consisted of TGRcyp1a1ren2 and Fischer F344 controls (n=5-6). Arrows represent the timing and duration of treatment with FK506 or water. The shaded area represents the timing and duration of dietary 0.3% (w/w) I3C. Group A began treatment with FK506 or water 3 days prior to the commencement of dietary I3C. Group B started treatment on day 3 of induction and group C on day 7. Animals in groups A, B and C were culled after 14 days of inducing diet. Group D animals were induced with I3C for 14 days before starting FK506 or water treatment, and were culled on day 21. The timing of specific vascular events previously described in this model is indicated above the time line.

Administration of FK506 at days 3, 7 and 14 led to the immediate and sustained reduction of blood pressure to control levels (figure 4.5 a and b). Again, this occurred in the presence of normal transgene induction, confirmed by plasma renin-angiotensin assays (Table 4.2). Therefore, despite the presence of severe end organ damage, FK506 demonstrated potent antihypertensive effects.

Figure 4.5 Effect of Late FK506 Administration on Hypertension

a) Groups B and C

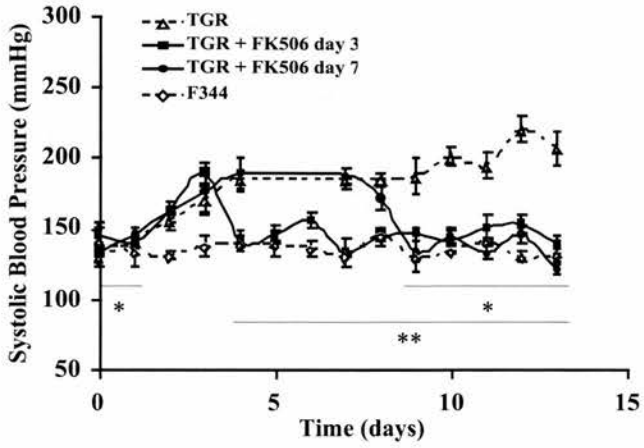

b) Group D

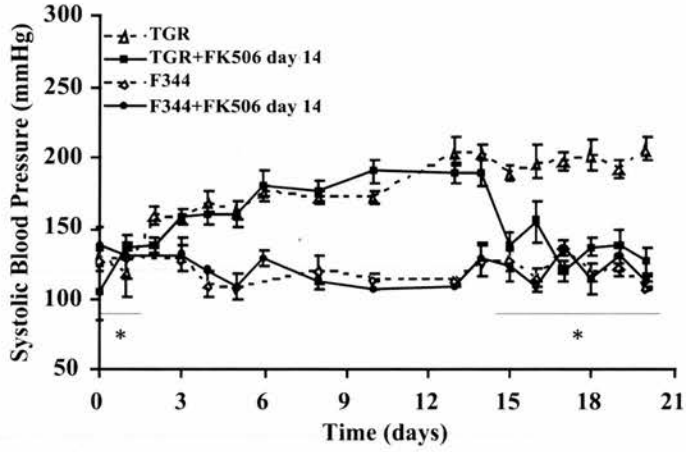

Late administration of FK506 after the establishment of hypertension at day 3, 7 (a), or 14 (b) resulted in normalisation of blood pressure to levels that were not significantly different to F344 control within 1-2 days. Mean ±SEM (n= 5). * TGR + FK506 vs F344 p=NS, ** TGR + FK506 day 3 vs F344 p=NS (all other time points TGR + FK506 vs F344 $p<0.001$). 2-way ANOVA, Bonferroni's post-hoc test.

4.5 Effect of FK506 on Vascular Injury and End Organ Damage

Induction of malignant hypertension in this model is characterised by the development of fibrinoid necrosis in distinct vascular beds at specific times.[581] Vehicle treated transgenic rats developed histological evidence of malignant vascular injury at day 14, with fibrinoid necrosis and perivascular inflammatory infiltrates in the heart, mesentery and kidney (fig 4.5a-d). By day 21, vascular injury was more florid (figure 4.5e-h). Concomitant with the antihypertensive effect, we observed complete abolition of vascular pathology in transgenic rats treated with FK506 in groups A and B (fig 4.6i-p). Vascular injury was ameliorated in animals treated with FK506 at day 7, with prevention of renal injury, though mesenteric and cardiac beds showed fibrinoid necrosis (fig 4.6q-t). However, treatment at day 14 (group D) had no influence on the severity of damage, despite the reduction in blood pressure (fig 4.6u-x).

Vehicle treated transgenic rats were significantly polyuric compared to nontransgenic animals at day 14 of induction (fig 4.7). In comparison, pretreatment with FK506 abolished the polyuria in transgenics, and an intermediate effect on polyuria was observed in animals treated with FK506 at days 3, 7 and 14 of induction (fig 4.7).

In order to distinguish between the possibilities that FK506 inhibited vascular damage simply through blood pressure reduction, versus a specific blood pressure-independent effect, an experiment was performed in which one group of TGRcyp1a1ren2 received nifedipine 0.5% w/w in the powdered diet. Nifedipine is a dihydropyridine calcium channel blocker that lowers blood pressure without effects on the renin angiotensin system. Half this dose has previously been demonstrated to control blood pressure in SHR.[731] Surprisingly, blood pressure could not be controlled using this dose of nifedipine (figure 4.8), and therefore, the question remains unanswered. Further experiments of this nature were not undertaken due to limitations of animal availability.

Figure 4.6 TGRcyp1a1ren2 Histology after FK506 Treatment

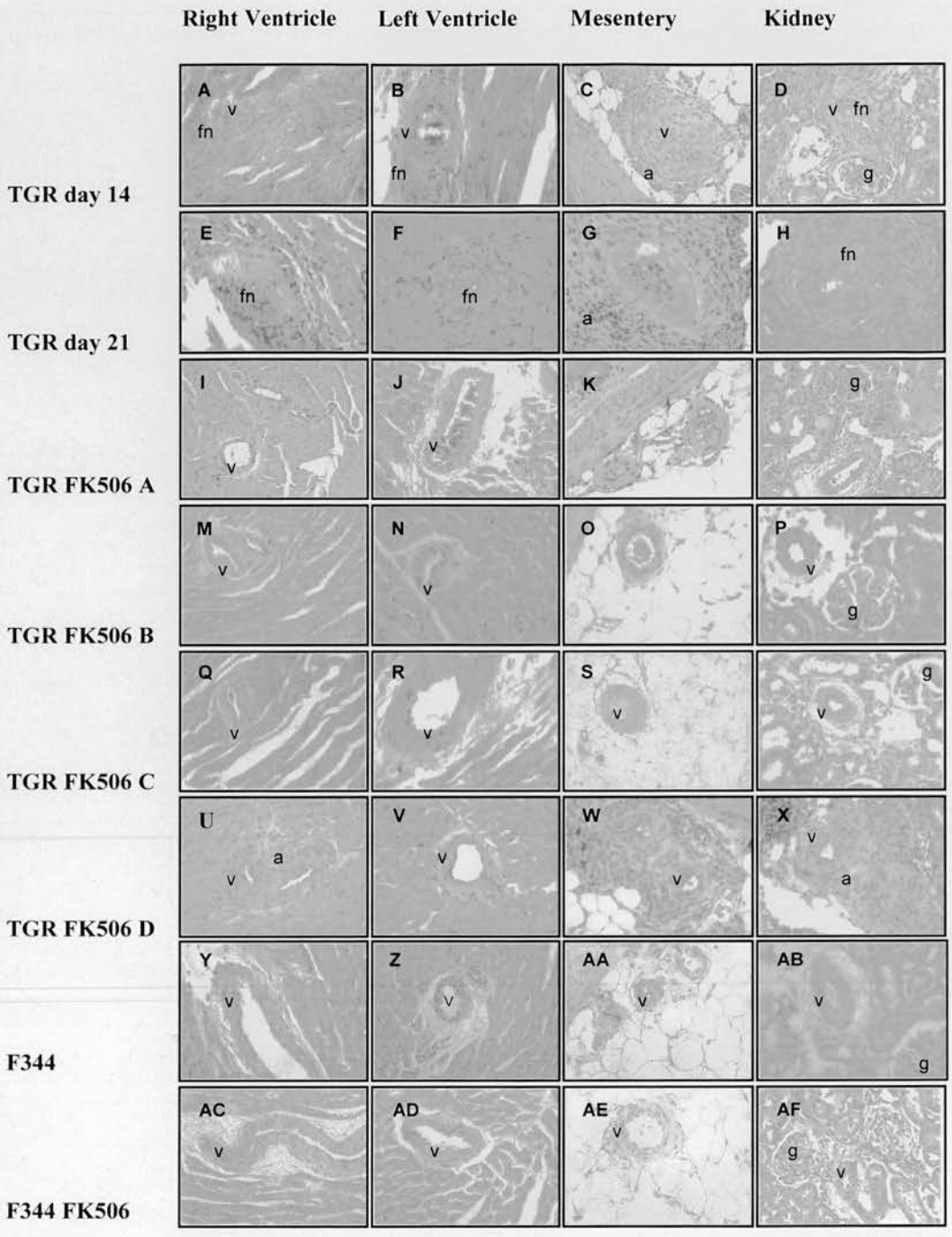

Representative haematoxylin and eosin stained tissue sections from water and FK506 treated TGRcyp1a1ren2 and F344 rats fed 0.3% I3C. TGR: TGRcyp1a1ren2, F344: Fischer control, FK506; FK506 treated. A – D: experimental group. v: arterial vessel, a: adventitial expansion, g: glomerulus, fn: fibrinoid necrosis.

Figure 4.7 Effect of FK506 on Weight-Adjusted Urine Output

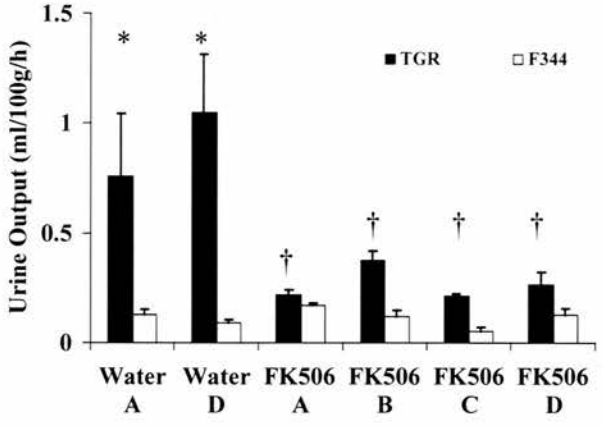

Profound polyuria was observed in water-treated TGRcyp1a1ren2 at days 14 and 21 of induction. This was dramatically reduced by FK506 treatment at all time points. (n=5 per group, mean ± SEM). * $p < 0.05$ vs F344. † p=NS vs F344. 2-way ANOVA, Bonferroni's post hoc test.

Figure 4.8 Effect of Nifedipine on Blood Pressure in TGRcyp1a1ren2

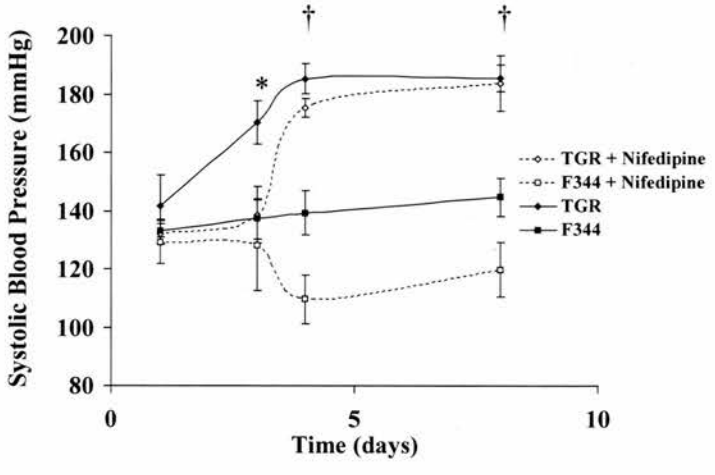

TGRcyp1a1ren2 and F344 animals were fed powdered diet supplemented with 0.3% I3C (w/w). In one group the diet was supplemented with 0.5% Nifedipine. Nifedipine had no sustained effect on the development of hypertension in transgenic animals, but significantly lowered blood pressure in F344 controls. * $p < 0.01$, † p=NS TGR vs TGR nifedipine. 2-way ANOVA, Bonferroni's test.

4.6 Effect of FK506 on Left Ventricular Hypertrophy

Analysis of LVH demonstrated a significant increase in LVMI in water-treated TGRcyp1a1ren2 group after 14 (23% vs F344) or 21 days (39% vs control)($p<0.01$ vs. control). FK506 treatment prevented LVH when started early (groups A – C) but had no effect when administered late (group D) (table 4.1). In view of the severe weight loss seen in transgenic groups, LV mass corrected by tibial length was also analysed. When this was used as the reference, significant differences between water treated transgenic groups and water treated controls remained, whilst all FK506 treated transgenic groups demonstrated suppression of LVH (table 4.1). Left ventricular brain natriuretic peptide (BNP) mRNA expression was measured by real time PCR to assess the inhibition of LVH. In untreated TGRcyp1a1ren2 there was a 1.8-fold induction of BNP expression, in keeping with the development of LVH (figures 4.9, A2.3 and tables A2.3, A2.4).

Figure 4.9 Left Ventricular BNP Expression

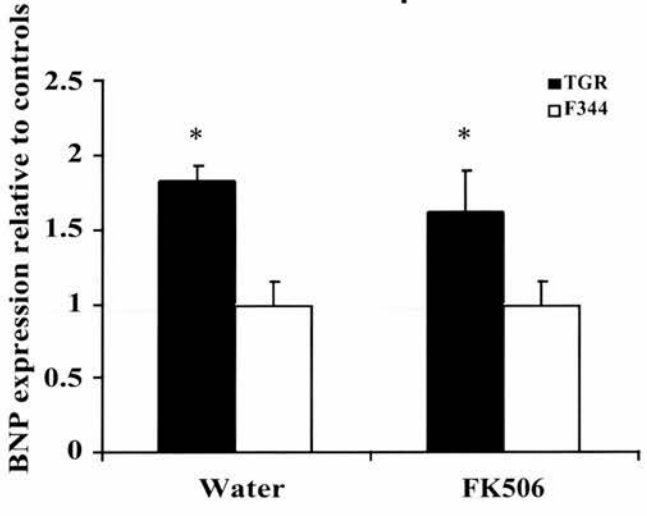

BNP expression was measured relative to 18S ribosomal RNA expression in left ventricles from experimental group A. Water treated TGRcyp1a1ren2 animals exhibited a 1.8-fold induction relative to controls. FK506 did not significantly diminish BNP induction in transgenics despite inhibition of hypertension and gravimetric LVH. N=4 per group (mean ± SEM). *$p<0.05$ vs control. 2-way ANOVA, Bonferroni's post-hoc test.

However BNP levels in FK506 treated transgenics did not differ significantly from untreated transgenics (figure 4.9). Therefore the protective effect of FK506 on ventricular remodelling was incomplete, despite the absence of haemodynamic load.

4.7 Effect of FK506 on Left Ventricular Function

Theoretically FK506 may impair cardiac function by altering sarcoplasmic calcium regulation,[491] reducing cardiac output and thereby blood pressure. Previous reports have demonstrated a similar effect with CsA.[521] To exclude this as an anti-hypertensive mechanism, heart function was examined by M-mode and Doppler echocardiography. Doppler echocardiography examines the velocity and direction of blood flow within the heart, allowing cardiac output to be estimated using equation 5 (chapter 2).[103,732] In addition, LVH leads to increased ventricular stiffness, causing altered diastolic function,[672,733,734] which is reflected in changes in transmitral Doppler spectra such as peak inflow velocities, early filling deceleration time (dt), rate of early filling deceleration (dV/dt) and isovolumic relaxation time (IVRT) as illustrated in figures 4.10 – 4.12.

There was no difference in, heart rate, fractional shortening, dt, dV/dt, V_{max} or E/A ratio between treated and untreated transgenic groups. Cardiac output was increased in FK506 treated transgenic and non-transgenic animals, though this was only statistically significant in group A transgenic animals (table 4.3). Furthermore, endocardial fractional shortening was increased in all transgenic groups compared to water treated controls. All TGRcyp1a1ren2 animals developed evidence of diastolic dysfunction, with prolongation of the isovolumic relaxation time (IVRT)($p<0.001$), and interestingly this was not corrected by FK506 treatment (table 4.3). Therefore, cardiac systolic function appeared to be increased in TGRcyp1a1ren2 animals, whilst early relaxation was impaired. Furthermore, FK506 appeared to increase rather than impair cardiac output.

Figure 4.10 Apical Four-Chamber View and Pulse Wave Doppler Sampling Position

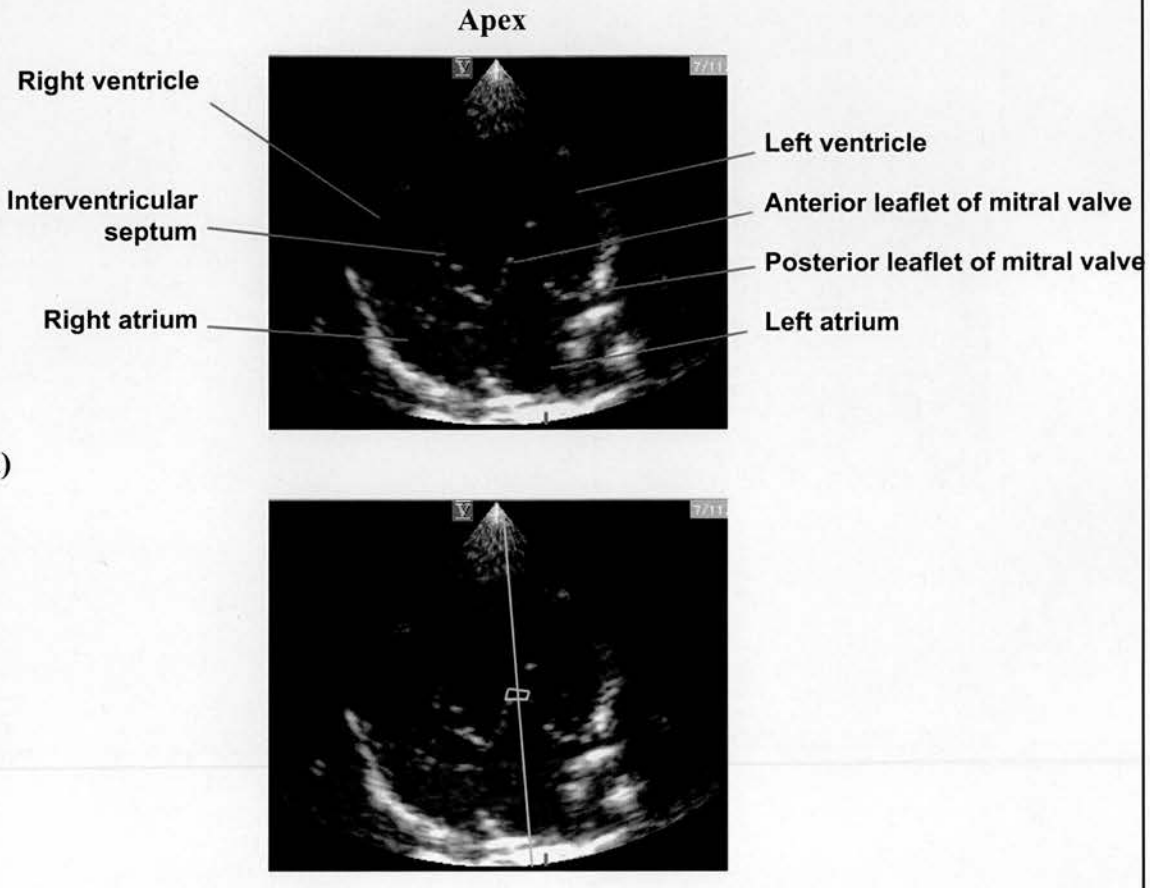

Echocardiographic B mode apical 4 chamber view of rat heart to illustrate sample position for mitral valve inflow Doppler measurement. a) Early diastole: mitral valve is opening. b) Doppler probe is aligned from apex to transect mitral valve as shown by the yellow line below. The approximate position of the sampling volume is indicated by the yellow box.

Figure 4.11 Transmitral Doppler Inflow Parameters.

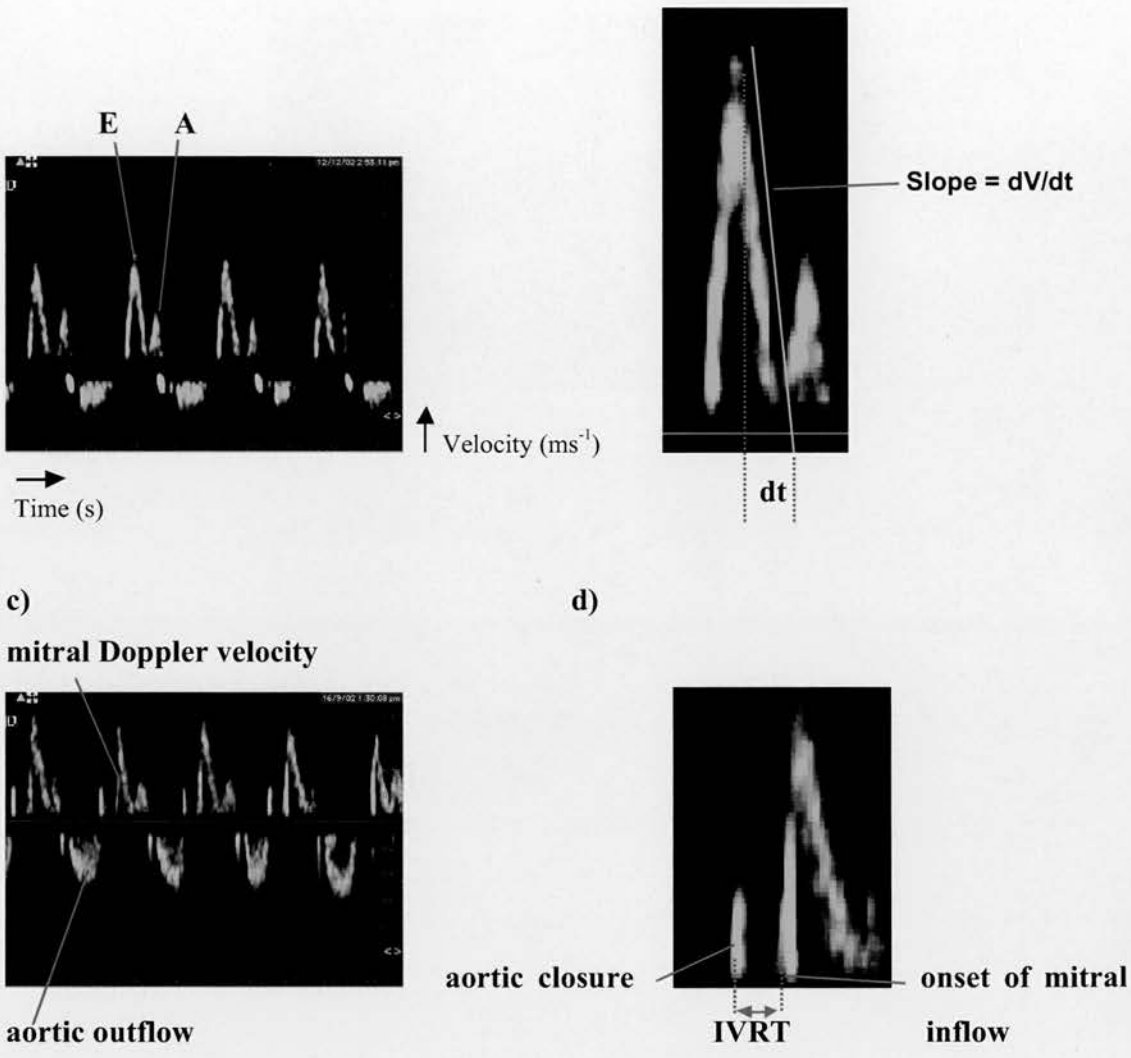

Isovolumic relaxation time (IVRT) was measured as illustrated in figure 4.10. a) Transmitral Doppler inflow velocity comprises E and A waves as indicated. b) Measurement of early filling deceleration time was taken from the peak early velocity to the end of the early filling wave. The rate of deceleration was measured as indicated by the solid yellow line. c) Pulse wave sampling volume was placed between aortic and mitral flows so that velocity spectra of both aortic and mitral flows are detected simultaneously. c) detail of c demonstrating the IVRT between the signal generated by aortic closure and the onset of mitral inflow.

Figure 4.12 Apical Five-Chamber View and LVOT Doppler Velocities

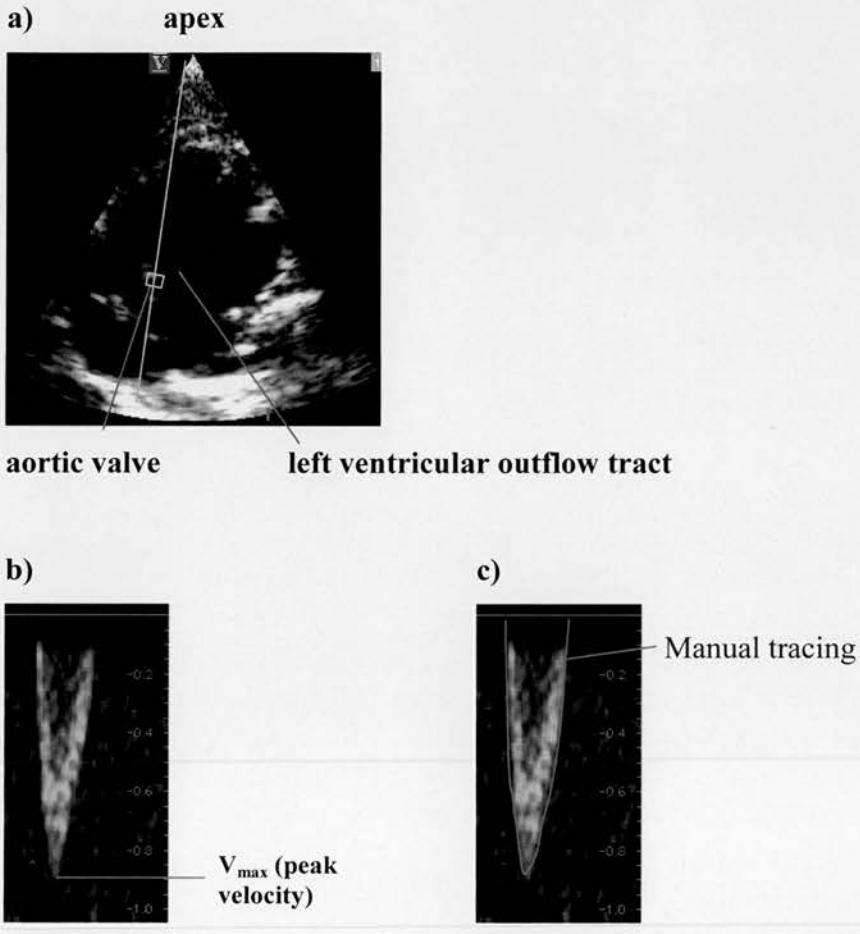

Echocardiographic B mode apical 5-chamber view of rat heart to illustrate sample position for left ventricular outflow tract Doppler measurement. a) The apical five-chamber view was used to obtain left ventricular outflow tract velocities, by positioning the Doppler probe as indicated. b) Pulse wave Doppler was sampled in the outflow tract to allow measurement of peak velocity. c) Velocity time integral (VTI) was calculated by manually tracing round the outflow tract velocity spectra. Cardiac output could be calculated from VTI, heart rate and outflow tract diameter using equation 5, chapter 2.[103]

Table 4.3. Effect of FK506 on Cardiac Function in TGRcyp1a1ren2

Group	Treatment	HR (bpm)	eFS (%)	E/A (ratio)	dt (ms)	dV/dt (ms^{-2})	IVRT (ms)	Vmax (ms^{-1})	CO ($ml\ min^{-1}$)
F344	H_2O	294 ±7	53.6 ±1.9	1.66 ±0.08	0.051 ±0.002	14.1 ±0.8	28.2 ±1.1	0.75 ±0.00	75.8 ±6.2
F344	FK506	292 ±7	71.7 [A] ±1.4	1.48 ±0.06	0.050 ±0.002	14.0 ±0.7	30.0 ±1.4	0.84 ±0.05	94.1 ±4.9
A TGR	H_2O	274 ±6	73.6[B] ±3.9	1.63 ±0.14	0.049 ±0.001	13.5 ±0.7	35.4 [A] ±0.2	0.95 ±0.15	66.9 ±9.2
D TGR	H_2O	281 ±10	66.6 [A] ±4.0	1.50 ±0.18	0.052 ±0.006	13.7 ±1.9	43.3 [B] ±3.4	0.73 ±0.10	68.4 ±1.0
A TGR	FK506	304 ±12	82.7 [A] ±2.2	1.39 ±0.10	0.059 ±0002	11.9 ±0.5	35.7 [B] ±2.5	0.91 ±0.01	99.1 [A] ±6.0
D TGR	FK506	262 ±10	71.7 [B] ±5.1	1.56 ±0.16	0.050 ±0.003	12.3 ±0.8	37.8 [A] ±1.6	0.93 0.19	73.0 ±1.1

Control groups were pooled for analysis according to treatment. H_2O: water treatment, FK: FK506 treatment, TG: TGRcyp1a1ren2 transgenic, F344: Fischer F344 control, HR: heart rate, FS: endocardial fractional shortening, bpm: beats per minute, E/A: ratio of early and late transmitral filling velocities, dt: deceleration time of early mitral fillling, dV/dt: rate of early filling deceleration, IVRT: isovolumic relaxation time, Vmax: maximal left ventricular outflow tract velocity, CO: cardiac output. [A] $p<0.05$, [B] $p<0.01$and [C] $p<0.001$ vs water treated control. 1-way ANOVA, Dunnett's test.

4.8 Effect of FK506 on TGRα1ATren2

FK506 treatment has been used in several different animal models of hypertension, without any antihypertensive effects being reported. Therefore, to broaden the scope of these experiments FK506 was administered to another ren2-based transgenic rat model of hypertension, TGRα1ATren2.[408] In this model mouse ren-2^d is expressed constitutively from the liver under the control of the human α1-antitrypsin promoter, leading to hypertension and premature death at around 7 weeks after birth. This model is on an inbred F344 background and can be considered to be congenic with

TGRcyp1a1ren2. Therefore, TGRα1ATren2 is almost identical to TGRcyp1a1ren2, except that transgene expression is more highly restricted to the liver, hypertension develops at an early age and malignant hypertension develops unpredictably around 7 weeks of age.

Figure 4.13 Systolic Blood Pressure in TGRα1ATren2.

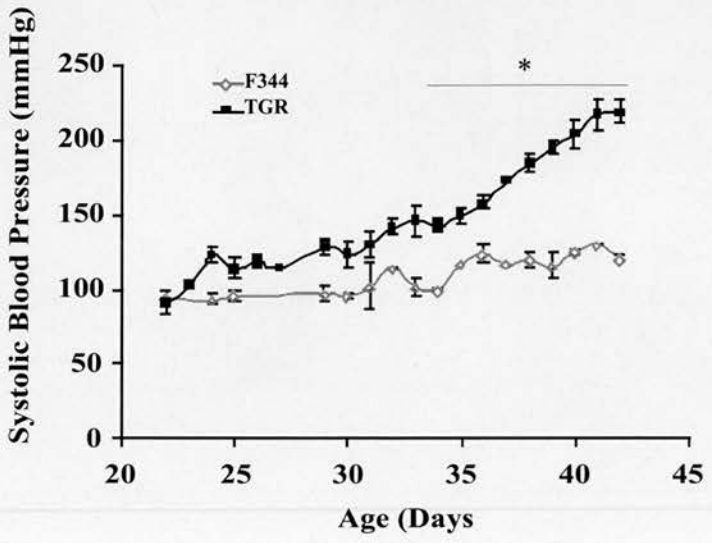

Male TGRα_1ATren2 develop severe hypertension after weaning compared to non-transgenic littermates (* $p<0.05$ vs control). n=6 per group. 1-way ANOVA, Dunnett's test.

Male TGRα_1ATren2 and nontransgenic littermates were studied from weaning (day 21) to 42 days of age. During this time hypertension developed with a final blood pressure of 218±8 mmHg in transgenics and 120±2 mmHg in controls (figure 4.13). Treatment with FK506 abolished hypertension, with a blood pressure of 137±6 mmHg at day 42, without any effect on hepatic transgene expression (figure 4.14a and 4.15). Similarly LVH was also abolished by FK506 treatment (figure 4.15b). However, for reasons that are not clear 2 of 10 transgenic animals failed to respond to FK506, and developed hypertension and LVH. The effect of FK506 on weight gain was studied. Vehicle treated transgenic animals had a reduced growth rate compared to nontransgenic

littermates. However, FK506 treatment reduced weight gain in nontransgenic animals but had little additional effect in transgenics (figure 4.16).

Figure 4.14 Effect of FK506 on Systolic Blood Pressure and LVH in TGRα_1ATren2

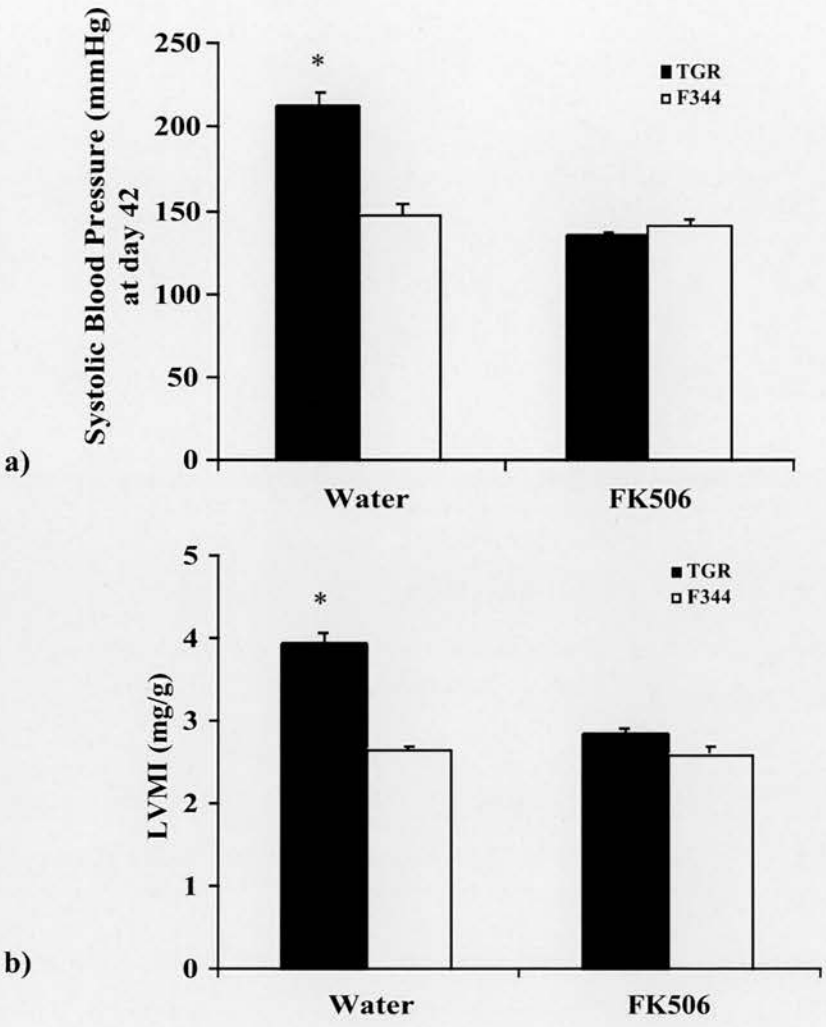

FK506 treatment in TGRα_1ATren2 completely abrogated hypertension at day 42. Left ventricular mass index was significantly elevated in water treated transgenic animals compared to controls. FK506 treatment reduced LVMI to control levels. (* $p<0.05$ vs control) (n=6). 2-way ANOVA, Bonferroni's test.

Figure 4.15 Hepatic Renin Expression in TGRα_1ATren2

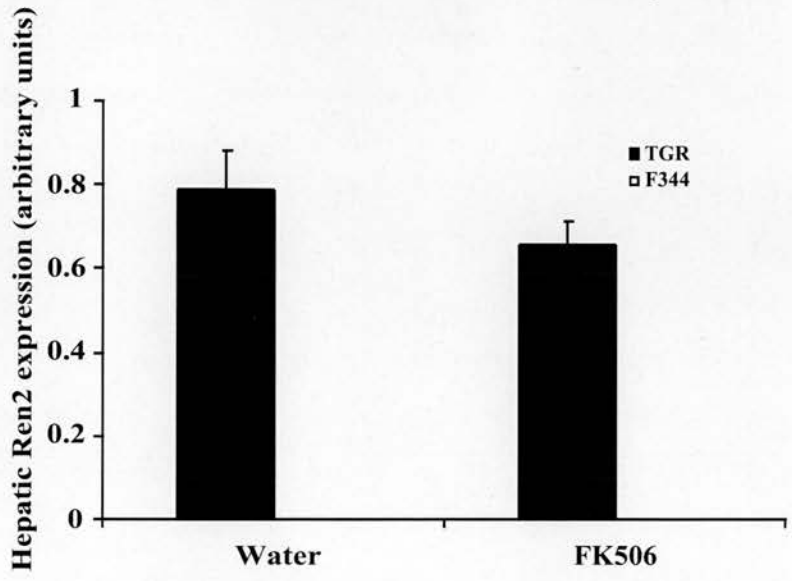

No hepatic ren2 expression was detected in controls: there was no significant difference between transgenics treated with water or FK506 († p=NS TGR + water vs TGR +FK506). p=NS, 2-way ANOVA, Bonferroni's test. Mean ± SEM.

Figure 4.16 Growth Curves for TGRα_1ATren2

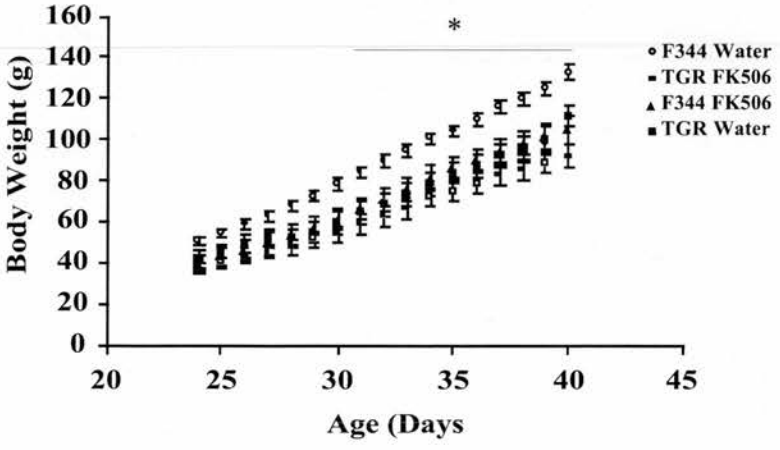

Growth was no different between groups except TGR treated with FK506 and controls treated with water * p<0.05 TGR+FK506 vs Control +water. n=5 per group, means ± SEM. ANOVA, Bonferroni's test.

4.9 Possible Mechanisms of Action

The mechanisms by which FK506 exerts an antihypertensive effect are not obvious, but the data described so far may provide some clues. The potent antihypertensive effect of FK506 contrasts with the lack of effect of nifedipine, a conventional antihypertensive agent. This suggests that FK506 may have a novel mode of action, or that it inhibits a critical pathway in the maintenance of hypertension in these models.

The fact that FK506 had immediate effects on blood pressure at all time points, but did not lower blood pressure in control animals implies that the mechanism is specific to the development of hypertension, as opposed to normal homeostatic regulation of blood pressure. Furthermore, since FK506 has not been shown to affect blood pressure in other diverse models of hypertension, the likelihood is that the effect of FK506 is particularly important for the development of ren-2-mediated hypertension. Current knowledge of the RAS suggests that ren-2-mediated hypertension is dependent on the production of angiotensin II, which leads to vasoconstriction and salt retention. Therefore, it seemed likely that FK506 might inhibit angiotensin II signalling in either the kidney or resistance vessels. Previous work has demonstrated that angiotensin II-mediated vasoconstriction involves activation of PKC,[735] ras-GTPase,[736] and MAPK pathways.[737,738] Specific inhibitors of these signalling molecules can ameliorate hypertension and vascular injury in animal models.[736,739,740] For example p38 and ERK inhibitors administered to homozygous TGRmren2-27 animals diminish renal injury independently of blood pressure.[740] It has also been shown that calcineurin interacts with some of these pathways in the heart, and that calcineurin inhibition leads to inhibition of MAPK and PKC signalling.[547] Therefore it seemed plausible that the effect of FK506 might be to block AII-mediated vasoconstrictor pathways in resistance vessels.

To explore this possibility the activation of MAPK signalling pathways in mesenteric vessels was examined by Western blotting of protein extracts from mesenteric tissues. Mesentery was studied as this is a well-vascularised tissue from which resistance vessels can be easily dissected. In order to examine processes involved in the development of

hypertension, as opposed to processes activated by hypertension itself, an early time point, day 4 of induction, was chosen. TGRcyp1a1ren2 and F344 animals were induced for 4 days, and treated with either vehicle or FK506. Western blots of mesenteric protein extracts were probed with antibodies specific for activated forms of p44/42 MAPK (ERK) p38 MAPK and p54/56 JNK. Unfortunately no reproducible pattern could be identified, and the role of these signalling pathways remains to be defined (data not shown).

4.10 Summary

Experiments designed to allow the study of pressure-independent inhibition of LVH were confounded by the unexpected antihypertensive effect of FK506. This phenomenon was explored in more detail, and it was shown that FK506 was a potent antihypertensive even after the development of severe end organ damage, including renal injury. In addition to lowering blood pressure, FK506 inhibited end organ damage at a histological level, though in the heart, expression of a hypertrophic marker, BNP was not diminished, nor was diastolic dysfunction corrected. These findings were also generalisable to another transgenic model of hypertension, TGRα1ATren2. Although the antihypertensive mechanism of FK506 is unknown, an interaction between FK506/calcineurin and vasoconstrictor signalling pathways is a theoretical possibility that remains to be substantiated.

4.11 Discussion

4.11.1 Mechanism of Antihypertensive Action of FK506

The finding that FK506 exerted an antihypertensive effect in TGRcyp1a1ren2 and TGRα1ATren2 was surprising. FK506 has been studied in several animal models of hypertension, including the Dahl salt-sensitive rats,[507,516-518] abdominal aortic constriction models,[498,502,506] and mineralocorticoid-induced hypertension,[520] with only one report of a minor blood pressure reduction.[498] Indeed, hypertension is a common side effect of FK506 in organ transplant patients.[729]

The mechanism by which this effect is mediated is obscure, but several possibilities, which are not mutually exclusive warrant further discussion.

1. Immunosuppression.
2. Inhibition of angiotensin II-mediated inflammatory processes.
3. Inhibition of angiotensin II-mediated vasoconstriction and salt/water retention.

These will be discussed in more detail.

4.11.2 Immunopathologic Mechanisms in Hypertension

The fact that FK506 is an immunosuppressant raises the possibility that this lies behind the observed antihypertensive effect. It is well established that calcineurin is crucial for the activation of T-cell responses, which orchestrate immune responses to foreign antigen.[741] This occurs via calcineurin-dependent mechanisms such as inhibition of lymphokine secretion,[464,741,742] as well as calcineurin independent mechanisms such as TGFβ-induced p21 WAF/CIP1 inhibition.[743] Furthermore, FK506 has been shown to inhibit lymphocytic transendothelial extravasation.[744] In our studies FK506 was used at a dose that has previously been shown to immunosuppressive in rats.[745]

Early studies in Okamoto strain SHR demonstrated that hypertension may have an immune contribution. Thymectomy at 4 weeks of age, or thymus grafts/extracts transplanted at birth delayed the onset and degree of hypertension in later life,[746,747]

whilst immunosuppression of SHR with cyclophosphamide or mycophenolate can ameliorate hypertension.[748,749] These findings are not restricted to SHR: mycophenolate prevents hypertension in dTGR[750] and rats made hypertensive by angiotensin II infusion, partial nephrectomy or nitric oxide synthase inhibition.[749,751-753] Therefore, there are several precedents for our observations.

Exactly how immunosuppression may be antihypertensive is not clear, but it is pertinent to note that AT_1R stimulation on lymphocytes triggers proliferation and augments immune responses in a calcineurin-dependent manner.[754] Therefore, it is possible that angiotensin II stimulates lymphocyte vascular infiltration and activation, which in turn provide as yet undefined signals to vascular cells that cause endothelial dysfunction, vasoconstriction and remodelling, or alter renal sodium/water handling.

The focus of the immune response in hypertension is not obvious. What antigen(s) drives the process? Haemodynamic stress may damage vascular cells and initiate an inflammatory/immune response, but in this study treatment prior to the development of hypertension prevented any rise in blood pressure, so this potential mechanism seems unlikely to be important. In the hypertensive models studied here, an immune response against renin would be feasible, since mouse renin is antigenically distinct to rat renin, and transgene expression is induced in adult animals. However, it seems more likely that a response against transgene-derived renin would neutralize its activity, thereby preventing hypertension. Such an effect has been observed in naïve SHR transfused with anti-renin T cells.[755]

4.11.3 Inflammatory mechanisms in hypertension

Although it has long been recognised that hypertensive end organ damage stimulates tissue injury and inflammation, it has only recently been appreciated that vascular inflammation may underlie the development of hypertension itself.[756] Indeed, angiotensin II is a pro-inflammatory agent, with direct effects on chemotaxis, proliferation and differentiation of monocytes in to macrophages.[757] In addition,

angiotensin II signalling stimulates reactive oxygen species (ROS) that may secondarily stimulate inflammatory processes.[758]

Evidence points to a role for angiotensin II in stimulating inflammatory cell recruitment and activation in vascular tissues. Angiotensin II infusion in rats induces hypertension as well as marked aortic monocyte infiltration [759,760] by directly inducing MCP-1 expression in endothelial, vascular smooth muscle cells and monocytes.[761-763] In addition, angiotensin II induces expression of cell adhesion molecules (VCAM-1) and chemoattractants (IL-8, IL-10) on endothelial cells, vascular smooth muscle cells and neutrophils,[764,765] and upregulates IL-6 and TNFα expression in macrophages.[766,767] Many of these effects are dependent on AT_1 / AT_2 receptor signalling and NFκB activation.[767,768] Evidence from mice deficient in CCR-2 (MCP-1 receptor) demonstrates that failure to recruit macrophages to the vessel wall prevents vascular hypertrophy in response to angiotensin II,[769,770] thereby indicating the importance of immune infiltrates in mediating vascular remodelling: however, hypertension was mildly exacerbated rather than inhibited.[769]

Angiotensin II induces generation of reactive oxygen species via activation of vascular and neutrophil NADPH oxidase.[758] Since ROS are prime activators of NFkB signalling, and hence inflammatory responses, it seems plausible that they may have a key role in vascular inflammation and endothelial dysfunction. Angiotensin II promotes ROS generation both directly as a consequence of receptor coupling to NADPH oxidase, but also by induction of NADPH oxidase expression in the vascular wall.[771,772] The importance of this is highlighted by the failure of mice deficient in the p47 (phox) component of vascular NADPH oxidase to develop hypertension in response to angiotensin II,[771] with evidence of blunted vascular superoxide production. In addition, neutrophil activation is influenced by angiotensin II, via redox pathways and calcineurin.[758] This suggests that angiotensin II promotes vascular inflammation at multiple levels.

The question therefore arises as to how FK506 may interact with inflammatory pathways in the vascular wall, and at what level of the inflammatory cascade? The effects of calcineurin are cell-type specific, diverse and complex. Angiotensin II-mediated neutrophil NADPH oxidase induction is calcineurin-dependent, and thereby amenable to suppression by FK506.[758] In addition, neutrophil motility also appears to be regulated by calcineurin.[773] In contrast in macrophages calcineurin appears to have a suppressive role, preventing activation via IκB dephosphorylation.[774] Therefore under certain conditions FK506 and CsA activate macrophages though the doses required for this effect are greater than those generally required for lymphocyte inhibition.[774] Furthermore, in mesenteric endothelium, CsA (and presumably FK506) increases leukocyte binding and decreases expression of iNOS, suggesting another paradoxical proinflammatory effect.[775]

Interestingly, treatment of rats transgenic for both human angiotensinogen and renin (dTGR) with ciclosporin A was reported to cause a 35mmHg reduction in blood pressure, though this was not thought to be of any significance since blood pressure remained markedly raised.[514] This study found that vascular injury was ameliorated by CsA treatment, with evidence of inhibition of NFκB activity and IL-6/iNOS expression, suggesting an anti-inflammatory mechanism. Similar findings have been presented for the same transgenic model treated with dexamethasone,[750] mycophenolate,[750] etanercept[750] (anti-TNFα antibody) aspirin,[776] HMG CoA-reductase inhibitor[777] and NFκB inhibitor.[778] It is also worthwhile noting that dTGR resembles TGRcyp1a1ren2 and TGRα1ATren2 in that all are based on activation of the RAS, suggesting that angiotensin-II mediated inflammation/hypertension may be susceptible to inhibition by drugs of this type.

4.11.4 Inhibition of Angiotensin II Signalling

Angiotensin II causes hypertension and vascular injury by several distinct mechanisms. The most widely recognised effect is the vasoconstrictor response of arterioles to angiotensin II. This is dependent on AT_1 receptor activation leading to activation of

downstream signal cascades such as PKC,[735] ras-GTPase,[736] and MAPK pathways.[737,738] The interrelation of these distinct pathways is not clear, but studies of cardiac hypertrophy in mice suggest that permissive interactions, or crosstalk, between calcineurin and MAPK/PKC pathways occur.[547] Therefore, it seems plausible to speculate that FK506 may inhibit vasoconstrictor pathways, possibly via removal of essential crosstalk influences. Calcineurin is expressed in vascular smooth muscle cells, endothelium and vascular fibroblasts, and angiotensin induced dephosphorylation of STAT3,[779] and angiotensin-induced regulation of phenotypic differentiation of vascular smooth muscle cells [780,781] are mediated by calcineurin/NFAT. However, evidence for calcineurin/NFAT-mediated effects in angiotensin-induced vasoconstriction has not been described. A study of preglomerular vascular smooth muscle cells from Wistar Kyoto rats and SHR found no role for calcineurin in angiotensin II/isoproterenol induced cAMP formation.[782] Studies of isolated vessels exposed acutely to CsA or FK506 demonstrate impaired vasorelaxation[783] or even potentiation of vasoconstriction.[784]

In this study no consistent effect could be found with regard to the phosphorylation status of key MAPK enzymes required for vasocontriction, using antibodies specific for phosphorylated ERK1/2, JNK and p38 MAPK. The main reasons for this are likely to be the heterogeneity of cell types present in tissue samples as complex as whole artery, as well as alterations in signalling due to tissue handling and hypoxia during prolonged dissection.

4.11.5 Inhibition of Vascular Injury

Vehicle treated transgenic rats developed histological evidence of malignant vascular injury at day 14, characterised by fibrinoid necrosis and perivascular inflammatory infiltrates in the heart, mesentery and kidney. By day 21, vascular injury was more florid. The antihypertensive effect of FK506 was evident at all time points studied, even in the presence of substantial vascular and renal damage. Early treatment with FK506 prevented the development of vascular injury and remodelling, whilst later treatment appeared to ameliorate, or at least arrest progression.

Whether the beneficial effect of FK506 on vascular damage was purely a result of blood pressure reduction, or if there was specific inhibition of angiotensin-mediated injury was not clear. Previous studies in a variety of hypertensive animal models have indicated that vascular injury can be ameliorated by blocking calcineurin, MAPK, TNFα, NFκB and RAS signalling, without lowering blood pressure.[514,627,628,739,740,750,776,778,785] In dTGR suppression of blood pressure does not prevent vascular inflammation and end organ damage unless a renin inhibitor is used.[786] Attempts to lower blood pressure with a non-RAS antihypertensive agent in this study were unsuccessful, leaving this important question unanswered. The difference in efficacy between FK506 and nifedipine was striking, and the reason for the failure of nifedipine was unclear. As previously stated half this dose has been used to control blood pressure in SHR.[731] Nifedipine is known to be photosensitive, but care was taken to ensure fresh drug was prepared daily, so that this is unlikely to have been a problem. Since nifedipine is metabolised by P450 3A,[787,788] an interaction with I3C is a possibility.[592] Certain dihydropyridine calcium channel blockers induce cyp1a1 which would lead to transgene overexpression, but this does not appear to be a property of nifedipine.[789] It is likely that effective blood pressure control may require more than one antihypertensive agent: triple-drug therapy has been required to maintain normotension in dTGR.[786] Indeed, telemetric studies in TGRmren2-27 demonstrated that constant dose titration is required to achieve and maintain normal blood pressures with antihypertensive agents, which is rarely done in practice.[579]

4.11.6 Inhibition of LVH

A modest degree of LVH (39%) was observed in vehicle treated TGRcyp1a1ren2 rats after 21 days of severe hypertension, and a lesser degree of LVH was observed at day 14 (22%). FK506 treatment prevented an increase in LVMI, except for group D where treatment was administered late (days 14 and 21): however, using tibial length to correct LV mass (Lvtib) FK506 suppressed LVH effectively in all groups. The correct measure of LVH is controversial, particularly when there are changes in body mass. This has been investigated in a variety of species,[528-532,790] and LV mass appears to adjust in

proportion to body weight. Therefore, LVMI is probably the best surrogate marker of LVH if microscopic or cell capacitance studies are not performed.

The induction of BNP also confirmed that LVH was induced in response to malignant hypertension. However the failure of FK506 to inhibit BNP expression contradicts the assertion that FK506 inhibits LVH. This anomaly is intriguing, since the BNP promoter contains NFAT consensus elements,[82] and should be sensitive to calcineurin inhibition. Similar observations have been made with respect to CnAβ, NFATc3 and GSK-3β knockout mice, in which LVH is attenuated, without full inhibition of the LVH gene program.[87,474,536] This suggests that even in the absence of hypertension, an activated RAS initiates the molecular programme for LVH, without other phenotypic changes such as an increase in cardiac mass. In other words, various aspects of LVH can be dissociated. Exactly how this occurs is not known, but one could speculate that some aspects of LVH are dependent on humoral signals, whilst others require haemodynamic stimuli. For example, in some studies BNP expression is only increased after the development of diastolic heart failure, as opposed to LVH with normal diastolic function.[111] Alternatively, genetic markers of LVH such as BNP may simply be epiphenomena, or markers of myocyte stress/haemodynamic alteration. Some credance for this view is provided by studies of cardiac unloading in rats in which hearts were transplanted to the abdomen of recipient rats: transplanted hearts demonstrated gene expression profiles similar to LVH, despite a regression of cardiac mass. [88]

Echocardiographic studies demonstrated that endocardial fractional shortening was increased in water treated transgenic groups compared to controls. Since eFS is a load-dependent measure of LV function, this may simply reflect the effects of increased afterload (hypertension) on cardiac function.[94] Furthermore, the development of LVH may be associated with a compensatory increase in radial cardiac function, whilst longitudinal parameters decline.[104,676-679] FK506 did not have a detrimental effect on cardiac performance, in so far as fractional shortening and cardiac output were increased in some FK506 treated groups compared to water treated controls. Similar observations

have been made in invasive studies using intravenous FK506.[791] Furthermore in vitro studies of papillary muscle function during FK506 exposure also found no adverse effects on contractility.[792]

A variety of alterations occur during LVH that impact on ventricular diastolic function, such as impaired myocyte relaxation, myocyte ischaemia, altered myocyte metabolism, increased myocyte stiffness and increased fibrosis.[69,152,197,200,201,650,793] Diastolic dysfunction is due to abnormalities of myocardial relaxation in diastole, causing alterations in left ventricular filling. This is reflected in changes in Doppler transmitral flow indices, including prolongation of the deceleration time (dt) of early transmitral filling, decline in the rate of deceleration (dv/dt), as well as decreased peak early transmitral velocity to peak late transmitral velocity ratio (e/a ratio).[672,794,795] Such changes were not observed in this study. Isovolumic relaxation time (IVRT) is a measure of myocardial relaxation during the earliest phase of diastole, in the phase between aortic valve closure and mitral vave opening, when blood neither enters nor leaves the left ventricle (ie isovolumic phase of cardiac diastole). Prolongation of IVRT is an early indicator of diastolic dysfunction, occuring before changes in other parameters.[794] IVRT was prolonged in all transgenic groups, even after FK506 treatment. This suggests that diastolic dysfunction may be induced by RAS signalling that is not inhibited by FK506, and can be dissociated from LVH and hypertension.

4.11.7 Effect of FK506 on Transgene Induction

It was striking that FK506 treated animals demonstrated increased transgene expression compared to water treated controls. This was particularly so for animals in group A that received FK506 for the longest period, and was evident at both mRNA and enzyme activity levels. The most likely explanation is that FK506 causes transgene induction directly via cyp1a1 promoter induction. Alternatively it may be that FK506 treated animals remain healthier due to inhibition of malignant hypertension, and therefore eat more inducing diet. Although this was not formally examined it is unlikely because weight loss in FK506 treated transgenics was as severe as in water treated counterparts.

Chapter 5

Investigation of Prorenin (ren2) Uptake

5.1 Introduction

Transgenic rats such as TGRcyp1a1ren2 over express prorenin at extra-renal sites resulting in vascular damage and/or hypertension[288,408,562,581] despite the fact that prorenin is considered inactive. In these models plasma levels of transgene-derived prorenin are generally 100-1000 fold in excess of those of active renin, and angiotensins are only modestly elevated if at all.[288,408,562,581] However, angiotensin converting enzyme inhibitors and angiotensin receptor antagonists are highly effective in preventing the development of hypertension in these models,[567,577,579,627] indicating that RAS activation must be occurring somewhere. This suggests that prorenin is converted to renin at an extra-renal site, stimulating the tissue-based RAS in various organs. Some circumstantial evidence supports this hypothesis, in that subpressor doses of ACE inhibitors ameliorate end organ damage without lowering blood pressure,[567,628] though definitive interpretation of this type of experiment can never be certain. In support of this hypothesis, Ogg[408] demonstrated immunostaining for renin in coronary arteries of TGRα1ATren2 using a rabbit polyclonal antibody which recognises both rat and mouse renin. However, it is not inconceivable that such a result could be an artefact of cross-reactivity with other aspartyl proteinases such as cathepsins, which share homology with renin,[796] and are known to be present in vessel walls.[797] Peters et al. (2002)[407] demonstrated that intracardiomyocyte levels of proren2 within the hearts of TGRcyp1a1ren2 are elevated above levels expected for simple diffusion, whilst isolated adult cardiomyocytes internalize in vitro translated prorenin ($ren2^d$), leading to the generation of angiotensins. This supports a concept of prorenin uptake and local RAS activation within the heart of $ren2^d$ transgenic rats. However, the mechanism of uptake

for ren2 is completely unknown, as it is non-glycosylated and therefore unlikely to be bound by the mannose-6 phosphate receptor (M6PR) which has previously been implicated as the mechanism for human (pro)renin uptake in endothelial cells and cardiomyocytes.[399-402,798] Furthermore, uptake and activation of prorenin by this mechanism has not been shown conclusively to lead to RAS activation or to have physiological consequences.[402] We therefore hypothesised that a separate uptake mechanism for ren2^{d} exists which is distinct to M6PR, and that ren2^{d} uptake leads to activation of prorenin in cardiomyocytes.

One strategy to explore this further is to study the uptake of recombinant prorenin in vitro, in different cell types (eg cardiomyocytes, vascular smooth muscle cells, endothelial cells). Subsequent experiments to identify the mechanism responsible would require diverse approaches such as the use of pharmacological inhibitors, screening of expression libraries for prorenin binding, or the use of gene transfer techniques to express candidate receptor molecules in cell culture. In vivo uptake experiments may also be fruitful, particularly with the availability of mouse knockout models to test the role of specific molecules on renin distribution and processing.

Since there is no commercially available source for recombinant renin, we chose to produce recombinant mouse ren2. Mice are unique in that certain strains possess two renin genes (e.g. Ren-1^{d} and Ren-2^{d} in the DBA/2 strain vs Ren-1^{c} in the C57BL strain).[799-801] This appears to have arisen as a result of a gene duplication event after the divergence of mice and rats as separate species 10-20 million years ago.[802,803] All mouse renin genes consist of 9 exons and 8 introns with high homology existing between cDNA sequences, 97% between Ren-1^{c} and Ren-2^{d} and 99% between Ren-1^{c} and Ren-1^{d}.[804] Ren2^{d} protein is structurally similar to other renins:[799,805,806] prorenin (43kDa) is processed to a 38kDa active renin comprising a 33kDa heavy chain and a 5kDa light chain linked by a disulphide bridge, with an intrachain disulphide bridge.[266,807] Notably Ren-2^{d} lacks glycosylation sites,[261,805,808,809] and is therefore ideal for investigating glycosylation independent mechanisms of prorenin uptake. The crystal structure for

ren2^{d} is similar to other aspartyl proteinases, comprising an active site within a deep cleft between the N- and the C-terminal domains, with ten sub-sites within the active site that determine specificity for angiotensinogen.[810] Ren2^{d} has extreme substrate specificity, cleaving only between a leu-leu peptide bond in angiotensinogen from mouse, rat, horse, hog and dog, but not human.[811,812] Ren-2^{d} is highly expressed in granular convoluted tubules of the submaxillary gland, but also in the kidney at a level approximately equivalent to ren-1^{d}.[804,813] Deletion of ren-2^{d} in two renin gene mice has no discernable effect on blood pressure or renal structure, but causes an increase in plasma active renin and a decrease in prorenin.[814] In contrast ren-1$^{d-/-}$ mice have increased plasma concentrations of prorenin and decreased levels of active renin, with altered JGA and macula densa morphology.[815] Female ren-1$^{d-/-}$ mice are hypotensive.[815] Therefore, ren1^{d} and ren2^{d} are not functionally equivalent and ren2^{d} cannot substitute for the absence of ren1^{d}. The role of ren2^{d} is as yet undetermined.

5.2 Overview of Recombinant Renin

Previous investigators have produced recombinant (pro)renin of various species (human, marmoset, rat and mouse) using a variety of methods including in vitro translation systems, E.coli, insect cells, and mammalian cells (CHO cells, AtT-20 pituitary cells, 293, COS-1 and COS-7 kidney cells, and dog cells).[263,290,298,314,317,403,407,816-841] Purification has been carried out using methods such as antisera affinity columns,[831] pepstatin and H77-affinity chromatography,[842] immobilised synthetic renin inhibitors, ion exchange chromatography, concavalin-A-sepharose columns[825] and GST-fusion proteins.[832] In some studies the prosegment has been found to be essential for efficient expression and correct protein folding.[298,819,838] Recombinant renin has been used in a variety of situations, to study crystal structure, in vitro activity, as well as physiological role in cell culture and in vivo. The choice of expression system ultimately depends on the final use of the protein, and therefore the desired quantity, purity, and functionality.

We chose a baculoviral expression system to produce recombinant ren2^{d} as this approach has several theoretical advantages over other methods for recombinant protein

production. Insect cells are eukaryotic, and therefore should allow the generation of functionally active ren2^{d}, given the availability of cellular machinery for protein folding and disulphide bond formation.[843,844] Ren2^{d} contains two disulphide bonds that are critical to its structure and function[800,808] (Swissprot P00796), and this is therefore an important consideration. Although other post-translational modifications such as glycosylation are more primitive than mammalian cells,[816,845] this does not affect the production of ren2^{d}. The ability to grow insect cells in bulk suspension greatly enhances productivity, theoretically allowing the generation of several grammes of recombinant protein per litre of culture. If in vivo experiments are to be feasible, quantity is an important factor.

5.3 Overview of Baculoviral Expression Systems

Autographa californica multicapsid nucleopolyhedrovirus (AcMNPV) is the prototypical baculovirus used in insect-based protein expression systems.[603,604,844] This is a large double stranded DNA virus that infects arthropods. The genome is relatively large (130kb), accommodating sizeable foreign DNA inserts. The viral life cycle involves cell infection via adsorptive endocytosis, followed by replication of viral DNA in the host nucleus. Waves of gene expression occur, which can be divided into immediate early, early, late and very late. Replicated viral particles are assembled in the host nucleus, and comprise two types: occluded and non-occluded. Non-occluded viral particles are released from the cell via budding and cell lysis, infecting neighbouring cells. Occluded viral particles form aggregates of virus and protein called polyhedra, of which polyhedrin is a major component. This protein is expressed in the very late phase of infection, at around 18 hours. Polyhedrin coated particles contain several hundred viral particles and protect them from destruction: consumption by other insects leads to breakdown of occluded particles and release of infective virus, thereby completing the life cycle. Since occlusion bodies are not essential for viral propagation in a laboratory setting the polyhedrin gene can be replaced with a gene of interest, which will be highly expressed in the very late phase of infection. A variety of other viral promoters have also been used for this purpose, including p10, and basic protein.[844]

Insect cell lines available for protein expression include *Spodoptera frugiperda* (Sf),[846] *Trichoplusia ni*,[847] *Mamestra brassicae*,[848] and *Estigmene acrea*.[849] Sf9 cells are the most commonly used and have the advantage of ease of culture, high culture density and ability to grow in both monolayers and suspension. Since insect cells are eukaryotic, post-translational modification of proteins is carried out, such as phosphorylation, myristylation, glycosylation, disulphide bonding, and prosegment cleavage. However, the scope of these processes is less advanced compared to mammalian cells: for example N-glycosylation is limited to high mannose oligosaccharides, and more complex oligosaccharides are not generally seen.[845,850] Glycosylation patterns similar to mammalian cells are possible either using Estigmene acrea[851] or baculoviral vectors containing glycosylation enzymes such as β-1,4-galactosyltransferase.[845,850]

A cloned gene of interest can be introduced into the AcMNPV genome by homologous recombination using intermediate vectors containing viral sequence homologous to sequences flanking the polyhedrin locus. Recombination occurs following the introduction of virus and vector into Sf9 cells. Since this is a relatively rare event, a mechanism for selecting for appropriate recombination enhances the efficiency and removes the need for laborious screening processes. The development of modifed baculoviral DNA (*Bsu 36* I linearised) with a lethal deletion of the open reading frame (ORF) 1629 near the polyhedrin locus has facilitated the production of recombinant baculovirus. Homologous recombination between the deletant baculovirus and vector containing the gene of interest restores ORF1629 generating viable baculovirus, with a very low background of contaminating wild type virus. Furthermore, identification of recombinant baculovirus has been aided by the incorporation of lacZ reporter gene downstream to the baculoviral early to late promoter within the transfer vector, allowing screening by X-gal visualisation. Vectors are available which include immuno-tags, purification tags (His, GST) and signal sequences (gp67, mellitin, human placental alkaline phosphatase) so that a fusion protein can be produced if desired.

5.4 Recombinant ren2: General Strategy

The basic requirement for our experiments was to produce active ren2^{d} that could be used in vitro and in vivo to study cellular uptake and distribution. Therefore a method of identifying recombinant prorenin was desirable. We chose to incorporate epitope tags at the N- and C- termini of prorenin, using the 9e10 myc and haemagluttinin (HA) epitopes respectively. These epitopes have been used widely in recombinant and transgenic expression experiments, allowing convenient distinction of recombinant and endogenous protein,[852] either in vitro, or in vivo. In addition, identification of N- and C-termini in this manner enables proteolytic loss of the prosegment to be identified. Co-immunoprecipitation studies to identify interacting proteins may also be facilitated. Since protein modification in this way could alter function, it was decided to generate variants in which one or other of the epitopes was omitted. An additional design feature was the incorporation of a hexa-histidine motif (6xHis tag) to aid purification from complex protein mixtures.[853-855] Under appropriate conditions histidine rich proteins bind via imidazole groups through open co-ordination sites on transition metals such as cobalt, nickel, copper, zinc and iron with high affinity.[854-856] Immobilisation of the metal ions to a matrix through chelating compounds allows capture of histidine rich proteins, which can then be eluted using free imidazole (immobilised metal affinity chelation, IMAC).

The general strategy used to generate immuno-tagged prorenin-encoding baculovirus (illustrated in figures 5.1-5.3) is based on the method of Liu et al (1998)[857] and involves a 3 step process: 1. assembly of a ren2^{d} cDNA construct incorporating immunotags by TA-cloning PCR amplification products into an intermediate vector: 2. generation of a baculoviral transfer vector in which the ren2^{d} construct is flanked by baculoviral homology arms, lacZ gene and ORF1629 sequence: 3. recombination of Bsu36I linearised baculovirus with the intermediate vector to generate a viable recombinant baculovirus.

Figure 5.1. Step 1: TA-cloning ren2 PCR products into pUniV5HisTOPO vector.

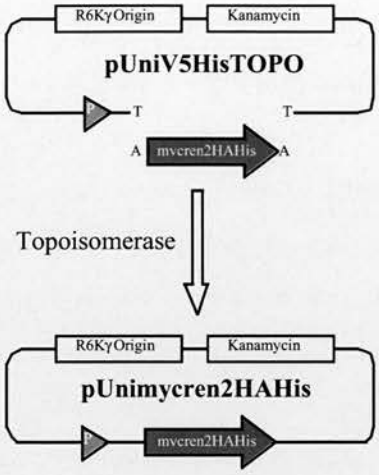

PCR amplified ren2 constructs (red arrow) were cloned into pUniV5HisTOPO using topoisomerase bound to the linearised vector. Ligation mixtures were transfected into PIR1 E.coli and selected using kanamycin. Clones were screened for incorporation of ren2 by restriction digestion, and appropriate clones were sequenced. LoxP site grey triangle.

Figure 5.2. Step 2: Generation of Donor Vector by Cre-Mediated Recombination Between pUnimycren2HAHis and pBlueBac4.5E

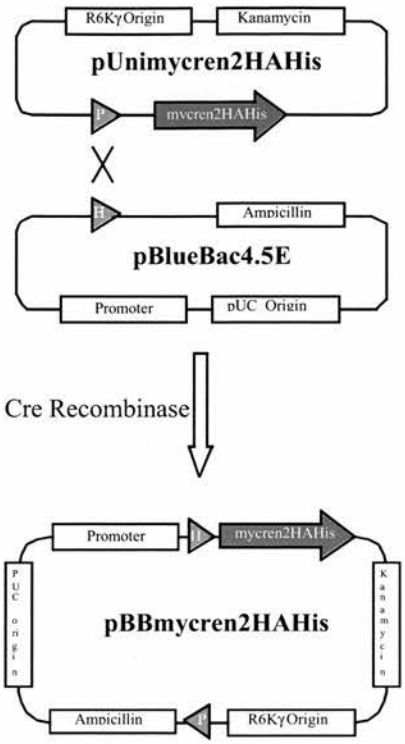

pUni constructs containing Ren2 (red arrow) were introduced into the baculoviral transfer vector pBlueBac4.5E by *Cre*-mediated recombination. A fusion vector, pBBmycren2HAHis was generated. Recombination mixtures were transfected into TOP10 One Shot *E.coli* and cultured under kanamycin selection. The fidelity of recombination was verified by sequencing. Grey triangles: *lox*P or *lox*H sites.

Figure 5.3 Step 3: Generation of Recombinant Baculovirus by Homologous Recombination.

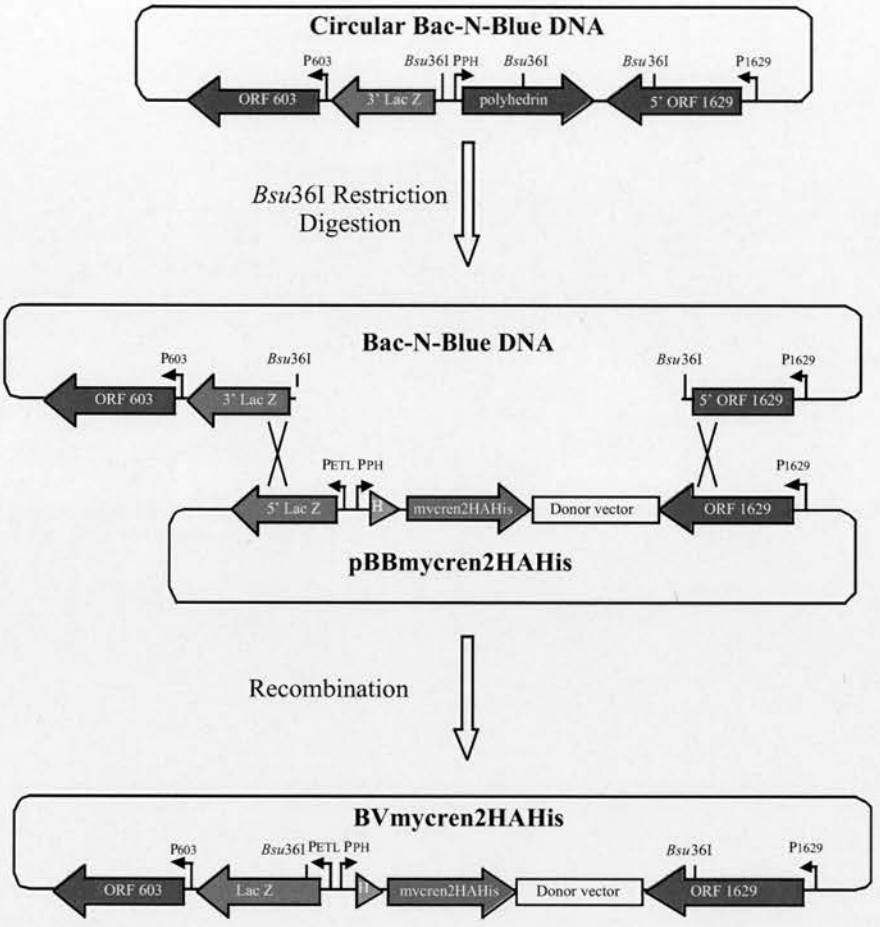

Homologous recombination between pBB vectors and *Bsu*36I linearised Bac-N-Blue DNA results in the generation of recombinant baculovirus, with restoration of the essential gene ORF 1629, and full length *Lac Z*. Blue: baculoviral sequence, turquoise: *Lac Z*, red: mycren2HAHis, white: donor vector, grey: *lox* H.

5.5 Baculoviral Expression of Recombinant Prorenin

5.5.1 Generation of a Renin cDNA Series

Ren2^d cDNA (1.2 kb) was amplified from pBS-α_1AT-Ren2 (JJM4), using a combination of primers (Table A1). Primer JJM 55 was designed to amplify the native signal sequence, whilst JJM 361 led to incorporation of a 5' myc tag without inclusion of the signal sequence. JJM 362 and JJM 363 both incorporated 3' HA motifs. JJM 362 was designed to allow read through, whilst JJM 363 included a consensus stop codon to prevent this. Combinations of 5' and 3' primers were used to create ren2^d cDNA with or without signal sequence or tags as illustrated in figure 5.4. In addition, two ren2^d cDNA's mutated at the prosegment cleavage site were amplified from pα_1AT-Ren2-7180 and pBS-α_1AT-Ren2-5136 using primers JJM 361 and JJM 362. As previously discussed prosegment cleavage in ren2 occurs between lysine$_{64}$-arginine$_{65}$. Substitution of serine for arginine (designated PRO7180), or replacing both lysine/arginine with alanine/alanine (PRO5136) theoretically render the site uncleavable by known proteases (figure 5.5).[311,318] These modifications were generated by Dr R Molina using site directed mutagenesis.

5.5.2 TA Cloning ren2^d cDNA into pUniV5HisTOPO® Donor Vector

pUniV5His TOPO® is a 2.3 kb plasmid vector with a R6Kγ replication origin, kanamycin resistance cassette (neo gene), V5 and 6xHis tag sequences, loxP site and a TOPO® cloning site for direct cloning of PCR products. TA-cloning, is a technique that takes advantage of the fact that Taq polymerase amplification of DNA leads to non-template-dependent 3' terminal adenosine bases in the amplification product. Free adenosine bases can base pair with thymidine bases present at the 3' termini of linearised vector. The vector is supplied in an "activated" form i.e. linearised, with free thymidine bases at the 3' ends, and covalently bound Topoisomerase I. Topoisomerase I mediates ligation of the vector and PCR product,[858] whilst non-ligated vector remains linearised and cannot replicate. The R6Kγ replication origin only allows vector propagation in E.coli strains expressing the pir gene, such as PIR1 and PIR2. This

feature prevents replication of pUniV5HisTopo in subsequent cloning steps in non-pir strains.

Figure 5.4 Restriction Maps of ren2 PCR Constructs

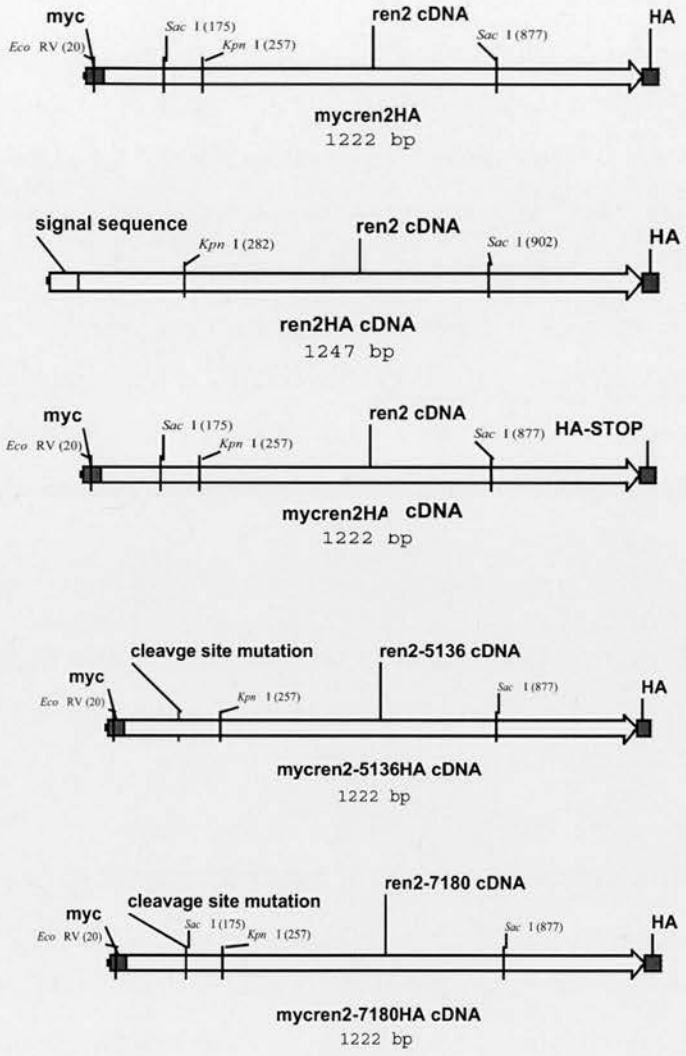

Ren2[d] cDNA was amplified using primers that incorporated 5' myc or 3' HA immunotags (blue). Ren2-5136 and ren2-7180 incorporated prosegment cleavage site mutations as illustrated in figure 5.5. Restriction enzyme cleavage sites are indicated with nucleotide positions in parentheses.

Figure 5.5 Prosegment Cleavage Site Mutations

5' GAC GTA TTC ACA AAG AGC TCT TCC TTG ACT GAT C PRO7180
Lys_{64} Ser_{65}

5' GAC GTA TTC ACA GCT GCT TCT TCC TTG ACT GAT C PRO5136
Ala_{64} Ala_{65}

5' GAC GTA TTC ACA AAG AGG TCT TCC TTG ACT GAT C Ren2
Lys_{64} Arg_{65}

Prosegment cleavage site mutations in ren2 were introduced by site-directed mutagenesis. The resulting amino acid sequences are thought to be non-cleavable by known proteases.

Table 5.1 Predicted Restriction Fragments of pUni Constructs

Plasmid	Restriction enzyme	Correct ren2 cDNA orientation (bp)
pUnimycren2HAHis	*Kpn* I	3163, 320
	Xho I/*Sac* I	2227, 702, 364,190
pUnimycren2HA	*Kpn* I	3106, 320
	Xho I/*Sac* I	2227, 702, 364, 133
pUniren2HAHis	*Kpn* I	3163, 350
	Xho I/*Sac* I	2227, 702, 364, 220
pUnimycren2-5136HAHis	*Kpn* I	3163, 320
	Xho I/*Sac* I	2227, 702, 364, 190
pUnimycren2-7180HAHis	*Kpn* I	3163, 320
	Xho I/*Sac* I	2227, 702, 364, 190

Figure 5.6 Restriction Maps of pUni Vectors

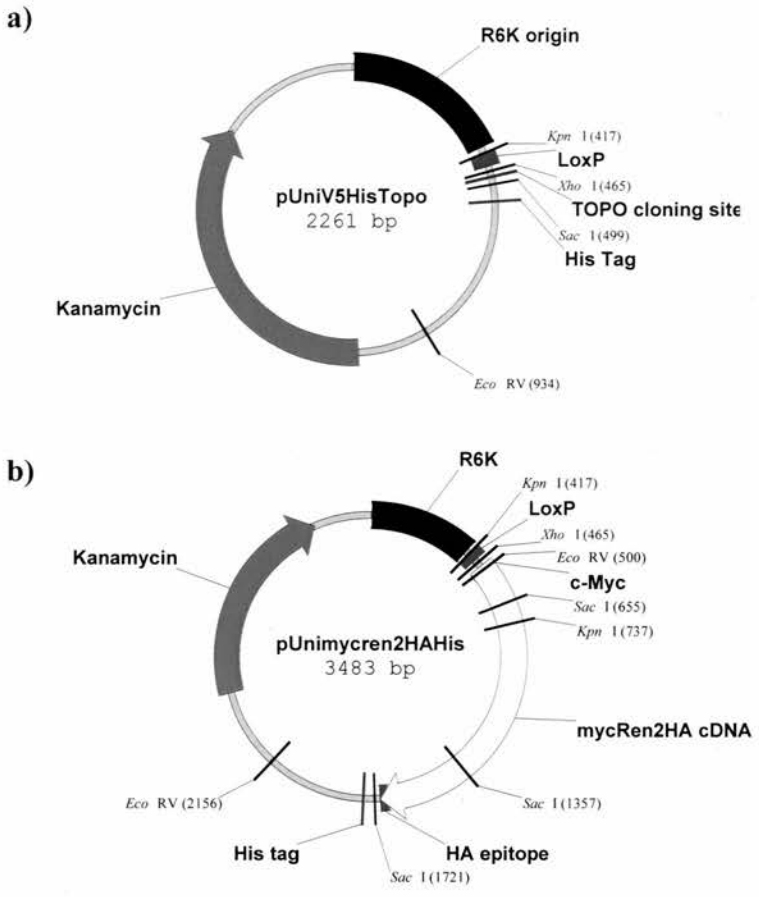

Restriction maps of pUniV5HisTOPO (a) and pUnimycren2HAHis (b). Nucleotide positions are relative to the plasmid replication origin.

Amplified ren2^{d} cDNA's were TA-cloned into the TOPO® cloning site of pUniV5HisTOPO® (2.3 kb), in frame with adjacent V5 and His tags, generating pUnimycren2HAHis (3483 bp), pUniren2HAHis (3513 bp), pUnimycren2HA (3426 bp), pUnimycren2-5136HAHis (3483 bp), pUnimycren2-7180HAHis (3483 bp). The orientation of cDNA inserts was distinguishable by restriction enzyme digestion with *Kpn* I, and *Sac* I/*Xho* I (Figure 5.7a and b for pUnimycren2HAHis). The restriction maps for vectors and ren2 constructs with myc and HA tags are shown in figures 5.4 and 5.6.

Clones were repeatedly sequenced on both strands to confirm the fidelity of PCR amplification and insert orientation using primers JJM 56, 57, 58, and 59 (Table A2).

Figure 5.7 Screening pUnimycren2HAHis Clones

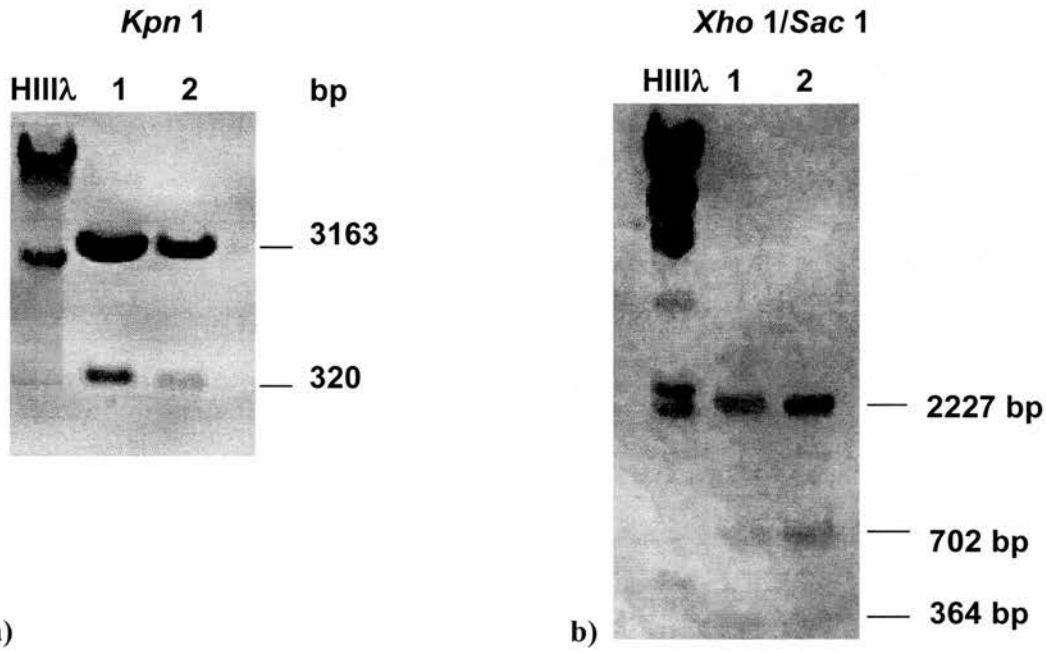

Clones (1 and 2) of pUnimycren2HAHis were restriction enzyme digested and fragments separated on 0.8% agarose gels. a) *Kpn* I digestion. Correct orientation of the ren2 cDNA insert yielded fragments of 3163 and 320 bp. b) *Xho* I/*Sac* I digestion. Correct orientation of the ren2 cDNA inserted yielded fragments of 2227, 702 and 364 bp. HIIIλ: *Hind*III digested λ bacteriophage DNA.

5.5.3 Generation of Baculoviral Recombination Vector

pBlueBac is a baculoviral transfer vector (4919 bp) used for introducing a gene of interest into *Bsu 36* I deletant baculovirus genome by homologous recombination (figure 5.3). It contains a pUC origin, ampicillin resistance gene, LoxH site, LacZ under the control of the baculoviral early to late promoter, and other baculoviral sequences, including ORF1629 and the polyhedrin promoter (figure 5.8). The recombination vectors were constructed by Cre-mediated recombination between pUni constructs and the donor vector pBlueBac (pBB) (figure 5.2). Cre is a site-directed recombinase from the bacteriophage λ, which recognises a 19 bp pallindromic recombination sequence

termed loxP.[859] In vitro Cre-mediated recombination between two supercoiled substrates, each containing loxP sites, results in a supercoiled dimer at an efficiency of 10-20%.[860,861] pBB contains a modified loxP site, termed loxH, which has reduced recombination efficiency, but interferes less with expression of the gene of interest in Sf9 cells.[857] Recombination between pUnimycren2HAHis and pBB results in a fusion plasmid, pBBmycren2HAHis (8.4 kb) in which ren2^{d} cDNA is placed under the transcriptional control of the polyhedrin promoter, and is flanked by baculoviral sequence (0.4 kb and 1.0 kb), and 5' lacZ sequence. Recombination products were transfected into TOP 10 One Shot *E.coli* and selected using kanamycin. Since TOP 10 One Shot E.coli lack the pir gene, only pBBmycren2HAHis (containing both the pUC origin and the neo gene) were propagated. Recombinant clones were verified by restriction enzyme digestion with *EcoR* V and *Kpn* I, (Figure 5.9 pBBmycren2HA) and checked by sequencing on both strands.

Table 5.2 Predicted Restriction Fragments of pBB Constructs

Plasmid	Restriction enzyme	Correct orientation (bp)
pBBmycren2HAHis	*Kpn* I	5239, 3163
	EcoR V	6530, 1656, 216
pBBren2HAHis	*Kpn* I	5264, 3163
	EcoR V	6530, 1897
pBBmycren2HA	*Kpn* I	5239, 3163
	EcoR V	6530, 1656, 216
pBBmycren2-5136HAHis	*Kpn* I	5239, 3163
	EcoR V	6530, 1656, 216
pUnimycren2-7180HAHis	*Kpn* I	5239, 3163
	EcoR V	6530, 1656, 216

Figure 5.8 Restriction Maps of pBlueBac4.5E and pBBmycren2HAHis

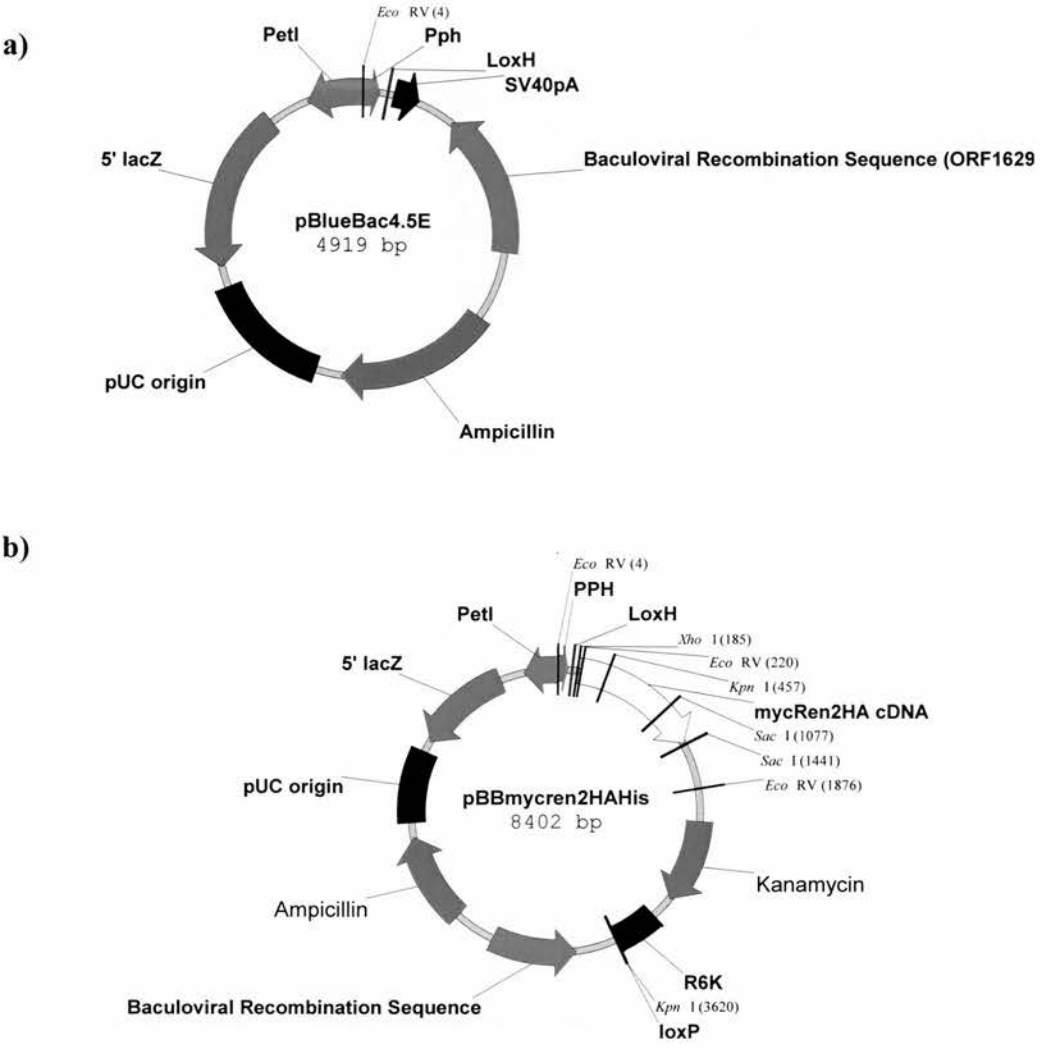

pBlueBac4.5E (a) contains a loxH site for Cre-mediated recombination with pUni vectors, such as pUnimycren2HA, leading to generation of pBBmycren2HAHis (b) In addition, it contains baculoviral sequences that allow homologous recombination with Bac-N-Blue ACNPV. PetI: baculoviral early-to-late promoter, PPH: polyhedrin promoter, R6K: replication origin, LoxH: recombination site, LoxP: recombination site, SV40pA: SV40 poly A sequence.

Figure 5.9 Screening pBBmycren2HAHis Clones

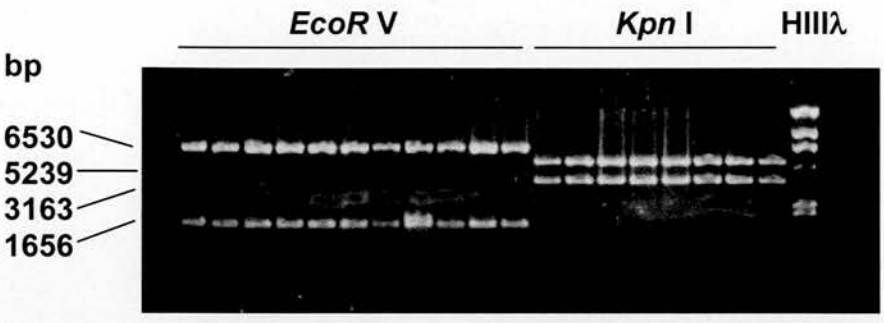

pBBmycren2HAHis clones were screened for correct recombination by restriction digestion with *EcoR* V and *Kpn* I digestion. All clones demonstrated correct recombination. *EcoR* V: 6530 and 1656 bp. *Kpn* I: 5239 and 3163 bp. 0.8% agarose. HIIIλ: *Hind*III digested λ bacteriophage DNA.

5.5.4 Baculoviral Recombination

Bsu36 I digestion of Bac-N-Blue baculoviral DNA results in deletion of the 3' sequence of ORF 1629, polyhedrin promoter and polyhedrin (figure 5.3). Whilst polyhedrin is dispensible for viral replication, ORF1629 is vital. Homologous recombination between pBB constructs and deletant virus rescues viral competency, whilst incorporating ren2^{d} cDNA into the viral genome.[862] The homology arms of the pBB constructs are 5' LacZ fragment (888 bp of shared homology) and ORF1629 (800 bp of shared homology). Recombination was mediated by transfection of Bsu36 I deleted baculovirus and pBB constructs into Sf9 insect cells using liposomes. Correct recombination also generated a full length Lac Z cDNA under the control of the baculoviral early to late promoter, allowing visual identification of recombinant viral plaques with X-gal. The recombinant baculoviruses were named using the prefix BV (e.g. pBBmycren2HAHis and Bsu 36 I Bac-N-Blue recombination generated BVmycren2HAHis).

5.5.6 Identification and Isolation of Recombinant Baculovirus

Recombination between pBB and *Bsu 36* I digested Bac-N-Blue initiated baculoviral infection in Sf9 cells. The development of blue-green plaques in the presence of X-gal within the Sf9 monolayer indicated that recombination had occurred successfully, producing full-length β-galactosidase. Under the conditions used, we routinely obtained around 10-20 individual recombinant plaques per 80mm plate. Within plaques morphological evidence of viral infection was apparent, such as cell enlargement and cell lysis (Figure 5.10). Recombinant plaques are initiated by a single recombination event: virus isolates were obtained from each plaque by aspiration of agarose gel plugs using a Pasteur pipette. Each isolate was individually propagated on a small scale for further characterisation of recombination and protein expression.

Figure 5.10 Morphology of Baculoviral Plaques

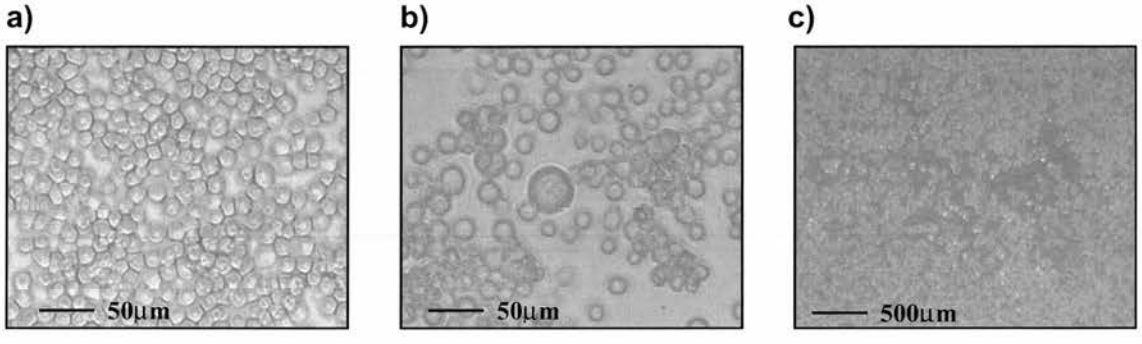

Bright-field microscopy of Sf9 cultures a) Subconfluent non-infected Sf9 cells of uniform size (high power). b) Baculoviral (BVmycren2HAHis) infected Sf9 cells show growth arrest, and gross swelling (high power). c) Low power view of b) recombinant plaque stained with X-gal. Note central area of cell lysis.

Although the use of Bsu 36 I deletant baculovirus significantly reduces contamination by wild type baculovirus, low level contamination is possible, presumably because of incomplete restriction digestion of Bac-N-Blue DNA, or complex recombination events. The presence of wild type virus reduces the efficiency of protein expression due to competition with recombinant virus for cellular resources, and more efficient replication. Therefore, it was important to ensure that viral stocks were free of wild type baculovirus. A PCR assay was used to distinguish recombinant and wild type baculovirus, using primers flanking the polyhedrin region (JJM 396: nucleotides -44 to –21: JJM 397: +794 to +774 (nomenclature of O'Reilly et al, 1992[863]) Appendix A, table B), and therefore spanning the ren2^{d} cDNA. Wild type baculovirus led to amplification of an 839 bp fragment, whilst recombinant virus produced a 3.9 kb fragment (figure 5.11). Non-contaminated viral isolates were selected and characterised further.

Figure 5.11 PCR Screening of Recombinant Viral Isolates

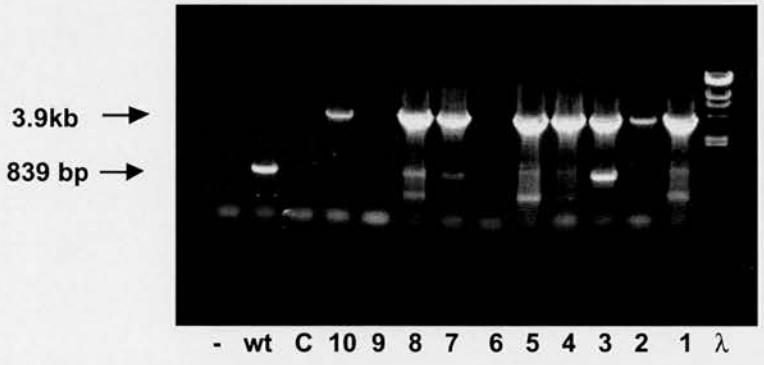

Mini cultures of isolated recombinant viral plaques were grown for 3-5 days. DNA was isolated and screened for the presence of recombinant and wild type baculovirus using primers flanking the polyhedrin region. wt: Bac-N-Blue wild type control, C: uninfected Sf9 cell DNA control, 1-10: recombinant viral plaque isolates, λ : λ*Hind*III marker.

5.5.7 Analysis of Protein Expression by Baculoviral Plaque Isolates

Viral isolates expressing ren2 protein were identified by Western blotting of whole cell lysates from 6 well plates (Figure 5.9), using anti-haemagglutin antibody. The agreement between PCR and Western blotting results was imperfect, in that only a few viral isolates appeared to give rise to recombinant renin production. This is likely to be due to differences in the sensitivity of the two screening techniques as well as variations in viral titre: if individual infections proceed at different rates some will fail to produce detectable levels of protein at that time point, whilst giving positive PCR results. Alternatively, DNA preparation from small cultures did not allow high quality DNA to be prepared, so PCR may have failed for this reason.

Figure 5.12 Screening for Recombinant Prorenin

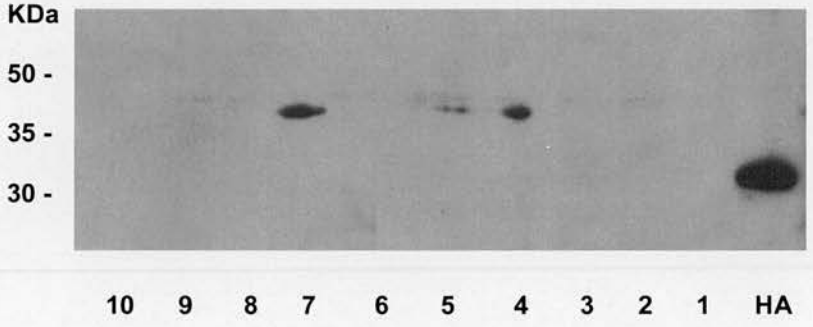

Western blot. Mini cultures of viral recombinants were grown for 5 days. Crude protein extracts were made and screened for the presence of recombinant prorenin using αHA antibody. 1-10: BVmycren2 HAHis isolates. HA: hepatic protein from 11βHydroxysteroid dehydrogenase-2 transgenic mice expressing HA-tagged HSD-2. Primary α-HA, 1 : 1000, secondary α-mouse IgG, 1 : 1000. 10% PAGE-SDS gel.

5.5.8. Generation and Purification of Recombinant Prorenin

On the basis of PCR and Western blotting results suitable viral isolates were identified for each construct. High titre stocks (>10^8 pfu) were generated in 100 ml suspension cultures of Sf9 cells, according to the method described in section 2.2.30. Time course and infectivity studies with BVmycren2HAHis indicated that protein yield was optimal

at 72 hours of infection using a multiplicity of infection of 1.0 (Figure 5.13). Similar results were obtained for the other recombinant baculoviruses. Although some studies have suggested that very low MOI's (0.0001) lead to better yields,[864] this was not found to be the case in this instance (data not shown). Recombinant protein was present entirely in cellular lysates and none was in the culture medium: the vast majority of renin was in the pelleted insoluble fraction (Figure 5.14). BVren2HAHis retains the endogenous prorenin signal sequence but was also insoluble (data not shown). Using these parameters recombinant prorenin was purified under native conditions by immobilised metal affinity chromatography (IMAC) using a cobalt column. Polyacrylamide gel electrophoresis and Western blotting identified recombinant renin using anti-HA and anti-renin antibodies (Figure 5.15 and 5.16). Silver staining showed that the purity of recombinant protein was low (Figure 5.17).

Figure 5.13 BVmycren2HAHis Infection Timecourse

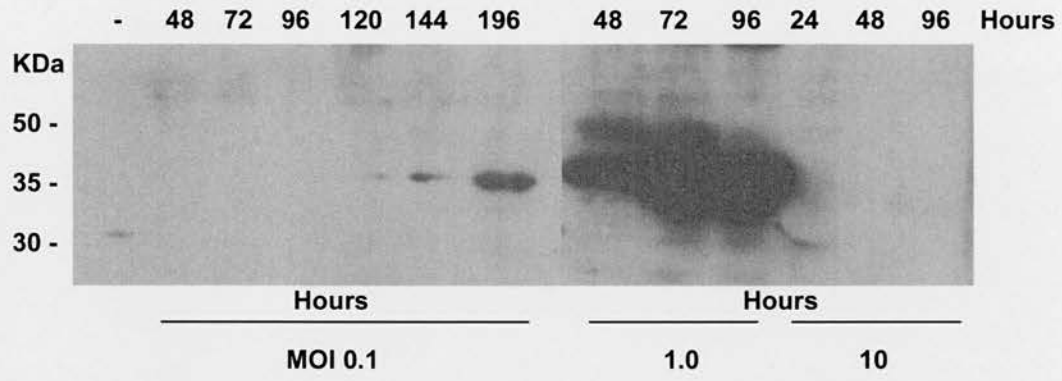

Suspension cultures were infected with BVmycren2HAHis at different multiplicities of infection and sampled at intervals of 24 hours after infection. Optimum infectivity and time point is MOI 1.0 at 72 hours. Primary α HA, 1 : 1000, secondary SAPU rabbit αmouse, 1 : 1000. - negative control. 10% SDS-PAGE gel.

Figure 5.14 Solubility of Recombinant Prorenin

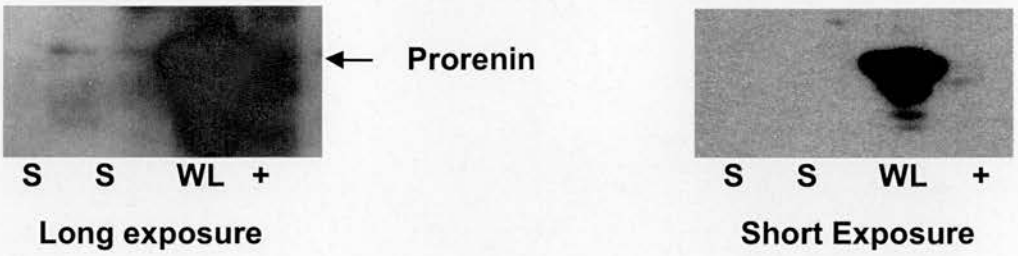

Soluble recombinant prorenin (BVmycren2HAHis) was separated from whole lysate by centrifugation at 10,000 rpm for 1 hour in a Sorvall SS34 rotor. Supernatant and whole lysate were analysed by Western blotting after PAGE. WL: whole lysate, S : supernatant after centrifugation of whole lysate, + : positive control. αHA 1: 1000, rabbit αmouse 1 : 1000. 10% SDS-PAGE gel.

Figure 5.15 IMAC Purification of Recombinant Prorenin

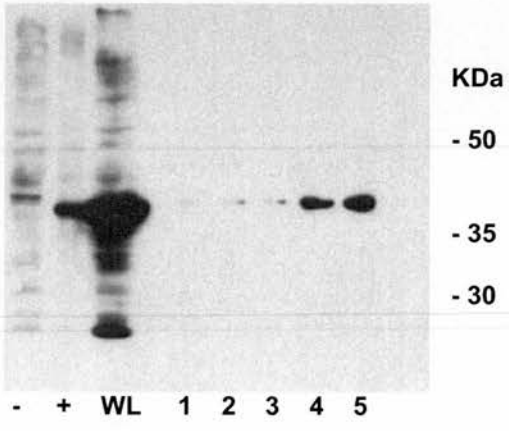

BVmycren2HAHis recombinant prorenin was purified by IMAC, separated by PAGE and analysed by Western blotting. Primary αHA 1:1000, secondary SAPU rabbit αmouse 1:1000. - negative control, + positive control, WL whole lysate (nonpurified), 1 – 5 elution fractions.

Figure 5.16 Purified Recombinant Prorenin

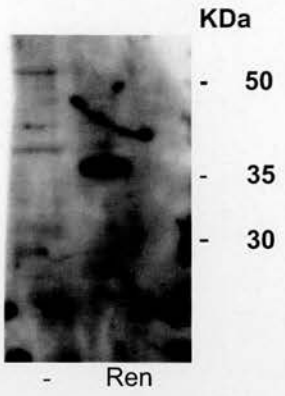

Purified BVmycren2HAHis was analysed by Western blotting using a polyclonal antirenin antibody. Primary polyclonal antirenin antibody [363] 1/10000. Secondary SAPU rabbit αmouse 1:1000. - negative control, Ren: BVmycren2HAHis sample.

Figure 5.17 Analysis of Recombinant Prorenin Purity

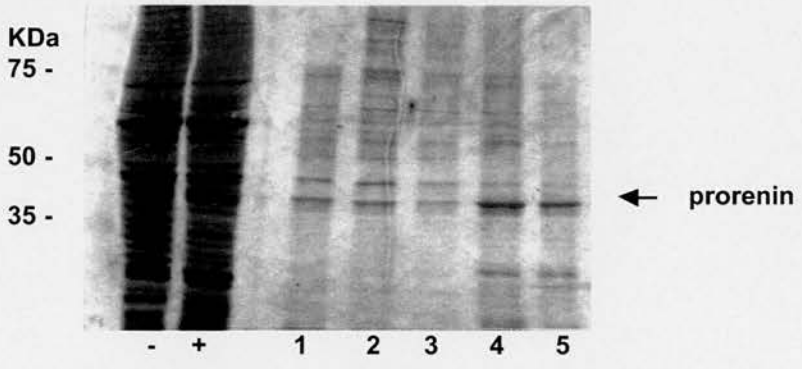

BVmycren2HAHis recombinant prorenin was purified by IMAC and analysed by silver staining of PAGE gels. - unpurified negative control, + unpurified positive control, 1 – 5 aliquots of eluate containing purified prorenin. Samples are identical to figure 5.15.

5.3 Enzymatic Activity of Recombinant Prorenin Constructs

Soluble BVmycren2HAHis was partially purified from whole cell lysates by IMAC using a cobalt resin. Five 1 ml fractions of eluate were collected in Tris buffer and samples one and four were tested for renin activity against porcine angiotensinogen before and after trypsin activation over a range of pH values. Assays were performed by Prof J. Peters. Figures 5.18 and 5.19 demonstrate that both samples contained prorenin which was activated to renin by trypsin treatment: marked pH-dependence was seen, with pH 7.3-8.0 being optimal. Above pH8.0, renin activity was severely curtailed. Renin activity was also detected in both samples prior to trypsin treatment (figure 5.18), suggesting either intrinsic activity due to cryoactivation or possible contamination with active renin. Renin activity was substantially greater for sample 1 compared to sample 4 (90,000 ngAI/ml/h vs 20,000ngAI/ml/h), though this was not in agreement with the appearance of Western blotting and silver staining data (Figures 5.15 and 5.16).

Figure 5.18 Renin Activity of Recombinant Prorenin

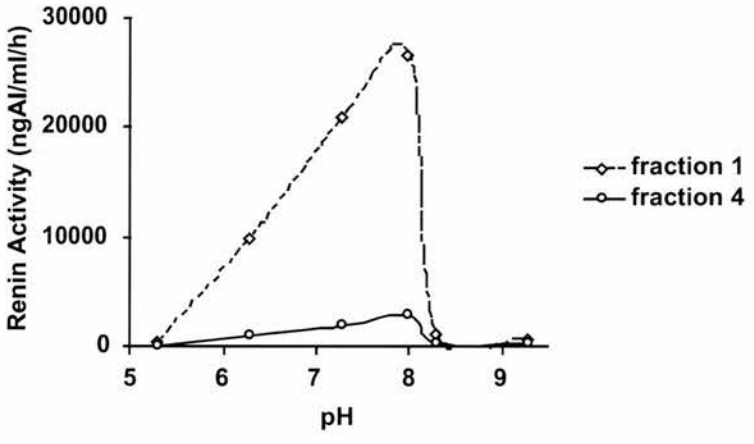

Recombinant prorenin BVmycren2HA was purified by IMAC. Enzymatic activity was measured as the production of angiotensin I from porcine angiotensinogen, by radioimmunoassay. Fractions 1 and 4 refer to figure 5.15 and 5.17.

Figure 5.19 Activity of Recombinant Prorenin

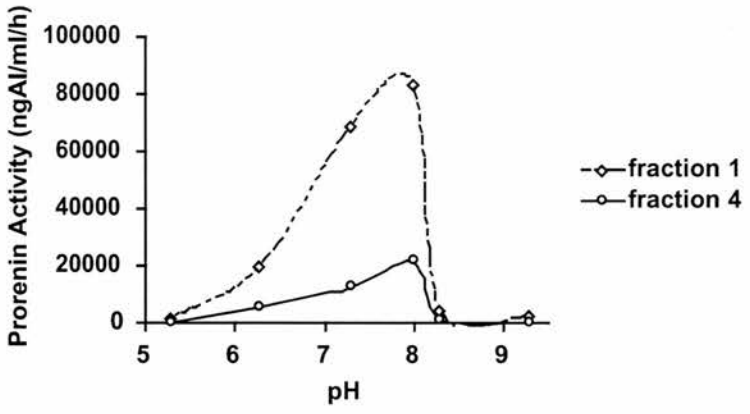

Recombinant prorenin BVmycren2HA was purified by IMAC, and activated to renin by trypsin digestion. Enzymatic activity was measured as the production of angiotensin I from porcine angiotensinogen, by radioimmunoassay. Fractions 1 and 4 refer to figure 5.15 and 5.17.

BVren2HA differs from BVmycren2HA in that it lacks an N-terminal myc epitope and retains the endogenous signal sequence. This construct was also shown to have proteolytic activity against porcine angiotensinogen (data not shown). Renin activity of BVmycren2HA was destroyed by freezing, even in the presence of 20% glycerol or 10% bovine serum albumin (data not shown).

5.4 Alternative Strategies for Recombinant Protein Purification

Silver staining suggested that there was significant contamination with baculoviral proteins using the IMAC method. The reasons for inefficient purification by IMAC may have been due to a high proportion of histidine rich insect proteins, or a problem with the accessibility of the hexa-histidine tag for interaction with the column. Therefore, other purification strategies were explored, including modifications of the IMAC protocol, immunoaffinity, and ion exchange chromatography. These will be discussed in more detail.

5.4.1. Modified IMAC

In order to improve the purification of recombinant prorenin by IMAC, strategies were employed to reduce non-specific binding of insect cell proteins to the cobalt column. These included the following modifications:

5.4.1.1 Additional centrifugation.

Crude lysates were centrifuged at 10,000 rpm for 30 minutes using an SS34 rotor to pellet insoluble contaminants. This strategy helped to improve IMAC column flow rate, but did not significantly affect purity of soluble fractions (figure 5.20).

Figure 5.20 IMAC Purification using Additional Centrifugation

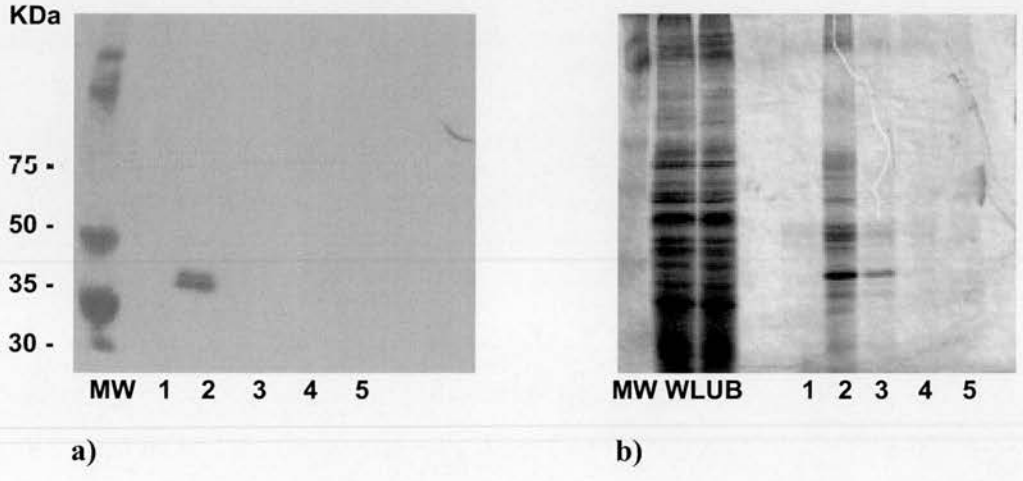

IMAC purification of BVmycren2HAHis was preceded by centrifugation of whole cell lysate at 10,000rpm for 30 minutes in a Sorvall SS34 rotor. a) Western blot: Primary α–HA 1:1000, secondary SAPU rabbit α-mouse 1:1000. b) Silver stain of purified fractions. MW: molecular weight marker, WL: whole lysate, UB, fraction unbound by IMAC column, 1 – 5 elution fractions.

5.4.1.2 Non-ionic detergents (1% NP-40).

NP-40 is a non-ionic surfactant that improves protein solubility and reduces protein-protein interactions. Use of 1% NP-40 in wash steps appeared to inhibit binding of recombinant renin to the cobalt column (figure 5.21).

Figure 5.21 IMAC Purification Using 1% NP40.

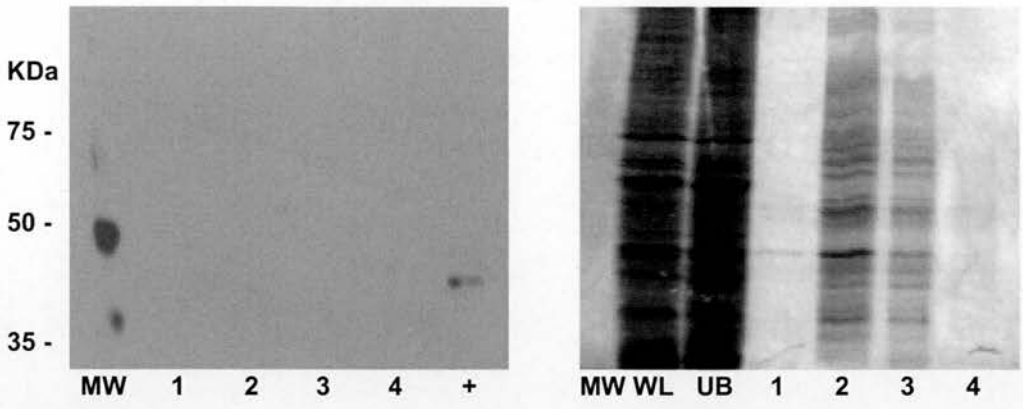

Recombinant BVmycren2HAHis was purified by IMAC. All solutions used contained 1% NP40. a) Western blot: Primary α-HA 1:1000, secondary SAPU rabbit α-mouse 1:1000. b) Silver stain of purified fractions. MW: molecular weight marker, WL: whole cell lysate, UB: unbound protein, 1-4: elution fractions. +: positive control.

5.4.1.3 Acid-elution (pH 5.0).

pH affects protein solubility and ionic charge, and hexa-histidine binding to the cobalt column is also pH-dependent. Acidic solutions may be used to elute bound proteins. Use of 300mM NaCl pH5.0 in the elution step did not appear to improve purity (figure 5.20). Although sample 3 appeared to be relatively pure and contain high levels of recombinant prorenin (figure 5.22), concentration of this sample using an Amicon centrifugation column demonstrated significant contamination.

5.4.1.4 β-mercaptoethanol (5mM).

β-mercaptoethanol reduces disulphide bonds and thereby disrupts intermolecular interactions. Use of low concentrations of β-mercaptoethanol is widely recommended for enhancing protein purification, but appeared to prevent recombinant prorenin binding in this instance (figure 5.23).

Figure 5.22 IMAC Purification Using Acid Elution

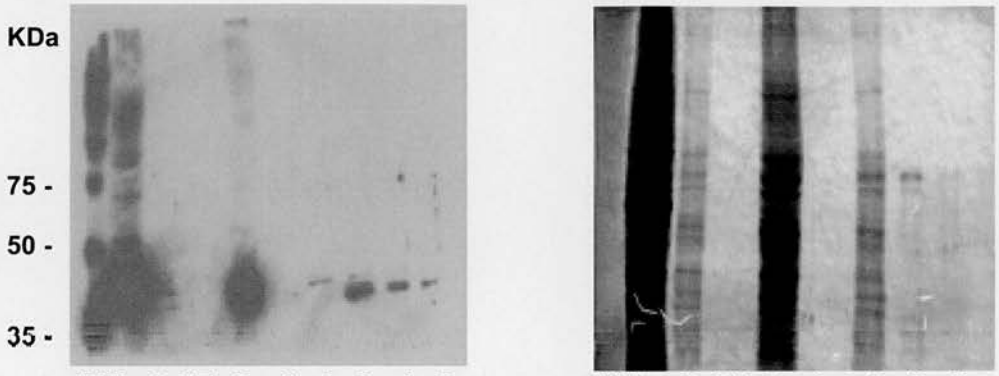

Recombinant BVmycren2HAHis was purified by IMAC, and eluted with 300mM NaCl pH5.0. a) Western blot: Primary αHA 1:1000, secondary SAPU rabbit αmouse 1:1000. b) Silver stain. + positive control, P: pooled unconcentrated purified sample, FT: column flow through, Co: concentrated purified sample, 1-5: elution fractions.

Figure 5.23 IMAC Purification Using β-mercaptoethanol

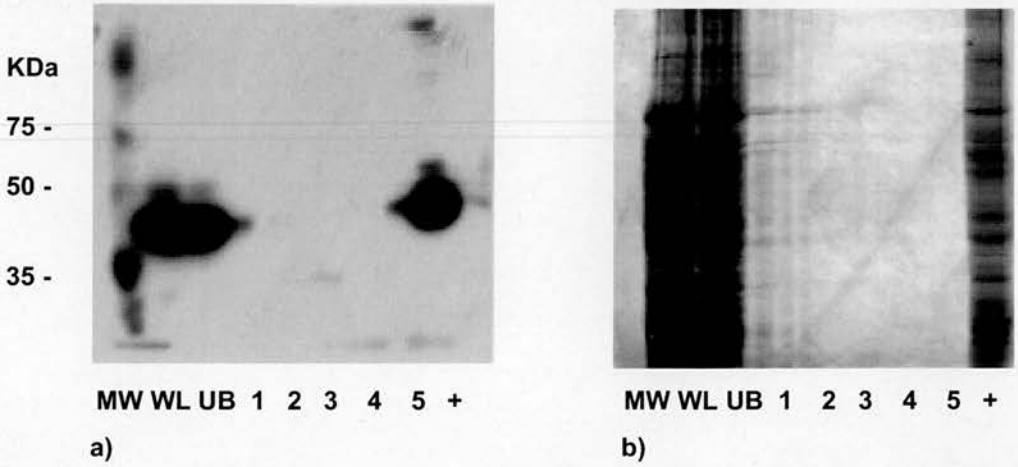

Recombinant BVmycren2HAHis was purified by IMAC. All solutions used contained 5mM β-mercaptoethanol. a) Western blot: Primary αHA 1:1000, secondary SAPU rabbit αmouse 1:1000. b) Silver stain of purified fractions. WL: whole lysate, UB: fraction unbound to cobalt column, 1-5: eluate samples, +: positive control.

5.4.1.5 High Salt Extraction Buffer (500mM NaCl)

Salt concentration alters protein ionic charge, and may therefore be expected to alter the binding characteristics of histidine-rich proteins to the cobalt column. Such a strategy has been employed previously to enhance purification of recombinant green fluorescent protein (GFP) by IMAC.[865] Use of 600mM NaCl solutions throughout the purification process did not reduce contamination (figure 5.24).

5.4.1.6 Glycerol 10% (v/v)

Glycerol is commonly used as a buffer to stabilise enzymes, and is sometime s recommended to reduce non-specific protein binding during purification. Inclusion of glycerol 10% (v/v) appeared to inhibit recombinant protein binding to the IMAC column (figure 5.24).

Figure 5.24 IMAC Purification Using High Salt or Glycerol

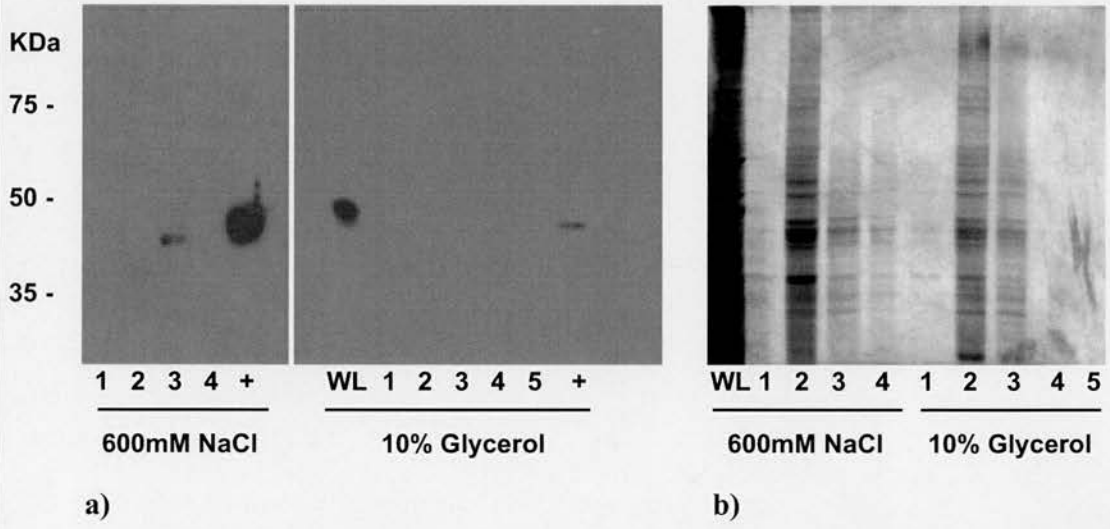

Recombinant BVmycren2HAHis was purifed by IMAC. Solutions contained either 600mM NaCl or 10% glycerol. a) Western blot: Primary αHA 1:1000, secondary SAPU rabbit αmouse 1:1000. b) Silver stain. WL: whole cell lysate, 1 – 5: elution fractions, +: positive control.

5.4.1.7 Low Concentrations of Imidazole (1 mM)

Theoretically the affinity of histidine-rich insect cell proteins for the IMAC column is of lower affinity than that of the hexa-histidine motif, and should elute with low concentrations of imidazole. This strategy is widely used to improve protein purity.[866] However, there was little evidence that this significantly affected the purity of recombinant ren2 (figures 5.25).

5.4.1.8 Nickel-Based IMAC

The physicochemical properties of different IMAC columns vary according to the chelation agent and metal used. In the literature conflicting reports regarding the superiority of different columns suggest that optimal conditions vary for the protein being studied.[866-868] A nickel-based resin (Qiagen) did not significantly alter protein purification (data not shown).

Figure 5.25 IMAC Purification Using 1mM Imidazole

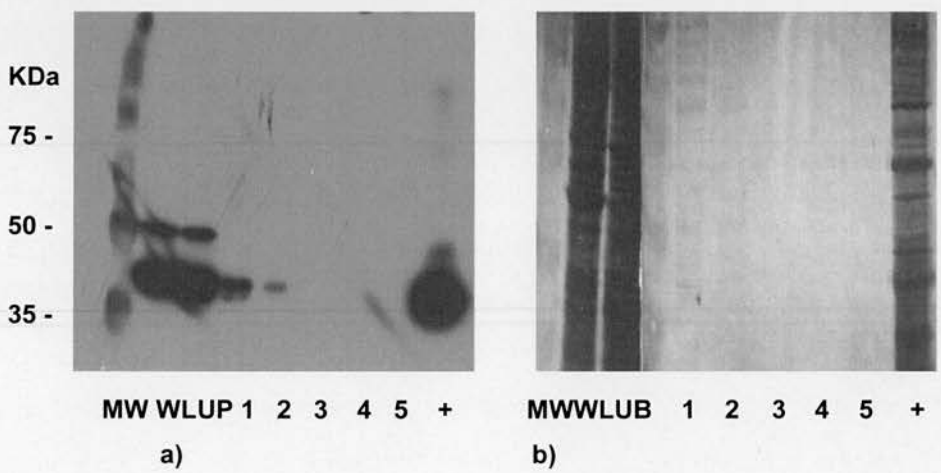

Recombinant BVmycren2HAHis was purified by IMAC: all solutions contained 1mM Imidazole. 150mM Imidazole was used for elution. a) Western blot: Primary αHA 1:1000, secondary SAPU rabbit αmouse 1:1000. b) Silver stain. WL: whole cell lysate, UB: unbound to cobalt column, 1-5: eluate samples +: positive control.

5.4.1.9 Denaturation – Renaturation

Although the original intention had been to purify native prorenin, denaturing purification conditions theoretically circumvent some of the problems encountered with purification. In particular, because a major proportion of recombinant renin was insoluble, it was hypothesised that purity and yield might be improved by solubilising renin, thereby augmenting the availability of renin for binding. In addition, denaturation may also improve the accessibility of the hexa-histidine tag for binding, since it is possible that this was sterically hindered by secondary and tertiary protein structures. Indeed a major determinant of the success of IMAC is thought to be surface exposure and availability of the histidine tag.[854] Denaturation of cell lysates with 6M guanidine HCl, and IMAC purification under denaturing conditions was followed by overnight dialysis in 50mM Tris pH7.5. This resulted in precipitation of protein, and this strategy was not pursued further.

5.4.2 Immunoprecipitation and Immunoaffinity Purification

Since the hexa-histidine tag did not allow efficient purification by IMAC, the possibility of using the epitope tags for immunoaffinity purification was explored. In the first instance, an immunoprecipitation procedure was carried out to demonstrate the feasibility of this approach. Agarose-conjugated anti-HA monoclonal antibody (Santa Cruz) was used in a standard protocol (section 2.2.35). Western blotting demonstrated that the recombinant prorenin could be captured by this method (figure 5.26a). Immunoprecipitated prorenin was not detectable by silver stain, but the level of contaminating proteins was also negligible (figure 5.26b). This indicated that the HA epitope is accessible to soluble antibody in the native state, and that selective capture of prorenin is possible.

Using a commercial sepharose-conjugated rat monoclonal anti-HA column (Roche), large-scale immunoaffinity purification was attempted using HA peptide (1mg/ml) to competitively elute recombinant protein. No HA-tagged recombinant protein was detected in the eluates by Western blotting despite several attempts (figure 5.27).

Analysis of eluates demonstrated that recombinant protein was not bound by the column. The reasons for this are not clear.

Figure 5.26 Immunoprecipitation of Recombinant Prorenin

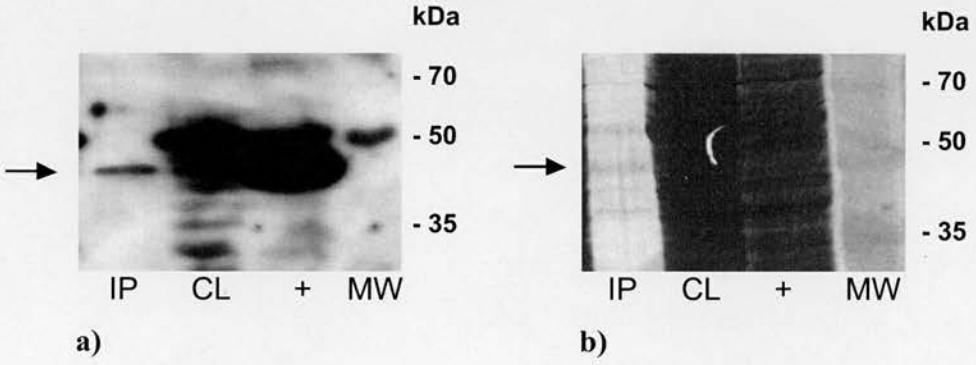

a) Western blot. Prorenin was immunoprecipitated with 1µg monoclonal agarose-conjugated anti-HA. Arrow indicates prorenin. Western blot: primary, rabbit polyclonal anti-HA 1:1000, secondary, goat anti-rabbit polyclonal HRP-conjugated 1:1000. ECL+plus detection. b) Silver stain. IP, immunoprecipitate, CL, cleared lysate, +, positive control, MW, molecular weight markers.

Figure 5.27 Immunoaffinity Purification of Recombinant Prorenin

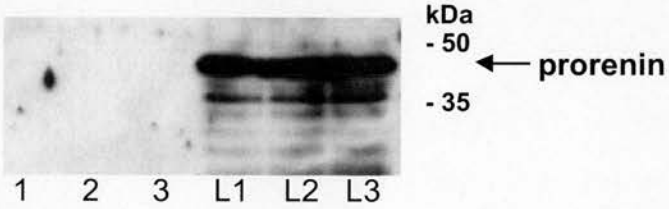

Recombinant prorenin present in cleared lysate (L1-3) was not present in elution fractions (1,2,3) collected after application to a rat monoclonal anti-HA affinity column. By molecular weight criteria the upper band is likely to be prorenin. Primary Rabbit polyclonal anti-HA, 1:1000, secondary goat anti-rabbit HRP-conjugated, 1:1000. ECL detection. L1: lysate cleared by 30 minutes centrifugation at 10,000 g. L2: 60 minutes at 10,000g. L3: 60 minutes at 10, 000 g and 0.22µm filter.

5.4.3 Ion Exchange Chromatography

Ion exchange chromatography exploits the pH-dependent ionic properties of proteins, allowing differential binding to a charged column and separation according to pH or binding affinity. The pH at which a protein is in a zwitterionic or isoelectric state (pI) can be predicted from its amino acid sequence, allowing purification conditions to be chosen. Using ExPASy on-line tools (http://us.expasy.org) the pI value of BVmycren2HAHis was calculated to be 5.32, suggesting that an anion exchange column would be suitable for purification under alkali conditions.[869] In general a pH at least 1.0 unit above or below the pI is required. Since renin activity is pH-dependent and maximal around pH 7.5, this was chosen as the optimal pH. In addition, it was felt that a physiological pH would simplify further experimental use.

Figure 5.28 Ion Exchange Chromatography

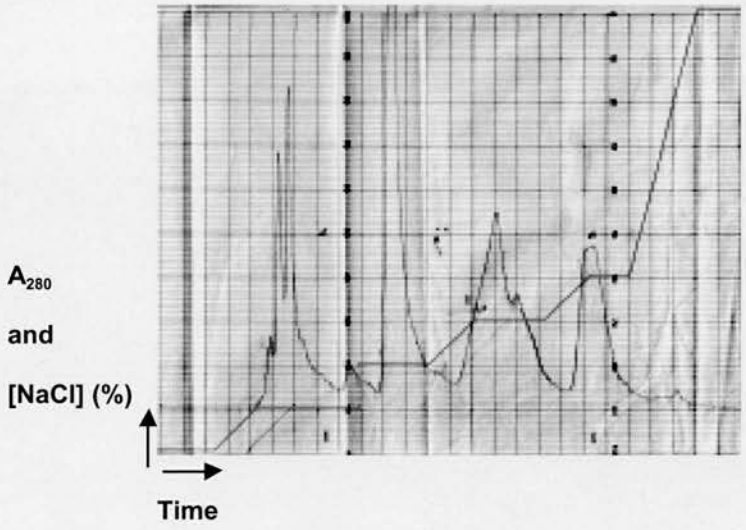

Ion exchange chromatography was performed on a BVmycren2HAHis preparation using an Äkta FPLC system and a MonoQ anion resin. Protein was eluted using a buffered NaCl gradient (red line represents salt concentration). Elution was monitored by A280 absorbance (Blue line). Fractions of eluate were collected over 5 minute intervals as salt concentration was increased

A series of pilot studies were performed using conditions described in the methods section (2.2.36). Figure 5.28 illustrates a typical baculoviral protein elution profile monitored by A280 nm absorbance. Approximately 90 10ml eluate fractions were collected and screened for the presence of recombinant renin. Since the level of recombinant prorenin expression was low all samples had to be screened by Western blotting. Samples identified as containing prorenin were subjected to a further round of ion exchange chromatography, and rescreened (figure 5.29b). Purity was checked using silver staining (fig 5.29a). Unfortunately, purity remained poor and yield was low. Further ion exchange experiments were therefore not performed.

Figure 5.29 Ion Exchange Chromatography Purified Recombinant Renin

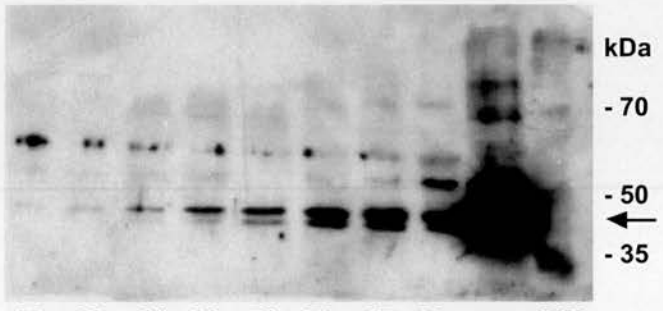

a) 83 82 81 80 79 78 77 76 + MW

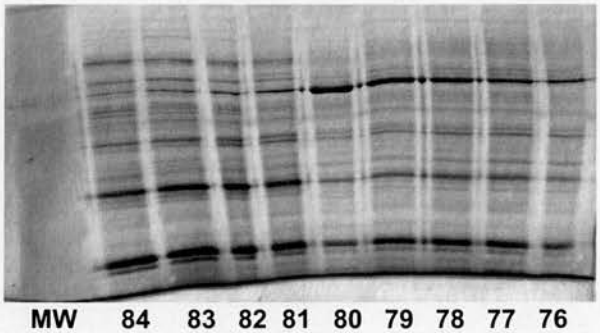

b) MW 84 83 82 81 80 79 78 77 76

a) Silver stained polyacrylamide gel. Recombinant prorenin was purified by two rounds of ion exchange chromatography using Mono Q Sepharose with a 500mM NaCl elution gradient. b) Western blotting of ion exchange purified fractions. Lanes: 76 – 83: elution fractions, + : positive control, MW: molecular weight. Primary Rabbit polyclonal α-HA, 1:1000, secondary goat α-rabbit HRP-conjugated, 1:1000.

5.5 Discussion

Although the basic aim of producing epitope-tagged recombinant prorenin with enzymatic activity was successfully achieved, difficulties regarding yield and purity limited its usefulness as a research tool.

5.5.1 Recombinant Renin Activity

The fact that BVmycren2HAHis was active suggests that production in a baculoviral system allowed appropriate folding and formation of secondary/tertiary structure. In addition, the purification conditions (IMAC) were also suitable for the maintenance of enzymatic activity. The extensive modification of $ren2^d$ by the incorporation of several epitope and purification tags did not inactivate enzymatic activity, although this was not systematically explored to determine any subtle effect. Previous studies have found variable effects depending on the location of tags within the protein,[870,871] and this might be an avenue for future investigation. pH 6.5-7.0 is optimal for mouse submaxillary prorenin,[810] with little activity above pH 8.0. This is consistent with the observed optima (pH 7.3-8.0) for trypsin activated BVmycren2HAHis prorenin enzymatic activity against porcine angiotensinogen, though the difference is not easily explained. Presumably this reflects the effect of tags on the overall molecular charge of recombinant prorenin. Although the samples tested for activity were not 100% pure, it is unlikely that contaminants accounted for the enzymatic activity.

Prorenin exhibits a small degree of renin activity due to non-proteolytic activation, generally in the order of less than 2%.[872] The recombinant prorenin samples studied here had about 30% intrinsic renin activity prior to trypsin digestion. This probably reflects cryo-activation due to prolonged storage at 4°C prior to analysis as well as proteolytic activation during purification. Indeed, Western blotting using anti-HA antibody demonstrated doublet bands, rather than a single band, suggesting slight proteolytic breakdown. A further mechanism of activation includes a possible effect of the myc epitope on prosegment function. Mutational analysis has indicated that autoinhibition of renin by the prosegment is dependent on amino acids within the region P10-P20.[298]

Amino acid substitutions, particularly alterations in charge may lead to renin activation. Therefore, it is feasible that the myc epitope disrupts prosegment function, either sterically, or by charge effects. It is notable that the sample with the least recombinant renin present, as assessed by Western blotting and silver staining, had the higher activity. The likely explanation for this must be that not all purified renin was in an activatible form, possibly due to protein misfolding.

5.5.2 Recombinant Renin Yield

Yield was greatly reduced due to protein insolubility, which may have been caused by several factors. Firstly, high-level production of a single protein may have saturated processing pathways, leading to abnormal folding, resulting in insoluble secondary and tertiary structures. BVmycren2HA was deliberately designed without a signal peptide, in order to accommodate the myc epitope tag. This may have contributed to the insolubility problem since it would have prevented normal cellular export leading to intracellular accumulation. To control for the effect of this BVren2HA was generated, which lacked the myc tag, but retained the endogenous signal peptide. This recombinant protein was not secreted in any significant amount in to the culture medium, and was also insoluble, suggesting that the prorenin solubility was not dependent on secretion. Although endogenous signal sequences have been shown to be effective in baculoviral systems,[868,873,874] it may have been worthwhile using established high expression signal sequences such as those from honey bee mellitin,[874,875] baculoviral gp67[876] or bombyxin.[877] The prosegment was retained in all constructs as previous reports have indicated that this may be important for successful renin folding and yield.[298,819,838]

Very high concentrations of a single protein can lead to protein-protein interactions that form insoluble quaternary structures. Indeed, the His tag itself may promote cation-dependent oligomerization.[878] In addition, the acidic conditions of the baculoviral system may have been close to the pI value of the recombinant protein (pH 5.32), at which precipitation is more likely to occur. Strategies to resolubilise precipitated protein by denaturation and renaturation were not successful due to precipitation of protein

during dialysis. Although this method may have been viable with extensive refinement, previous studies have also reported problems dialysing His-tagged proteins.[878]

Although Sf9 cells are easy to grow, it is possible that other insect cell lines may have given better yields. In particular, High Five™ (BRI-TN-5B1-4) cells, derived from Trichopluisa ni are better adapted than Sf9 cells to protein secretion, but have the disadvantages of more fastidious growth conditions and lower culture density.

5.5.3 Recombinant Protein Purity

A hexa-histidine tag was incorporated in to the design of the recombinant prorenin series in order to facilitate purification. Although it was recognised that purity would not be 100% using this strategy alone, it was likely to be a simple and effective first step towards purification. Numerous reports in the literature testify to the usefulness of this approach. In reality the IMAC strategy was very poor despite numerous attempts to enhance its success. The reason for this is not immediately clear. Some authors report better purity using 10xHis tags, as opposed to the more commonly used 6xHis tag used here.[878] Histidine-rich proteins present in baculoviral cells may have been bound by the IMAC column and therefore co-purified. Attempts to reduce low affinity binding using low concentrations of imidazole, high salt concentration, and acid elution were not particularly successful, though assessment of purity was semiquantitative and subjective. Since silver staining is very sensitive for detecting proteins, purity may have appeared to have been more acceptable using less sensitive methods such as Coomasie staining. Other measures such as β-mercaptoethanol, glycerol and NP-40 appeared to inhibit recombinant protein binding altogether. It is also possible that there was steric hindrance of the hexa-histidine motif by the HA epitope tag, given that this was not the most C-terminal motif. Emphasis has previously been placed on the surface availability of the His tag for interaction with chelated cations,[879] though this is impossible to predict. Systematic studies of the position of the His tag within proteins have detected variable effects on binding efficiency and yield.[870,871,880,881] However, this seems to be unlikely

to have been a major factor as the problem was one of contamination, rather than inability to bind the column.

The failure of immuno-affinity purification was surprising since immunoprecipitation experiments had been encouraging. The reason for this discrepancy is not clear, but may relate to the use of different antibodies for the two procedures. In any case, such a method would not have been suitable for large-scale protein purification both in terms of logistics and expense.

Finally, ion exchange chromatography was an attractive method for large-scale purification of native prorenin. Given the physico-chemical properties of the recombinant prorenin, purification was feasible. However, the level of soluble prorenin expression relative to that of background contaminants was probably too low for this method to work efficiently, particularly as large volumes of solute are used, and the sample becomes very dilute. Successive rounds of purification did not enhance purity. Furthermore, the possibility of oligomerization of recombinant renin via His tags may have contributed to the broad elution profile observed.

Chapter 6

Conclusions

6.1 Introduction

Cardiac hypertrophy is a serious complication of hypertension, with a significant impact on long-term prognosis due to deleterious effects on cardiac function and arrhythmias.[624,882] Whilst it was once regarded as an essential process to maintain cardiac output in the face of increased workload, it is increasingly apparent that hypertrophic remodelling is unnecessary. The work described in this thesis addresses several aspects of cardiac hypertrophy and cardiac physiology in transgenic rat models of hypertension which may have relevance to clinical practice. Experiments in chapter 3 concentrated on the functional consequences of LVH in TGRcyp1a1ren2 in the context of chronic hypertension, and regression of hypertension. Chapter 4 describes attempts to ameliorate LVH via calcineurin inhibition using FK506, and the unexpected finding that this abolished hypertension. Chapter 5 reports the production of recombinant prorenin in a baculoviral expression system in an effort to study potential mechanisms of prorenin uptake in the heart, and its contribution to LH in prorenin-based transgenic models of hypertension/LVH.

6.2 Low Dose Induction Experiments in TGRcyp1a1Ren2

6.2.1 Introduction

Whilst the blood pressure response of TGRcyp1a1ren2 to indole-3-carbinol has been shown to be dose-dependent,[581,587] the only dose investigated in detail so far has been 0.3% I3C (w/w). In this chapter experiments describing the phenotype of TGRcyp1a1ren2 in response to 0.15% I3C (w/w) were detailed. Given that a lower dose of inducing agent was used, a milder phenotype was to be expected, and indeed chronic hypertension ensued, with a moderate degree of LVH. No evidence of MH was found, although a proportion of transgenic animals died suddenly of unknown cause at around

day 140 of induction. The degree of hypertension reached was similar to that using 0.3% (w/w) I3C, except that the onset was slower, and the level of transgene induction was less.

6.2.2 Phenotype of TGRcyp1a1ren2

In this model LVH did not give rise to any evidence of LV systolic dysfunction, as assessed by a variety of techniques. Although significant electrical remodelling occurred, few significant arrhythmias were detected. Therefore, LVH appears to have a benign impact on cardiac function, at least at the time points studied in this model. In this respect the data presented here is consistent with early, compensated cardiac hypertrophy in humans. Comparison with other models of pressure overload suggests that longer duration of hypertension may have led to significant cardiac problems, although the severity of this appears to be highly variable between models. Analysis was carried out under anaesthesia under a single set of haemodynamic conditions, and it is possible that different afterload or preload may have affected function differently between hypertrophied and non-hypertrophied hearts. More sophisticated analysis of in vivo cardiac function using microconductance catheters may have detected subtle abnormalities of LV function that were missed.

Reversal of hypertension by withdrawing the inducing agent from the diet of TGRcyp1a1ren2 animals led to a prompt reduction in blood pressure back to control levels, and regression of LVH, with evidence of normalisation of cardiac functional, electrical and molecular changes. This is encouraging in that it suggests that effect treatment of hypertension may be able to completely reverse the detrimental consequences of LVH in humans.

6.2.3 Future studies

Demonstrating evidence of LV dysfunction in this model would be a significant finding, providing a model of heart failure secondary to hypertensive heart disease. Such a model would be a powerful resource for investigating manipulations that either exacerbate or

ameliorate the transition from LVH to heart failure in an inbred monogenic model of hypertension. It is likely that prolonged induction of hypertension in a large cohort of TGRcyp1a1ren2 animals may allow a proportion to survive long enough to develop heart failure. Alternatively, manipulations such as high salt diet, or chronic aldosterone infusion may stimulate cardiac fibrosis and lead to earlier cardiac dysfunction. Given the availability of congenic strains of TGRcyp1a1ren2 varying at loci encompassing ACE and At_1 it would be interesting to assess the effect of these loci on the susceptibility to LVH and heart failure. Future studies should involve assessment of cardiac function under variable haemodynamic conditions, and use microconductance catheter technology to obtain reliable pressure-volume data.

The current data on LVH regression was obtained relatively early in the time course of LVH development and later time points may be interesting in that certain aspects of ventricular remodelling, such as fibrosis may be irreversible.

6.3 Studies of FK506 in TGRcyp1a1ren2 and TGRα1ATren2

6.3.1 Background to Calcineurin

Calcineurin-dependent LVH has received substantial interest in recent years,[486,496] largely because calcineurin inhibitors are widely available, so that relevant experiments have been easy to perform. Initial optimism was tempered by a series of reports that demonstrated negative effects of calcineurin inhibition in the setting of pressure overload.[498,504] In particular calicneurin inhibitors appeared to either have no effect on cardiac hypertrophy, or else, increase mortality. Subsequently, a more detailed and balanced view has built up from transgenic and knockout experiments, which support a central role for calcineurin signalling in the development of cardiac hypertrophy.[443,456,501,533,535,536] This function is not exclusive to calcineurin, and a similar case for other interacting signalling pathways can also be made, such as GSK-3β,[87] so that at present identification of a single critical mediator of LVH remains elusive. A pivotal observation of many of these studies has been that prevention of LVH leads to reduced mortality despite increased cardiac wall stress.[417,535] This is a paradoxical

situation, since theories of LVH that have remained unchallenged for almost 30 years are based around the assumption that normalisation of wall stress by LVH was beneficial.[10] However, elegant experiments in various knockout mouse strains have demonstrated that LVH rather than increased wall stress is detrimental, and that long-term survival occurs in the absence of LVH despite chronically raised wall stress.[417,535] The obvious questions therefore arise as to why LVH is harmful, and whether this is always the case. Furthermore, if wall stress is irrelevant, what compensatory mechanism occurs to prevent the onset of heart failure? We hypothesised that increased contractility may be a mechanism to compensate for raised wall stress.

6.3.2 Effect of FK506 Cardiac Hypertrophy and Blood Pressure

With these questions in mind experiments were undertaken in TGRcyp1a1ren2 to investigate the effect of the calcineurin inhibitor FK506 on LVH, and to determine if changes in contractility occurred that might comprise part of a compensatory mechanism. Rather surprisingly FK506 treatment inhibited hypertension and end organ damage in this model, as well as in TGRα1ATren2. LVH was inhibited, but this effect could not be distinguished from the antihypertensive effect of the drug, and therefore detailed studies of cardiac contractility were not relevant. Likewise it was not possible to demonstrate whether the beneficial effect on vascular damage was a direct effect of the drug, or a secondary effect of blood pressure reduction, and these points require further clarification.

FK506 exerted an antihypertensive effect that was evident at all time points studied, even after the establishment of severe end organ damage. The mechanism of blood pressure reduction is unknown, but several possibilities exist, including direct inhibition of angiotensin II induced vasoconstriction, or else anti-inflammatory or immunoinhibitory effects. Studies of MAPK signalling in mesenteric arteries were inconsistent and conclusions could not be drawn from the data. A different approach to analysing MAPK signalling in vessels might be more successful, such as the use of

conditional knockout models lacking key signalling components in vascular smooth muscle cells, or else the use of pharmacological MAPK inhibitors.

Precedents of immunosuppressant treatments reducing blood pressure in animal models of hypertension exist,[749-753,883] and this relatively novel area of hypertension research warrants more investigation. Whether this will ever lead to clinical treatments is far from clear, as existing immunosuppressants are probably too toxic to be used except in life-threatening hypertension. Paradoxically, agents such as FK506 frequently cause hypertension at immunosuppressive doses in humans,[729] suggesting that species differences in drug metabolism, immunology or mechanisms of hypertension exist. Furthermore it is not clear whether the observed effects on blood pressure were due to calcineurin inhibition, or non-calcineurin-dependent effects of FK506.

6.2.3 Future Experiments

6.2.3.1 Antihypertensive effect

An experiment that I consider imperative to clarify the possible antihypertensive mechanism of FK506 would be to study vasoconstrictor responses of resistance vessels from FK506 and vehicle treated animals in an organ bath apparatus. If FK506 is having a direct effect on vasoconstrictor responses to angiotensin II, this should be evident. A failure to demonstrate any effect on vasoconstrictor responses suggests that an immune/inflammatory mechanism may be more likely. Although previous studies have demonstrated impaired vasorelaxation/vasoconstriction after treatment with FK506 in response to AngII [783,784] these studies were after acute exposure to drug, and may not be relevant to renin-induced hypertension. Indeed, a study by De Lima et al. (1999)[884] found that acute incubation of rat resistance vessels with FK506 caused an enhanced vasoconstrictor response to norepinephrine and impaired vasodilation to nitrate donors, whilst longterm treatment of rats had the opposite effects. Responses to angiotensin II were not studied however.

Another relevant experiment would be to study the effect of FK506 on angiotensin II induced hypertension in rats. This would establish whether the mechanism is related to angiotensin II pathways, or an unknown effect of prorenin. Furthermore, it may be important to repeat the current experiments using ciclosporin to establish if the effect is likely to be calcineurin-dependent. However, given the pharmacological differences between the two agents interpretation of a negative result may not be straightforward.

It would be desirable to study the blood pressure response of calcineurin Aβ knockout mice to angiotensin II. Such mice have been shown to be resistant to angiotensin II-induced cardiac hypertrophy, but the blood pressure response was not reported.[536] Since these mice have deficient T cell responses,[445] this experiment would not help to distinguish between an immune or vasoconstrictor effect, so ideally one would want to generate tissue specific CnAβ knockouts targeted to vascular smooth muscle cells or T cells.

The effect of blood pressure lowering without inhibition of the RAS has not been adequately addressed in these studies, and requires further analysis. A combination of antihypertensives in high doses such as nifedipine and hydralazine may be sufficient. Ideally the agents used should have little effect on the RAS, and should not interact with I3C.

It may be possible to explore immune/inflammatory interactions with hypertension in TGRcyp1a1ren2 by non-pharmacological methods. In particular, the role of NFkB warrants further investigation. This transcription factor mediates many aspects of inflammation by inducing expression of cytokines and cell adhesion molecules. Previous work in models of hypertension has demonstrated NFkB activation in the kidney and vasculature, pharmacological inhibition of which ameliorates tissue damage.[778] A more specific method to investigate this further would be to use an adenoviral construct to deliver an IkB superinhibitor of NFkB to the vasculature.[885-887]

Another approach might be to selectively inactivate immune cell subsets using specific monoclonal antibodies.[888]

6.3.3.2 Investigating Non-hypertrophic Mechanisms of Left Ventricular Compensation

The original intention to study non-hypertrophic mechanisms of left ventricular compensation for increased wall stress remains an area of personal interest. Clearly the best way to pursue this is to study an existing model of non-hypertrophic compensation, such as CnAβ mice. The hypothesis that enhanced cardiac contractility compensates for increased wall stress remains to be tested. It is also possible that altered myocardial energetics may play a compensatory role.[223] Ideally such an endeavour would involve detailed analysis of cardiac function by pressure-volume analysis, as well as in vitro studies of cardiomyocyte/papillary muscle function. Furthermore, since cardiac contractility is the functional consequence of altered gene expression, protein regulation, structural reorganisation, and altered metabolism, the use of high-throughput technologies such as microarrays and proteomics would be essential starting points for further investigation.

6.4 Investigation of Prorenin (ren2) Uptake

6.4.1 Introduction

Numerous strands of evidence suggest that the cardiac based renin-angiotensin system imports renin/prorenin, and that this exerts a physiological effect on the heart.[353,393,395,396,400-402,407,889-891] This theory is an attractive explanation for some of the phenotypes observed in transgenic rats overexpressing prorenin, in which there is little systemic activation of the RAS, yet profound end organ remodelling and damage occurs.[288,408,562] The pathway by which circulating renin/prorenin enters the heart is not well defined, although the mannose-6 phosphate receptor/ IGF-II receptor has been identified as a renin receptor in cardiomyocytes.[400-402] However this candidate lacks credibility in so far as the renin imported by this mechanism has to be glycosylated, and it appears to be degraded rather than contributing to local RAS activation.

We therefore sought to identify a mechanism of ren2 protein uptake by cardiomyocytes that may be relevant to the transgenic models produced in our laboratory. The strategy adopted was to study recombinant prorenin uptake in a cell culture system. A variety of different forms of ren2 were produced in a baculoviral expression system, incorporating immuno tags and purification tags to aid identification and isolation of the recombinant protein. Whilst active recombinant prorenin was produced study of uptake mechanisms was hampered by low yield and purity of the recombinant protein, and efforts to address this using alternative purification strategies were not successful.

6.4.2 Future Experiments

6.4.2.1 Redesigning Recombinant Prorenin

As previously discussed certain features of the recombinant protein design may have contributed to the problems encountered. In particular it seems likely that an insect-compatible signal sequence may have allowed secretion of prorenin into culture medium. Mathews et al. (1996)[400] used the signal sequence from honey-bee mellitin to express human renin in Sf9 cells, and this method has been used for other proteins with success.[875,876] However, Park et al 1999[892] found that mellitin signal sequence did not improve the secretion of Thyroid Stimulating Hormone Receptor in Sf9 cells, though yields were generally improved. An alternative strategy might be to modify the endogenous renin signal sequence. Expression of HIV gp120 in Sf9 cells has been enhanced by reducing the number of positively charged amino acids in the endogenous signal sequence, or using heterologous signal sequences with low charge such as mellitin or murine interleukin-3.[893] $Ren2^d$ signal sequence contains 3 arginine residues and it is possible that deletion or substitution of these may improve $ren2^d$ secretion in Sf9 cells.

Alternative purification strategies available may include the use of different fusion tags which may be less subject to non-specific binding than hexa-histidine (e.g. Arg-tag, calmodulin-binding peptide, cellulose-binding domain, DsbA, glutathione S-transferase, FLAG-tag, HAT-tag, maltose-binding protein, NusA, S-tag, SBP-tag, Strep-tag, and

thioredoxin).[894] However, no information is available to indicate whether one or other of these tags is better suited to recombinant renin production. or which tags might interfere with renin activity. Indeed, there are no published reports demonstrating successful use of tag sequences in recombinant renin production, so the effect on renin function is entirely unpredictable. Therefore, a decision to follow a particular strategy would be speculative.

6.4.2.2 Alternative Recombinant Protein Expression Systems

Transient mammalian cell transfection has been the most widely used expression system for recombinant renin,[290,407,819,826,827,831,833,834,839,841] suggesting that this might be the preferred strategy. Using such systems renin is correctly processed and modified, and is therefore active. Although such advantages are offset by low yields, quantities are certainly sufficient for in vitro studies,[398,407] and possibly even in vivo work [404].

Cell-free translation systems[895] have been used to express renin[407] allowing high purity protein to be produced, but serious drawbacks are the small quantities and lack of regulated protein folding/secondary protein processing. Chaperone proteins can help correct folding,[896-898] and it is also possible to generate disulphide bonds under appropriate conditions.[896,899] However, there is no published evidence to suggest that renin produced in this manner is active.[379,407] Since the folding of recombinant renin produced in this manner may be suboptimal, it is hard to see how any firm conclusions can be made about the cellular uptake using such preparations.

E. coli have been used to produce human prorenin[840] and a rat renin-GST fusion protein.[832] In both cases the protein was expressed as an inclusion body, which required denaturation and refolding: use of co-expressed chaperone proteins may prevent this problem.[900] trxB deficient E.coli strains can be used for disulphide bond formation, but at present this rarely occurs in a native pattern.[901] Therefore E.coli are probably not an ideal protein expression system for the purposes of this work.

6.4.3 Renin Receptor

Nguyen et al. (2002)[412] recently reported the identification of a specific renin receptor which binds renin and prorenin with high affinity (K_d 5.0-7.8 nM). This molecule appears to be novel in that renin/prorenin binding leads to signal transduction, receptor phosphorylation and cellular activation, as well as enhancing renin/prorenin catalytic efficiency by four fold.[412] It therefore serves a dual purpose, transducing signals in response to renin binding, as well as augmenting local RAS activation through kinetic effects on renin activity. The receptor comprises 350 amino acids (45kDa) with a single predicted transmembrane segment. It has no known homologues and is highly conserved between species. Expression has been demonstrated in the heart, as well as brain, kidney, placenta and liver. Preliminary evidence suggests that it is localised to the mesangium of glomeruli and the subendothelium of coronary and renal arteries, associated with smooth muscle cells, though the exact locations are not well defined.[412] Cardiomyocyte expression has not been reported which suggests that although the receptor may contribute to certain vascular effects, perhaps even control of blood pressure and vascular remodelling, it is unlikely to have a direct effect on cardiac hypertrophy or cardiac prorenin uptake.

This molecule is an attractive candidate for mediating tissue responses to renin/prorenin. It may explain the observations from rat renin transgenic rats in which supraphysiological levels of prorenin cause profound vascular remodeling without hypertension or systemic activation of the RAS.[288] Initial work has confirmed the existence of a rat homologue of the renin receptor in the heart. cDNA sequence is 89% identical to human, and 93% identical to mouse, whilst at the amino acid level it is 92.3% and 96% identity to human and mouse sequences respectively (data not shown). Previous analysis of the human amino acid sequence suggests a hydropathic transmembrane portion between amino acids 306-326, and a phosphorylatable tyrosine at position 335. Interestingly, both rat and mouse sequences diverge from human within the transmembrane portion, though the phosphorylation site is conserved.

Development of this work should aim to confirm the original findings of Nguyen et al (2002),[412] in particular the binding characteristics of the receptor, the cellular responses to stimulation, and the precise cellular location. Expression of mutant variants in cell culture would allow identification of important structural/functional motifs, and perhaps define portions dedicated to enzyme kinetics versus signal transduction. It should also be possible to identify the region of renin involved in receptor binding and therefore design antagonists. Further investigation would involve transgenic studies, as described below.

6.4.4 Transgenic Strategies to Investigate Prorenin Uptake by the Heart

Given the difficulty of producing pure recombinant prorenin it may be worthwhile considering transgenic approaches to study prorenin uptake by the heart in vivo. The existing literature has been discussed in detail previously,[353,407,902] and confirms the existence of pathways allowing (pro)renin uptake in the heart, but does not identify the specific mechanism involved.

If M6PR is involved in prorenin uptake by tissues, one approach to confirm this might be to generate mice deficient for the M6PR gene. Conditional M6PR knockout mice, including cardiac specific knockouts have recently been described [903] and would be an ideal tool for investigation of this. Interestingly, such mice do not display any cardiac abnormalities, perhaps suggesting that the M6PR has no significant role in cardiac physiology. This does not necessarily exclude a role in prorenin uptake, and it would be necessary to look at cardiac renin levels in these mice. Theoretically this would be best examined by cross-breeding the human prorenin / human angiotensinogen transgenic mice of Prescott et al., (2000)[353] on to this strain, although the breeding strategy for this would be complex. Equally, normal cardiac development does not indicate that hypertrophic responses are normal, so it would be worthwhile investigating the effects of hypertrophic stimuli such as aortic constriction.

Confirmation of the reported role of the putative renin receptor could also be investigated by transgenic/knockout strategies. In particular the precise cell types

expressing the receptor could be better defined using the renin receptor promoter to drive expression of GFP or lac Z. Further evaluation of this molecule will obviously involve targeted deletion in murine embryonic stem cells. In addition, it would be interesting to study the effect of conditional ablation in the heart and other tissues if possible. Given the vascular distribution however, tissue specific deletion may not be feasible with currently available tissue specific promoters. Furthermore initial BLAST searches of the published human sequence against genome sequences demonstrate complete homology of the 3' sequence with the M8-9 subunit of H^+ vacuolar ATPase. This suggests that the ATPase subunit is derived from the renin receptor gene. The significance of this is unknown though it is worth noting that mice deficent in other subunits of the H^+ ATPase are inviable. [903,904] It is therefore likely that a renin receptor knockout may have profound gestational abnormalities. An alternative approach would be cardiomyocyte-specific overexpression of the renin receptor, either in the presence of normal RAS activity/normotension, as well as in response to pressure overload/prorenin excess.

Surprisingly no one has reported transgenic overexpression of renin in the heart, though this experiment would be interesting for several reasons. Firstly, it would help to establish whether prorenin in the heart has any physiological effect, since this is not immediately apparent from other transgenic or in vitro uptake studies. Since overexpressed cardiac renin may be secreted and cause systemic effects, it may be necessary to generate a non-secretable form lacking the signal sequence. A non-secreted splice variant of renin has been described in rat heart [379] and the effects of this specific form could also be explored. The phenotype of such animals would have to be carefully evaluated given the potential for even cardiac-targeted GFP overexpression to cause dilated cardiomyopathy [905].

6.5 Concluding Remarks

The studies of left ventricular hypertrophy described in this thesis demonstrate that much is still to be learned regarding the mechanisms controlling hypertrophy, and the

relationship between LVH, wall stress and adverse cardiac prognosis. The hypothesis that increased contractility may compensate for increased wall stress warrants further systematic investigation as this may revolutionise understanding of LVH and its treatment. A prediction of this hypothesis is that LVH may be preceded by a hypercontractile state, and that LVH develops as contractility declines towards normality. Further decline eventually leads to heart failure. This theory therefore implicates the inotropic state of the heart as the prime determinant of the hypertrophic response.

The beneficial effect of immunosuppressive treatment with FK506 on blood pressure suggests that this may be a novel approach to treating some severe forms of hypertension. In addition, it refocuses attention on the inflammatory aspects of hypertension and vascular remodelling, which may be amenable to therapeutic intervention. This is likely to be an important area for future research.

Recombinant protein production has advanced in recent years, yet it still presents challenges. It is likely that modification of the strategy described in this thesis will yield a viable method of recombinant prorenin production, of acceptable purity and activity. Such a resource will allow detailed investigation of the cardiac renin-angiotensin system, and clarification of the role of the putative renin receptor in this.

References

1. Hunter JJ, Chien KR. Signaling pathways for cardiac hypertrophy and failure. *N Engl J Med*. 1999;341:1276-83.
2. Soonpaa MH, Field LJ. Survey of studies examining mammalian cardiomyocyte DNA synthesis. *Circ Res*. 1998;83:15-26.
3. Pasumarthi KBS, Field LJ. Cardiomyocyte Cell Cycle Regulation. *Circ Res*. 2002;90:1044-1054.
4. Li F, Wang X, Capasso JM, Gerdes AM. Rapid transition of cardiac myocytes from hyperplasia to hypertrophy during postnatal development. *J Mol Cell Cardiol*. 1996;28:1737-46.
5. O'Connell TD, Ishizaka S, Nakamura A, Swigart PM, Rodrigo MC, Simpson GL, Cotecchia S, Rokosh DG, Grossman W, Foster E, Simpson PC. The alpha(1A/C)- and alpha(1B)-adrenergic receptors are required for physiological cardiac hypertrophy in the double-knockout mouse. *J Clin Invest*. 2003;111:1783-91.
6. Belke DD, Betuing S, Tuttle MJ, Graveleau C, Young ME, Pham M, Zhang D, Cooksey RC, McClain DA, Litwin SE, Taegtmeyer H, Severson D, Kahn CR, Abel ED. Insulin signaling coordinately regulates cardiac size, metabolism, and contractile protein isoform expression. *J Clin Invest*. 2002;109:629-39.
7. Shioi T, Kang PM, Douglas PS, Hampe J, Yballe CM, Lawitts J, Cantley LC, Izumo S. The conserved phosphoinositide 3-kinase pathway determines heart size in mice. *EMBO J*. 2000;19:2537-2548.
8. Bueno OF, Molkentin JD. Involvement of extracellular signal-regulated kinases 1/2 in cardiac hypertrophy and cell death. *Circ Res*. 2002;91:776-81.
9. Colan SD. Mechanics of left ventricular systolic and diastolic function in physiologic hypertrophy of the athlete's heart. *Cardiol Clin*. 1997;15:355-72.
10. Grossman W, Jones D, McLaurin LP. Wall stress and patterns of hypertrophy in the human left ventricle. *J Clin Invest*. 1975;56:56-64.
11. Sasayama S, Ross J, Jr., Franklin D, Bloor CM, Bishop S, Dilley RB. Adaptations of the left ventricle to chronic pressure overload. *Circ Res*. 1976;38:172-8.
12. Ganau A, Devereux RB, Roman MJ, de Simone G, Pickering TG, Saba PS, Vargiu P, Simongini I, Laragh JH. Patterns of left ventricular hypertrophy and geometric remodeling in essential hypertension. *J Am Coll Cardiol*. 1992;19:1550-8.
13. Gerdes AM, Onodera T, Tamura T, Said S, Bohlmeyer TJ, Abraham WT, Bristow MR. New method to evaluate myocyte remodeling from formalin-fixed biopsy and autopsy material. *J Card Fail*. 1998;4:343-8.

14. Thoss K, Roth J. The use of fluorescein isothiocyanate labelled lectins for immuno-histological demonstration of saccharides. III. Studies by use of Ricinus communis lectin and wheat germ agglutinin. *Exp Pathol (Jena).* 1977;14:215-9.
15. Said S, Tamura T, Gerdes AM. Measurement of isolated myocyte volume using the Coulter models Z2 and ZM/C256: a comparison of instrument function. *Biotechniques.* 1998;25:522-5.
16. Nordin C, Siri F, Aronson RS. Electrophysiologic characteristics of single myocytes isolated from hypertrophied guinea-pig hearts. *J Mol Cell Cardiol.* 1989;21:729-39.
17. Myerson SG, Montgomery HE, World MJ, Pennell DJ. Left ventricular mass: reliability of M-mode and 2-dimensional echocardiographic formulas. *Hypertension.* 2002;40:673-8.
18. Levy D, Savage DD, Garrison RJ, Anderson KM, Kannel WB, Castelli WP. Echocardiographic criteria for left ventricular hypertrophy: the Framingham Heart Study. *Am J Cardiol.* 1987;59:956-60.
19. Levy D, Anderson KM, Savage DD, Kannel WB, Christiansen JC, Castelli WP. Echocardiographically detected left ventricular hypertrophy: prevalence and risk factors. The Framingham Heart Study. *Ann Intern Med.* 1988;108:7-13.
20. Devereux RB, de Simone G, Pickering TG, Schwartz JE, Roman MJ. Relation of left ventricular midwall function to cardiovascular risk factors and arterial structure and function. *Hypertension.* 1998;31:929-36.
21. Lauer MS, Anderson KM, Levy D. Separate and joint influences of obesity and mild hypertension on left ventricular mass and geometry: the Framingham Heart Study. *J Am Coll Cardiol.* 1992;19:130-4.
22. Rasooly Y, Sasson Z, Gupta R. Relation between body fat distribution and left ventricular mass in men without structural heart disease or systemic hypertension. *Am J Cardiol.* 1993;71:1477-9.
23. Hammond IW, Devereux RB, Alderman MH, Lutas EM, Spitzer MC, Crowley JS, Laragh JH. The prevalence and correlates of echocardiographic left ventricular hypertrophy among employed patients with uncomplicated hypertension. *J Am Coll Cardiol.* 1986;7:639-50.
24. Goble MM, Mosteller M, Moskowitz WB, Schieken RM. Sex differences in the determinants of left ventricular mass in childhood. The Medical College of Virginia Twin Study. *Circulation.* 1992;85:1661-5.
25. de Simone G, Devereux RB, Daniels SR, Meyer RA. Gender differences in left ventricular growth. *Hypertension.* 1995;26:979-83.
26. de Simone G, Devereux RB, Kimball TR, Mureddu GF, Roman MJ, Contaldo F, Daniels SR. Interaction between body size and cardiac workload: influence on left ventricular mass during body growth and adulthood. *Hypertension.* 1998;31:1077-82.
27. Verdecchia P, Porcellati C, Schillaci G, Borgioni C, Ciucci A, Battistelli M, Guerrieri M, Gatteschi C, Zampi I, Santucci A, et al. Ambulatory blood

pressure. An independent predictor of prognosis in essential hypertension. *Hypertension*. 1994;24:793-801.
28. Verdecchia P, Reboldi G, Schillaci G, Borgioni C, Ciucci A, Telera MP, Santeusanio F, Porcellati C, Brunetti P. Circulating insulin and insulin growth factor-1 are independent determinants of left ventricular mass and geometry in essential hypertension. *Circulation*. 1999;100:1802-7.
29. Chen CH, Ting CT, Lin SJ, Hsu TL, Ho SJ, Chou P, Chang MS, O'Connor F, Spurgeon H, Lakatta E, Yin FC. Which arterial and cardiac parameters best predict left ventricular mass? *Circulation*. 1998;98:422-8.
30. Post WS, Larson MG, Myers RH, Galderisi M, Levy D. Heritability of left ventricular mass: the Framingham Heart Study. *Hypertension*. 1997;30:1025-8.
31. Bielen E, Fagard R, Amery A. Inheritance of heart structure and physical exercise capacity: a study of left ventricular structure and exercise capacity in 7-year-old twins. *Eur Heart J*. 1990;11:7-16.
32. Bielen E, Fagard R, Amery A. The inheritance of left ventricular structure and function assessed by imaging and Doppler echocardiography. *Am Heart J*. 1991;121:1743-9.
33. Verdecchia P, Schillaci G, Reboldi G, Franklin SS, Porcellati C. Ambulatory monitoring for prediction of cardiac and cerebral events. *Blood Press Monit*. 2001;6:211-5.
34. Garner C, Lecomte E, Visvikis S, Abergel E, Lathrop M, Soubrier F. Genetic and environmental influences on left ventricular mass. A family study. *Hypertension*. 2000;36:740-6.
35. Rowlands DB, Glover DR, Ireland MA, McLeay RA, Stallard TJ, Watson RD, Littler WA. Assessment of left-ventricular mass and its response to antihypertensive treatment. *Lancet*. 1982;1:467-70.
36. Abi-Samra F, Fouad FM, Tarazi RC. Determinants of left ventricular hypertrophy and function in hypertensive patients. An echocardiographic study. *Am J Med*. 1983;75:26-33.
37. Drayer JI, Gardin JM, Weber MA. Echocardiographic left ventricular hypertrophy in hypertension. *Chest*. 1983;84:217-21.
38. Devereux RB, Savage DD, Sachs I, Laragh JH. Relation of hemodynamic load to left ventricular hypertrophy and performance in hypertension. *Am J Cardiol*. 1983;51:171-6.
39. Devereux RB, Roman MJ, de Simone G, O'Grady MJ, Paranicas M, Yeh JL, Fabsitz RR, Howard BV. Relations of left ventricular mass to demographic and hemodynamic variables in American Indians: the Strong Heart Study. *Circulation*. 1997;96:1416-23.
40. Ganau A, Devereux RB, Pickering TG, Roman MJ, Schnall PL, Santucci S, Spitzer MC, Laragh JH. Relation of left ventricular hemodynamic load and contractile performance to left ventricular mass in hypertension. *Circulation*. 1990;81:25-36.

41. de Simone G, Verdecchia P, Pede S, Gorini M, Maggioni AP. Prognosis of inappropriate left ventricular mass in hypertension: the MAVI Study. *Hypertension*. 2002;40:470-6.
42. Palmieri V, de Simone G, Roman MJ, Schwartz JE, Pickering TG, Devereux RB. Ambulatory blood pressure and metabolic abnormalities in hypertensive subjects with inappropriately high left ventricular mass. *Hypertension*. 1999;34:1032-40.
43. Palmieri V, Wachtell K, Gerdts E, Bella JN, Papademetriou V, Tuxen C, Nieminen MS, Dahlof B, de Simone G, Devereux RB. Left ventricular function and hemodynamic features of inappropriate left ventricular hypertrophy in patients with systemic hypertension: the LIFE study. *Am Heart J*. 2001;141:784-91.
44. Vakili BA, Okin PM, Devereux RB. Prognostic implications of left ventricular hypertrophy. *Am Heart J*. 2001;141:334-41.
45. Casale PN, Devereux RB, Milner M, Zullo G, Harshfield GA, Pickering TG, Laragh JH. Value of echocardiographic measurement of left ventricular mass in predicting cardiovascular morbid events in hypertensive men. *Ann Intern Med*. 1986;105:173-8.
46. Levy D, Garrison RJ, Savage DD, Kannel WB, Castelli WP. Prognostic implications of echocardiographically determined left ventricular mass in the Framingham Heart Study. *N Engl J Med*. 1990;322:1561-6.
47. Koren MJ, Devereux RB, Casale PN, Savage DD, Laragh JH. Relation of left ventricular mass and geometry to morbidity and mortality in uncomplicated essential hypertension. *Ann Intern Med*. 1991;114:345-52.
48. Schillaci G, Verdecchia P, Porcellati C, Cuccurullo O, Cosco C, Perticone F. Continuous relation between left ventricular mass and cardiovascular risk in essential hypertension. *Hypertension*. 2000;35:580-6.
49. Verdecchia P, Schillaci G, Borgioni C, Ciucci A, Gattobigio R, Zampi I, Santucci A, Santucci C, Reboldi G, Porcellati C. Prognostic value of left ventricular mass and geometry in systemic hypertension with left ventricular hypertrophy. *Am J Cardiol*. 1996;78:197-202.
50. Krumholz HM, Larson M, Levy D. Prognosis of left ventricular geometric patterns in the Framingham Heart Study. *J Am Coll Cardiol*. 1995;25:879-84.
51. Ghali JK, Liao Y, Cooper RS. Influence of left ventricular geometric patterns on prognosis in patients with or without coronary artery disease. *J Am Coll Cardiol*. 1998;31:1635-40.
52. Verdecchia P, Schillaci G, Borgioni C, Ciucci A, Gattobigio R, Zampi I, Reboldi G, Porcellati C. Prognostic significance of serial changes in left ventricular mass in essential hypertension. *Circulation*. 1998;97:48-54.
53. Messerli FH, Ventura HO, Elizardi DJ, Dunn FG, Frohlich ED. Hypertension and sudden death. Increased ventricular ectopic activity in left ventricular hypertrophy. *Am J Med*. 1984;77:18-22.

54. McLenachan JM, Henderson E, Morris KI, Dargie HJ. Ventricular arrhythmias in patients with hypertensive left ventricular hypertrophy. *N Engl J Med*. 1987;317:787-92.
55. Verdecchia P, Porcellati C, Reboldi G, Gattobigio R, Borgioni C, Pearson TA, Ambrosio G. Left ventricular hypertrophy as an independent predictor of acute cerebrovascular events in essential hypertension. *Circulation*. 2001;104:2039-44.
56. Haider AW, Larson MG, Benjamin EJ, Levy D. Increased left ventricular mass and hypertrophy are associated with increased risk for sudden death. *J Am Coll Cardiol*. 1998;32:1454-9.
57. Schunkert H, Weinberg EO, Bruckschlegel G, Riegger AJ, Lorell BH. Alteration of growth responses in established cardiac pressure overload hypertrophy in rats with aortic banding. *J Clin Invest*. 1995;96:2768-74.
58. Schunkert H, Jahn L, Izumo S, Apstein C, Lorell B. Localization and Regulation of c-fos and c-jun Protooncogene Induction by Systolic Wall Stress in Normal and Hypertrophied Rat Heart. *PNAS*. 1991;88:11480-11484.
59. Chien KR, Knowlton KU, Zhu H, Chien S. Regulation of cardiac gene expression during myocardial growth and hypertrophy: molecular studies of an adaptive physiologic response. *Faseb J*. 1991;5:3037-46.
60. Brand T, Sharma HS, Schaper W. Expression of nuclear proto-oncogenes in isoproterenol-induced cardiac hypertrophy. *J Mol Cell Cardiol*. 1993;25:1325-37.
61. Sadoshima J, Jahn L, Takahashi T, Kulik T, Izumo S. Molecular characterization of the stretch-induced adaptation of cultured cardiac cells. An in vitro model of load-induced cardiac hypertrophy. *J. Biol. Chem.* 1992;267:10551-10560.
62. Saadane N, Alpert L, Chalifour LE. Expression of immediate early genes, GATA-4, and Nkx-2.5 in adrenergic-induced cardiac hypertrophy and during regression in adult mice. *Br J Pharmacol*. 1999;127:1165-76.
63. Thompson JT, Rackley MS, O'Brien TX. Upregulation of the cardiac homeobox gene Nkx2-5 (CSX) in feline right ventricular pressure overload. *Am J Physiol Heart Circ Physiol*. 1998;274:H1569-1573.
64. Brown LA, Nunez DJ, Wilkins MR. Differential regulation of natriuretic peptide receptor messenger RNAs during the development of cardiac hypertrophy in the rat. *J Clin Invest*. 1993;92:2702-12.
65. Black FM, Packer SE, Parker TG, Michael LH, Roberts R, Schwartz RJ, Schneider MD. The vascular smooth muscle alpha-actin gene is reactivated during cardiac hypertrophy provoked by load. *J Clin Invest*. 1991;88:1581-8.
66. Dorn GW, 2nd, Robbins J, Ball N, Walsh RA. Myosin heavy chain regulation and myocyte contractile depression after LV hypertrophy in aortic-banded mice. *Am J Physiol*. 1994;267:H400-5.

67. Miyata S, Minobe W, Bristow MR, Leinwand LA. Myosin heavy chain isoform expression in the failing and nonfailing human heart. *Circ Res.* 2000;86:386-90.
68. Nadal-Ginard B, Mahdavi V. Molecular basis of cardiac performance. Plasticity of the myocardium generated through protein isoform switches. *J Clin Invest.* 1989;84:1693-700.
69. Schunkert H, Dzau VJ, Tang SS, Hirsch AT, Apstein CS, Lorell BH. Increased rat cardiac angiotensin converting enzyme activity and mRNA expression in pressure overload left ventricular hypertrophy. Effects on coronary resistance, contractility, and relaxation. *J Clin Invest.* 1990;86:1913-20.
70. Schultz Jel J, Witt SA, Glascock BJ, Nieman ML, Reiser PJ, Nix SL, Kimball TR, Doetschman T. TGF-beta1 mediates the hypertrophic cardiomyocyte growth induced by angiotensin II. *J Clin Invest.* 2002;109:787-96.
71. Edgren J, von Knorring J, Lindy S, Turto H. Heart volume and myocardial connective tissue during development and regression of thyroxine-induced cardiac hypertrophy in rats. *Acta Physiol Scand.* 1976;97:514-8.
72. Turto H, Lindy S. Collagen metabolism of the rat heart during experimental cardiac hypertrophy and the effect of digitoxin treatment. *Adv Cardiol.* 1976;18:41-5.
73. Blankesteijn MW, Essers-Janssen YPG, Ulrich MMW, Smits JFM. Increased Expression of a Homologue of Drosophila Tissue Polarity Gene "Frizzled" in Left Ventricular Hypertrophy in the Rat, as Identified by Subtractive Hybridization. *Journal of Molecular and Cellular Cardiology.* 1996;28:1187-1191.
74. Yussman MG, Toyokawa T, Odley A, Lynch RA, Wu G, Colbert MC, Aronow BJ, Lorenz JN, Dorn GW, 2nd. Mitochondrial death protein Nix is induced in cardiac hypertrophy and triggers apoptotic cardiomyopathy. *Nat Med.* 2002;8:725-30.
75. Friddle CJ, Koga T, Rubin EM, Bristow J. Expression profiling reveals distinct sets of genes altered during induction and regression of cardiac hypertrophy. *Proc Natl Acad Sci U S A.* 2000;97:6745-50.
76. Aronow BJ, Toyokawa T, Canning A, Haghighi K, Delling U, Kranias E, Molkentin JD, Dorn GW, 2nd. Divergent transcriptional responses to independent genetic causes of cardiac hypertrophy. *Physiol Genomics.* 2001;6:19-28.
77. Hwang DM, Dempsey AA, Lee CY, Liew CC. Identification of differentially expressed genes in cardiac hypertrophy by analysis of expressed sequence tags. *Genomics.* 2000;66:1-14.
78. Johnatty SE, Dyck JR, Michael LH, Olson EN, Abdellatif M. Identification of genes regulated during mechanical load-induced cardiac hypertrophy. *J Mol Cell Cardiol.* 2000;32:805-15.
79. Kiarash A, Pagano PJ, Tayeh M, Rhaleb NE, Carretero OA. Upregulated Expression of Rat Heart Intercellular Adhesion Molecule-1 in Angiotensin

II- but Not Phenylephrine- Induced Hypertension. *Hypertension*. 2001;37:58-65.

80. Cappola TP, Cope L, Cernetich A, Barouch LA, Minhas K, Irizarry RA, Parmigiani G, Durrani S, Lavoie T, Hoffman EP, Ye SQ, Garcia JGN, Hare JM. Deficiency of different nitric oxide synthase isoforms activates divergent transcriptional programs in cardiac hypertrophy. *Physiol. Genomics*. 2003;14:25-34.
81. Crackower MA, Oudit GY, Kozieradzki I, Sarao R, Sun H, Sasaki T, Hirsch E, Suzuki A, Shioi T, Irie-Sasaki J, Sah R, Cheng HY, Rybin VO, Lembo G, Fratta L, Oliveira-dos-Santos AJ, Benovic JL, Kahn CR, Izumo S, Steinberg SF, Wymann MP, Backx PH, Penninger JM. Regulation of myocardial contractility and cell size by distinct PI3K-PTEN signaling pathways. *Cell*. 2002;110:737-49.
82. Molkentin JD, Lu JR, Antos CL, Markham B, Richardson J, Robbins J, Grant SR, Olson EN. A calcineurin-dependent transcriptional pathway for cardiac hypertrophy. *Cell*. 1998;93:215-28.
83. Sato Y, Ferguson DG, Sako H, Dorn GW, 2nd, Kadambi VJ, Yatani A, Hoit BD, Walsh RA, Kranias EG. Cardiac-specific overexpression of mouse cardiac calsequestrin is associated with depressed cardiovascular function and hypertrophy in transgenic mice. *J Biol Chem*. 1998;273:28470-7.
84. D'Angelo DD, Sakata Y, Lorenz JN, Boivin GP, Walsh RA, Liggett SB, Dorn GW, 2nd. Transgenic Galphaq overexpression induces cardiac contractile failure in mice. *Proc Natl Acad Sci U S A*. 1997;94:8121-6.
85. Mochly-Rosen D, Wu G, Hahn H, Osinska H, Liron T, Lorenz JN, Yatani A, Robbins J, Dorn GW, 2nd. Cardiotrophic effects of protein kinase C epsilon: analysis by in vivo modulation of PKCepsilon translocation. *Circ Res*. 2000;86:1173-9.
86. Takeishi Y, Ping P, Bolli R, Kirkpatrick DL, Hoit BD, Walsh RA. Transgenic overexpression of constitutively active protein kinase C epsilon causes concentric cardiac hypertrophy. *Circ Res*. 2000;86:1218-23.
87. Antos CL, McKinsey TA, Frey N, Kutschke W, McAnally J, Shelton JM, Richardson JA, Hill JA, Olson EN. Activated glycogen synthase-3beta suppresses cardiac hypertrophy in vivo. *PNAS*. 2002;99:907-912.
88. Depre C, Shipley GL, Chen W, Han Q, Doenst T, Moore ML, Stepkowski S, Davies PJ, Taegtmeyer H. Unloaded heart in vivo replicates fetal gene expression of cardiac hypertrophy. *Nat Med*. 1998;4:1269-75.
89. Molkentin JD, Dorn IG, 2nd. Cytoplasmic signaling pathways that regulate cardiac hypertrophy. *Annu Rev Physiol*. 2001;63:391-426.
90. Boknik P, Khorchidi S, Bodor GS, Huke S, Knapp J, Linck B, Luss H, Muller FU, Schmitz W, Neumann J. Role of protein phosphatases in regulation of cardiac inotropy and relaxation. *Am J Physiol Heart Circ Physiol*. 2001;280:H786-94.

91. Boknik P, Heinroth-Hoffmann I, Kirchhefer U, Knapp J, Linck B, Luss H, Muller T, Schmitz W, Brodde O, Neumann J. Enhanced protein phosphorylation in hypertensive hypertrophy. *Cardiovasc Res.* 2001;51:717-28.
92. Nemoto S, DeFreitas G, Mann DL, Carabello BA. Effects of changes in left ventricular contractility on indexes of contractility in mice. *Am J Physiol Heart Circ Physiol.* 2002;283:H2504-10.
93. Noble MI. The Frank--Starling curve. *Clin Sci Mol Med.* 1978;54:1-7.
94. Carabello BA. Evolution of the study of left ventricular function: everything old is new again. *Circulation.* 2002;105:2701-3.
95. Chaves AA, Weinstein DM, Bauer JA. Non-invasive echocardiographic studies in mice: influence of anesthetic regimen. *Life Sci.* 2001;69:213-22.
96. Takuma S, Suehiro K, Cardinale C, Hozumi T, Yano H, Shimizu J, Mullis-Jansson S, Sciacca R, Wang J, Burkhoff D, Di Tullio MR, Homma S. Anesthetic inhibition in ischemic and nonischemic murine heart: comparison with conscious echocardiographic approach. *Am J Physiol Heart Circ Physiol.* 2001;280:H2364-2370.
97. Strauer BE. Ventricular function and coronary hemodynamics in hypertensive heart disease. *Am J Cardiol.* 1979;44:999-1006.
98. Topol EJ, Traill TA, Fortuin NJ. Hypertensive hypertrophic cardiomyopathy of the elderly. *N Engl J Med.* 1985;312:277-83.
99. Alpert NR, Hamrell BB, Halpern W. Mechanical and biochemical correlates of cardiac hypertrophy. *Circ Res.* 1974;35:suppl II:71-82.
100. Bing OH, Matsushita S, Fanburg BL, Levine HJ. Mechanical properties of rat cardiac muscle during experimental hypertrophy. *Circ Res.* 1971;28:234-45.
101. Sasayama S, Franklin D, Ross J, Jr. Hyperfunction with normal inotropic state of the hypertrophied left ventricle. *Am J Physiol.* 1977;232:H418-25.
102. Kahn JK. Correlates of supranormal (ejection fraction greater than or equal to 85%) left ventricular performance. *Am J Cardiol.* 1988;61:1145-6.
103. Litwin SE, Katz SE, Morgan JP, Douglas PS. Serial echocardiographic assessment of left ventricular geometry and function after large myocardial infarction in the rat. *Circulation.* 1994;89:345-54.
104. Nakamura A, Rokosh DG, Paccanaro M, Yee RR, Simpson PC, Grossman W, Foster E. LV systolic performance improves with development of hypertrophy after transverse aortic constriction in mice. *Am J Physiol Heart Circ Physiol.* 2001;281:H1104-12.
105. Engelhardt S, Hein L, Wiesmann F, Lohse MJ. Progressive hypertrophy and heart failure in beta1-adrenergic receptor transgenic mice. *Proc Natl Acad Sci U S A.* 1999;96:7059-64.
106. Bing OH, Brooks WW, Robinson KG, Slawsky MT, Hayes JA, Litwin SE, Sen S, Conrad CH. The spontaneously hypertensive rat as a model of the

transition from compensated left ventricular hypertrophy to failure. *J Mol Cell Cardiol*. 1995;27:383-96.
107. Boluyt MO, O'Neill L, Meredith AL, Bing OH, Brooks WW, Conrad CH, Crow MT, Lakatta EG. Alterations in cardiac gene expression during the transition from stable hypertrophy to heart failure. Marked upregulation of genes encoding extracellular matrix components. *Circ Res*. 1994;75:23-32.
108. Doi R, Masuyama T, Yamamoto K, Doi Y, Mano T, Sakata Y, Ono K, Kuzuya T, Hirota S, Koyama T, Miwa T, Hori M. Development of different phenotypes of hypertensive heart failure: systolic versus diastolic failure in Dahl salt-sensitive rats. *J Hypertens*. 2000;18:111-20.
109. Capasso JM, Palackal T, Olivetti G, Anversa P. Severe myocardial dysfunction induced by ventricular remodeling in aging rat hearts. *Am J Physiol*. 1990;259:H1086-96.
110. Iwanaga Y, Kihara Y, Hasegawa K, Inagaki K, Yoneda T, Kaburagi S, Araki M, Sasayama S. Cardiac endothelin-1 plays a critical role in the functional deterioration of left ventricles during the transition from compensatory hypertrophy to congestive heart failure in salt-sensitive hypertensive rats. *Circulation*. 1998;98:2065-73.
111. Yamamoto K, Masuyama T, Sakata Y, Doi R, Ono K, Mano T, Kondo H, Kuzuya T, Miwa T, Hori M. Local neurohumoral regulation in the transition to isolated diastolic heart failure in hypertensive heart disease: absence of AT1 receptor downregulation and 'overdrive' of the endothelin system. *Cardiovasc Res*. 2000;46:421-32.
112. Rothermund L, Pinto YM, Hocher B, Vetter R, Leggewie S, Kobetamehl P, Orzechowski HD, Kreutz R, Paul M. Cardiac endothelin system impairs left ventricular function in renin-dependent hypertension via decreased sarcoplasmic reticulum Ca(2+) uptake. *Circulation*. 2000;102:1582-8.
113. Zolk O, Quattek J, Seeland U, El-Armouche A, Eschenhagen T, Bohm M. Activation of the cardiac endothelin system in left ventricular hypertrophy before onset of heart failure in TG(mREN2)27 rats. *Cardiovasc Res*. 2002;53:363-71.
114. Yamamoto K, Masuyama T, Sakata Y, Mano T, Nishikawa N, Kondo H, Akehi N, Kuzuya T, Miwa T, Hori M. Roles of renin-angiotensin and endothelin systems in development of diastolic heart failure in hypertensive hearts. *Cardiovasc Res*. 2000;47:274-83.
115. Barlucchi L, Leri A, Dostal DE, Fiordaliso F, Tada H, Hintze TH, Kajstura J, Nadal-Ginard B, Anversa P. Canine ventricular myocytes possess a renin-angiotensin system that is upregulated with heart failure. *Circ Res*. 2001;88:298-304.
116. Iwanaga Y, Kihara Y, Inagaki K, Onozawa Y, Yoneda T, Kataoka K, Sasayama S. Differential effects of angiotensin II versus endothelin-1 inhibitions in hypertrophic left ventricular myocardium during transition to heart failure. *Circulation*. 2001;104:606-12.

117. Weinberg EO, Schoen FJ, George D, Kagaya Y, Douglas PS, Litwin SE, Schunkert H, Benedict CR, Lorell BH. Angiotensin-converting enzyme inhibition prolongs survival and modifies the transition to heart failure in rats with pressure overload hypertrophy due to ascending aortic stenosis. *Circulation*. 1994;90:1410-22.
118. Serneri GG, Boddi M, Cecioni I, Vanni S, Coppo M, Papa ML, Bandinelli B, Bertolozzi I, Polidori G, Toscano T, Maccherini M, Modesti PA. Cardiac angiotensin II formation in the clinical course of heart failure and its relationship with left ventricular function. *Circ Res*. 2001;88:961-8.
119. Zolk O, Ng LL, O'Brien RJ, Weyand M, Eschenhagen T. Augmented expression of cardiotrophin-1 in failing human hearts is accompanied by diminished glycoprotein 130 receptor protein abundance. *Circulation*. 2002;106:1442-6.
120. Takimoto Y, Aoyama T, Iwanaga Y, Izumi T, Kihara Y, Pennica D, Sasayama S. Increased expression of cardiotrophin-1 during ventricular remodeling in hypertensive rats. *Am J Physiol Heart Circ Physiol*. 2002;282:H896-901.
121. Rohrbach S, Yan X, Weinberg EO, Hasan F, Bartunek J, Marchionni MA, Lorell BH. Neuregulin in cardiac hypertrophy in rats with aortic stenosis. Differential expression of erbB2 and erbB4 receptors. *Circulation*. 1999;100:407-12.
122. Sordahl LA, McCollum WB, Wood WG, Schwartz A. Mitochondria and sarcoplasmic reticulum function in cardiac hypertrophy and failure. *Am J Physiol*. 1973;224:497-502.
123. Gwathmey JK, Morgan JP. Altered calcium handling in experimental pressure-overload hypertrophy in the ferret. *Circ Res*. 1985;57:836-43.
124. Whitmer JT, Kumar P, Solaro RJ. Calcium transport properties of cardiac sarcoplasmic reticulum from cardiomyopathic Syrian hamsters (BIO 53.58 and 14.6): evidence for a quantitative defect in dilated myopathic hearts not evident in hypertrophic hearts. *Circ Res*. 1988;62:81-5.
125. Mercadier JJ, Lompre AM, Duc P, Boheler KR, Fraysse JB, Wisnewsky C, Allen PD, Komajda M, Schwartz K. Altered sarcoplasmic reticulum Ca2(+)-ATPase gene expression in the human ventricle during end-stage heart failure. *J Clin Invest*. 1990;85:305-9.
126. Meyer M, Schillinger W, Pieske B, Holubarsch C, Heilmann C, Posival H, Kuwajima G, Mikoshiba K, Just H, Hasenfuss G, et al. Alterations of sarcoplasmic reticulum proteins in failing human dilated cardiomyopathy. *Circulation*. 1995;92:778-84.
127. Ito K, Yan X, Tajima M, Su Z, Barry WH, Lorell BH. Contractile reserve and intracellular calcium regulation in mouse myocytes from normal and hypertrophied failing hearts. *Circ Res*. 2000;87:588-95.
128. Pieske B, Maier LS, Bers DM, Hasenfuss G. Ca2+ handling and sarcoplasmic reticulum Ca2+ content in isolated failing and nonfailing human myocardium. *Circ Res*. 1999;85:38-46.

129. Qi M, Shannon TR, Euler DE, Bers DM, Samarel AM. Downregulation of sarcoplasmic reticulum Ca(2+)-ATPase during progression of left ventricular hypertrophy. *Am J Physiol.* 1997;272:H2416-24.
130. Arai M, Suzuki T, Nagai R. Sarcoplasmic reticulum genes are upregulated in mild cardiac hypertrophy but downregulated in severe cardiac hypertrophy induced by pressure overload. *J Mol Cell Cardiol.* 1996;28:1583-90.
131. Schultz JEJ, Glascock BJ, Witt SA, Nieman ML, Nattamai KJ, Liu LH, Lorenz JN, Shull GE, Kimball TR, Periasamy M. Accelerated onset of heart failure in mice during pressure overload with chronically decreased SERCA2 calcium pump activity. *Am J Physiol Heart Circ Physiol.* 2004;286:H1146-1153.
132. Giordano FJ, He H, McDonough P, Meyer M, Sayen MR, Dillmann WH. Adenovirus-mediated gene transfer reconstitutes depressed sarcoplasmic reticulum Ca2+-ATPase levels and shortens prolonged cardiac myocyte Ca2+ transients. *Circulation.* 1997;96:400-3.
133. He H, Giordano FJ, Hilal-Dandan R, Choi DJ, Rockman HA, McDonough PM, Bluhm WF, Meyer M, Sayen MR, Swanson E, Dillmann WH. Overexpression of the rat sarcoplasmic reticulum Ca2+ ATPase gene in the heart of transgenic mice accelerates calcium transients and cardiac relaxation. *J Clin Invest.* 1997;100:380-9.
134. Baker DL, Hashimoto K, Grupp IL, Ji Y, Reed T, Loukianov E, Grupp G, Bhagwhat A, Hoit B, Walsh R, Marban E, Periasamy M. Targeted overexpression of the sarcoplasmic reticulum Ca2+-ATPase increases cardiac contractility in transgenic mouse hearts. *Circ Res.* 1998;83:1205-14.
135. Loukianov E, Ji Y, Grupp IL, Kirkpatrick DL, Baker DL, Loukianova T, Grupp G, Lytton J, Walsh RA, Periasamy M. Enhanced myocardial contractility and increased Ca2+ transport function in transgenic hearts expressing the fast-twitch skeletal muscle sarcoplasmic reticulum Ca2+-ATPase. *Circ Res.* 1998;83:889-97.
136. del Monte F, Hajjar RJ, Harding SE. Overwhelming evidence of the beneficial effects of SERCA gene transfer in heart failure. *Circ Res.* 2001;88:E66-7.
137. Miyamoto MI, del Monte F, Schmidt U, DiSalvo TS, Kang ZB, Matsui T, Guerrero JL, Gwathmey JK, Rosenzweig A, Hajjar RJ. Adenoviral gene transfer of SERCA2a improves left-ventricular function in aortic-banded rats in transition to heart failure. *Proc Natl Acad Sci U S A.* 2000;97:793-8.
138. Ito K, Yan X, Feng X, Manning WJ, Dillmann WH, Lorell BH. Transgenic expression of sarcoplasmic reticulum Ca(2+) atpase modifies the transition from hypertrophy to early heart failure. *Circ Res.* 2001;89:422-9.
139. O'Donnell JM, Sumbilla CM, Ma H, Farrance IK, Cavagna M, Klein MG, Inesi G. Tight control of exogenous SERCA expression is required to

obtain acceleration of calcium transients with minimal cytotoxic effects in cardiac myocytes. *Circ Res*. 2001;88:415-21.
140. Toyoshima C, Asahi M, Sugita Y, Khanna R, Tsuda T, MacLennan DH. Inaugural Article: Modeling of the inhibitory interaction of phospholamban with the Ca2+ ATPase. *Proc Natl Acad Sci U S A*. 2003;100:467-72.
141. Hasenfuss G. Alterations of calcium-regulatory proteins in heart failure. *Cardiovasc Res*. 1998;37:279-89.
142. Luo W, Grupp IL, Harrer J, Ponniah S, Grupp G, Duffy JJ, Doetschman T, Kranias EG. Targeted ablation of the phospholamban gene is associated with markedly enhanced myocardial contractility and loss of beta-agonist stimulation. *Circ Res*. 1994;75:401-9.
143. Minamisawa S, Hoshijima M, Chu G, Ward CA, Frank K, Gu Y, Martone ME, Wang Y, Ross J, Jr., Kranias EG, Giles WR, Chien KR. Chronic phospholamban-sarcoplasmic reticulum calcium ATPase interaction is the critical calcium cycling defect in dilated cardiomyopathy. *Cell*. 1999;99:313-22.
144. Sato Y, Kiriazis H, Yatani A, Schmidt AG, Hahn H, Ferguson DG, Sako H, Mitarai S, Honda R, Mesnard-Rouiller L, Frank KF, Beyermann B, Wu G, Fujimori K, Dorn GW, 2nd, Kranias EG. Rescue of contractile parameters and myocyte hypertrophy in calsequestrin overexpressing myocardium by phospholamban ablation. *J Biol Chem*. 2001;276:9392-9.
145. Haghighi K, Schmidt AG, Hoit BD, Brittsan AG, Yatani A, Lester JW, Zhai J, Kimura Y, Dorn GW, 2nd, MacLennan DH, Kranias EG. Superinhibition of sarcoplasmic reticulum function by phospholamban induces cardiac contractile failure. *J Biol Chem*. 2001;276:24145-52.
146. Zvaritch E, Backx PH, Jirik F, Kimura Y, de Leon S, Schmidt AG, Hoit BD, Lester JW, Kranias EG, MacLennan DH. The transgenic expression of highly inhibitory monomeric forms of phospholamban in mouse heart impairs cardiac contractility. *J Biol Chem*. 2000;275:14985-91.
147. Kiriazis H, Sato Y, Kadambi VJ, Schmidt AG, Gerst MJ, Hoit BD, Kranias EG. Hypertrophy and functional alterations in hyperdynamic phospholamban-knockout mouse hearts under chronic aortic stenosis. *Cardiovasc Res*. 2002;53:372-81.
148. Chu G, Carr AN, Young KB, Lester JW, Yatani A, Sanbe A, Colbert MC, Schwartz SM, Frank KF, Lampe PD, Robbins J, Molkentin JD, Kranias EG. Enhanced myocyte contractility and Ca2+ handling in a calcineurin transgenic model of heart failure. *Cardiovasc Res*. 2002;54:105-16.
149. Marx SO, Reiken S, Hisamatsu Y, Jayaraman T, Burkhoff D, Rosemblit N, Marks AR. PKA phosphorylation dissociates FKBP12.6 from the calcium release channel (ryanodine receptor): defective regulation in failing hearts. *Cell*. 2000;101:365-76.
150. Schmidt AG, Kadambi VJ, Ball N, Sato Y, Walsh RA, Kranias EG, Hoit BD. Cardiac-specific overexpression of calsequestrin results in left ventricular hypertrophy, depressed force-frequency relation and pulsus alternans in vivo. *J Mol Cell Cardiol*. 2000;32:1735-44.

151. Zeitz O, Maass AE, Van Nguyen P, Hensmann G, Kogler H, Moller K, Hasenfuss G, Janssen PM. Hydroxyl radical-induced acute diastolic dysfunction is due to calcium overload via reverse-mode Na(+)-Ca(2+) exchange. *Circ Res*. 2002;90:988-95.
152. Hasenfuss G, Schillinger W, Lehnart SE, Preuss M, Pieske B, Maier LS, Prestle J, Minami K, Just H. Relationship between Na+-Ca2+-exchanger protein levels and diastolic function of failing human myocardium. *Circulation*. 1999;99:641-8.
153. Hasenfuss G, Pieske B. Calcium cycling in congestive heart failure. *J Mol Cell Cardiol*. 2002;34:951-69.
154. Litten RZ, 3rd, Brayden JE, Alpert NR. The ATPase activity of subfragment-1 from the hypertrophied heart. *Biochim Biophys Acta*. 1978;523:377-84.
155. Lowes BD, Minobe W, Abraham WT, Rizeq MN, Bohlmeyer TJ, Quaife RA, Roden RL, Dutcher DL, Robertson AD, Voelkel NF, Badesch DB, Groves BM, Gilbert EM, Bristow MR. Changes in gene expression in the intact human heart. Downregulation of alpha-myosin heavy chain in hypertrophied, failing ventricular myocardium. *J Clin Invest*. 1997;100:2315-24.
156. Krenz M, Sanbe A, Bouyer-Dalloz F, Gulick J, Klevitsky R, Hewett TE, Osinska HE, Lorenz JN, Brosseau C, Federico A, Alpert NR, Warshaw DM, Perryman MB, Helmke SM, Robbins J. Analysis of myosin heavy chain functionality in the heart. *J Biol Chem*. 2003;278:17466-74.
157. Lompre AM, Schwartz K, d'Albis A, Lacombe G, Van Thiem N, Swynghedauw B. Myosin isoenzyme redistribution in chronic heart overload. *Nature*. 1979;282:105-7.
158. Kameyama T, Chen Z, Bell SP, VanBuren P, Maughan D, LeWinter MM. Mechanoenergetic alterations during the transition from cardiac hypertrophy to failure in Dahl salt-sensitive rats. *Circulation*. 1998;98:2919-29.
159. Yang J, Moravec CS, Sussman MA, DiPaola NR, Fu D, Hawthorn L, Mitchell CA, Young JB, Francis GS, McCarthy PM, Bond M. Decreased SLIM1 expression and increased gelsolin expression in failing human hearts measured by high-density oligonucleotide arrays. *Circulation*. 2000;102:3046-52.
160. Ohno M, Takemura G, Ohno A, Misao J, Hayakawa Y, Minatoguchi S, Fujiwara T, Fujiwara H. "Apoptotic" myocytes in infarct area in rabbit hearts may be oncotic myocytes with DNA fragmentation: analysis by immunogold electron microscopy combined with In situ nick end-labeling. *Circulation*. 1998;98:1422-30.
161. Kanoh M, Takemura G, Misao J, Hayakawa Y, Aoyama T, Nishigaki K, Noda T, Fujiwara T, Fukuda K, Minatoguchi S, Fujiwara H. Significance of myocytes with positive DNA in situ nick end-labeling (TUNEL) in hearts with dilated cardiomyopathy: not apoptosis but DNA repair. *Circulation*. 1999;99:2757-64.

162. Kang PM, Izumo S. Apoptosis and heart failure: A critical review of the literature. *Circ Res*. 2000;86:1107-13.
163. Anversa P. Myocyte death in the pathological heart. *Circ Res*. 2000;86:121-4.
164. Lee P, Morley G, Huang Q, Fischer A, Seiler S, Horner JW, Factor S, Vaidya D, Jalife J, Fishman GI. Conditional lineage ablation to model human diseases. *Proc Natl Acad Sci U S A*. 1998;95:11371-6.
165. Condorelli G, Roncarati R, Ross J, Jr., Pisani A, Stassi G, Todaro M, Trocha S, Drusco A, Gu Y, Russo MA, Frati G, Jones SP, Lefer DJ, Napoli C, Croce CM. Heart-targeted overexpression of caspase3 in mice increases infarct size and depresses cardiac function. *Proc Natl Acad Sci U S A*. 2001;98:9977-82.
166. Teiger E, Than VD, Richard L, Wisnewsky C, Tea BS, Gaboury L, Tremblay J, Schwartz K, Hamet P. Apoptosis in pressure overload-induced heart hypertrophy in the rat. *J Clin Invest*. 1996;97:2891-7.
167. Nitahara JA, Cheng W, Liu Y, Li B, Leri A, Li P, Mogul D, Gambert SR, Kajstura J, Anversa P. Intracellular calcium, DNase activity and myocyte apoptosis in aging Fischer 344 rats. *J Mol Cell Cardiol*. 1998;30:519-35.
168. Kajstura J, Cheng W, Sarangarajan R, Li P, Li B, Nitahara JA, Chapnick S, Reiss K, Olivetti G, Anversa P. Necrotic and apoptotic myocyte cell death in the aging heart of Fischer 344 rats. *Am J Physiol*. 1996;271:H1215-28.
169. Condorelli G, Morisco C, Stassi G, Notte A, Farina F, Sgaramella G, de Rienzo A, Roncarati R, Trimarco B, Lembo G. Increased cardiomyocyte apoptosis and changes in proapoptotic and antiapoptotic genes bax and bcl-2 during left ventricular adaptations to chronic pressure overload in the rat. *Circulation*. 1999;99:3071-8.
170. Ding B, Price RL, Goldsmith EC, Borg TK, Yan X, Douglas PS, Weinberg EO, Bartunek J, Thielen T, Didenko VV, Lorell BH. Left ventricular hypertrophy in ascending aortic stenosis mice: anoikis and the progression to early failure. *Circulation*. 2000;101:2854-62.
171. Ikeda S, Hamada M, Hiwada K. Contribution of non-cardiomyocyte apoptosis to cardiac remodelling that occurs in the transition from compensated hypertrophy to heart failure in spontaneously hypertensive rats. *Clin Sci (Lond)*. 1999;97:239-46.
172. Li Z, Bing OH, Long X, Robinson KG, Lakatta EG. Increased cardiomyocyte apoptosis during the transition to heart failure in the spontaneously hypertensive rat. *Am J Physiol*. 1997;272:H2313-9.
173. Hirota H, Chen J, Betz UA, Rajewsky K, Gu Y, Ross J, Jr., Muller W, Chien KR. Loss of a gp130 cardiac muscle cell survival pathway is a critical event in the onset of heart failure during biomechanical stress. *Cell*. 1999;97:189-98.
174. Rogers JH, Tamirisa P, Kovacs A, Weinheimer C, Courtois M, Blumer KJ, Kelly DP, Muslin AJ. RGS4 causes increased mortality and reduced

cardiac hypertrophy in response to pressure overload. *J Clin Invest.* 1999;104:567-76.
175. Brancaccio M, Fratta L, Notte A, Hirsch E, Poulet R, Guazzone S, De Acetis M, Vecchione C, Marino G, Altruda F, Silengo L, Tarone G, Lembo G. Melusin, a muscle-specific integrin beta(1)-interacting protein, is required to prevent cardiac failure in response to chronic pressure overload. *Nat Med.* 2003;9:68-75.
176. Shai SY, Harpf AE, Babbitt CJ, Jordan MC, Fishbein MC, Chen J, Omura M, Leil TA, Becker KD, Jiang M, Smith DJ, Cherry SR, Loftus JC, Ross RS. Cardiac myocyte-specific excision of the beta1 integrin gene results in myocardial fibrosis and cardiac failure. *Circ Res.* 2002;90:458-64.
177. Crone SA, Zhao YY, Fan L, Gu Y, Minamisawa S, Liu Y, Peterson KL, Chen J, Kahn R, Condorelli G, Ross J, Jr., Chien KR, Lee KF. ErbB2 is essential in the prevention of dilated cardiomyopathy. *Nat Med.* 2002;8:459-65.
178. Badorff C, Ruetten H, Mueller S, Stahmer M, Gehring D, Jung F, Ihling C, Zeiher AM, Dimmeler S. Fas receptor signaling inhibits glycogen synthase kinase 3{beta} and induces cardiac hypertrophy following pressure overload. *J. Clin. Invest.* 2002;109:373-381.
179. Lemire I, Ducharme A, Tardif JC, Poulin F, Jones LR, Allen BG, Hebert TE, Rindt H. Cardiac-directed overexpression of wild-type alpha1B-adrenergic receptor induces dilated cardiomyopathy. *Am J Physiol Heart Circ Physiol.* 2001;281:H931-8.
180. Adams JW, Sakata Y, Davis MG, Sah VP, Wang Y, Liggett SB, Chien KR, Brown JH, Dorn GW, 2nd. Enhanced Galphaq signaling: a common pathway mediates cardiac hypertrophy and apoptotic heart failure. *Proc Natl Acad Sci U S A.* 1998;95:10140-5.
181. Kubota T, McTiernan CF, Frye CS, Slawson SE, Lemster BH, Koretsky AP, Demetris AJ, Feldman AM. Dilated cardiomyopathy in transgenic mice with cardiac-specific overexpression of tumor necrosis factor-alpha. *Circ Res.* 1997;81:627-35.
182. Geng YJ, Ishikawa Y, Vatner DE, Wagner TE, Bishop SP, Vatner SF, Homcy CJ. Apoptosis of cardiac myocytes in Gsalpha transgenic mice. *Circ Res.* 1999;84:34-42.
183. Pellieux C, Foletti A, Peduto G, Aubert JF, Nussberger J, Beermann F, Brunner HR, Pedrazzini T. Dilated cardiomyopathy and impaired cardiac hypertrophic response to angiotensin II in mice lacking FGF-2. *J Clin Invest.* 2001;108:1843-51.
184. Duerr RL, McKirnan MD, Gim RD, Clark RG, Chien KR, Ross J, Jr. Cardiovascular effects of insulin-like growth factor-1 and growth hormone in chronic left ventricular failure in the rat. *Circulation.* 1996;93:2188-96.
185. Duerr RL, Huang S, Miraliakbar HR, Clark R, Chien KR, Ross J, Jr. Insulin-like growth factor-1 enhances ventricular hypertrophy and function during the onset of experimental cardiac failure. *J Clin Invest.* 1995;95:619-27.

186. Palmen M, Daemen MJ, Bronsaer R, Dassen WR, Zandbergen HR, Kockx M, Smits JF, van der Zee R, Doevendans PA. Cardiac remodeling after myocardial infarction is impaired in IGF-1 deficient mice. *Cardiovasc Res*. 2001;50:516-24.
187. Li Q, Li B, Wang X, Leri A, Jana KP, Liu Y, Kajstura J, Baserga R, Anversa P. Overexpression of insulin-like growth factor-1 in mice protects from myocyte death after infarction, attenuating ventricular dilation, wall stress, and cardiac hypertrophy. *J Clin Invest*. 1997;100:1991-9.
188. Welch S, Plank D, Witt S, Glascock B, Schaefer E, Chimenti S, Andreoli AM, Limana F, Leri A, Kajstura J, Anversa P, Sussman MA. Cardiac-specific IGF-1 expression attenuates dilated cardiomyopathy in tropomodulin-overexpressing transgenic mice. *Circ Res*. 2002;90:641-8.
189. Janssen PM, Hasenfuss G, Zeitz O, Lehnart SE, Prestle J, Darmer D, Holtz J, Schumann H. Load-dependent induction of apoptosis in multicellular myocardial preparations. *Am J Physiol Heart Circ Physiol*. 2002;282:H349-56.
190. Pimentel DR, Amin JK, Xiao L, Miller T, Viereck J, Oliver-Krasinski J, Baliga R, Wang J, Siwik DA, Singh K, Pagano P, Colucci WS, Sawyer DB. Reactive oxygen species mediate amplitude-dependent hypertrophic and apoptotic responses to mechanical stretch in cardiac myocytes. *Circ Res*. 2001;89:453-60.
191. Leri A, Claudio PP, Li Q, Wang X, Reiss K, Wang S, Malhotra A, Kajstura J, Anversa P. Stretch-mediated release of angiotensin II induces myocyte apoptosis by activating p53 that enhances the local renin-angiotensin system and decreases the Bcl-2-to-Bax protein ratio in the cell. *J Clin Invest*. 1998;101:1326-42.
192. Cook SA, Sugden PH, Clerk A. Regulation of bcl-2 family proteins during development and in response to oxidative stress in cardiac myocytes: association with changes in mitochondrial membrane potential. *Circ Res*. 1999;85:940-9.
193. Sawyer DB, Colucci WS. Mitochondrial oxidative stress in heart failure: "oxygen wastage" revisited. *Circ Res*. 2000;86:119-20.
194. Ide T, Tsutsui H, Kinugawa S, Suematsu N, Hayashidani S, Ichikawa K, Utsumi H, Machida Y, Egashira K, Takeshita A. Direct evidence for increased hydroxyl radicals originating from superoxide in the failing myocardium. *Circ Res*. 2000;86:152-7.
195. Li JM, Gall NP, Grieve DJ, Chen M, Shah AM. Activation of NADPH oxidase during progression of cardiac hypertrophy to failure. *Hypertension*. 2002;40:477-84.
196. Beggah AT, Escoubet B, Puttini S, Cailmail S, Delage V, Ouvrard-Pascaud A, Bocchi B, Peuchmaur M, Delcayre C, Farman N, Jaisser F. Reversible cardiac fibrosis and heart failure induced by conditional expression of an antisense mRNA of the mineralocorticoid receptor in cardiomyocytes. *Proc Natl Acad Sci U S A*. 2002;99:7160-5.

197. Weber KT. Fibrosis and hypertensive heart disease. *Curr Opin Cardiol.* 2000;15:264-72.
198. Diez J, Laviades C, Mayor G, Gil MJ, Monreal I. Increased serum concentrations of procollagen peptides in essential hypertension. Relation to cardiac alterations. *Circulation*. 1995;91:1450-6.
199. Annoni G, Luvara G, Arosio B, Gagliano N, Fiordaliso F, Santambrogio D, Jeremic G, Mircoli L, Latini R, Vergani C, Masson S. Age-dependent expression of fibrosis-related genes and collagen deposition in the rat myocardium. *Mech Ageing Dev*. 1998;101:57-72.
200. Yamamoto K, Masuyama T, Sakata Y, Nishikawa N, Mano T, Yoshida J, Miwa T, Sugawara M, Yamaguchi Y, Ookawara T, Suzuki K, Hori M. Myocardial stiffness is determined by ventricular fibrosis, but not by compensatory or excessive hypertrophy in hypertensive heart. *Cardiovasc Res*. 2002;55:76-82.
201. Burlew BS, Weber KT. Cardiac fibrosis as a cause of diastolic dysfunction. *Herz*. 2002;27:92-8.
202. Iwanaga Y, Aoyama T, Kihara Y, Onozawa Y, Yoneda T, Sasayama S. Excessive activation of matrix metalloproteinases coincides with left ventricular remodeling during transition from hypertrophy to heart failure in hypertensive rats. *J Am Coll Cardiol*. 2002;39:1384-91.
203. Brower GL, Janicki JS. Contribution of ventricular remodeling to pathogenesis of heart failure in rats. *Am J Physiol Heart Circ Physiol*. 2001;280:H674-83.
204. Spinale FG, Coker ML, Thomas CV, Walker JD, Mukherjee R, Hebbar L. Time-dependent changes in matrix metalloproteinase activity and expression during the progression of congestive heart failure: relation to ventricular and myocyte function. *Circ Res*. 1998;82:482-95.
205. Janicki JS, Brower GL, Henegar JR, Wang L. Ventricular remodeling in heart failure: the role of myocardial collagen. *Adv Exp Med Biol*. 1995;382:239-45.
206. Gunja-Smith Z, Morales AR, Romanelli R, Woessner JF, Jr. Remodeling of human myocardial collagen in idiopathic dilated cardiomyopathy. Role of metalloproteinases and pyridinoline cross-links. *Am J Pathol*. 1996;148:1639-48.
207. Peterson JT, Hallak H, Johnson L, Li H, O'Brien PM, Sliskovic DR, Bocan TM, Coker ML, Etoh T, Spinale FG. Matrix metalloproteinase inhibition attenuates left ventricular remodeling and dysfunction in a rat model of progressive heart failure. *Circulation*. 2001;103:2303-9.
208. Chancey AL, Brower GL, Peterson JT, Janicki JS. Effects of matrix metalloproteinase inhibition on ventricular remodeling due to volume overload. *Circulation*. 2002;105:1983-8.
209. Woodiwiss AJ, Tsotetsi OJ, Sprott S, Lancaster EJ, Mela T, Chung ES, Meyer TE, Norton GR. Reduction in myocardial collagen cross-linking parallels left ventricular dilatation in rat models of systolic chamber dysfunction. *Circulation*. 2001;103:155-60.

210. Beltrami CA, Finato N, Rocco M, Feruglio GA, Puricelli C, Cigola E, Quaini F, Sonnenblick EH, Olivetti G, Anversa P. Structural basis of end-stage failure in ischemic cardiomyopathy in humans. *Circulation*. 1994;89:151-63.
211. Siwik DA, Chang DL, Colucci WS. Interleukin-1beta and tumor necrosis factor-alpha decrease collagen synthesis and increase matrix metalloproteinase activity in cardiac fibroblasts in vitro. *Circ Res*. 2000;86:1259-65.
212. Bozkurt B, Kribbs SB, Clubb FJ, Jr., Michael LH, Didenko VV, Hornsby PJ, Seta Y, Oral H, Spinale FG, Mann DL. Pathophysiologically relevant concentrations of tumor necrosis factor-alpha promote progressive left ventricular dysfunction and remodeling in rats. *Circulation*. 1998;97:1382-91.
213. Diwan A, Dibbs Z, Nemoto S, DeFreitas G, Carabello BA, Sivasubramanian N, Wilson EM, Spinale FG, Mann DL. Targeted Overexpression of Noncleavable and Secreted Forms of Tumor Necrosis Factor Provokes Disparate Cardiac Phenotypes. *Circulation*. 2004;109:262-268.
214. Bradham WS, Bozkurt B, Gunasinghe H, Mann D, Spinale FG. Tumor necrosis factor-alpha and myocardial remodeling in progression of heart failure: a current perspective. *Cardiovasc Res*. 2002;53:822-30.
215. Bozkurt B, Torre-Amione G, Warren MS, Whitmore J, Soran OZ, Feldman AM, Mann DL. Results of targeted anti-tumor necrosis factor therapy with etanercept (ENBREL) in patients with advanced heart failure. *Circulation*. 2001;103:1044-7.
216. Kadokami T, Frye C, Lemster B, Wagner CL, Feldman AM, McTiernan CF. Anti-tumor necrosis factor-alpha antibody limits heart failure in a transgenic model. *Circulation*. 2001;104:1094-7.
217. Pinto YM, Pinto-Sietsma SJ, Philipp T, Engler S, Kossamehl P, Hocher B, Marquardt H, Sethmann S, Lauster R, Merker HJ, Paul M. Reduction in left ventricular messenger RNA for transforming growth factor beta(1) attenuates left ventricular fibrosis and improves survival without lowering blood pressure in the hypertensive TGR(mRen2)27 Rat. *Hypertension*. 2000;36:747-54.
218. Zhang J. Myocardial energetics in cardiac hypertrophy. *Clin Exp Pharmacol Physiol*. 2001;29:351-359.
219. Weiss RG, Chatham JC, Georgakopoulos D, Charron MJ, Wallimann T, Kay L, Walzel B, Wang Y, Kass DA, Gerstenblith G, Chacko VP. An increase in the myocardial PCr/ATP ratio in GLUT4 null mice. *FASEB J*. 2002;16:613-615.
220. Kaasik A, Veksler V, Boehm E, Novotova M, Minajeva A, Ventura-Clapier R. Energetic crosstalk between organelles: architectural integration of energy production and utilization. *Circ Res*. 2001;89:153-159.

221. Murakami Y, Zhang J, Eijgelshoven MHJ. Myocardial creatine kinase kinetics in hearts with postinfarction left ventricular remodelling. *Am J Physiol Heart Circ Physiol*. 1999;276:H892-900.
222. Tian R, Ingwall JS. Energetic basis for reduced contractile reserve in isolated rat hearts. *Am J Physiol Heart Circ Physiol*. 1996;270:H1207-16.
223. Liao R, Jain M, Cui L, D'Agostino J, Aiello F, Luptak I, Ngoy S, Mortensen RM, Tian R. Cardiac-Specific Overexpression of GLUT1 Prevents the Development of Heart Failure Attributable to Pressure Overload in Mice. *Circulation*. 2002;106:2125-2131.
224. Nitenberg A, Loiseau A, Antony I. Left ventricular mechanical efficiency in hypertensive patients with and without increased myocardial mass and with normal pump function. *Am J Hypertens*. 2001;14:1231-8.
225. Morii I, Kihara Y, Inoko M, Sasayama S. Myocardial contractile efficiency and oxygen cost of contractility are preserved during transition from compensated hypertrophy to failure in rats with salt-sensitive hypertension. *Hypertension*. 1998;31:949-60.
226. Kameyama T, Chen Z, Bell SP, VanBuren P, Maughan D, LeWinter MM. Mechanoenergetic alterations during the transition from cardiac hypertrophy to failure in Dahl salt-sensitive rats. *Circulation*. 1998;98:2919-29.
227. Sadoshima J, Izumo S. Mechanotransduction in stretch-induced hypertrophy of cardiac myocytes. *J Recept Res*. 1993;13:777-94.
228. Sadoshima J, Takahashi T, Jahn L, Izumo S. Roles of mechano-sensitive ion channels, cytoskeleton, and contractile activity in stretch-induced immediate-early gene expression and hypertrophy of cardiac myocytes. *Proc Natl Acad Sci U S A*. 1992;89:9905-9.
229. Vandenburgh HH, Solerssi R, Shansky J, Adams JW, Henderson SA, Lemaire J. Response of neonatal rat cardiomyocytes to repetitive mechanical stimulation in vitro. *Ann N Y Acad Sci*. 1995;752:19-29.
230. Mann DL, Kent RL, Cooper Gt. Load regulation of the properties of adult feline cardiocytes: growth induction by cellular deformation. *Circ Res*. 1989;64:1079-90.
231. Yamazaki T, Komuro I, Yazaki Y. Molecular aspects of mechanical stress-induced cardiac hypertrophy. *Mol Cell Biochem*. 1996;163-164:197-201.
232. Kira Y, Kochel PJ, Gordon EE, Morgan HE. Aortic perfusion pressure as a determinant of cardiac protein synthesis. *Am J Physiol*. 1984;246:C247-58.
233. Palmieri EA, Benincasa G, Di Rella F, Casaburi C, Monti MG, De Simone G, Chiariotti L, Palombini L, Bruni CB, Sacca L, Cittadini A. Differential expression of TNF-alpha , IL-6, and IGF-1 by graded mechanical stress in normal rat myocardium. *Am J Physiol Heart Circ Physiol*. 2002;282:H926-934.
234. Li J, Hampton T, Morgan JP, Simons M. Stretch-induced VEGF Expression in the Heart. *J. Clin. Invest.* 1997;100:18-24.

235. Baumgarten G, Knuefermann P, Kalra D, Gao F, Taffet GE, Michael L, Blackshear PJ, Carballo E, Sivasubramanian N, Mann DL. Load-dependent and -independent regulation of proinflammatory cytokine and cytokine receptor gene expression in the adult mammalian heart. *Circulation*. 2002;105:2192-7.
236. Wiesner RJ, Ehmke H, Faulhaber J, Zak R, Ruegg JC. Dissociation of left ventricular hypertrophy, beta-myosin heavy chain gene expression, and myosin isoform switch in rats after ascending aortic stenosis. *Circulation*. 1997;95:1253-9.
237. Sadoshima J, Xu Y, Slayter HS, Izumo S. Autocrine release of angiotensin II mediates stretch-induced hypertrophy of cardiac myocytes in vitro. *Cell*. 1993;75:977-84.
238. Sadoshima J, Izumo S. Molecular characterization of angiotensin II--induced hypertrophy of cardiac myocytes and hyperplasia of cardiac fibroblasts. Critical role of the AT1 receptor subtype. *Circ Res*. 1993;73:413-23.
239. Gray MO, Long CS, Kalinyak JE, Li HT, Karliner JS. Angiotensin II stimulates cardiac myocyte hypertrophy via paracrine release of TGF-beta 1 and endothelin-1 from fibroblasts. *Cardiovasc Res*. 1998;40:352-63.
240. Sano M, Fukuda K, Kodama H, Pan J, Saito M, Matsuzaki J, Takahashi T, Makino S, Kato T, Ogawa S. Interleukin-6 family of cytokines mediate angiotensin II-induced cardiac hypertrophy in rodent cardiomyocytes. *J Biol Chem*. 2000;275:29717-23.
241. Zhang X, Dostal DE, Reiss K, Cheng W, Kajstura J, Li P, Huang H, Sonnenblick EH, Meggs LG, Baker KM, et al. Identification and activation of autocrine renin-angiotensin system in adult ventricular myocytes. *Am J Physiol*. 1995;269:H1791-802.
242. Ruwhof C, van der Laarse A. Mechanical stress-induced cardiac hypertrophy: mechanisms and signal transduction pathways. *Cardiovasc Res*. 2000;47:23-37.
243. Ross RS, Borg TK. Integrins and the Myocardium. *Circ Res*. 2001;88:1112-1119.
244. Franchini KG, Torsoni AS, Soares PHA, Saad MJA. Early Activation of the Multicomponent Signaling Complex Associated With Focal Adhesion Kinase Induced by Pressure Overload in the Rat Heart. *Circ Res*. 2000;87:558-565.
245. Pham CG, Harpf AE, Keller RS, Vu HT, Shai SY, Loftus JC, Ross RS. Striated muscle-specific beta(1D)-integrin and FAK are involved in cardiac myocyte hypertrophic response pathway. *Am J Physiol Heart Circ Physiol*. 2000;279:H2916-26.
246. Keller RS, Shai SY, Babbitt CJ, Pham CG, Solaro RJ, Valencik ML, Loftus JC, Ross RS. Disruption of integrin function in the murine myocardium leads to perinatal lethality, fibrosis, and abnormal cardiac performance. *Am J Pathol*. 2001;158:1079-90.

247. Taylor JM, Rovin JD, Parsons JT. A role for focal adhesion kinase in phenylephrine-induced hypertrophy of rat ventricular cardiomyocytes. *J Biol Chem*. 2000;275:19250-7.
248. Eble DM, Strait JB, Govindarajan G, Lou J, Byron KL, Samarel AM. Endothelin-induced cardiac myocyte hypertrophy: role for focal adhesion kinase. *Am J Physiol Heart Circ Physiol*. 2000;278:H1695-707.
249. Heidkamp MC, Bayer AL, Kalina JA, Eble DM, Samarel AM. GFP-FRNK disrupts focal adhesions and induces anoikis in neonatal rat ventricular myocytes. *Circ Res*. 2002;90:1282-9.
250. Aikawa R, Nagai T, Kudoh S, Zou Y, Tanaka M, Tamura M, Akazawa H, Takano H, Nagai R, Komuro I. Integrins play a critical role in mechanical stress-induced p38 MAPK activation. *Hypertension*. 2002;39:233-8.
251. Fuller SJ. Stimulation of gene expression in neonatal cardiac myocytes by raised extracellular pH. *Biochem Soc Trans*. 1997;25:210S.
252. Yamazaki T, Komuro I, Kudoh S, Zou Y, Nagai R, Aikawa R, Uozumi H, Yazaki Y. Role of ion channels and exchangers in mechanical stretch-induced cardiomyocyte hypertrophy. *Circ Res*. 1998;82:430-7.
253. Cingolani HE, Alvarez BV, Ennis IL, Camilion de Hurtado MC. Stretch-induced alkalinization of feline papillary muscle: an autocrine-paracrine system. *Circ Res*. 1998;83:775-80.
254. Loennechen JP, Wisloff U, Falck G, Ellingsen O. Effects of cariporide and losartan on hypertrophy, calcium transients, contractility, and gene expression in congestive heart failure. *Circulation*. 2002;105:1380-6.
255. Camilion de Hurtado MC, Portiansky EL, Perez NG, Rebolledo OR, Cingolani HE. Regression of cardiomyocyte hypertrophy in SHR following chronic inhibition of the Na(+)/H(+) exchanger. *Cardiovasc Res*. 2002;53:862-8.
256. Spitznagel H, Chung O, Xia Q, Rossius B, Illner S, Jahnichen G, Sandmann S, Reinecke A, Daemen MJ, Unger T. Cardioprotective effects of the Na(+)/H(+)-exchange inhibitor cariporide in infarct-induced heart failure. *Cardiovasc Res*. 2000;46:102-10.
257. Yoshida H, Karmazyn M. Na(+)/H(+) exchange inhibition attenuates hypertrophy and heart failure in 1-wk postinfarction rat myocardium. *Am J Physiol Heart Circ Physiol*. 2000;278:H300-4.
258. Marano G, Vergari A, Catalano L, Gaudi S, Palazzesi S, Musumeci M, Stati T, Ferrari AU. Na+/H+ exchange inhibition attenuates left ventricular remodeling and preserves systolic function in pressure-overloaded hearts. *Br J Pharmacol*. 2004;141:526-32.
259. Inagami T, Misono K, Michelakis AM. Definitive evidence for similarity in the active site of renin and acidic protease. *Biochem Biophys Res Commun*. 1974;56:503-9.
260. McKown MM, Gregerman RI. Human renin inhibition by a diazoacyl reagent: relationship of the enzyme to other proteinases. *Life Sci*. 1975;16:71-9.

261. Misono KS, Inagami T. Characterization of the active site of mouse submaxillary gland renin. *Biochemistry*. 1980;19:2616-22.
262. Rahuel J, Priestle JP, Grutter MG. The crystal structures of recombinant glycosylated human renin alone and in complex with a transition state analog inhibitor. *J Struct Biol*. 1991;107:227-36.
263. Sielecki AR, Hayakawa K, Fujinaga M, Murphy ME, Fraser M, Muir AK, Carilli CT, Lewicki JA, Baxter JD, James MN. Structure of recombinant human renin, a target for cardiovascular-active drugs, at 2.5 A resolution. *Science*. 1989;243:1346-51.
264. Blundell T, Sibanda BL, Pearl L. Three-dimensional structure, specificity and catalytic mechanism of renin. *Nature*. 1983;304:273-5.
265. Catanzaro DF, Mullins JJ, Morris BJ. The biosynthetic pathway of renin in mouse submandibular gland. *J Biol Chem*. 1983;258:7364-8.
266. Misono KS, Inagami T. Structure of mouse submaxillary gland renin. Identification of two disulfide-linked polypeptide chains and the complete amino acid sequence of the light chain. *J Biol Chem*. 1982;257:7536-40.
267. Hein L, Stevens ME, Barsh GS, Pratt RE, Kobilka BK, Dzau VJ. Overexpression of angiotensin AT1 receptor transgene in the mouse myocardium produces a lethal phenotype associated with myocyte hyperplasia and heart block. *Proc Natl Acad Sci U S A*. 1997;94:6391-6.
268. Paradis P, Dali-Youcef N, Paradis FW, Thibault G, Nemer M. Overexpression of angiotensin II type I receptor in cardiomyocytes induces cardiac hypertrophy and remodeling. *Proc Natl Acad Sci U S A*. 2000;97:931-6.
269. Milano CA, Dolber PC, Rockman HA, Bond RA, Venable ME, Allen LF, Lefkowitz RJ. Myocardial expression of a constitutively active alpha 1B-adrenergic receptor in transgenic mice induces cardiac hypertrophy. *Proc Natl Acad Sci U S A*. 1994;91:10109-13.
270. Zuscik MJ, Chalothorn D, Hellard D, Deighan C, McGee A, Daly CJ, Waugh DJJ, Ross SA, Gaivin RJ, Morehead AJ, Thomas JD, Plow EF, McGrath JC, Piascik MT, Perez DM. Hypotension, Autonomic Failure, and Cardiac Hypertrophy in Transgenic Mice Overexpressing the alpha 1B-Adrenergic Receptor. *J. Biol. Chem.* 2001;276:13738-13743.
271. Sakata Y, Hoit BD, Liggett SB, Walsh RA, Dorn GW, 2nd. Decompensation of pressure-overload hypertrophy in G alpha q-overexpressing mice. *Circulation*. 1998;97:1488-95.
272. Mende U, Kagen A, Cohen A, Aramburu J, Schoen FJ, Neer EJ. Transient cardiac expression of constitutively active Galphaq leads to hypertrophy and dilated cardiomyopathy by calcineurin-dependent and independent pathways. *Proc Natl Acad Sci U S A*. 1998;95:13893-8.
273. Iwase M, Bishop SP, Uechi M, Vatner DE, Shannon RP, Kudej RK, Wight DC, Wagner TE, Ishikawa Y, Homcy CJ, Vatner SF. Adverse effects of chronic endogenous sympathetic drive induced by cardiac GS alpha overexpression. *Circ Res*. 1996;78:517-24.

274. Hunter JJ, Tanaka N, Rockman HA, Ross J, Jr., Chien KR. Ventricular expression of a MLC-2v-ras fusion gene induces cardiac hypertrophy and selective diastolic dysfunction in transgenic mice. *J Biol Chem*. 1995;270:23173-8.
275. Sussman MA, Welch S, Walker A, Klevitsky R, Hewett TE, Price RL, Schaefer E, Yager K. Altered focal adhesion regulation correlates with cardiomyopathy in mice expressing constitutively active rac1. *J. Clin. Invest.* 2000;105:875-886.
276. Wakasaki H, Koya D, Schoen FJ, Jirousek MR, Ways DK, Hoit BD, Walsh RA, King GL. Targeted overexpression of protein kinase C beta2 isoform in myocardium causes cardiomyopathy. *Proc Natl Acad Sci U S A*. 1997;94:9320-5.
277. Bowman JC, Steinberg SF, Jiang T, Geenen DL, Fishman GI, Buttrick PM. Expression of protein kinase C beta in the heart causes hypertrophy in adult mice and sudden death in neonates. *J Clin Invest.* 1997;100:2189-95.
278. Chen L, Hahn H, Wu G, Chen CH, Liron T, Schechtman D, Cavallaro G, Banci L, Guo Y, Bolli R, Dorn GW, 2nd, Mochly-Rosen D. Opposing cardioprotective actions and parallel hypertrophic effects of delta PKC and epsilon PKC. *Proc Natl Acad Sci U S A*. 2001;98:11114-9.
279. Gruver CL, DeMayo F, Goldstein MA, Means AR. Targeted developmental overexpression of calmodulin induces proliferative and hypertrophic growth of cardiomyocytes in transgenic mice. *Endocrinology*. 1993;133:376-88.
280. Passier R, Zeng H, Frey N, Naya FJ, Nicol RL, McKinsey TA, Overbeek P, Richardson JA, Grant SR, Olson EN. CaM kinase signaling induces cardiac hypertrophy and activates the MEF2 transcription factor in vivo. *J Clin Invest*. 2000;105:1395-406.
281. Hirota H, Yoshida K, Kishimoto T, Taga T. Continuous activation of gp130, a signal-transducing receptor component for interleukin 6-related cytokines, causes myocardial hypertrophy in mice. *Proc Natl Acad Sci U S A*. 1995;92:4862-6.
282. Kunisada K, Negoro S, Tone E, Funamoto M, Osugi T, Yamada S, Okabe M, Kishimoto T, Yamauchi-Takihara K. Signal transducer and activator of transcription 3 in the heart transduces not only a hypertrophic signal but a protective signal against doxorubicin-induced cardiomyopathy. *Proc Natl Acad Sci U S A*. 2000;97:315-9.
283. Delaughter MC, Taffet GE, Fiorotto ML, Entman ML, Schwartz RJ. Local insulin-like growth factor I expression induces physiologic, then pathologic, cardiac hypertrophy in transgenic mice. *Faseb J*. 1999;13:1923-9.
284. Bueno OF, De Windt LJ, Tymitz KM, Witt SA, Kimball TR, Klevitsky R, Hewett TE, Jones SP, Lefer DJ, Peng CF, Kitsis RN, Molkentin JD. The MEK1-ERK1/2 signaling pathway promotes compensated cardiac hypertrophy in transgenic mice. *Embo J*. 2000;19:6341-50.

285. Matsui T, Li L, Wu JC, Cook SA, Nagoshi T, Picard MH, Liao R, Rosenzweig A. Phenotypic spectrum caused by transgenic overexpression of activated Akt in the heart. *J Biol Chem*. 2002;277:22896-901.
286. Zhang D, Gaussin V, Taffet GE, Belaguli NS, Yamada M, Schwartz RJ, Michael LH, Overbeek PA, Schneider MD. TAK1 is activated in the myocardium after pressure overload and is sufficient to provoke heart failure in transgenic mice. *Nat Med*. 2000;6:556-63.
287. Zhang X, Azhar G, Chai J, Sheridan P, Nagano K, Brown T, Yang J, Khrapko K, Borras AM, Lawitts J, Misra RP, Wei JY. Cardiomyopathy in transgenic mice with cardiac-specific overexpression of serum response factor. *Am J Physiol Heart Circ Physiol*. 2001;280:H1782-92.
288. Veniant M, Menard J, Bruneval P, Morley S, Gonzales MF, Mullins J. Vascular damage without hypertension in transgenic rats expressing prorenin exclusively in the liver. *J Clin Invest*. 1996;98:1966-70.
289. Depre C, Hase M, Gaussin V, Zajac A, Wang L, Hittinger L, Ghaleb B, Yu X, Kudej RK, Wagner T, Sadoshima J, Vatner SF. H11 kinase is a novel mediator of myocardial hypertrophy in vivo. *Circ Res*. 2002;91:1007-14.
290. Aeed PA, Guido DM, Mathews WR, Elhammer AP. Characterization of the oligosaccharide structures on recombinant human prorenin expressed in Chinese hamster ovary cells. *Biochemistry*. 1992;31:6951-61.
291. Baxter JD, Duncan K, Chu W, James MN, Russell RB, Haidar MA, DeNoto FM, Hsueh W, Reudelhuber TL. Molecular biology of human renin and its gene. *Recent Prog Horm Res*. 1991;47:211-57; discussion 257-8.
292. Weaver D, Skinner S, Walker L, Sangster M. Phenotypic inhibition of the renin-angiotensin system, emergence of the Ren-2 gene, and adaptive radiation of mice. *Gen Comp Endocrinol*. 1991;83:306-15.
293. Yokosawa H, Holladay LA, Inagami T, Haas E, Murakami K. Human renal renin. Complete purification and characterization. *J Biol Chem*. 1980;255:3498-502.
294. Oliver WJ, Gross F. Effect of testosterone and duct ligation on submaxillary renin-like principle. *Am J Physiol*. 1967;213:341-6.
295. Hatae T, Takimoto E, Murakami K, Fukamizu A. Comparative studies on species-specific reactivity between renin and angiotensinogen. *Mol Cell Biochem*. 1994;131:43-7.
296. Hirose S, Kim S, Miyazaki H, Park YS, Murakami K. In vitro biosynthesis of human renin and identification of plasma inactive renin as an activation intermediate. *J Biol Chem*. 1985;260:16400-5.
297. Dzau VJ, Tanaka A, Pratt RE. The nature of renin precursor and inactive renin. *Clin Exp Hypertens A*. 1982;4:1973-85.
298. Mercure C, Thibault G, Lussier-Cacan S, Davignon J, Schiffrin EL, Reudelhuber TL. Molecular analysis of human prorenin prosegment variants in vitro and in vivo. *J Biol Chem*. 1995;270:16355-9.

299. Derkx FH, Deinum J, Lipovski M, Verhaar M, Fischli W, Schalekamp MA. Nonproteolytic "activation" of prorenin by active site-directed renin inhibitors as demonstrated by renin-specific monoclonal antibody. *J Biol Chem*. 1992;267:22837-42.
300. Yamauchi T, Nagahama M, Watanabe T, Ishizuka Y, Hori H, Murakami K. Site-directed mutagenesis of human prorenin. Substitution of three arginine residues in the propeptide with glutamine residues yields active prorenin. *J Biochem (Tokyo)*. 1990;107:27-31.
301. Higashimori K, Mizuno K, Nakajo S, Boehm F, Marcotte P, Egan D, Holleman W, Heusser C, Poisner A, Inagami T. Pure human inactive renin. Evidence that native inactive renin is prorenin. *J. Biol. Chem.* 1989;264:14662-14667.
302. Almeida PC, Chagas JR, Cezari MH, Juliano MA, Juliano L. Hydrolysis by plasma kallikrein of fluorogenic peptides derived from prorenin processing site. *Biochim Biophys Acta*. 2000;1479:83-90.
303. Almeida PC, Oliveira V, Chagas JR, Meldal M, Juliano MA, Juliano L. Hydrolysis by cathepsin B of fluorescent peptides derived from human prorenin. *Hypertension*. 2000;35:1278-83.
304. Jutras I, Reudelhuber TL. Prorenin processing by cathepsin B in vitro and in transfected cells. *FEBS Lett*. 1999;443:48-52.
305. Laframboise M, Reudelhuber TL, Jutras I, Brechler V, Seidah NG, Day R, Gross KW, Deschepper CF. Prorenin activation and prohormone convertases in the mouse As4.1 cell line. *Kidney Int*. 1997;51:104-9.
306. Mercure C, Jutras I, Day R, Seidah NG, Reudelhuber TL. Prohormone convertase PC5 is a candidate processing enzyme for prorenin in the human adrenal cortex. *Hypertension*. 1996;28:840-6.
307. Jutras I, Seidah NG, Reudelhuber TL, Brechler V. Two activation states of the prohormone convertase PC1 in the secretory pathway. *J Biol Chem*. 1997;272:15184-8.
308. Kim WS, Hatsuzawa K, Ishizuka Y, Hashiba K, Murakami K, Nakayama K. A processing enzyme for prorenin in mouse submandibular gland. Purification and characterization. *J Biol Chem*. 1990;265:5930-3.
309. Derkx FH, Schalekamp MP, Schalekamp MA. Two-step prorenin-renin conversion. Isolation of an intermediary form of activated prorenin. *J Biol Chem*. 1987;262:2472-7.
310. Heinrikson RL, Hui J, Zurcher-Neely H, Poorman RA. A structural model to explain the partial catalytic activity of human prorenin. *Am J Hypertens*. 1989;2:367-80.
311. Reudelhuber TL, Brechler V, Jutras I, Mercure C, Methot D. Proteolytic and non-proteolytic activation of prorenin. *Adv Exp Med Biol*. 1998;436:229-38.
312. Suzuki F, Hayakawa M, Nakagawa T, Nasir UM, Ebihara A, Iwasawa A, Ishida Y, Nakamura Y, Murakami K. Human prorenin has "gate and handle" regions for its non-proteolytic activation. *J Biol Chem*. 2003;278:22217-22.

313. Muller DN, Hilgers KF, Mathews S, Breu V, Fischli W, Uhlmann R, Luft FC. Effects of Human Prorenin in Rats Transgenic for Human Angiotensinogen. *Hypertension*. 1999;33:312-317.
314. Hosoi M, Kim S, Takada T, Suzuki F, Murakami K, Yamamoto K. Effects of prorenin on blood pressure and plasma renin concentrations in stroke-prone spontaneously hypertensive rats. *Am J Physiol*. 1992;262:E234-9.
315. Lenz T, Sealey JE, Lappe RW, Carilli C, Oshiro GT, Baxter JD, Laragh JH. Infusion of recombinant human prorenin into rhesus monkeys. Effects on hemodynamics, renin-angiotensin-aldosterone axis and plasma testosterone. *Am J Hypertens*. 1990;3:257-61.
316. Lenz T, Sealey JE, Maack T, James GD, Heinrikson RL, Marion D, Laragh JH. Half-life, hemodynamic, renal, and hormonal effects of prorenin in cynomolgus monkeys. *Am J Physiol*. 1991;260:R804-10.
317. Kim S, Hosoi M, Ikemoto F, Murakami K, Ishizuka Y, Yamamoto K. Conversion to renin of exogenously administered recombinant human prorenin in liver and kidney of monkeys. *Am J Physiol*. 1990;258:E451-8.
318. Methot D, Silversides DW, Reudelhuber TL. In vivo enzymatic assay reveals catalytic activity of the human renin precursor in tissues. *Circ Res*. 1999;84:1067-72.
319. Mollina RaM, J. In; 2000.
320. Franken AA, Derkx FH, Blankestijn PJ, Janssen JA, Mannesse CK, Hop W, Boomsma F, Weber R, Peperkamp E, De Jong PT, et al. Plasma prorenin as an early marker of microvascular disease in patients with diabetes mellitus. *Diabete Metab*. 1992;18:137-43.
321. Wilson DM, Luetscher JA. Plasma prorenin activity and complications in children with insulin-dependent diabetes mellitus. *N Engl J Med*. 1990;323:1101-6.
322. Luetscher JA, Kraemer FB. Microalbuminuria and increased plasma prorenin. Prevalence in diabetics followed up for four years. *Arch Intern Med*. 1988;148:937-41.
323. Gomez RA, Lynch KR, Sturgill BC, Elwood JP, Chevalier RL, Carey RM, Peach MJ. Distribution of renin mRNA and its protein in the developing kidney. *Am J Physiol*. 1989;257:F850-8.
324. JONES CA, HURLEY MI, BLACK TA, KANE CM, PAN L, PRUITT SC, GROSS KW. Expression of a renin/GFP transgene in mouse embryonic, extra-embryonic, and adult tissues. *Physiol. Genomics*. 2000;4:75-81.
325. Naruse K, Takii Y, Inagami T. Immunohistochemical localization of renin in luteinizing hormone-producing cells of rat pituitary. *Proc Natl Acad Sci U S A*. 1981;78:7579-83.
326. Li C, Ansari R, Yu Z, Shah D. Definitive Molecular Evidence of Renin-Angiotensin System in Human Uterine Decidual Cells. *Hypertension*. 2000;36:159-164.
327. Re R, Fallon JT, Dzau V, Ouay SC, Haber E. Renin synthesis by canine aortic smooth muscle cells in culture. *Life Sci*. 1982;30:99-106.

328. Field LJ, McGowan RA, Dickinson DP, Gross KW. Tissue and gene specificity of mouse renin expression. *Hypertension*. 1984;6:597-603.
329. Field LJ, Philbrick WM, Howles PN, Dickinson DP, McGowan RA, Gross KW. Expression of tissue-specific Ren-1 and Ren-2 genes of mice: comparative analysis of 5'-proximal flanking regions. *Mol Cell Biol*. 1984;4:2321-31.
330. Lilly LS, Pratt RE, Alexander RW, Larson DM, Ellison KE, Gimbrone MA, Jr., Dzau VJ. Renin expression by vascular endothelial cells in culture. *Circ Res*. 1985;57:312-8.
331. Danser AH, van den Dorpel MA, Deinum J, Derkx FH, Franken AA, Peperkamp E, de Jong PT, Schalekamp MA. Renin, prorenin, and immunoreactive renin in vitreous fluid from eyes with and without diabetic retinopathy. *J Clin Endocrinol Metab*. 1989;68:160-7.
332. Cooper AC, Robinson G, Vinson GP, Cheung WT, Broughton Pipkin F. The localization and expression of the renin-angiotensin system in the human placenta throughout pregnancy. *Placenta*. 1999;20:467-74.
333. Dostal DE, Baker KM. The cardiac renin-angiotensin system: conceptual, or a regulator of cardiac function? *Circ Res*. 1999;85:643-50.
334. Engeli S, Negrel R, Sharma AM. Physiology and pathophysiology of the adipose tissue renin-angiotensin system. *Hypertension*. 2000;35:1270-7.
335. Ganten D, Schelling P, Vecsei P, Ganten U. Iso-renin of extrarenal origin. "The tissue angiotensinogenase systems". *Am J Med*. 1976;60:760-72.
336. Dzau VJ, Brenner A, Emmett NL. Evidence for renin in rat brain: differentiation from other reninlike enzymes. *Am J Physiol*. 1982;242:E292-7.
337. Hirose S, Naruse M, Ohtsuki K, Inagami T. Totally inactive renin zymogen and different forms of active renin in hog brain tissues. *J Biol Chem*. 1981;256:5572-6.
338. Dzau VJ, Pratt RE. Renin gene expression, biosynthesis, and cellular pathways of secretion. *Clin Physiol Biochem*. 1988;6:210-6.
339. Pratt RE, Carleton JE, Roth TP, Dzau VJ. Evidence for two cellular pathways of renin secretion by the mouse submandibular gland. *Endocrinology*. 1988;123:1721-7.
340. Pratt RE, Flynn JA, Hobart PM, Paul M, Dzau VJ. Different secretory pathways of renin from mouse cells transfected with the human renin gene. *J Biol Chem*. 1988;263:3137-41.
341. Derkx FH, Schalekamp MA. Human prorenin: pathophysiology and clinical implications. *Clin Exp Hypertens A*. 1988;10:1213-25.
342. Sealey JE, Moon C, Laragh JH, Atlas SA. Plasma prorenin in normal, hypertensive, and anephric subjects and its effect on renin measurements. *Circ Res*. 1977;40:I41-5.
343. Hosoi M, Kim S, Tabata T, Nishitani H, Nishizawa Y, Morii H, Murakami K, Yamamoto K. Evidence for the presence of differently glycosylated forms of prorenin in the plasma of anephric man. *J Clin Endocrinol Metab*. 1992;74:680-4.

344. Baker KM, Aceto JF. Angiotensin II stimulation of protein synthesis and cell growth in chick heart cells. *Am J Physiol*. 1990;259:H610-8.
345. Miyata S, Haneda T. Hypertrophic growth of cultured neonatal rat heart cells mediated by type 1 angiotensin II receptor. *Am J Physiol*. 1994;266:H2443-51.
346. Liu Y, Leri A, Li B, Wang X, Cheng W, Kajstura J, Anversa P. Angiotensin II stimulation in vitro induces hypertrophy of normal and postinfarcted ventricular myocytes. *Circ Res*. 1998;82:1145-59.
347. Pennica D, King KL, Shaw KJ, Luis E, Rullamas J, Luoh SM, Darbonne WC, Knutzon DS, Yen R, Chien KR, et al. Expression cloning of cardiotrophin 1, a cytokine that induces cardiac myocyte hypertrophy. *Proc Natl Acad Sci U S A*. 1995;92:1142-6.
348. Booz GW, Baker KM. Role of type 1 and type 2 angiotensin receptors in angiotensin II-induced cardiomyocyte hypertrophy. *Hypertension*. 1996;28:635-40.
349. Kuwahara K, Saito Y, Harada M, Ishikawa M, Ogawa E, Miyamoto Y, Hamanaka I, Kamitani S, Kajiyama N, Takahashi N, Nakagawa O, Masuda I, Nakao K. Involvement of Cardiotrophin-1 in Cardiac Myocyte-Nonmyocyte Interactions During Hypertrophy of Rat Cardiac Myocytes In Vitro. *Circulation*. 1999;100:1116-1124.
350. Dostal DE, Baker KM. Angiotensin II stimulation of left ventricular hypertrophy in adult rat heart. Mediation by the AT1 receptor. *Am J Hypertens*. 1992;5:276-80.
351. Bendall JK, Cave AC, Heymes C, Gall N, Shah AM. Pivotal role of a gp91(phox)-containing NADPH oxidase in angiotensin II-induced cardiac hypertrophy in mice. *Circulation*. 2002;105:293-6.
352. Mazzolai L, Nussberger J, Aubert JF, Brunner DB, Gabbiani G, Brunner HR, Pedrazzini T. Blood pressure-independent cardiac hypertrophy induced by locally activated renin-angiotensin system. *Hypertension*. 1998;31:1324-30.
353. Prescott G, Silversides DW, Chiu SM, Reudelhuber TL. Contribution of circulating renin to local synthesis of angiotensin peptides in the heart. *Physiol Genomics*. 2000;4:67-73.
354. Hoffmann S, Krause T, van Geel PP, Willenbrock R, Pagel I, Pinto YM, Buikema H, van Gilst WH, Lindschau C, Paul M, Inagami T, Ganten D, Urata H. Overexpression of the human angiotensin II type 1 receptor in the rat heart augments load induced cardiac hypertrophy. *J Mol Med*. 2001;79:601-8.
355. van Kats JP, Methot D, Paradis P, Silversides DW, Reudelhuber TL. Use of a biological peptide pump to study chronic peptide hormone action in transgenic mice. Direct and indirect effects of angiotensin II on the heart. *J Biol Chem*. 2001;276:44012-7.
356. Harada K, Komuro I, Zou Y, Kudoh S, Kijima K, Matsubara H, Sugaya T, Murakami K, Yazaki Y. Acute pressure overload could induce

hypertrophic responses in the heart of angiotensin II type 1a knockout mice. *Circ Res*. 1998;82:779-85.
357. Hamawaki M, Coffman TM, Lashus A, Koide M, Zile MR, Oliverio MI, DeFreyte G, Cooper Gt, Carabello BA. Pressure-overload hypertrophy is unabated in mice devoid of AT1A receptors. *Am J Physiol*. 1998;274:H868-73.
358. Koide M, Carabello BA, Conrad CC, Buckley JM, DeFreyte G, Barnes M, Tomanek RJ, Wei CC, Dell'Italia LJ, Cooper Gt, Zile MR. Hypertrophic response to hemodynamic overload: role of load vs. renin-angiotensin system activation. *Am J Physiol*. 1999;276:H350-8.
359. Katz SA, Opsahl JA, Wernsing SE, Forbis LM, Smith J, Heller LJ. Myocardial renin is neither necessary nor sufficient to initiate or maintain ventricular hypertrophy. *Am J Physiol Regul Integr Comp Physiol*. 2000;278:R578-86.
360. van Kesteren CA, van Heugten HA, Lamers JM, Saxena PR, Schalekamp MA, Danser AH. Angiotensin II-mediated growth and antigrowth effects in cultured neonatal rat cardiac myocytes and fibroblasts. *J Mol Cell Cardiol*. 1997;29:2147-57.
361. Fischer TA, Singh K, O'Hara DS, Kaye DM, Kelly RA. Role of AT1 and AT2 receptors in regulation of MAPKs and MKP-1 by ANG II in adult cardiac myocytes. *Am J Physiol*. 1998;275:H906-16.
362. Pachori AS, Numan MT, Ferrario CM, Diz DM, Raizada MK, Katovich MJ. Blood pressure-independent attenuation of cardiac hypertrophy by AT(1)R-AS gene therapy. *Hypertension*. 2002;39:969-75.
363. Ichihara S, Senbonmatsu T, Price E, Jr., Ichiki T, Gaffney FA, Inagami T. Angiotensin II type 2 receptor is essential for left ventricular hypertrophy and cardiac fibrosis in chronic angiotensin II-induced hypertension. *Circulation*. 2001;104:346-51.
364. Senbonmatsu T, Ichihara S, Price E, Jr., Gaffney FA, Inagami T. Evidence for angiotensin II type 2 receptor-mediated cardiac myocyte enlargement during in vivo pressure overload. *J Clin Invest*. 2000;106:R25-9.
365. Kudoh S, Komuro I, Hiroi Y, Zou Y, Harada K, Sugaya T, Takekoshi N, Murakami K, Kadowaki T, Yazaki Y. Mechanical stretch induces hypertrophic responses in cardiac myocytes of angiotensin II type 1a receptor knockout mice. *J Biol Chem*. 1998;273:24037-43.
366. Sadoshima J, Izumo S. Autocrine secretion of angiotensin II mediates stretch-induced hypertrophy of cardiac myocytes in vitro. *Contrib Nephrol*. 1996;118:214-21.
367. Akishita M, Iwai M, Wu L, Zhang L, Ouchi Y, Dzau VJ, Horiuchi M. Inhibitory effect of angiotensin II type 2 receptor on coronary arterial remodeling after aortic banding in mice. *Circulation*. 2000;102:1684-9.
368. Schneider MD, Lorell BH. AT(2), judgment day: which angiotensin receptor is the culprit in cardiac hypertrophy? *Circulation*. 2001;104:247-8.

369. Kurisu S, Ozono R, Oshima T, Kambe M, Ishida T, Sugino H, Matsuura H, Chayama K, Teranishi Y, Iba O, Amano K, Matsubara H. Cardiac angiotensin II type 2 receptor activates the kinin/NO system and inhibits fibrosis. *Hypertension*. 2003;41:99-107.
370. Karmazyn M, Liu Q, Gan XT, Brix BJ, Fliegel L. Aldosterone increases NHE-1 expression and induces NHE-1-dependent hypertrophy in neaonatal rat ventricular myocytes. *Hypertension*. 2003;42:1171-6.
371. Takeda Y, Yoneda T, Demura M, Miyamori I, Mabuchi H. Cardiac aldosterone production in genetically hypertensive rats. *Hypertension*. 2000;36:495-500.
372. Pitt B, Reichek N, Willenbrock R, Zannad F, Phillips RA, Roniker B, Kleiman J, Krause S, Burns D, Williams GH. Effects of Eplerenone, Enalapril, and Eplerenone/Enalapril in patients with essential hypertension and left ventricular hypertrophy. The 4E-left ventricular hypertrophy study. *Circulation*. 2003;108:1831-38.
373. Silvestre JS, Robert V, Heymes C, Aupetit-Faisant B, Mouas C, Moalic JM, Swynghedauw B, Delcayre C. Myocardial production of aldosterone and corticosterone in the rat. Physiological regulation. *J Biol Chem*. 1998;273:4883-91.
374. Silvestre JS, Heymes C, Oubenaissa A, Robert V, Aupetit-Faisant B, Carayon A, Swynghedauw B, Delcayre C. Activation of cardiac aldosterone production in rat myocardial infarction: effect of angiotensin II receptor blockade and role in cardiac fibrosis. *Circulation*. 1999;99:2694-701.
375. Gomez-Sanchez EP, Ahmad N, Romero DG, Gomez -Sanchez CE. Origin of aldosterone in the rat heart. *Endocrinology*. 2004;145:4796-802.
376. Garnier A, Bendall JK, Fuchs S, Escoubet B, Rochais F, Hoerter J, Nehme J, Ambroiseine M-L, De Angelis N, Morineau G, d'Estienne P, Fischmeister R, Heymes C, Pinet F, Delcayre C. Cardiac specific increase in aldosterone production induces coronary dysfunction in aldosterone synthase-transgenic mice. *Circulation*. 2004;110:1819-1825.
377. Dostal DE, Rothblum KN, Chernin MI, Cooper GR, Baker KM. Intracardiac detection of angiotensinogen and renin: a localized renin-angiotensin system in neonatal rat heart. *Am J Physiol*. 1992;263:C838-50.
378. Dostal DE, Rothblum KN, Conrad KM, Cooper GR, Baker KM. Detection of angiotensin I and II in cultured rat cardiac myocytes and fibroblasts. *Am J Physiol*. 1992;263:C851-63.
379. Clausmeyer S, Reinecke A, Farrenkopf R, Unger T, Peters J. Tissue-specific expression of a rat renin transcript lacking the coding sequence for the prefragment and its stimulation by myocardial infarction. *Endocrinology*. 2000;141:2963-70.
380. Clausmeyer S, Sturzebecher R, Peters J. An alternative transcript of the rat renin gene can result in a truncated prorenin that is transported into adrenal mitochondria. *Circ Res*. 1999;84:337-44.

381. De Mello WC, Danser AH. Angiotensin II and the heart : on the intracrine renin-angiotensin system. *Hypertension*. 2000;35:1183-8.
382. van Kats JP, de Lannoy LM, Jan Danser AH, van Meegen JR, Verdouw PD, Schalekamp MA. Angiotensin II type 1 (AT1) receptor-mediated accumulation of angiotensin II in tissues and its intracellular half-life in vivo. *Hypertension*. 1997;30:42-9.
383. Neri Serneri GG, Boddi M, Coppo M, Chechi T, Zarone N, Moira M, Poggesi L, Margheri M, Simonetti I. Evidence for the existence of a functional cardiac renin-angiotensin system in humans. *Circulation*. 1996;94:1886-93.
384. de Lannoy LM, Danser AH, van Kats JP, Schoemaker RG, Saxena PR, Schalekamp MA. Renin-angiotensin system components in the interstitial fluid of the isolated perfused rat heart. Local production of angiotensin I. *Hypertension*. 1997;29:1240-51.
385. de Lannoy LM, Danser AH, Bouhuizen AM, Saxena PR, Schalekamp MA. Localization and production of angiotensin II in the isolated perfused rat heart. *Hypertension*. 1998;31:1111-7.
386. Neri Serneri GG, Boddi M, Poggesi L, Simonetti I, Coppo M, Papa ML, Lisi GF, Maccherini M, Becherini R, Boncompagni A, Toscano T, Modesti PA. Activation of cardiac renin-angiotensin system in unstable angina. *J Am Coll Cardiol*. 2001;38:49-55.
387. Malhotra R, Sadoshima J, Brosius FC, 3rd, Izumo S. Mechanical stretch and angiotensin II differentially upregulate the renin-angiotensin system in cardiac myocytes In vitro. *Circ Res*. 1999;85:137-46.
388. Iwai N, Shimoike H, Kinoshita M. Cardiac renin-angiotensin system in the hypertrophied heart. *Circulation*. 1995;92:2690-6.
389. Boer PH, Ruzicka M, Lear W, Harmsen E, Rosenthal J, Leenen FH. Stretch-mediated activation of cardiac renin gene. *Am J Physiol*. 1994;267:H1630-6.
390. Tokuda K, Kai H, Kuwahara F, Yasukawa H, Tahara N, Kudo H, Takemiya K, Koga M, Yamamoto T, Imaizumi T. Pressure-Independent Effects of Angiotensin II on Hypertensive Myocardial Fibrosis. *Hypertension*. 2004;43:499-503.
391. von Lutterotti N, Catanzaro DF, Sealey JE, Laragh JH. Renin is not synthesized by cardiac and extrarenal vascular tissues. A review of experimental evidence. *Circulation*. 1994;89:458-70.
392. Danser AH, Admiraal PJ, Derkx FH, de Bruyn JH, Schalekamp MA. Changes in plasma renin and angiotensin run in parallel after nephrectomy. *J Hypertens Suppl*. 1993;11 Suppl 5:S238-9.
393. Danser AH, Schalekamp MA. Is there an internal cardiac renin-angiotensin system? *Heart*. 1996;76:28-32.
394. Katz SA, Opsahl JA, Lunzer MM, Forbis LM, Hirsch AT. Effect of bilateral nephrectomy on active renin, angiotensinogen, and renin glycoforms in plasma and myocardium. *Hypertension*. 1997;30:259-66.

395. Danser AH, van Kats JP, Admiraal PJ, Derkx FH, Lamers JM, Verdouw PD, Saxena PR, Schalekamp MA. Cardiac renin and angiotensins. Uptake from plasma versus in situ synthesis. *Hypertension*. 1994;24:37-48.
396. Danser AH, Admiraal PJ, Derkx FH, Lamers JM, Verdouw PD, Saxena PR, Schalekamp MA. Cardiac renin is kidney-derived. *J Hypertens Suppl*. 1993;11 Suppl 5:S224-5.
397. Katz SA, Opsahl JA, Forbis LM. Myocardial enzymatic activity of renin and cathepsin D before and after bilateral nephrectomy. *Basic Res Cardiol*. 2001;96:659-68.
398. van Kesteren CA, Saris JJ, Dekkers DH, Lamers JM, Saxena PR, Schalekamp MA, Danser AH. Cultured neonatal rat cardiac myocytes and fibroblasts do not synthesize renin or angiotensinogen: evidence for stretch-induced cardiomyocyte hypertrophy independent of angiotensin II. *Cardiovasc Res*. 1999;43:148-56.
399. van den Eijnden MM, Saris JJ, de Bruin RJ, de Wit E, Sluiter W, Reudelhuber TL, Schalekamp MA, Derkx FH, Danser AH. Prorenin accumulation and activation in human endothelial cells: importance of mannose 6-phosphate receptors. *Arterioscler Thromb Vasc Biol*. 2001;21:911-6.
400. Saris JJ, Derkx FH, Lamers JM, Saxena PR, Schalekamp MA, Danser AH. Cardiomyocytes bind and activate native human prorenin : role of soluble mannose 6-phosphate receptors. *Hypertension*. 2001;37:710-5.
401. Saris JJ, Derkx FH, De Bruin RJ, Dekkers DH, Lamers JM, Saxena PR, Schalekamp MA, Jan Danser AH. High-affinity prorenin binding to cardiac man-6-P/IGF-II receptors precedes proteolytic activation to renin. *Am J Physiol Heart Circ Physiol*. 2001;280:H1706-15.
402. Saris JJ, van den Eijnden MM, Lamers JM, Saxena PR, Schalekamp MA, Danser AH. Prorenin-induced myocyte proliferation: no role for intracellular angiotensin II. *Hypertension*. 2002;39:573-7.
403. Marks DL, Kost LJ, Kuntz SM, Romero JC, LaRusso NF. Hepatic processing of recombinant human renin: mechanisms of uptake and degradation. *Am J Physiol*. 1991;261:G349-58.
404. Hiruma M, Kim S, Ikemoto F, Murakami K, Yamamoto K. Fate of recombinant human renin administered exogenously to anesthetized monkeys. *Hypertension*. 1988;12:317-23.
405. Blanchard F, Raher S, Duplomb L, Vusio P, Pitard V, Taupin JL, Moreau JF, Hoflack B, Minvielle S, Jacques Y, Godard A. The mannose 6-phosphate/insulin-like growth factor II receptor is a nanomolar affinity receptor for glycosylated human leukemia inhibitory factor. *J Biol Chem*. 1998;273:20886-93.
406. Dennis PA, Rifkin DB. Cellular activation of latent transforming growth factor beta requires binding to the cation-independent mannose 6-phosphate/insulin-like growth factor type II receptor. *Proc Natl Acad Sci U S A*. 1991;88:580-4.

407. Peters J, Farrenkopf R, Clausmeyer S, Zimmer J, Kantachuvesiri S, Sharp MG, Mullins JJ. Functional significance of prorenin internalization in the rat heart. *Circ Res*. 2002;90:1135-41.
408. Ogg D. Characterisation of Rat Lines Transgenic for the Mouse *Ren-2d* cDNA. In. Edinburgh: PhD Thesis, University of Edinburgh; 1997.
409. Tada M, Takahashi S, Miyano M, Miyake Y. Tissue-specific regulation of renin-binding protein gene expression in rats. *J Biochem (Tokyo)*. 1992;112:175-82.
410. Schmitz C, Gotthardt M, Hinderlich S, Leheste J-R, Gross V, Vorum H, Christensen EI, Luft FC, Takahashi S, Willnow TE. Normal Blood Pressure and Plasma Renin Activity in Mice Lacking the Renin-binding Protein, a Cellular Renin Inhibitor. *J. Biol. Chem*. 2000;275:15357-15362.
411. Campbell DJ, Valentijn AJ. Identification of vascular renin-binding proteins by chemical cross-linking: inhibition of binding of renin by renin inhibitors. *J Hypertens*. 1994;12:879-90.
412. Nguyen G, Delarue F, Burckle C, Bouzhir L, Giller T, Sraer JD. Pivotal role of the renin/prorenin receptor in angiotensin II production and cellular responses to renin. *J Clin Invest*. 2002;109:1417-27.
413. Re RN. Implications of intracrine hormone action for physiology and medicine. *Am J Physiol Heart Circ Physiol*. 2003;284:H751-7.
414. Simpson P. Stimulation of hypertrophy of cultured neonatal rat heart cells through an alpha 1-adrenergic receptor and induction of beating through an alpha 1- and beta 1-adrenergic receptor interaction. Evidence for independent regulation of growth and beating. *Circ Res*. 1985;56:884-94.
415. Bisognano JD, Weinberger HD, Bohlmeyer TJ, Pende A, Raynolds MV, Sastravaha A, Roden R, Asano K, Blaxall BC, Wu SC, Communal C, Singh K, Colucci W, Bristow MR, Port DJ. Myocardial-directed overexpression of the human beta(1)-adrenergic receptor in transgenic mice. *J Mol Cell Cardiol*. 2000;32:817-30.
416. Rapacciuolo A, Esposito G, Caron K, Mao L, Thomas SA, Rockman HA. Important role of endogenous norepinephrine and epinephrine in the development of in vivo pressure-overload cardiac hypertrophy. *J Am Coll Cardiol*. 2001;38:876-82.
417. Esposito G, Rapacciuolo A, Naga Prasad SV, Takaoka H, Thomas SA, Koch WJ, Rockman HA. Genetic alterations that inhibit in vivo pressure-overload hypertrophy prevent cardiac dysfunction despite increased wall stress. *Circulation*. 2002;105:85-92.
418. Ito H, Hirata Y, Hiroe M, Tsujino M, Adachi S, Takamoto T, Nitta M, Taniguchi K, Marumo F. Endothelin-1 induces hypertrophy with enhanced expression of muscle-specific genes in cultured neonatal rat cardiomyocytes. *Circ Res*. 1991;69:209-15.
419. Ito H, Hiroe M, Hirata Y, Fujisaki H, Adachi S, Akimoto H, Ohta Y, Marumo F. Endothelin ETA receptor antagonist blocks cardiac hypertrophy provoked by hemodynamic overload. *Circulation*. 1994;89:2198-203.

420. Kurihara Y, Kurihara H, Suzuki H, Kodama T, Maemura K, Nagai R, Oda H, Kuwaki T, Cao WH, Kamada N, et al. Elevated blood pressure and craniofacial abnormalities in mice deficient in endothelin-1. *Nature*. 1994;368:703-10.
421. Kurihara Y, Kurihara H, Oda H, Maemura K, Nagai R, Ishikawa T, Yazaki Y. Aortic arch malformations and ventricular septal defect in mice deficient in endothelin-1. *J Clin Invest*. 1995;96:293-300.
422. Clouthier DE, Hosoda K, Richardson JA, Williams SC, Yanagisawa H, Kuwaki T, Kumada M, Hammer RE, Yanagisawa M. Cranial and cardiac neural crest defects in endothelin-A receptor-deficient mice. *Development*. 1998;125:813-24.
423. Akhter SA, Luttrell LM, Rockman HA, Iaccarino G, Lefkowitz RJ, Koch WJ. Targeting the receptor-Gq interface to inhibit in vivo pressure overload myocardial hypertrophy. *Science*. 1998;280:574-7.
424. Wettschureck N, Rutten H, Zywietz A, Gehring D, Wilkie TM, Chen J, Chien KR, Offermanns S. Absence of pressure overload induced myocardial hypertrophy after conditional inactivation of Galphaq/Galpha11 in cardiomyocytes. *Nat Med*. 2001;7:1236-40.
425. Wollert KC, Taga T, Saito M, Narazaki M, Kishimoto T, Glembotski CC, Vernallis AB, Heath JK, Pennica D, Wood WI, Chien KR. Cardiotrophin-1 activates a distinct form of cardiac muscle cell hypertrophy. Assembly of sarcomeric units in series VIA gp130/leukemia inhibitory factor receptor-dependent pathways. *J Biol Chem*. 1996;271:9535-45.
426. Yoshida K, Taga T, Saito M, Suematsu S, Kumanogoh A, Tanaka T, Fujiwara H, Hirata M, Yamagami T, Nakahata T, Hirabayashi T, Yoneda Y, Tanaka K, Wang WZ, Mori C, Shiota K, Yoshida N, Kishimoto T. Targeted disruption of gp130, a common signal transducer for the interleukin 6 family of cytokines, leads to myocardial and hematological disorders. *Proc Natl Acad Sci U S A*. 1996;93:407-11.
427. Uozumi H, Hiroi Y, Zou Y, Takimoto E, Toko H, Niu P, Shimoyama M, Yazaki Y, Nagai R, Komuro I. gp130 plays a critical role in pressure overload-induced cardiac hypertrophy. *J Biol Chem*. 2001;276:23115-9.
428. Clayton RN. Cardiovascular Function in Acromegaly. *Endocr Rev*. 2003;24:272-277.
429. Bell D, McDermott BJ. Contribution of de novo protein synthesis to the hypertrophic effect of IGF-1 but not of thyroid hormones in adult ventricular cardiomyocytes. *Mol Cell Biochem*. 2000;206:113-24.
430. Serneri GG, Modesti PA, Boddi M, Cecioni I, Paniccia R, Coppo M, Galanti G, Simonetti I, Vanni S, Papa L, Bandinelli B, Migliorini A, Modesti A, Maccherini M, Sani G, Toscano M. Cardiac growth factors in human hypertrophy. Relations with myocardial contractility and wall stress. *Circ Res*. 1999;85:57-67.
431. Modesti PA, Vanni S, Bertolozzi I, Cecioni I, Polidori G, Paniccia R, Bandinelli B, Perna A, Liguori P, Boddi M, Galanti G, Serneri GG. Early sequence of cardiac adaptations and growth factor formation in pressure-

and volume-overload hypertrophy. *Am J Physiol Heart Circ Physiol*. 2000;279:H976-85.
432. Donohue TJ, Dworkin LD, Lango MN, Fliegner K, Lango RP, Benstein JA, Slater WR, Catanese VM. Induction of myocardial insulin-like growth factor-I gene expression in left ventricular hypertrophy. *Circulation*. 1994;89:799-809.
433. Cittadini A, Stromer H, Katz SE, Clark R, Moses AC, Morgan JP, Douglas PS. Differential Cardiac Effects of Growth Hormone and Insulin-like Growth Factor1 in the Rat : A Combined In Vivo and In Vitro Evaluation. *Circulation*. 1996;93:800-809.
434. Redaelli G, Malhotra A, Li B, Li P, Sonnenblick EH, Hofmann PA, Anversa P. Effects of constitutive overexpression of insulin-like growth factor-1 on the mechanical characteristics and molecular properties of ventricular myocytes. *Circ Res*. 1998;82:594-603.
435. Knowles JW, Esposito G, Mao L, Hagaman JR, Fox JE, Smithies O, Rockman HA, Maeda N. Pressure-independent enhancement of cardiac hypertrophy in natriuretic peptide receptor A-deficient mice. *J Clin Invest*. 2001;107:975-84.
436. Vega RB, Rothermel BA, Weinheimer CJ, Kovacs A, Naseem RH, Bassel-Duby R, Williams RS, Olson EN. Dual roles of modulatory calcineurin-interacting protein 1 in cardiac hypertrophy. *Proc Natl Acad Sci U S A*. 2003;100:669-674.
437. Asakawa M, Takano H, Nagai T, Uozumi H, Hasegawa H, Kubota N, Saito T, Masuda Y, Kadowaki T, Komuro I. Peroxisome proliferator-activated receptor gamma plays a critical role in inhibition of cardiac hypertrophy in vitro and in vivo. *Circulation*. 2002;105:1240-6.
438. Abel ED, Kaulbach HC, Tian R, Hopkins JC, Duffy J, Doetschman T, Minnemann T, Boers ME, Hadro E, Oberste-Berghaus C, Quist W, Lowell BB, Ingwall JS, Kahn BB. Cardiac hypertrophy with preserved contractile function after selective deletion of GLUT4 from the heart. *J Clin Invest*. 1999;104:1703-14.
439. Kong Y, Shelton JM, Rothermel B, Li X, Richardson JA, Bassel-Duby R, Williams RS. Cardiac-specific LIM protein FHL2 modifies the hypertrophic response to beta-adrenergic stimulation. *Circulation*. 2001;103:2731-8.
440. Xin HB, Senbonmatsu T, Cheng DS, Wang YX, Copello JA, Ji GJ, Collier ML, Deng KY, Jeyakumar LH, Magnuson MA, Inagami T, Kotlikoff MI, Fleischer S. Oestrogen protects FKBP12.6 null mice from cardiac hypertrophy. *Nature*. 2002;416:334-8.
441. Ichinose F, Bloch KD, Wu JC, Hataishi R, Aretz HT, Picard MH, Scherrer-Crosbie M. Pressure overload-induced LV hypertrophy and dysfunction in mice are exacerbated by congenital NOS3 deficiency. *Am J Physiol Heart Circ Physiol*. 2004;286:H1070-1075.
442. Crabtree GR. Generic signals and specific outcomes: signaling through Ca2+, calcineurin, and NF-AT. *Cell*. 1999;96:611-4.

443. Taigen T, De Windt LJ, Lim HW, Molkentin JD. Targeted inhibition of calcineurin prevents agonist-induced cardiomyocyte hypertrophy. *Proc Natl Acad Sci U S A*. 2000;97:1196-201.
444. Haq S, Choukroun G, Lim H, Tymitz KM, del Monte F, Gwathmey J, Grazette L, Michael A, Hajjar R, Force T, Molkentin JD. Differential activation of signal transduction pathways in human hearts with hypertrophy versus advanced heart failure. *Circulation*. 2001;103:670-7.
445. Bueno OF, Brandt EB, Rothenberg ME, Molkentin JD. Defective T cell development and function in calcineurin A beta -deficient mice. *Proc Natl Acad Sci U S A*. 2002;99:9398-403.
446. Parsons SA, Wilkins BJ, Bueno OF, Molkentin JD. Altered Skeletal Muscle Phenotypes in Calcineurin A{alpha} and A{beta} Gene-Targeted Mice. *Mol. Cell. Biol.* 2003;23:4331-4343.
447. Ueki K, Muramatsu T, Kincaid RL. Structure and expression of two isoforms of the murine calmodulin-dependent protein phosphatase regulatory subunit (calcineurin B). *Biochem Biophys Res Commun*. 1992;187:537-43.
448. Crabtree GR, Olson EN. NFAT signaling: choreographing the social lives of cells. *Cell*. 2002;109 Suppl:S67-79.
449. Sugimoto T, Stewart S, Guan KL. The calcium/calmodulin-dependent protein phosphatase calcineurin is the major Elk-1 phosphatase. *J Biol Chem*. 1997;272:29415-8.
450. Tian J, Karin M. Stimulation of Elk1 transcriptional activity by mitogen-activated protein kinases is negatively regulated by protein phosphatase 2B (calcineurin). *J Biol Chem*. 1999;274:15173-80.
451. Biswas G, Anandatheerthavarada HK, Zaidi M, Avadhani NG. Mitochondria to nucleus stress signaling: a distinctive mechanism of NF{kappa}B/Rel activation through calcineurin-mediated inactivation of I{kappa}B{beta}. *J. Cell Biol.* 2003;161:507-519.
452. Hunton DL, Lucchesi PA, Pang Y, Cheng X, Dell'Italia LJ, Marchase RB. Capacitative calcium entry contributes to nuclear factor of activated T-cells nuclear translocation and hypertrophy in cardiomyocytes. *J Biol Chem*. 2002;277:14266-73.
453. Frey N, Richardson JA, Olson EN. Calsarcins, a novel family of sarcomeric calcineurin-binding proteins. *Proc Natl Acad Sci U S A*. 2000;97:14632-7.
454. Rothermel B, Vega RB, Yang J, Wu H, Bassel-Duby R, Williams RS. A protein encoded within the Down syndrome critical region is enriched in striated muscles and inhibits calcineurin signaling. *J Biol Chem*. 2000;275:8719-25.
455. Wang Y, De Keulenaer GW, Weinberg EO, Muangman S, Gualberto A, Landschulz KT, Turi TG, Thompson JF, Lee RT. Direct biomechanical induction of endogenous calcineurin inhibitor Down Syndrome Critical Region-1 in cardiac myocytes. *Am J Physiol Heart Circ Physiol*. 2002;283:H533-9.

456. Rothermel BA, McKinsey TA, Vega RB, Nicol RL, Mammen P, Yang J, Antos CL, Shelton JM, Bassel-Duby R, Olson EN, Williams RS. Myocyte-enriched calcineurin-interacting protein, MCIP1, inhibits cardiac hypertrophy in vivo. *Proc Natl Acad Sci U S A*. 2001;98:3328-33.
457. Sun L, Youn HD, Loh C, Stolow M, He W, Liu JO. Cabin 1, a negative regulator for calcineurin signaling in T lymphocytes. *Immunity*. 1998;8:703-11.
458. Lai MM, Burnett PE, Wolosker H, Blackshaw S, Snyder SH. Cain, a novel physiologic protein inhibitor of calcineurin. *J Biol Chem*. 1998;273:18325-31.
459. Lin X, Sikkink RA, Rusnak F, Barber DL. Inhibition of calcineurin phosphatase activity by a calcineurin B homologous protein. *J Biol Chem*. 1999;274:36125-31.
460. Coghlan VM, Perrino BA, Howard M, Langeberg LK, Hicks JB, Gallatin WM, Scott JD. Association of protein kinase A and protein phosphatase 2B with a common anchoring protein. *Science*. 1995;267:108-11.
461. Harding MW, Galat A, Uehling DE, Schreiber SL. A receptor for the immunosuppressant FK506 is a cis-trans peptidyl-prolyl isomerase. *Nature*. 1989;341:758-60.
462. Fischer G, Wittmann-Liebold B, Lang K, Kiefhaber T, Schmid FX. Cyclophilin and peptidyl-prolyl cis-trans isomerase are probably identical proteins. *Nature*. 1989;337:476-8.
463. Takahashi N, Hayano T, Suzuki M. Peptidyl-prolyl cis-trans isomerase is the cyclosporin A-binding protein cyclophilin. *Nature*. 1989;337:473-5.
464. Jain J, McCaffrey PG, Miner Z, Kerppola TK, Lambert JN, Verdine GL, Curran T, Rao A. The T-cell transcription factor NFATp is a substrate for calcineurin and interacts with Fos and Jun. *Nature*. 1993;365:352-5.
465. Okamura H, Aramburu J, Garcia-Rodriguez C, Viola JP, Raghavan A, Tahiliani M, Zhang X, Qin J, Hogan PG, Rao A. Concerted dephosphorylation of the transcription factor NFAT1 induces a conformational switch that regulates transcriptional activity. *Mol Cell*. 2000;6:539-50.
466. Haq S, Choukroun G, Kang ZB, Ranu H, Matsui T, Rosenzweig A, Molkentin JD, Alessandrini A, Woodgett J, Hajjar R, Michael A, Force T. Glycogen synthase kinase-3beta is a negative regulator of cardiomyocyte hypertrophy. *J Cell Biol*. 2000;151:117-30.
467. Gomez del Arco P, Martinez-Martinez S, Maldonado JL, Ortega-Perez I, Redondo JM. A role for the p38 MAP kinase pathway in the nuclear shuttling of NFATp. *J Biol Chem*. 2000;275:13872-8.
468. Porter CM, Havens MA, Clipstone NA. Identification of amino acid residues and protein kinases involved in the regulation of NFATc subcellular localization. *J Biol Chem*. 2000;275:3543-51.
469. Yang TT, Xiong Q, Enslen H, Davis RJ, Chow CW. Phosphorylation of NFATc4 by p38 mitogen-activated protein kinases. *Mol Cell Biol*. 2002;22:3892-904.

470. Chow CW, Dong C, Flavell RA, Davis RJ. c-Jun NH(2)-terminal kinase inhibits targeting of the protein phosphatase calcineurin to NFATc1. *Mol Cell Biol*. 2000;20:5227-34.
471. Zhu J, Shibasaki F, Price R, Guillemot JC, Yano T, Dotsch V, Wagner G, Ferrara P, McKeon F. Intramolecular masking of nuclear import signal on NF-AT4 by casein kinase I and MEKK1. *Cell*. 1998;93:851-61.
472. Xia Y, McMillin JB, Lewis A, Moore M, Zhu WG, Williams RS, Kellems RE. Electrical stimulation of neonatal cardiac myocytes activates the NFAT3 and GATA4 pathways and up-regulates the adenylosuccinate synthetase 1 gene. *J Biol Chem*. 2000;275:1855-63.
473. Yang J, Rothermel B, Vega RB, Frey N, McKinsey TA, Olson EN, Bassel-Duby R, Williams RS. Independent signals control expression of the calcineurin inhibitory proteins MCIP1 and MCIP2 in striated muscles. *Circ Res*. 2000;87:E61-8.
474. Wilkins BJ, De Windt LJ, Bueno OF, Braz JC, Glascock BJ, Kimball TF, Molkentin JD. Targeted Disruption of NFATc3, but Not NFATc4, Reveals an Intrinsic Defect in Calcineurin-Mediated Cardiac Hypertrophic Growth. *Mol. Cell. Biol.* 2002;22:7603-7613.
475. Hoey T, Sun YL, Williamson K, Xu X. Isolation of two new members of the NF-AT gene family and functional characterization of the NF-AT proteins. *Immunity*. 1995;2:461-72.
476. Ranger AM, Grusby MJ, Hodge MR, Gravallese EM, de la Brousse FC, Hoey T, Mickanin C, Baldwin HS, Glimcher LH. The transcription factor NF-ATc is essential for cardiac valve formation. *Nature*. 1998;392:186-90.
477. de la Pompa JL, Timmerman LA, Takimoto H, Yoshida H, Elia AJ, Samper E, Potter J, Wakeham A, Marengere L, Langille BL, Crabtree GR, Mak TW. Role of the NF-ATc transcription factor in morphogenesis of cardiac valves and septum. *Nature*. 1998;392:182-6.
478. Graef IA, Chen F, Chen L, Kuo A, Crabtree GR. Signals transduced by Ca(2+)/calcineurin and NFATc3/c4 pattern the developing vasculature. *Cell*. 2001;105:863-75.
479. Hodge MR, Ranger AM, Charles de la Brousse F, Hoey T, Grusby MJ, Glimcher LH. Hyperproliferation and dysregulation of IL-4 expression in NF-ATp-deficient mice. *Immunity*. 1996;4:397-405.
480. Oukka M, Ho IC, de la Brousse FC, Hoey T, Grusby MJ, Glimcher LH. The transcription factor NFAT4 is involved in the generation and survival of T cells. *Immunity*. 1998;9:295-304.
481. Peng SL, Gerth AJ, Ranger AM, Glimcher LH. NFATc1 and NFATc2 together control both T and B cell activation and differentiation. *Immunity*. 2001;14:13-20.
482. Ranger AM, Oukka M, Rengarajan J, Glimcher LH. Inhibitory function of two NFAT family members in lymphoid homeostasis and Th2 development. *Immunity*. 1998;9:627-35.

483. Xanthoudakis S, Viola JP, Shaw KT, Luo C, Wallace JD, Bozza PT, Luk DC, Curran T, Rao A. An enhanced immune response in mice lacking the transcription factor NFAT1. *Science*. 1996;272:892-5.
484. Horsley V, Friday BB, Matteson S, Kegley KM, Gephart J, Pavlath GK. Regulation of the growth of multinucleated muscle cells by an NFATC2-dependent pathway. *J Cell Biol*. 2001;153:329-38.
485. Kegley KM, Gephart J, Warren GL, Pavlath GK. Altered primary myogenesis in NFATC3(-/-) mice leads to decreased muscle size in the adult. *Dev Biol*. 2001;232:115-26.
486. Bueno OF, van Rooij E, Molkentin JD, Doevendans PA, De Windt LJ. Calcineurin and hypertrophic heart disease: novel insights and remaining questions. *Cardiovasc Res*. 2002;53:806-21.
487. Goto T, Kino T, Hatanaka H, Okuhara M, Kohsaka M, Aoki H, Imanaka H. FK 506: historical perspectives. *Transplant Proc*. 1991;23:2713-7.
488. Goto S, Stepkowski SM, Kahan BD. Effect of FK 506 and cyclosporine on heart allograft survival in rats. *Transplant Proc*. 1991;23:529-30.
489. Shiraga T, Matsuda H, Nagase K, Iwasaki K, Noda K, Yamazaki H, Shimada T, Funae Y. Metabolism of FK506, a potent immunosuppressive agent, by cytochrome P450 3A enzymes in rat, dog and human liver microsomes. *Biochem Pharmacol*. 1994;47:727-35.
490. Matsuda S, Shibasaki F, Takehana K, Mori H, Nishida E, Koyasu S. Two distinct action mechanisms of immunophilin-ligand complexes for the blockade of T-cell activation. *EMBO Reports*. 2000;1:428-434.
491. Bandyopadhyay A, Shin DW, Ahn JO, Kim DH. Calcineurin regulates ryanodine receptor/Ca(2+)-release channels in rat heart. *Biochem J*. 2000;352 Pt 1:61-70.
492. Mijares A, Malecot CO, Peineau N, Argibay JA. In vivo and in vitro inhibition of the L-type calcium current in isolated guinea-pig cardiomyocytes by the immunosuppressive agent cyclosporin A. *J Mol Cell Cardiol*. 1997;29:2067-76.
493. Terracciano CM. Sarcoplasmic reticulum calcium release function and FK binding proteins in heart failure: another piece of a complex jigsaw. *Cardiovasc Res*. 2000;48:191-3.
494. Shou W, Aghdasi B, Armstrong DL, Guo Q, Bao S, Charng MJ, Mathews LM, Schneider MD, Hamilton SL, Matzuk MM. Cardiac defects and altered ryanodine receptor function in mice lacking FKBP12. *Nature*. 1998;391:489-92.
495. Zhang W. Old and new tools to dissect calcineurin's role in pressure-overload cardiac hypertrophy. *Cardiovasc Res*. 2002;53:294-303.
496. Wilkins BJ, Molkentin JD. Calcineurin and cardiac hypertrophy: where have we been? Where are we going? *J Physiol*. 2002;541:1-8.
497. Sussman MA, Lim HW, Gude N, Taigen T, Olson EN, Robbins J, Colbert MC, Gualberto A, Wieczorek DF, Molkentin JD. Prevention of cardiac hypertrophy in mice by calcineurin inhibition. *Science*. 1998;281:1690-3.

498. Zhang W, Kowal RC, Rusnak F, Sikkink RA, Olson EN, Victor RG. Failure of calcineurin inhibitors to prevent pressure-overload left ventricular hypertrophy in rats. *Circ Res*. 1999;84:722-8.
499. Meguro T, Hong C, Asai K, Takagi G, McKinsey TA, Olson EN, Vatner SF. Cyclosporine attenuates pressure-overload hypertrophy in mice while enhancing susceptibility to decompensation and heart failure. *Circ Res*. 1999;84:735-40.
500. Lim HW, De Windt LJ, Steinberg L, Taigen T, Witt SA, Kimball TR, Molkentin JD. Calcineurin expression, activation, and function in cardiac pressure-overload hypertrophy. *Circulation*. 2000;101:2431-7.
501. Hill JA, Karimi M, Kutschke W, Davisson RL, Zimmerman K, Wang Z, Kerber RE, Weiss RM. Cardiac hypertrophy is not a required compensatory response to short-term pressure overload. *Circulation*. 2000;101:2863-9.
502. Shimoyama M, Hayashi D, Takimoto E, Zou Y, Oka T, Uozumi H, Kudoh S, Shibasaki F, Yazaki Y, Nagai R, Komuro I. Calcineurin plays a critical role in pressure overload-induced cardiac hypertrophy. *Circulation*. 1999;100:2449-54.
503. Eto Y, Yonekura K, Sonoda M, Arai N, Sata M, Sugiura S, Takenaka K, Gualberto A, Hixon ML, Wagner MW, Aoyagi T. Calcineurin is activated in rat hearts with physiological left ventricular hypertrophy induced by voluntary exercise training. *Circulation*. 2000;101:2134-7.
504. Ding B, Price RL, Borg TK, Weinberg EO, Halloran PF, Lorell BH. Pressure overload induces severe hypertrophy in mice treated with cyclosporine, an inhibitor of calcineurin. *Circ Res*. 1999;84:729-34.
505. Wang Z, Kutschke W, Richardson KE, Karimi M, Hill JA. Electrical remodeling in pressure-overload cardiac hypertrophy: role of calcineurin. *Circulation*. 2001;104:1657-63.
506. Luo Z, Shyu KG, Gualberto A, Walsh K. Calcineurin inhibitors and cardiac hypertrophy. *Nat Med*. 1998;4:1092-3.
507. Shimoyama M, Hayashi D, Zou Y, Takimoto E, Mizukami M, Monzen K, Kudoh S, Hiroi Y, Yazaki Y, Nagai R, Komuro I. Calcineurin inhibitor attenuates the development and induces the regression of cardiac hypertrophy in rats with salt-sensitive hypertension. *Circulation*. 2000;102:1996-2004.
508. Baumgarten G, Knuefermann P, Nozaki N, Sivasubramanian N, Mann DL, Vallejo JG. In vivo expression of proinflammatory mediators in the adult heart after endotoxin administration: the role of toll-like receptor-4. *J Infect Dis*. 2001;183:1617-24.
509. Muller JG, Nemoto, S, Laser, M, Carabello, B.A, Menick, D.R. Calcineurin inhibition and cardiac hypertrophy. *Science*. 1998;282:1007a.
510. Lim HW, De Windt LJ, Mante J, Kimball TR, Witt SA, Sussman MA, Molkentin JD. Reversal of cardiac hypertrophy in transgenic disease models by calcineurin inhibition. *J Mol Cell Cardiol*. 2000;32:697-709.

511. Fatkin D, McConnell BK, Mudd JO, Semsarian C, Moskowitz IGP, Schoen FJ, Giewat M, Seidman CE, Seidman JG. An abnormal Ca2+ response in mutant sarcomere protein-mediated familial hypertrophic cardiomyopathy. *J. Clin. Invest.* 2000;106:1351-1359.
512. Mervaala EM, Pere AK, Lindgren L, Laakso J, Teravainen TL, Karjala K, Vapaatalo H, Ahonen J, Karppanen H. Effects of dietary sodium and magnesium on cyclosporin A-induced hypertension and nephrotoxicity in spontaneously hypertensive rats. *Hypertension*. 1997;29:822-7.
513. Lassila M, Finckenberg P, Pere AK, Krogerus L, Ahonen J, Vapaatalo H, Nurminen ML. Comparison of enalapril and valsartan in cyclosporine A-induced hypertension and nephrotoxicity in spontaneously hypertensive rats on high-sodium diet. *Br J Pharmacol*. 2000;130:1339-47.
514. Mervaala E, Muller DN, Park JK, Dechend R, Schmidt F, Fiebeler A, Bieringer M, Breu V, Ganten D, Haller H, Luft FC. Cyclosporin A protects against angiotensin II-induced end-organ damage in double transgenic rats harboring human renin and angiotensinogen genes. *Hypertension*. 2000;35:360-6.
515. Murat A, Pellieux C, Brunner HR, Pedrazzini T. Calcineurin blockade prevents cardiac mitogen-activated protein kinase activation and hypertrophy in renovascular hypertension. *J Biol Chem*. 2000;275:40867-73.
516. Hayashida W, Kihara Y, Yasaka A, Sasayama S. Cardiac calcineurin during transition from hypertrophy to heart failure in rats. *Biochem Biophys Res Commun*. 2000;273:347-51.
517. Sakata Y, Masuyama T, Yamamoto K, Nishikawa N, Yamamoto H, Kondo H, Ono K, Otsu K, Kuzuya T, Miwa T, Takeda H, Miyamoto E, Hori M. Calcineurin inhibitor attenuates left ventricular hypertrophy, leading to prevention of heart failure in hypertensive rats. *Circulation*. 2000;102:2269-75.
518. Nagata K, Somura F, Obata K, Odashima M, Izawa H, Ichihara S, Nagasaka T, Iwase M, Yamada Y, Nakashima N, Yokota M. AT1 receptor blockade reduces cardiac calcineurin activity in hypertensive rats. *Hypertension*. 2002;40:168-74.
519. Goldspink PH, McKinney RD, Kimball VA, Geenen DL, Buttrick PM. Angiotensin II induced cardiac hypertrophy in vivo is inhibited by cyclosporin A in adult rats. *Mol Cell Biochem*. 2001;226:83-8.
520. Takeda Y, Yoneda T, Demura M, Usukura M, Mabuchi H. Calcineurin inhibition attenuates mineralocorticoid-induced cardiac hypertrophy. *Circulation*. 2002;105:677-9.
521. Oie E, Bjornerheim R, Clausen OP, Attramadal H. Cyclosporin A inhibits cardiac hypertrophy and enhances cardiac dysfunction during postinfarction failure in rats. *Am J Physiol Heart Circ Physiol*. 2000;278:H2115-23.

522. Kamiya H, Okumura K, Ito M, Saburi Y, Tomida T, Hayashi K, Matsui H, Hayakawa T. Calcineurin inhibitor attenuates cardiac hypertrophy due to energy metabolic disorder. *Can J Cardiol*. 2001;17:1292-8.
523. Lim HW, Molkentin JD. Calcineurin and human heart failure. *Nat Med*. 1999;5:246-7.
524. Mervaala E, Lassila M, Vaskonen T, Krogerus L, Lahteenmaki T, Vapaatalo H, Karppanen H. Effects of ACE inhibition on cyclosporine A-induced hypertension and nephrotoxicity in spontaneously hypertensive rats on a high-sodium diet. *Blood Press*. 1999;8:49-56.
525. Takeda Y, Miyamori I, Furukawa K, Inaba S, Mabuchi H. Mechanisms of FK 506-induced hypertension in the rat. *Hypertension*. 1999;33:130-6.
526. Kimura B, Mohuczy D, Tang X, Phillips MI. Attenuation of Hypertension and Heart Hypertrophy by Adeno-Associated Virus Delivering Angiotensinogen Antisense. *Hypertension*. 2001;37:376-380.
527. Sakata Y, Masuyama T, Yamamoto K, Doi R, Mano T, Kuzuya T, Miwa T, Takeda H, Hori M. Renin angiotensin system-dependent hypertrophy as a contributor to heart failure in hypertensive rats: different characteristics from renin angiotensin system-independent hypertrophy. *J Am Coll Cardiol*. 2001;37:293-9.
528. Freund HR, Holroyde J. Cardiac function during protein malnutrition and refeeding in the isolated rat heart. *JPEN J Parenter Enteral Nutr*. 1986;10:470-3.
529. Cicogna AC, Padovani CR, Okoshi K, Aragon FF, Okoshi MP. Myocardial function during chronic food restriction in isolated hypertrophied cardiac muscle. *Am J Med Sci*. 2000;320:244-8.
530. Samarel AM, Parmacek MS, Magid NM, Decker RS, Lesch M. Protein synthesis and degradation during starvation-induced cardiac atrophy in rabbits. *Circ Res*. 1987;60:933-41.
531. Stahl TJ, Alden PB, Madoff RD, Ring WS, Cerra FB. Cardiac beta-adrenergic responsiveness is well preserved in moderate protein calorie malnutrition from semistarvation. *JPEN J Parenter Enteral Nutr*. 1988;12:579-86.
532. de Simone G, Scalfi L, Galderisi M, Celentano A, Di Biase G, Tammaro P, Garofalo M, Mureddu GF, de Divitiis O, Contaldo F. Cardiac abnormalities in young women with anorexia nervosa. *Br Heart J*. 1994;71:287-92.
533. De Windt LJ, Lim HW, Bueno OF, Liang Q, Delling U, Braz JC, Glascock BJ, Kimball TF, del Monte F, Hajjar RJ, Molkentin JD. Targeted inhibition of calcineurin attenuates cardiac hypertrophy in vivo. *Proc Natl Acad Sci U S A*. 2001;98:3322-7.
534. Zou Y, Hiroi Y, Uozumi H, Takimoto E, Toko H, Zhu W, Kudoh S, Mizukami M, Shimoyama M, Shibasaki F, Nagai R, Yazaki Y, Komuro I. Calcineurin plays a critical role in the development of pressure overload-induced cardiac hypertrophy. *Circulation*. 2001;104:97-101.

535. Hill JA, Rothermel B, Yoo KD, Cabuay B, Demetroulis E, Weiss RM, Kutschke W, Bassel-Duby R, Williams RS. Targeted inhibition of calcineurin in pressure-overload cardiac hypertrophy. Preservation of systolic function. *J Biol Chem*. 2002;277:10251-5.
536. Bueno OF, Wilkins BJ, Tymitz KM, Glascock BJ, Kimball TF, Lorenz JN, Molkentin JD. Impaired cardiac hypertrophic response in Calcineurin Abeta -deficient mice. *Proc Natl Acad Sci U S A*. 2002;99:4586-91.
537. Tsao L, Neville C, Musaro A, McCullagh KJ, Rosenthal N. Revisiting calcineurin and human heart failure. *Nat Med*. 2000;6:2-3.
538. Ritter O, Hack S, Schuh K, Rothlein N, Perrot A, Osterziel KJ, Schulte HD, Neyses L. Calcineurin in human heart hypertrophy. *Circulation*. 2002;105:2265-9.
539. Lipkin GW, Tucker B, Giles M, Raine AE. Ambulatory blood pressure and left ventricular mass in cyclosporin- and non-cyclosporin-treated renal transplant recipients. *J Hypertens*. 1993;11:439-42.
540. Ventura HO, Malik FS, Mehra MR, Stapleton DD, Smart FW. Mechanisms of hypertension in cardiac transplantation and the role of cyclosporine. *Curr Opin Cardiol*. 1997;12:375-81.
541. Minamino T, Yujiri T, Terada N, Taffet GE, Michael LH, Johnson GL, Schneider MD. MEKK1 is essential for cardiac hypertrophy and dysfunction induced by Gq. *Proc Natl Acad Sci U S A*. 2002;99:3866-71.
542. Choukroun G, Hajjar R, Fry S, del Monte F, Haq S, Guerrero JL, Picard M, Rosenzweig A, Force T. Regulation of cardiac hypertrophy in vivo by the stress-activated protein kinases/c-Jun NH(2)-terminal kinases. *J Clin Invest*. 1999;104:391-8.
543. Bueno OF, De Windt LJ, Lim HW, Tymitz KM, Witt SA, Kimball TR, Molkentin JD. The dual-specificity phosphatase MKP-1 limits the cardiac hypertrophic response in vitro and in vivo. *Circ Res*. 2001;88:88-96.
544. Liao P, Georgakopoulos D, Kovacs A, Zheng M, Lerner D, Pu H, Saffitz J, Chien K, Xiao RP, Kass DA, Wang Y. The in vivo role of p38 MAP kinases in cardiac remodeling and restrictive cardiomyopathy. *Proc Natl Acad Sci U S A*. 2001;98:12283-8.
545. Braz JC, Bueno OF, Liang Q, Wilkins BJ, Dai Y-S, Parsons S, Braunwart J, Glascock BJ, Klevitsky R, Kimball TF, Hewett TE, Molkentin JD. Targeted inhibition of p38 MAPK promotes hypertrophic cardiomyopathy through upregulation of calcineurin-NFAT signaling. *J. Clin. Invest.* 2003;111:1475-1486.
546. Lim HW, New L, Han J, Molkentin JD. Calcineurin enhances MAPK phosphatase-1 expression and p38 MAPK inactivation in cardiac myocytes. *J Biol Chem*. 2001;276:15913-9.
547. De Windt LJ, Lim HW, Haq S, Force T, Molkentin JD. Calcineurin promotes protein kinase C and c-Jun NH2-terminal kinase activation in the heart. Cross-talk between cardiac hypertrophic signaling pathways. *J Biol Chem*. 2000;275:13571-9.

548. Hardt SE, Sadoshima J. Glycogen Synthase Kinase-3{beta}: A Novel Regulator of Cardiac Hypertrophy and Development. *Circ Res.* 2002;90:1055-1063.
549. Morisco C, Seta K, Hardt SE, Lee Y, Vatner SF, Sadoshima J. Glycogen synthase kinase 3beta regulates GATA4 in cardiac myocytes. *J Biol Chem.* 2001;276:28586-97.
550. Sheridan CM, Heist EK, Beals CR, Crabtree GR, Gardner P. Protein kinase A negatively modulates the nuclear accumulation of NF-ATc1 by priming for subsequent phosphorylation by glycogen synthase kinase-3. *J Biol Chem.* 2002;277:48664-76.
551. Beals CR, Sheridan CM, Turck CW, Gardner P, Crabtree GR. Nuclear export of NF-ATc enhanced by glycogen synthase kinase-3. *Science.* 1997;275:1930-4.
552. Graef IA, Mermelstein PG, Stankunas K, Neilson JR, Deisseroth K, Tsien RW, Crabtree GR. L-type calcium channels and GSK-3 regulate the activity of NF-ATc4 in hippocampal neurons. *Nature.* 1999;401:703-8.
553. Badorff C, Ruetten H, Mueller S, Stahmer M, Gehring D, Jung F, Ihling C, Zeiher AM, Dimmeler S. Fas receptor signaling inhibits glycogen synthase kinase 3 beta and induces cardiac hypertrophy following pressure overload. *J Clin Invest.* 2002;109:373-81.
554. Cross DA, Alessi DR, Cohen P, Andjelkovich M, Hemmings BA. Inhibition of glycogen synthase kinase-3 by insulin mediated by protein kinase B. *Nature.* 1995;378:785-9.
555. Shindo T, Manabe I, Fukushima Y, Tobe K, Aizawa K, Miyamoto S, Kawai-Kowase K, Moriyama N, Imai Y, Kawakami H, Nishimatsu H, Ishikawa T, Suzuki T, Morita H, Maemura K, Sata M, Hirata Y, Komukai M, Kagechika H, Kadowaki T, Kurabayashi M, Nagai R. Kruppel-like zinc-finger transcription factor KLF5/BTEB2 is a target for angiotensin II signaling and an essential regulator of cardiovascular remodeling. *Nat Med.* 2002;8:856-63.
556. de Simone G, Di Lorenzo L, Costantino G, Moccia D, Buonissimo S, de Divitiis O. Supernormal contractility in primary hypertension without left ventricular hypertrophy. *Hypertension.* 1988;11:457-63.
557. del Monte F, Harding SE, Dec GW, Gwathmey JK, Hajjar RJ. Targeting phospholamban by gene transfer in human heart failure. *Circulation.* 2002;105:904-7.
558. Sadoshima J, Montagne O, Wang Q, Yang G, Warden J, Liu J, Takagi G, Karoor V, Hong C, Johnson GL, Vatner DE, Vatner SF. The MEKK1-JNK pathway plays a protective role in pressure overload but does not mediate cardiac hypertrophy. *J Clin Invest.* 2002;110:271-9.
559. Ohkubo H, Kawakami H, Kakehi Y, Takumi T, Arai H, Yokota Y, Iwai M, Tanabe Y, Masu M, Hata J, et al. Generation of transgenic mice with elevated blood pressure by introduction of the rat renin and angiotensinogen genes. *Proc Natl Acad Sci U S A.* 1990;87:5153-7.

560. Ganten D, Wagner J, Zeh K, Bader M, Michel JB, Paul M, Zimmermann F, Ruf P, Hilgenfeldt U, Ganten U, et al. Species specificity of renin kinetics in transgenic rats harboring the human renin and angiotensinogen genes. *Proc Natl Acad Sci U S A*. 1992;89:7806-10.
561. Caron KM, James LR, Kim HS, Morham SG, Sequeira Lopez ML, Gomez RA, Reudelhuber TL, Smithies O. A genetically clamped renin transgene for the induction of hypertension. *Proc Natl Acad Sci U S A*. 2002;99:8248-52.
562. Mullins JJ, Peters J, Ganten D. Fulminant hypertension in transgenic rats harbouring the mouse Ren-2 gene. *Nature*. 1990;344:541-4.
563. Kantachuvesiri S, Haley CS, Fleming S, Kurian K, Whitworth CE, Wenham P, Kotelevtsev Y, Mullins JJ. Genetic mapping of modifier loci affecting malignant hypertension in TGRmRen2 rats. *Kidney Int*. 1999;56:414-20.
564. Whitworth CE, Fleming S, Kotelevtsev Y, Manson L, Brooker GA, Cumming AD, Mullins JJ. A genetic model of malignant phase hypertension in rats. *Kidney Int*. 1995;47:529-35.
565. Lee MA, Bohm M, Paul M, Bader M, Ganten U, Ganten D. Physiological characterization of the hypertensive transgenic rat TGR(mREN2)27. *Am J Physiol*. 1996;270:E919-29.
566. Peters J, Munter K, Bader M, Hackenthal E, Mullins JJ, Ganten D. Increased adrenal renin in transgenic hypertensive rats, TGR(mREN2)27, and its regulation by cAMP, angiotensin II, and calcium. *J Clin Invest*. 1993;91:742-7.
567. Bader M, Zhao Y, Sander M, Lee MA, Bachmann J, Bohm M, Djavidani B, Peters J, Mullins JJ, Ganten D. Role of tissue renin in the pathophysiology of hypertension in TGR(mREN2)27 rats. *Hypertension*. 1992;19:681-6.
568. Sander M, Bader M, Djavidani B, Maser-Gluth C, Vecsei P, Mullins J, Ganten D, Peters J. The role of the adrenal gland in hypertensive transgenic rat TGR(mREN2)27. *Endocrinology*. 1992;131:807-14.
569. Tokita Y, Franco-Saenz R, Reimann E, Mulrow P. Hypertension in the transgenic rat TGR(mRen-2)27 may be due to enhanced kinetics of the reaction between mouse renin and rat angiotensinogen. *Hypertension*. 1994;23:422-427.
570. Campbell DJ, Rong P, Kladis A, Rees B, Ganten D, Skinner SL. Angiotensin and bradykinin peptides in the TGR(mRen-2)27 rat. *Hypertension*. 1995;25:1014-20.
571. Senanayake PD, Moriguchi A, Kumagai H, Ganten D, Ferrario CM, Brosnihan KB. Increased expression of angiotensin peptides in the brain of transgenic hypertensive rats. *Peptides*. 1994;15:919-26.
572. Moriguchi A, Tallant EA, Matsumura K, Reilly TM, Walton H, Ganten D, Ferrario CM. Opposing actions of angiotensin-(1-7) and angiotensin II in the brain of transgenic hypertensive rats. *Hypertension*. 1995;25:1260-5.

573. Moriguchi A, Ferrario CM, Brosnihan KB, Ganten D, Morris M. Differential regulation of central vasopressin in transgenic rats harboring the mouse Ren-2 gene. *Am J Physiol.* 1994;267:R786-91.
574. Hilgers KF, Peters J, Veelken R, Sommer M, Rupprecht G, Ganten D, Luft FC, Mann JF. Increased vascular angiotensin formation in female rats harboring the mouse Ren-2 gene. *Hypertension*. 1992;19:687-91.
575. Peiro C, Rodriguez-Lopez AM, Angulo J, Regadera J, Marin J, Sanchez-Ferrer CF, Lopez-Novoa JM. Endogenous angiotensin II and cell hypertrophy in vascular smooth muscle cultures from hypertensive Ren-2 transgenic rats. *Cell Physiol Biochem*. 1998;8:106-16.
576. Fontes MA, Baltatu O, Caligiorne SM, Campagnole-Santos MJ, Ganten D, Bader M, Santos RA. Angiotensin peptides acting at rostral ventrolateral medulla contribute to hypertension of TGR(mREN2)27 rats. *Physiol Genomics*. 2000;2:137-42.
577. Bohm M, Lippoldt A, Wienen W, Ganten D, Bader M. Reduction of cardiac hypertrophy in TGR(mREN2)27 by angiotensin II receptor blockade. *Mol Cell Biochem.* 1996;163-164:217-21.
578. Ohta K, Kim S, Wanibuchi H, Ganten D, Iwao H. Contribution of Local Renin-Angiotensin System to Cardiac Hypertrophy, Phenotypic Modulation, and Remodeling in TGR(mRen2)27 Transgenic Rats. *Circulation*. 1996;94:785-791.
579. Witte K, Huser L, Knotter B, Heckmann M, Schiffer S, Lemmer B. Normalisation of blood pressure in hypertensive TGR(mREN2)27 rats by amlodipine vs. enalapril: effects on cardiac hypertrophy and signal transduction pathways. *Naunyn Schmiedebergs Arch Pharmacol.* 2001;363:101-9.
580. Bishop JE, Kiernan LA, Montgomery HE, Gohlke P, McEwan JR. Raised blood pressure, not renin-angiotensin systems, causes cardiac fibrosis in TGR m(Ren2)27 rats. *Cardiovascular Research*. 2000;47:57-67.
581. Kantachuvesiri S, Fleming S, Peters J, Peters B, Brooker G, Lammie AG, McGrath I, Kotelevtsev Y, Mullins JJ. Controlled hypertension, a transgenic toggle switch reveals differential mechanisms underlying vascular disease. *J Biol Chem*. 2001;276:36727-33.
582. Ryu DY, Levi PE, Fernandez-Salguero P, Gonzalez FJ, Hodgson E. Piperonyl butoxide and acenaphthylene induce cytochrome P450 1A2 and 1B1 mRNA in aromatic hydrocarbon-responsive receptor knock-out mouse liver. *Mol Pharmacol.* 1996;50:443-6.
583. Ryding AD, Sharp MG, Mullins JJ. Conditional transgenic technologies. *J Endocrinol*. 2001;171:1-14.
584. Zaher H, Yang TJ, Gelboin HV, Fernandez-Salguero P, Gonzalez FJ. Effect of phenobarbital on hepatic CYP1A1 and CYP1A2 in the Ahr-null mouse. *Biochem Pharmacol.* 1998;55:235-8.
585. Tomita S, Sinal CJ, Yim SH, Gonzalez FJ. Conditional disruption of the aryl hydrocarbon receptor nuclear translocator (Arnt) gene leads to loss

of target gene induction by the aryl hydrocarbon receptor and hypoxia-inducible factor 1alpha. *Mol Endocrinol.* 2000;14:1674-81.
586. Foussat J, Costet P, Galtier P, Pineau T, Lesca P. The 4S benzo(a)pyrene-binding protein is not a transcriptional activator of Cyp1a1 gene in Ah receptor-deficient (AHR -/-) transgenic mice. *Arch Biochem Biophys*. 1998;349:349-55.
587. Kantachuvesiri S. PhD Thesis. In: *Molecular Physiology Group*. Edinburgh: University of Edinburgh; 2000.
588. Campbell SJ, Carlotti F, Hall PA, Clark AJ, Wolf CR. Regulation of the CYP1A1 promoter in transgenic mice: an exquisitely sensitive on-off system for cell specific gene regulation. *J Cell Sci*. 1996;109 (Pt 11):2619-25.
589. Li H, Dong L, Whitlock J, Jr. Transcriptional activation function of the mouse Ah receptor nuclear translocator. *J. Biol. Chem.* 1994;269:28098-28105.
590. Dolwick KM, Schmidt JV, Carver LA, Swanson HI, Bradfield CA. Cloning and expression of a human Ah receptor cDNA. *Mol Pharmacol*. 1993;44:911-7.
591. Stresser DM, Williams DE, Griffin DA, Bailey GS. Mechanisms of tumor modulation by indole-3-carbinol. Disposition and excretion in male Fischer 344 rats. *Drug Metab Dispos*. 1995;23:965-75.
592. Katchamart S, Stresser DM, Dehal SS, Kupfer D, Williams DE. Concurrent flavin-containing monooxygenase down-regulation and cytochrome P-450 induction by dietary indoles in rat: implications for drug-drug interaction. *Drug Metab Dispos*. 2000;28:930-6.
593. *Molecular Cloning: A Laboratory Manual*: Cold Spring Harbour Laboratory Press; 1989.
594. *Current protocols in molecular biology*: John Wiley & Sons; 2003.
595. Coligan. *Current Protocols in Protein Science*. 2001 ed: John Wiley & Sons; 2001.
596. Growth and Maintenance of Insect Cell Lines (version G). In: Invitrogen Corporation; 2000.
597. pBlueBac4.5-E Echo Cloning System. In: Invitrogen Corporation; 1999.
598. Birnboim HC, Doly J. A rapid alkaline extraction procedure for screening recombinant plasmid DNA. *Nucleic Acids Res*. 1979;7:1513-23.
599. Sanger F, Nicklen S, Coulson AR. DNA sequencing with chain-terminating inhibitors. *Proc Natl Acad Sci U S A*. 1977;74:5463-7.
600. Tatusova TA, Madden TL. BLAST 2 Sequences, a new tool for comparing protein and nucleotide sequences. *FEMS Microbiol Lett*. 1999;174:247-50.
601. Southern EM. Detection of specific sequences among DNA fragments separated by gel electrophoresis. *J Mol Biol*. 1975;98:503-17.
602. Feinberg AP, Vogelstein B. A technique for radiolabeling DNA restriction endonuclease fragments to high specific activity. *Anal Biochem*. 1983;132:6-13.

603. Weiss S.A WWG, Gorfien S.F, Godwin G, P. Chapter 3: Insect Cell-Culture Techniques in Serum-Containing Medium. In: C.D. R, ed. *Methods in Molecular Biology*: Humana Press; 1995.
604. King L.A aPRD. The Baculovirus Expression System: a laboratory guide. In: Chapman and Hall; 1992.
605. Junqueira LC, Bignolas G, Brentani RR. Picrosirius staining plus polarization microscopy, a specific method for collagen detection in tissue sections. *Histochem J*. 1979;11:447-55.
606. Kojima M, Shiojima I, Yamazaki T, Komuro I, Zou Z, Wang Y, Mizuno T, Ueki K, Tobe K, Kadowaki T, et al. Angiotensin II receptor antagonist TCV-116 induces regression of hypertensive left ventricular hypertrophy in vivo and inhibits the intracellular signaling pathway of stretch-mediated cardiomyocyte hypertrophy in vitro. *Circulation*. 1994;89:2204-11.
607. Schelling P, Ganten U, Sponer G, Unger T, Ganten D. Components of the renin-angiotensin system in the cerebrospinal fluid of rats and dogs with special consideration of the origin and the fate of angiotensin II. *Neuroendocrinology*. 1980;31:297-308.
608. Pfeffer JM, Pfeffer MA, Frohlich ED. Validity of an indirect tail-cuff method for determining systolic arterial pressure in unanesthetized normotensive and spontaneously hypertensive rats. *J Lab Clin Med*. 1971;78:957-62.
609. Sahn DJ, DeMaria A, Kisslo J, Weyman A. Recommendations regarding quantitation in M-mode echocardiography: results of a survey of echocardiographic measurements. *Circulation*. 1978;58:1072-83.
610. Pawlush DG, Moore RL, Musch TI, Davidson WR, Jr. Echocardiographic evaluation of size, function, and mass of normal and hypertrophied rat ventricles. *J Appl Physiol*. 1993;74:2598-605.
611. Devereux RB, Reichek N. Echocardiographic determination of left ventricular mass in man. Anatomic validation of the method. *Circulation*. 1977;55:613-8.
612. de Simone G, Wallerson DC, Volpe M, Devereux RB. Echocardiographic measurement of left ventricular mass and volume in normotensive and hypertensive rats. Necropsy validation. *Am J Hypertens*. 1990;3:688-96.
613. Collins KA, Korcarz CE, Shroff SG, Bednarz JE, Fentzke RC, Lin H, Leiden JM, Lang RM. Accuracy of echocardiographic estimates of left ventricular mass in mice. *Am J Physiol Heart Circ Physiol*. 2001;280:H1954-62.
614. Shimizu G, Zile MR, Blaustein AS, Gaasch WH. Left ventricular chamber filling and midwall fiber lengthening in patients with left ventricular hypertrophy: overestimation of fiber velocities by conventional midwall measurements. *Circulation*. 1985;71:266-72.
615. Aytemir K, Maarouf N, Gallagher MM, Yap YG, Waktare JE, Malik M. Comparison of formulae for heart rate correction of QT interval in exercise electrocardiograms. *Pacing Clin Electrophysiol*. 1999;22:1397-401.

616. Lown B, Calvert AF, Armington R, Ryan M. Monitoring for serious arrhythmias and high risk of sudden death. *Circulation*. 1975;52:III189-98.
617. Bohlender J, Menard J, Ganten D, Luft FC. Angiotensinogen concentrations and renin clearance : implications for blood pressure regulation. *Hypertension*. 2000;35:780-6.
618. Bohlender J, Menard J, Luft FC, Ganten D. Dose effects of human renin in rats transgenic for human angiotensinogen. *Hypertension*. 1997;29:1031-8.
619. Theuer J, Dechend R, Muller DN, Park JK, Fiebeler A, Barta P, Ganten D, Haller H, Dietz R, Luft FC. Angiotensin II induced inflammation in the kidney and in the heart of double transgenic rats. *BMC Cardiovasc Disord*. 2002;2:3.
620. Haas GJ, McCune SA, Brown DM, Cody RJ. Echocardiographic characterization of left ventricular adaptation in a genetically determined heart failure rat model. *Am Heart J*. 1995;130:806-11.
621. Sharp J, Zammit T, Azar T, Lawson D. Recovery of male rats from major abdominal surgery after treatment with various analgesics. *Contemp Top Lab Anim Sci*. 2003;42:22-7.
622. Roy RN, Flynn TG. Organization of the gene for iso-rANP, a rat B-type natriuretic peptide. *Biochem Biophys Res Commun*. 1990;171:416-23.
623. de Simone G, Muiesan ML, Ganau A, Longhini C, Verdecchia P, Palmieri V, Agabiti-Rosei E, Mancia G. Reliability and limitations of echocardiographic measurement of left ventricular mass for risk stratification and follow-up in single patients: the RES trial. Working Group on Heart and Hypertension of the Italian Society of Hypertension. Reliability of M-mode Echocardiographic Studies. *J Hypertens*. 1999;17:1955-63.
624. Messerli FH. Hypertension and sudden cardiac death. *Am J Hypertens*. 1999;12:181S-188S.
625. Baillard C, Mansier P, Ennezat PV, Mangin L, Medigue C, Swynghedauw B, Chevalier B. Converting enzyme inhibition normalizes QT interval in spontaneously hypertensive rats. *Hypertension*. 2000;36:350-4.
626. Arribas S, Sanchez-Ferrer CF, Peiro C, Ponte A, Salaices M, Marin J. Functional vascular renin-angiotensin system in hypertensive transgenic rats for the mouse renin gene Ren-2. *Gen Pharmacol*. 1994;25:1163-70.
627. Bohm M, Lee M, Kreutz R, Kim S, Schinke M, Djavidani B, Wagner J, Kaling M, Wienen W, Bader M, et al. Angiotensin II receptor blockade in TGR(mREN2)27: effects of renin-angiotensin-system gene expression and cardiovascular functions. *J Hypertens*. 1995;13:891-9.
628. Montgomery HE, Kiernan LA, Whitworth CE, Fleming S, Unger T, Gohlke P, Mullins JJ, McEwan JR. Inhibition of tissue angiotensin converting enzyme activity prevents malignant hypertension in TGR(mREN2)27. *J Hypertens*. 1998;16:635-43.

629. Hilgers KF, Hartner A, Porst M, Veelken R, Mann JFE. Angiotensin II Type 1 Receptor Blockade Prevents Lethal Malignant Hypertension: Relation to Kidney Inflammation. *Circulation*. 2001;104:1436-1440.
630. Mervaala EM, Muller DN, Park JK, Schmidt F, Lohn M, Breu V, Dragun D, Ganten D, Haller H, Luft FC. Monocyte infiltration and adhesion molecules in a rat model of high human renin hypertension. *Hypertension*. 1999;33:389-95.
631. Whitworth CE, Fleming S, Cumming AD, Morton JJ, Burns NJ, Williams BC, Mullins JJ. Spontaneous development of malignant phase hypertension in transgenic Ren-2 rats. *Kidney Int*. 1994;46:1528-32.
632. Mayer NJ, Forsyth A, Kantachuvesiri S, Mullins JJ, Fleming S. Association of the D allele of the angiotensin I converting enzyme polymorphism with malignant vascular injury. *Mol Pathol*. 2002;55:29-33.
633. Stefansson B, Ricksten A, Rymo L, Aurell M, Herlitz H. Angiotensin-converting enzyme gene I/D polymorphism in malignant hypertension. *Blood Press*. 2000;9:104-9.
634. Nguyen G, Delarue F, Berrou J, Rondeau E, Sraer JD. Specific receptor binding of renin on human mesangial cells in culture increases plasminogen activator inhibitor-1 antigen. *Kidney Int*. 1996;50:1897-903.
635. Bohm M, Zolk O, Flesch M, Schiffer F, Schnabel P, Stasch J-P, Knorr A. Effects of Angiotensin II Type 1 Receptor Blockade and Angiotensin-Converting Enzyme Inhibition on Cardiac fl-Adrenergic Signal Transduction. *Hypertension*. 1998;31:747-754.
636. Arranz C, Tomat A, Fellet A, Garcia J, Balaszczuk AM, de los Angeles Costa M. Renal and vascular nitric oxide system in reduced renal mass saline hypertension. *Nephron Physiol*. 2003;95:p36-42.
637. Piech A, Dessy C, Havaux X, Feron O, Balligand JL. Differential regulation of nitric oxide synthases and their allosteric regulators in heart and vessels of hypertensive rats. *Cardiovasc Res*. 2003;57:456-67.
638. Parati G, Saul JP, Di Rienzo M, Mancia G. Spectral analysis of blood pressure and heart rate variability in evaluating cardiovascular regulation. A critical appraisal. *Hypertension*. 1995;25:1276-86.
639. Virtanen R, Jula A, Kuusela T, Helenius H, Voipio-Pulkki LM. Reduced heart rate variability in hypertension: associations with lifestyle factors and plasma renin activity. *J Hum Hypertens*. 2003;17:171-9.
640. Lucini D, Mela GS, Malliani A, Pagani M. Impairment in cardiac autonomic regulation preceding arterial hypertension in humans: insights from spectral analysis of beat-by-beat cardiovascular variability. *Circulation*. 2002;106:2673-9.
641. Mussalo H, Vanninen E, Ikaheimo R, Laitinen T, Laakso M, Lansimies E, Hartikainen J. Heart rate variability and its determinants in patients with severe or mild essential hypertension. *Clin Physiol*. 2001;21:594-604.
642. Baltatu O, Janssen BJ, Bricca G, Plehm R, Monti J, Ganten D, Bader M. Alterations in blood pressure and heart rate variability in transgenic rats with low brain angiotensinogen. *Hypertension*. 2001;37:408-13.

643. Gross V, Plehm R, Tank J, Jordan J, Diedrich A, Obst M, Luft FC. Heart rate variability and baroreflex function in AT2 receptor-disrupted mice. *Hypertension*. 2002;40:207-13.
644. Schiffrin EL. Vascular changes in hypertension in response to drug treatment: Effects of angiotensin receptor blockers. *Can J Cardiol*. 2002;18 Suppl A:15A-18A.
645. Radermacher J, Chavan A, Bleck J, Vitzthum A, Stoess B, Gebel MJ, Galanski M, Koch KM, Haller H. Use of Doppler ultrasonography to predict the outcome of therapy for renal-artery stenosis. *N Engl J Med*. 2001;344:410-7.
646. Kodama K, Adachi H, Sonoda J. Beneficial effects of long-term enalapril treatment and low-salt intake on survival rate of dahl salt-sensitive rats with established hypertension. *J Pharmacol Exp Ther*. 1997;283:625-9.
647. Ju H, Gros R, You X, Tsang S, Husain M, Rabinovitch M. Conditional and targeted overexpression of vascular chymase causes hypertension in transgenic mice. *PNAS*. 2001;98:7469-7474.
648. Bohlender J, Fukamizu A, Lippoldt A, Nomura T, Dietz R, Menard J, Murakami K, Luft FC, Ganten D. High human renin hypertension in transgenic rats. *Hypertension*. 1997;29:428-34.
649. Hayashida W, Kihara Y, Yasaka A, Inagaki K, Iwanaga Y, Sasayama S. Stage-specific differential activation of mitogen-activated protein kinases in hypertrophied and failing rat hearts. *J Mol Cell Cardiol*. 2001;33:733-44.
650. Flesch M, Schiffer F, Zolk O, Pinto Y, Rosenkranz S, Hirth-Dietrich C, Arnold G, Paul M, Bohm M. Contractile Systolic and Diastolic Dysfunction in Renin-Induced Hypertensive Cardiomyopathy. *Hypertension*. 1997;30:383-391.
651. Masciotra S, Picard S, Deschepper CF. Cosegregation Analysis in Genetic Crosses Suggests a Protective Role for Atrial Natriuretic Factor Against Ventricular Hypertrophy. *Circ Res*. 1999;84:1453-1458.
652. Deschepper CF, Masciotra S, Zahabi A, Boutin-Ganache I, Picard S, Reudelhuber TL. Functional Alterations of the Nppa Promoter Are Linked to Cardiac Ventricular Hypertrophy in WKY/WKHA Rat Crosses. *Circ Res*. 2001;88:223-228.
653. Harrap SB, Danes VR, Ellis JA, Griffiths CD, Jones EF, Delbridge LMD. The hypertrophic heart rat: a new normotensive model of genetic cardiac and cardiomyocyte hypertrophy. *Physiol. Genomics*. 2002;9:43-48.
654. Diet F, Graf C, Mahnke N, Wassmer G, Predel HG, Palma-Hohmann I, Rost R, Bohm M. ACE and angiotensinogen gene genotypes and left ventricular mass in athletes. *Eur J Clin Invest*. 2001;31:836-842.
655. Stella P, Bigatti G, Tizzoni L, Barlassina C, Lanzani C, Bianchi G, Cusi D. Association between aldosterone synthase (CYP11B2) polymorphism and left ventricular mass in human essential hypertension. *J Am Coll Cardiol*. 2004;43:265-70.

656. Winnicki M, Somers VK, Accurso V, Hoffmann M, Pawlowski R, Frigo G, Visentin P, Palatini P. alpha-Adducin Gly460Trp polymorphism, left ventricular mass and plasma renin activity. *J Hypertens*. 2002;20:1771-7.
657. Jamshidi Y, Montgomery HE, Hense H-W, Myerson SG, Torra IP, Staels B, World MJ, Doering A, Erdmann J, Hengstenberg C, Humphries SE, Schunkert H, Flavell DM. Peroxisome Proliferator-Activated Receptor {alpha} Gene Regulates Left Ventricular Growth in Response to Exercise and Hypertension. *Circulation*. 2002;105:950-955.
658. Semplicini A, Siffert W, Sartori M, Monari A, Naber C, Frigo G, Santonastaso M, Cozzutti E, Winnicki M, Palatini P. G protein beta3 subunit gene 825T allele is associated with increased left ventricular mass in young subjects with mild hypertension. *Am J Hypertens*. 2001;14:1191-5.
659. Diamantopoulos EJ, Andreadis EA, Vassilopoulos CV, Vlachonikolis IG, Tarassi KE, Chatzis NA, Giannakopoulos NS, Papasteriades CA. Association of specific HLA phenotypes with left ventricular mass and carotid intima-media thickness in hypertensives. *Am J Hypertens*. 2001;14:632-6.
660. Ortlepp JR, Breithardt O, Ohme F, Hanrath P, Hoffmann R. Lack of association among five genetic polymorphisms of the renin-angiotensin system and cardiac hypertrophy in patients with aortic stenosis. *Am Heart J*. 2001;141:671-6.
661. Shlyakhto EV, Shwartz EI, Nefedova YB, Zukova AV, Vinnic TA, Conrady AO. Lack of association of the renin-angiotensin system genes polymorphisms and left ventricular hypertrophy in hypertension. *Blood Press*. 2001;10:135-41.
662. Liao Y, Ishikura F, Beppu S, Asakura M, Takashima S, Asanuma H, Sanada S, Kim J, Ogita H, Kuzuya T, Node K, Kitakaze M, Hori M. Echocardiographic assessment of LV hypertrophy and function in aortic-banded mice: necropsy validation. *Am J Physiol Heart Circ Physiol*. 2002;282:H1703-8.
663. Wyatt HL, Heng MK, Meerbaum S, Hestenes JD, Cobo JM, Davidson RM, Corday E. Cross-sectional echocardiography. I. Analysis of mathematic models for quantifying mass of the left ventricle in dogs. *Circulation*. 1979;60:1104-13.
664. Devereux RB. Detection of left ventricular hypertrophy by M-mode echocardiography. Anatomic validation, standardization, and comparison to other methods. *Hypertension*. 1987;9:II9-26.
665. Roth DM, Swaney JS, Dalton ND, Gilpin EA, Ross J, Jr. Impact of anesthesia on cardiac function during echocardiography in mice. *Am J Physiol Heart Circ Physiol*. 2002;282:H2134-40.
666. Yang XP, Liu YH, Rhaleb NE, Kurihara N, Kim HE, Carretero OA. Echocardiographic assessment of cardiac function in conscious and anesthetized mice. *Am J Physiol*. 1999;277:H1967-74.

667. Shimizu G, Hirota Y, Kita Y, Kawamura K, Saito T, Gaasch WH. Left ventricular midwall mechanics in systemic arterial hypertension. Myocardial function is depressed in pressure-overload hypertrophy. *Circulation*. 1991;83:1676-84.
668. De Simone G, Devereux RB, Volpe M, Camargo MJ, Wallerson DC, Laragh JH. Midwall LV mechanics in rats with or without renovascular hypertension: effect of different Na+ intakes. *Am J Physiol*. 1996;270:H628-37.
669. de Simone G, Devereux RB, Koren MJ, Mensah GA, Casale PN, Laragh JH. Midwall left ventricular mechanics. An independent predictor of cardiovascular risk in arterial hypertension. *Circulation*. 1996;93:259-65.
670. Mayet J, Ariff B, Wasan B, Chapman N, Shahi M, Poulter NR, Sever PS, Foale RA, Thom SA. Improvement in midwall myocardial shortening with regression of left ventricular hypertrophy. *Hypertension*. 2000;36:755-9.
671. Perlini S, Muiesan ML, Cuspidi C, Sampieri L, Trimarco B, Aurigemma GP, Agabiti-Rosei E, Mancia G. Midwall mechanics are improved after regression of hypertensive left ventricular hypertrophy and normalization of chamber geometry. *Circulation*. 2001;103:678-83.
672. Masuyama T, Yamamoto K, Sakata Y, Doi R, Nishikawa N, Kondo H, Ono K, Kuzuya T, Sugawara M, Hori M. Evolving changes in Doppler mitral flow velocity pattern in rats with hypertensive hypertrophy. *J Am Coll Cardiol*. 2000;36:2333-8.
673. Greenbaum RA, Ho SY, Gibson DG, Becker AE, Anderson RH. Left ventricular fibre architecture in man. *Br Heart J*. 1981;45:248-63.
674. Greenbaum RA, Gibson DG. Regional non-uniformity of left ventricular wall movement in man. *Br Heart J*. 1981;45:29-34.
675. Shan K, Bick RJ, Poindexter BJ, Shimoni S, Letsou GV, Reardon MJ, Howell JF, Zoghbi WA, Nagueh SF. Relation of tissue Doppler derived myocardial velocities to myocardial structure and beta-adrenergic receptor density in humans. *J Am Coll Cardiol*. 2000;36:891-6.
676. Slotwiner DJ, Devereux RB, Schwartz JE, Pickering TG, de Simone G, Roman MJ. Relation of age to left ventricular function and systemic hemodynamics in uncomplicated mild hypertension. *Hypertension*. 2001;37:1404-9.
677. Vinereanu D, Florescu N, Sculthorpe N, Tweddel AC, Stephens MR, Fraser AG. Differentiation between pathologic and physiologic left ventricular hypertrophy by tissue Doppler assessment of long-axis function in patients with hypertrophic cardiomyopathy or systemic hypertension and in athletes. *Am J Cardiol*. 2001;88:53-8.
678. Wandt B, Bojo L, Hatle L, Wranne B. Left ventricular contraction pattern changes with age in normal adults. *J Am Soc Echocardiogr*. 1998;11:857-63.
679. Vinereanu D, Nicolaides E, Tweddel AC, Madler CF, Holst B, Boden LE, Cinteza M, Rees AE, Fraser AG. Subclinical left ventricular dysfunction in

asymptomatic patients with Type II diabetes mellitus, related to serum lipids and glycated haemoglobin. *Clin Sci (Lond)*. 2003;105:591-9.
680. Sutherland GR, Hatle L. Pulsed doppler myocardial imaging. A new approach to regional longitudinal function? *Eur J Echocardiogr*. 2000;1:81-3.
681. Hatle L, Sutherland GR. Regional myocardial function--a new approach. *Eur Heart J*. 2000;21:1337-57.
682. Patterson SW PH, Starling EH. The regulation of the heart beat. *Journal of Physiology*. 1914;48:465 - 513.
683. Gaasch WH, Zile MR, Hoshino PK, Apstein CS, Blaustein AS. Stress-shortening relations and myocardial blood flow in compensated and failing canine hearts with pressure-overload hypertrophy. *Circulation*. 1989;79:872-83.
684. Georgakopoulos D, Mitzner WA, Chen CH, Byrne BJ, Millar HD, Hare JM, Kass DA. In vivo murine left ventricular pressure-volume relations by miniaturized conductance micromanometry. *Am J Physiol.* 1998;274:H1416-22.
685. Feldman MD, Erikson JM, Mao Y, Korcarz CE, Lang RM, Freeman GL. Validation of a mouse conductance system to determine LV volume: comparison to echocardiography and crystals. *Am J Physiol Heart Circ Physiol*. 2000;279:H1698-707.
686. Sato T, Shishido T, Kawada T, Miyano H, Miyashita H, Inagaki M, Sugimachi M, Sunagawa K. ESPVR of in situ rat left ventricle shows contractility-dependent curvilinearity. *Am J Physiol.* 1998;274:H1429-34.
687. Little WC, Cheng CP, Mumma M, Igarashi Y, Vinten-Johansen J, Johnston WE. Comparison of measures of left ventricular contractile performance derived from pressure-volume loops in conscious dogs. *Circulation*. 1989;80:1378-87.
688. Williams RV, Lorenz JN, Witt SA, Hellard DT, Khoury PR, Kimball TR. End-systolic stress-velocity and pressure-dimension relationships by transthoracic echocardiography in mice. *Am J Physiol.* 1998;274:H1828-35.
689. Reichek N, Wilson J, St John Sutton M, Plappert TA, Goldberg S, Hirshfeld JW. Noninvasive determination of left ventricular end-systolic stress: validation of the method and initial application. *Circulation*. 1982;65:99-108.
690. Denault AY, Gorcsan J, 3rd, Mandarino WA, Kancel MJ, Pinsky MR. Left ventricular performance assessed by echocardiographic automated border detection and arterial pressure. *Am J Physiol.* 1997;272:H138-47.
691. Kang N, Walther T, Tian XL, Bohlender J, Fukamizu A, Ganten D, Bader M. Reduced hypertension-induced end-organ damage in mice lacking cardiac and renal angiotensinogen synthesis. *J Mol Med.* 2002;80:359-66.

692. Matsusaka T, Katori H, Inagami T, Fogo A, Ichikawa I. Communication between myocytes and fibroblasts in cardiac remodeling in angiotensin chimeric mice. *J Clin Invest.* 1999;103:1451-8.
693. Varo N, Iraburu MJ, Varela M, B Liqm, Etayo JC, J Diqm. Chronic AT(1) blockade stimulates extracellular collagen type I degradation and reverses myocardial fibrosis in spontaneously hypertensive rats. *Hypertension.* 2000;35:1197-202.
694. Forman DE, Cittadini A, Azhar G, Douglas PS, Wei JY. Cardiac morphology and function in senescent rats: gender-related differences. *J Am Coll Cardiol.* 1997;30:1872-7.
695. Tamura N, Ogawa Y, Chusho H, Nakamura K, Nakao K, Suda M, Kasahara M, Hashimoto R, Katsuura G, Mukoyama M, Itoh H, Saito Y, Tanaka I, Otani H, Katsuki M. Cardiac fibrosis in mice lacking brain natriuretic peptide. *Proc Natl Acad Sci U S A.* 2000;97:4239-44.
696. Oikarinen L, Nieminen MS, Viitasalo M, Toivonen L, Jern S, Dahlof B, Devereux RB, Okin PM, for the LIFE Study Investigators. QRS Duration and QT Interval Predict Mortality in Hypertensive Patients With Left Ventricular Hypertrophy. The Losartan Intervention for Endpoint Reduction in Hypertension Study. *Hypertension.* 2004:01.HYP.0000125230.46080.c6.
697. Swynghedauw B, Chevalier B, Charlemagne D, Mansier P, Carre F. Cardiac hypertrophy, arrhythmogenicity and the new myocardial phenotype. II. The cellular adaptational process. *Cardiovasc Res.* 1997;35:6-12.
698. Lee JK, Nishiyama A, Kambe F, Seo H, Takeuchi S, Kamiya K, Kodama I, Toyama J. Downregulation of voltage-gated K(+) channels in rat heart with right ventricular hypertrophy. *Am J Physiol.* 1999;277:H1725-31.
699. Meszaros J, Khananshvili D, Hart G. Mechanisms underlying delayed afterdepolarizations in hypertrophied left ventricular myocytes of rats. *Am J Physiol Heart Circ Physiol.* 2001;281:H903-14.
700. Assayag P, Carre F, Chevalier B, Delcayre C, Mansier P, Swynghedauw B. Compensated cardiac hypertrophy: arrhythmogenicity and the new myocardial phenotype. I. Fibrosis. *Cardiovasc Res.* 1997;34:439-44.
701. Bikkina M, Larson MG, Levy D. Asymptomatic ventricular arrhythmias and mortality risk in subjects with left ventricular hypertrophy. *J Am Coll Cardiol.* 1993;22:1111-6.
702. Carre F, Lessard Y, Coumel P, Ollivier L, Besse S, Lecarpentier Y, Swynghedauw B. Spontaneous arrhythmias in various models of cardiac hypertrophy and senescence of rats. A Holter monitoring study. *Cardiovasc Res.* 1992;26:698-705.
703. Stilli D, Sgoifo A, Macchi E, Zaniboni M, De Iasio S, Cerbai E, Mugelli A, Lagrasta C, Olivetti G, Musso E. Myocardial remodeling and arrhythmogenesis in moderate cardiac hypertrophy in rats. *Am J Physiol Heart Circ Physiol.* 2001;280:H142-50.

704. Diaz ME, Eisner DA, O'Neill SC. Depressed ryanodine receptor activity increases variability and duration of the systolic Ca2+ transient in rat ventricular myocytes. *Circ Res*. 2002;91:585-93.
705. Kameyama M, Hirayama Y, Saitoh H, Maruyama M, Atarashi H, Takano T. Possible contribution of the sarcoplasmic reticulum Ca pump function to electrical and mechanical alternans. *J Electrocardiol*. 2003;36:125-35.
706. Okin PM, Devereux RB, Liu JE, Oikarinen L, Jern S, Kjeldsen SE, Julius S, Wachtell K, Nieminen MS, Dahlof B. Regression of electrocardiographic left ventricular hypertrophy predicts regression of echocardiographic left ventricular mass: the LIFE study. *J Hum Hypertens*. 2004.
707. Oikarinen L, Nieminen MS, Toivonen L, Viitasalo M, Wachtell K, Papademetriou V, Jern S, Dahlof B, Devereux RB, Okin PM. Relation of QT interval and QT dispersion to regression of echocardiographic and electrocardiographic left ventricular hypertrophy in hypertensive patients: the Losartan Intervention For Endpoint Reduction (LIFE) study. *Am Heart J*. 2003;145:919-25.
708. Mathew J, Sleight P, Lonn E, Johnstone D, Pogue J, Yi Q, Bosch J, Sussex B, Probstfield J, Yusuf S. Reduction of cardiovascular risk by regression of electrocardiographic markers of left ventricular hypertrophy by the angiotensin-converting enzyme inhibitor ramipril. *Circulation*. 2001;104:1615-21.
709. Verdecchia P, Angeli F, Borgioni C, Gattobigio R, de Simone G, Devereux RB, Porcellati C. Changes in cardiovascular risk by reduction of left ventricular mass in hypertension: a meta-analysis. *Am J Hypertens*. 2003;16:895-9.
710. Botchway AN, Turner MA, Sheridan DJ, Flores NA, Fry CH. Electrophysiological effects accompanying regression of left ventricular hypertrophy. *Cardiovasc Res*. 2003;60:510-7.
711. Walther T, Schubert A, Falk V, Binner C, Kanev A, Bleiziffer S, Walther C, Doll N, Autschbach R, Mohr FW. Regression of left ventricular hypertrophy after surgical therapy for aortic stenosis is associated with changes in extracellular matrix gene expression. *Circulation*. 2001;104:I54-8.
712. Hickson RC, Hammons GT, Holoszy JO. Development and regression of exercise-induced cardiac hypertrophy in rats. *Am J Physiol*. 1979;236:H268-72.
713. Gerdes AM, Clark LC, Capasso JM. Regression of cardiac hypertrophy after closing an aortocaval fistula in rats. *Am J Physiol*. 1995;268:H2345-51.
714. Ruzicka M, Yuan B, Leenen FH. Effects of enalapril versus losartan on regression of volume overload-induced cardiac hypertrophy in rats. *Circulation*. 1994;90:484-91.

715. Yang CM, Kandaswamy V, Young D, Sen S. Changes in collagen phenotypes during progression and regression of cardiac hypertrophy. *Cardiovasc Res*. 1997;36:236-45.
716. Tea BS, Dam TV, Moreau P, Hamet P, deBlois D. Apoptosis during regression of cardiac hypertrophy in spontaneously hypertensive rats. Temporal regulation and spatial heterogeneity. *Hypertension*. 1999;34:229-35.
717. Frolov VA, Drozdova GA, Mustyatsa VF, Rieger P, Antoni Z, Kuzovkin AE. Possible mechanism of regression of myocardial hypertrophy. *Bull Exp Biol Med*. 2001;132:644-6.
718. Walther T, Schubert A, Falk V, Binner C, Walther C, Doll N, Fabricius A, Dhein S, Gummert J, Mohr FW. Left ventricular reverse remodeling after surgical therapy for aortic stenosis: correlation to Renin-Angiotensin system gene expression. *Circulation*. 2002;106:I23-6.
719. Moorjani N, Catarino P, El-Sayed R, Al-Ahmed S, Meyer B, Al-Mohanna F, Westaby S. A pressure overload model to track the molecular biology of heart failure. *Eur J Cardiothorac Surg*. 2003;24:920-5.
720. Cooper Gt, Marino TA. Complete reversibility of cat right ventricular chronic progressive pressure overload. *Circ Res*. 1984;54:323-31.
721. Wisenbaugh T, Allen P, Cooper Gt, O'Connor WN, Mezaros L, Streter F, Bahinski A, Houser S, Spann JF. Hypertrophy without contractile dysfunction after reversal of pressure overload in the cat. *Am J Physiol*. 1984;247:H146-54.
722. Lessick J, Mutlak D, Markiewicz W, Reisner SA. Failure of left ventricular hypertrophy to regress after surgery for aortic valve stenosis. *Echocardiography*. 2002;19:359-66.
723. Devereux RB, Palmieri V, Liu JE, Wachtell K, Bella JN, Boman K, Gerdts E, Nieminen MS, Papademetriou V, Dahlof B. Progressive hypertrophy regression with sustained pressure reduction in hypertension: the Losartan Intervention For Endpoint Reduction study. *J Hypertens*. 2002;20:1445-50.
724. Hohl CM, Altschuld RA. FK506 alters sarcoplasmic reticulum calcium release in neonatal piglet cardiac myocytes. *Pediatr Res*. 1999;46:316-9.
725. Timerman AP, Onoue H, Xin H-B, Barg S, Copello J, Wiederrecht G, Fleischer S. Selective Binding of FKBP12.6 by the Cardiac Ryanodine Receptor. *J. Biol. Chem.* 1996;271:20385-20391.
726. Yano M, Ono K, Ohkusa T, Suetsugu M, Kohno M, Hisaoka T, Kobayashi S, Hisamatsu Y, Yamamoto T, Kohno M, Noguchi N, Takasawa S, Okamoto H, Matsuzaki M. Altered Stoichiometry of FKBP12.6 Versus Ryanodine Receptor as a Cause of Abnormal Ca2+ Leak Through Ryanodine Receptor in Heart Failure. *Circulation*. 2000;102:2131-2136.
727. Yano M, Kobayashi S, Kohno M, Doi M, Tokuhisa T, Okuda S, Suetsugu M, Hisaoka T, Obayashi M, Ohkusa T, Matsuzaki M. FKBP12.6-mediated stabilization of calcium-release channel (ryanodine receptor) as a novel therapeutic strategy against heart failure. *Circulation*. 2003;107:477-84.

728. Shin DW, Pan Z, Bandyopadhyay A, Bhat MB, Kim DH, Ma J. Ca2+-Dependent Interaction between FKBP12 and Calcineurin Regulates Activity of the Ca2+ Release Channel in Skeletal Muscle. *Biophys. J.* 2002;83:2539-2549.
729. Rabkin JM, Corless CL, Rosen HR, Olyaei AJ. Immunosuppression impact on long-term cardiovascular complications after liver transplantation. *Am J Surg*. 2002;183:595-9.
730. Nakatani T, Uchida J, Iwai T, Matsumura K, Naganuma T, Kuratsukuri K, Sugimura K. Renin mRNA expression and renal dysfunction in tacrolimus-induced acute nephrotoxicity. *Int J Mol Med*. 2003;11:75-8.
731. Saleh FH, Jurjus AR. A comparative study of morphological changes in spontaneously hypertensive rats and normotensive Wistar Kyoto rats treated with an angiotensin-converting enzyme inhibitor or a calcium-channel blocker. *J Pathol*. 2001;193:415-20.
732. Slama M, Susic D, Varagic J, Ahn J, Frohlich ED. Echocardiographic measurement of cardiac output in rats. *Am J Physiol Heart Circ Physiol*. 2003;284:H691-697.
733. Ono K, Masuyama T, Yamamoto K, Doi R, Sakata Y, Nishikawa N, Mano T, Kuzuya T, Takeda H, Hori M. Echo doppler assessment of left ventricular function in rats with hypertensive hypertrophy. *Journal of the American Society of Echocardiography*. 2002;15:109-117.
734. Cingolani OH, Yang X-P, Cavasin MA, Carretero OA. Increased Systolic Performance With Diastolic Dysfunction in Adult Spontaneously Hypertensive Rats. *Hypertension*. 2003;41:249-254.
735. Massett MP, Ungvari Z, Csiszar A, Kaley G, Koller A. Different roles of PKC and MAP kinases in arteriolar constrictions to pressure and agonists. *Am J Physiol Heart Circ Physiol*. 2002;283:H2282-2287.
736. Muthalif MM, Karzoun NA, Gaber L, Khandekar Z, Benter IF, Saeed AE, Parmentier JH, Estes A, Malik KU. Angiotensin II-induced hypertension: contribution of Ras GTPase/Mitogen-activated protein kinase and cytochrome P450 metabolites. *Hypertension*. 2000;36:604-9.
737. Touyz RM, He G, Deng LY, Schiffrin EL. Role of extracellular signal-regulated kinases in angiotensin II-stimulated contraction of smooth muscle cells from human resistance arteries. *Circulation*. 1999;99:392-9.
738. Ishihata A, Tasaki K, Katano Y. Involvement of p44/42 mitogen-activated protein kinases in regulating angiotensin II- and endothelin-1-induced contraction of rat thoracic aorta. *Eur J Pharmacol*. 2002;445:247-56.
739. Behr TM, Nerurkar SS, Nelson AH, Coatney RW, Woods TN, Sulpizio A, Chandra S, Brooks DP, Kumar S, Lee JC, Ohlstein EH, Angermann CE, Adams JL, Sisko J, Sackner-Bernstein JD, Willette RN. Hypertensive end-organ damage and premature mortality are p38 mitogen-activated protein kinase-dependent in a rat model of cardiac hypertrophy and dysfunction. *Circulation*. 2001;104:1292-8.
740. de Borst MH, Navis G, de Boer RA, Huitema S, Vis LM, van Gilst WH, van Goor H. Specific MAP-kinase blockade protects against renal

damage in homozygous TGR(mRen2)27 rats. *Lab Invest.* 2003;83:1761-70.
741. Clipstone NA, Crabtree GR. Identification of calcineurin as a key signalling enzyme in T-lymphocyte activation. *Nature*. 1992;357:695-7.
742. Stankunas K, Graef IA, Neilson JR, Park SH, Crabtree GR. Signaling through calcium, calcineurin, and NF-AT in lymphocyte activation and development. *Cold Spring Harb Symp Quant Biol.* 1999;64:505-16.
743. Khanna AK. The immunosuppressive agent tacrolimus induces p21WAF/CIP1WAF1/CIP1 via TGF-beta secretion. *Biochem Biophys Res Commun*. 2003;303:266-72.
744. Tsuzuki S, Toyama-Sorimachi N, Kitamura F, Tobita Y, Miyasaka M. FK506 (tacrolimus) inhibits extravasation of lymphoid cells by abrogating VLA-4/VCAM-1 mediated transendothelial migration. *FEBS Lett*. 1998;430:414-8.
745. Stephen M, Woo J, Hasan NU, Whiting PH, Thomson AW. Immunosuppressive activity, lymphocyte subset analysis, and acute toxicity of FK-506 in the rat. A comparative and combination study with cyclosporine. *Transplantation*. 1989;47:60-5.
746. Ba D, Takeichi N, Kodama T, Kobayashi H. Restoration of T cell depression and suppression of blood pressure in spontaneously hypertensive rats (SHR) by thymus grafts or thymus extracts. *J Immunol.* 1982;128:1211-6.
747. Khraibi AA, Smith TL, Hutchins PM, Lynch CD, Dusseau JW. Thymectomy delays the development of hypertension in Okamoto spontaneously hypertensive rats. *J Hypertens*. 1987;5:537-41.
748. Khraibi AA, Norman RA, Jr., Dzielak DJ. Chronic immunosuppression attenuates hypertension in Okamoto spontaneously hypertensive rats. *Am J Physiol.* 1984;247:H722-6.
749. Rodriguez-Iturbe B, Quiroz Y, Nava M, Bonet L, Chavez M, Herrera-Acosta J, Johnson RJ, Pons HA. Reduction of renal immune cell infiltration results in blood pressure control in genetically hypertensive rats. *Am J Physiol Renal Physiol*. 2002;282:F191-201.
750. Muller DN, Shagdarsuren E, Park J-K, Dechend R, Mervaala E, Hampich F, Fiebeler A, Ju X, Finckenberg P, Theuer J, Viedt C, Kreuzer J, Heidecke H, Haller H, Zenke M, Luft FC. Immunosuppressive Treatment Protects Against Angiotensin II-Induced Renal Damage. *Am J Pathol*. 2002;161:1679-1693.
751. Quiroz Y, Pons H, Gordon KL, Rincon J, Chavez M, Parra G, Herrera-Acosta J, Gomez-Garre D, Largo R, Egido J, Johnson RJ, Rodriguez-Iturbe B. Mycophenolate mofetil prevents salt-sensitive hypertension resulting from nitric oxide synthesis inhibition. *Am J Physiol Renal Physiol*. 2001;281:F38-47.
752. Rodriguez-Iturbe B, Pons H, Quiroz Y, Gordon K, Rincon J, Chavez M, Parra G, Herrera-Acosta J, Gomez-Garre D, Largo R, Egido J, Johnson

RJ. Mycophenolate mofetil prevents salt-sensitive hypertension resulting from angiotensin II exposure. *Kidney Int.* 2001;59:2222-32.
753. Romero F, Rodriguez-Iturbe B, Parra G, Gonzalez L, Herrera-Acosta J, Tapia E. Mycophenolate mofetil prevents the progressive renal failure induced by 5/6 renal ablation in rats. *Kidney Int.* 1999;55:945-55.
754. Nataraj C, Oliverio MI, Mannon RB, Mannon PJ, Audoly LP, Amuchastegui CS, Ruiz P, Smithies O, Coffman TM. Angiotensin II regulates cellular immune responses through a calcineurin-dependent pathway. *J. Clin. Invest.* 1999;104:1693-1701.
755. Castedo M, Pelletier L, Pasquier R, Guettier C, Huygen K, Michel JB, Druet P. Anti-renin T cells trigger normal B cells to produce anti-renin antibodies and normalize blood pressure in spontaneously hypertensive rats. *Int Immunol.* 1993;5:1569-76.
756. Luft FC. Workshop: mechanisms and cardiovascular damage in hypertension. *Hypertension.* 2001;37:594-8.
757. Ruiz-Ortega M, Lorenzo O, Ruperez M, Esteban V, Suzuki Y, Mezzano S, Plaza JJ, Egido J. Role of the Renin-Angiotensin System in Vascular Diseases: Expanding the Field. *Hypertension.* 2001;38:1382-1387.
758. El Bekay R, Alvarez M, Monteseirin J, Alba G, Chacon P, Vega A, Martin-Nieto J, Jimenez J, Pintado E, Bedoya FJ, Sobrino F. Oxidative stress is a critical mediator of the angiotensin II signal in human neutrophils: involvement of mitogen-activated protein kinase, calcineurin, and the transcription factor NF-{kappa}B. *Blood.* 2003;102:662-671.
759. Tummala PE, Chen XL, Sundell CL, Laursen JB, Hammes CP, Alexander RW, Harrison DG, Medford RM. Angiotensin II induces vascular cell adhesion molecule-1 expression in rat vasculature: A potential link between the renin-angiotensin system and atherosclerosis. *Circulation.* 1999;100:1223-9.
760. Capers Qt, Alexander RW, Lou P, De Leon H, Wilcox JN, Ishizaka N, Howard AB, Taylor WR. Monocyte chemoattractant protein-1 expression in aortic tissues of hypertensive rats. *Hypertension.* 1997;30:1397-402.
761. Hernandez-Presa M, Bustos C, Ortego M, Tunon J, Renedo G, Ruiz-Ortega M, Egido J. Angiotensin-converting enzyme inhibition prevents arterial nuclear factor-kappa B activation, monocyte chemoattractant protein-1 expression, and macrophage infiltration in a rabbit model of early accelerated atherosclerosis. *Circulation.* 1997;95:1532-41.
762. Ruiz-Ortega M, Bustos C, Hernandez-Presa MA, Lorenzo O, Plaza JJ, Egido J. Angiotensin II participates in mononuclear cell recruitment in experimental immune complex nephritis through nuclear factor-kappa B activation and monocyte chemoattractant protein-1 synthesis. *J Immunol.* 1998;161:430-9.
763. Chen XL, Tummala PE, Olbrych MT, Alexander RW, Medford RM. Angiotensin II induces monocyte chemoattractant protein-1 gene expression in rat vascular smooth muscle cells. *Circ Res.* 1998;83:952-9.

764. Pueyo ME, Gonzalez W, Nicoletti A, Savoie F, Arnal JF, Michel JB. Angiotensin II stimulates endothelial vascular cell adhesion molecule-1 via nuclear factor-kappaB activation induced by intracellular oxidative stress. *Arterioscler Thromb Vasc Biol*. 2000;20:645-51.
765. Hernandez-Presa MA, Bustos C, Ortego M, Tunon J, Ortega L, Egido J. ACE inhibitor quinapril reduces the arterial expression of NF-kappaB-dependent proinflammatory factors but not of collagen I in a rabbit model of atherosclerosis. *Am J Pathol*. 1998;153:1825-37.
766. Nakamura A, Johns EJ, Imaizumi A, Yanagawa Y, Kohsaka T. Effect of beta(2)-adrenoceptor activation and angiotensin II on tumour necrosis factor and interleukin 6 gene transcription in the rat renal resident macrophage cells. *Cytokine*. 1999;11:759-65.
767. Han Y, Runge MS, Brasier AR. Angiotensin II induces interleukin-6 transcription in vascular smooth muscle cells through pleiotropic activation of nuclear factor-kappa B transcription factors. *Circ Res*. 1999;84:695-703.
768. Ruiz-Ortega M, Lorenzo O, Ruperez M, Konig S, Wittig B, Egido J. Angiotensin II activates nuclear transcription factor kappaB through AT(1) and AT(2) in vascular smooth muscle cells: molecular mechanisms. *Circ Res*. 2000;86:1266-72.
769. Bush E, Maeda N, Kuziel WA, Dawson TC, Wilcox JN, DeLeon H, Taylor WR. CC chemokine receptor 2 is required for macrophage infiltration and vascular hypertrophy in angiotensin II-induced hypertension. *Hypertension*. 2000;36:360-3.
770. Ishibashi M, Hiasa KI, Zhao Q, Inoue S, Ohtani K, Kitamoto S, Tsuchihashi M, Sugaya T, Charo IF, Kura S, Tsuzuki T, Ishibashi T, Takeshita A, Egashira K. Critical Role of Monocyte Chemoattractant Protein-1 Receptor CCR2 on Monocytes in Hypertension-Induced Vascular Inflammation and Remodeling. *Circ Res*. 2004.
771. Touyz RM, Chen X, Tabet F, Yao G, He G, Quinn MT, Pagano PJ, Schiffrin EL. Expression of a Functionally Active gp91phox-Containing Neutrophil-Type NAD(P)H Oxidase in Smooth Muscle Cells From Human Resistance Arteries: Regulation by Angiotensin II. *Circ Res*. 2002;90:1205-1213.
772. Cifuentes ME, Rey FE, Carretero OA, Pagano PJ. Upregulation of p67(phox) and gp91(phox) in aortas from angiotensin II-infused mice. *Am J Physiol Heart Circ Physiol*. 2000;279:H2234-40.
773. Hendey B, Lawson M, Marcantonio EE, Maxfield FR. Intracellular calcium and calcineurin regulate neutrophil motility on vitronectin through a receptor identified by antibodies to integrins alphav and beta3. *Blood*. 1996;87:2038-48.
774. Conboy IM, Manoli D, Mhaiskar V, Jones PP. Calcineurin and vacuolar-type H+-ATPase modulate macrophage effector functions. *Proc Natl Acad Sci U S A*. 1999;96:6324-9.

775. Rafiee P, Johnson CP, Li MS, Ogawa H, Heidemann J, Fisher PJ, Lamirand TH, Otterson MF, Wilson KT, Binion DG. Cyclosporine A enhances leukocyte binding by human intestinal microvascular endothelial cells through inhibition of p38 MAPK and iNOS. Paradoxical proinflammatory effect on the microvascular endothelium. *J Biol Chem*. 2002;277:35605-15.
776. Muller DN, Heissmeyer V, Dechend R, Hampich F, Park JK, Fiebeler A, Shagdarsuren E, Theuer J, Elger M, Pilz B, Breu V, Schroer K, Ganten D, Dietz R, Haller H, Scheidereit C, Luft FC. Aspirin inhibits NF-kappaB and protects from angiotensin II-induced organ damage. *Faseb J*. 2001;15:1822-4.
777. Dechend R, Fiebeler A, Park JK, Muller DN, Theuer J, Mervaala E, Bieringer M, Gulba D, Dietz R, Luft FC, Haller H. Amelioration of angiotensin II-induced cardiac injury by a 3-hydroxy-3-methylglutaryl coenzyme a reductase inhibitor. *Circulation*. 2001;104:576-81.
778. Muller DN, Dechend R, Mervaala EM, Park JK, Schmidt F, Fiebeler A, Theuer J, Breu V, Ganten D, Haller H, Luft FC. NF-kappaB inhibition ameliorates angiotensin II-induced inflammatory damage in rats. *Hypertension*. 2000;35:193-201.
779. Liang H, Venema VJ, Wang X, Ju H, Venema RC, Marrero MB. Regulation of angiotensin II-induced phosphorylation of STAT3 in vascular smooth muscle cells. *J Biol Chem*. 1999;274:19846-51.
780. Wada H, Hasegawa K, Morimoto T, Kakita T, Yanazume T, Abe M, Sasayama S. Calcineurin-GATA-6 pathway is involved in smooth muscle-specific transcription. *J. Cell Biol.* 2002;156:983-991.
781. Suzuki E, Nishimatsu H, Satonaka H, Walsh K, Goto A, Omata M, Fujita T, Nagai R, Hirata Y. Angiotensin II induces myocyte enhancer factor 2- and calcineurin/nuclear factor of activated T cell-dependent transcriptional activation in vascular myocytes. *Circ Res*. 2002;90:1004-11.
782. Mokkapatti R, Vyas SJ, Romero GG, Mi Z, Inoue T, Dubey RK, Gillespie DG, Stout AK, Jackson EK. Modulation by Angiotensin II of Isoproterenol-Induced cAMP Production in Preglomerular Microvascular Smooth Muscle Cells from Normotensive and Genetically Hypertensive Rats. *J Pharmacol Exp Ther.* 1998;287:223-231.
783. Jeanmart H, Malo O, Carrier M, Nickner C, Desjardins N, Perrault LP. Comparative study of cyclosporine and tacrolimus vs newer immunosuppressants mycophenolate mofetil and rapamycin on coronary endothelial function. *J Heart Lung Transplant*. 2002;21:990-8.
784. Schwertfeger E, Wehrens J, Oberhauser V, Katzenwadel A, Rump LC. Contractile effects of tacrolimus in human and rat isolated renal arteries. *J Auto Pharmacol.* 2001;21:205-210.
785. Park J-K, Muller DN, Mervaala EMA, Dechend R, Fiebeler A, Schmidt F, Bieringer M, Schafer O, Lindschau C, Schneider W, Ganten D, Luft FC, Haller H. Cerivastatin prevents angiotensin II-induced renal injury

independent of blood pressure- and cholesterol-lowering effects. *Kidney Int.* 2000;58:1420-1430.
786. Mervaala E, Muller DN, Schmidt F, Park JK, Gross V, Bader M, Breu V, Ganten D, Haller H, Luft FC. Blood pressure-independent effects in rats with human renin and angiotensinogen genes. *Hypertension*. 2000;35:587-94.
787. Guengerich FP, Martin MV, Beaune PH, Kremers P, Wolff T, Waxman DJ. Characterization of rat and human liver microsomal cytochrome P-450 forms involved in nifedipine oxidation, a prototype for genetic polymorphism in oxidative drug metabolism. *J Biol Chem*. 1986;261:5051-60.
788. Shimada T, Mimura M, Inoue K, Nakamura S, Oda H, Ohmori S, Yamazaki H. Cytochrome P450-dependent drug oxidation activities in liver microsomes of various animal species including rats, guinea pigs, dogs, monkeys, and humans. *Arch Toxicol*. 1997;71:401-8.
789. Konno Y, Nemoto K, Degawa M. Induction of hepatic cytochrome P450s responsible for the metabolism of xenobiotics by nicardipine and other calcium channel antagonists in the male rat. *Xenobiotica*. 2003;33:119-29.
790. Fioretto JR, Querioz SS, Padovani CR, Matsubara LS, Okoshi K, Matsubara BB. Ventricular remodeling and diastolic myocardial dysfunction in rats submitted to protein-calorie malnutrition. *Am J Physiol Heart Circ Physiol*. 2002;282:H1327-33.
791. Gardiner SM, March JE, Kemp PA, Fallgren B, Bennett T. Regional haemodynamic effects of cyclosporine A, tacrolimus and sirolimus in conscious rats. *Br J Pharmacol*. 2004.
792. Milting H, Janssen PM, Wangemann T, Kogler H, Domeier E, Seidler T, Hakim K, Grapow M, Zeitz O, Prestle J, Zerkowski HR. FK506 does not affect cardiac contractility and adrenergic response in vitro. *Eur J Pharmacol*. 2001;430:299-304.
793. Lamb HJ, Beyerbacht HP, van der Laarse A, Stoel BC, Doornbos J, van der Wall EE, de Roos A. Diastolic dysfunction in hypertensive heart disease is associated with altered myocardial metabolism. *Circulation*. 1999;99:2261-7.
794. Naqvi TZ. Diastolic function assessment incorporating new techniques in Doppler echocardiography. *Rev Cardiovasc Med*. 2003;4:81-99.
795. Mandinov L, Eberli FR, Seiler C, Hess OM. Diastolic heart failure. *Cardiovasc Res*. 2000;45:813-25.
796. Hanssens M, Vercruysse L, Verbist L, Pijnenborg R, Keirse MJ, Van Assche FA. Renin-like immunoreactivity in human placenta and fetal membranes. *Histochem Cell Biol*. 1995;104:435-42.
797. Cheng XW, Kuzuya M, Sasaki T, Arakawa K, Kanda S, Sumi D, Koike T, Maeda K, Tamaya-Mori N, Shi GP, Saito N, Iguchi A. Increased expression of elastolytic cysteine proteases, cathepsins S and K, in the

neointima of balloon-injured rat carotid arteries. *Am J Pathol.* 2004;164:243-51.
798. van Kesteren CAM, Danser AHJ, Derkx FHM, Dekkers DHW, Lamers JMJ, Saxena PR, Schalekamp MADH. Mannose 6-Phosphate Receptor Mediated Internalization and Activation of Prorenin by Cardiac Cells. *Hypertension.* 1997;30:1389-1396.
799. Mullins JJ, Burt DW, Windass JD, McTurk P, George H, Brammar WJ. Molecular cloning of two distinct renin genes from the DBA/2 mouse. *Embo J.* 1982;1:1461-6.
800. Panthier JJ, Foote S, Chambraud B, Strosberg AD, Corvol P, Rougeon F. Complete amino acid sequence and maturation of the mouse submaxillary gland renin precursor. *Nature.* 1982;298:90-2.
801. Panthier JJ, Dreyfus M, Roux TL, Rougeon F. Mouse kidney and submaxillary gland renin genes differ in their 5' putative regulatory sequences. *Proc Natl Acad Sci U S A.* 1984;81:5489-93.
802. Holm I, Ollo R, Panthier JJ, Rougeon F. Evolution of aspartyl proteases by gene duplication: the mouse renin gene is organized in two homologous clusters of four exons. *Embo J.* 1984;3:557-62.
803. Dickinson DP, Gross KW, Piccini N, Wilson CM. Evolution and variation of renin genes in mice. *Genetics.* 1984;108:651-67.
804. Sigmund CD, Gross KW. Structure, expression, and regulation of the murine renin genes. *Hypertension.* 1991;18:446-57.
805. Misono KS, Chang JJ, Inagami T. Amino acid sequence of mouse submaxillary gland renin. *Proc Natl Acad Sci U S A.* 1982;79:4858-62.
806. Dhanaraj V, Dealwis CG, Frazao C, Badasso M, Sibanda BL, Tickle IJ, Cooper JB, Driessen HP, Newman M, Aguilar C, et al. X-ray analyses of peptide-inhibitor complexes define the structural basis of specificity for human and mouse renins. *Nature.* 1992;357:466-72.
807. Morris BJ, Catanzaro DF, Mullins JJ, Hardman J, Shine J. Synthesis of mouse renin as a 2-5-33-5 kilodalton pre-pro-two-chain molecule and use of its cDNA to identify the human gene. *Clin Exp Pharmacol Physiol.* 1983;10:293-7.
808. Misono KS, Holladay LA, Murakami K, Kuromizu K, Inagami T. Rapid and large-scale purification and characterization of renin from mouse submaxillary gland. *Arch Biochem Biophys.* 1982;217:574-81.
809. Corvol P, Panthier JJ, Foote S, Rougeon F. Structure of the mouse submaxillary gland renin precursor and a model for renin processing. Arthur C. Corcoran Memorial Lecture. *Hypertension.* 1983;5:I3-9.
810. Dealwis CG, Frazao C, Badasso M, Cooper JB, Tickle IJ, Driessen H, Blundell TL, Murakami K, Miyazaki H, Sueiras-Diaz J, et al. X-ray analysis at 2.0 A resolution of mouse submaxillary renin complexed with a decapeptide inhibitor CH-66, based on the 4-16 fragment of rat angiotensinogen. *J Mol Biol.* 1994;236:342-60.
811. Poe M, Wu JK, Lin TY, Hoogsteen K, Bull HG, Slater EE. Renin cleavage of a human kidney renin substrate analogous to human angiotensinogen,

H-Asp-Arg-Val-Tyr-Ile-His-Pro-Phe-His-Leu-Val-Ile-His-Ser-OH, that is human renin specific and is resistant to cathepsin D. *Anal Biochem*. 1984;140:459-67.

812. Burton J, Quinn T. The amino-acid residues on the C-terminal side of the cleavage site of angiotensinogen influence the species specificity of reaction with renin. *Biochim Biophys Acta*. 1988;952:8-12.
813. Field LJ, Gross KW. Ren-1 and Ren-2 loci are expressed in mouse kidney. *Proc Natl Acad Sci U S A*. 1985;82:6196-200.
814. Sharp MG, Fettes D, Brooker G, Clark AF, Peters J, Fleming S, Mullins JJ. Targeted inactivation of the Ren-2 gene in mice. *Hypertension*. 1996;28:1126-31.
815. Clark AF, Sharp MG, Morley SD, Fleming S, Peters J, Mullins JJ. Renin-1 is essential for normal renal juxtaglomerular cell granulation and macula densa morphology. *J Biol Chem*. 1997;272:18185-90.
816. Aeed PA, Elhammer AP. Glycosylation of recombinant prorenin in insect cells: the insect cell line Sf9 does not express the mannose 6-phosphate recognition signal. *Biochemistry*. 1994;33:8793-7.
817. Pitarresi TM, Rubattu S, Heinrikson R, Sealey JE. Reversible cryoactivation of recombinant human prorenin. *J Biol Chem*. 1992;267:11753-9.
818. Valdenaire O, Breu V, Giller T, Bur D, Fischli W. Cloning and characterization of marmoset renin: comparison with human renin. *J Cardiovasc Pharmacol*. 1999;34:893-7.
819. Mathews S, Dobeli H, Pruschy M, Bosser R, D'Arcy A, Oefner C, Zulauf M, Gentz R, Breu V, Matile H, Schlaeger J, Fischli W. Recombinant human renin produced in different expression systems: biochemical properties and 3D structure. *Protein Expr Purif*. 1996;7:81-91.
820. Grueninger-Leitch F, D'Arcy A, D'Arcy B, Chene C. Deglycosylation of proteins for crystallization using recombinant fusion protein glycosidases. *Protein Sci*. 1996;5:2617-22.
821. Pilote L, McKercher G, Thibeault D, Lamarre D. Enzymatic characterization of purified recombinant human renin. *Biochem Cell Biol*. 1995;73:163-70.
822. Tong L, Pav S, Lamarre D, Pilote L, LaPlante S, Anderson PC, Jung G. High resolution crystal structures of recombinant human renin in complex with polyhydroxymonoamide inhibitors. *J Mol Biol*. 1995;250:211-22.
823. Asselbergs FA, Rahuel J, Cumin F, Leist C. Scaled-up production of recombinant human renin in CHO cells for enzymatic and X-ray structure analysis. *J Biotechnol*. 1994;32:191-202.
824. Shibasaki M, Sudoh K, Asano M, Murakami K. The effect of intravenous recombinant human renin on blood pressure in pithed spontaneously hypertensive rats. *Eur J Pharmacol*. 1992;215:271-6.
825. Hosoi M, Kim S, Yamauchi T, Watanabe T, Murakami K, Suzuki F, Takahashi A, Nakamura Y, Yamamoto K. Similarity between

physicochemical properties of recombinant rat prorenin and native inactive renin. *Biochem J.* 1991;275 (Pt 3):727-31.
826. Norman JA, Hadjilambris O, Baska R, Sharp DY, Kumar R. Stable expression, secretion, and characterization of active human renin in mammalian cells. *Mol Pharmacol.* 1992;41:53-9.
827. Yamauchi T, Suzuki F, Takahashi A, Tsutsumi I, Hori H, Watanabe T, Ishizuka Y, Nakamura Y, Murakami K. Expression of rat renin in mammalian cells and its purification. *Clin Exp Hypertens A.* 1992;14:377-92.
828. Holzman TF, Chung CC, Edalji R, Egan DA, Martin M, Gubbins EJ, Krafft GA, Wang GT, Thomas AM, Rosenberg SH, et al. Characterization of recombinant human renin: kinetics, pH-stability, and peptidomimetic inhibitor binding. *J Protein Chem.* 1991;10:553-63.
829. Edalji R, Holzman TF, Gubbins EJ. Active prorenin: evidence for the formation of a conformational variant of recombinant human prorenin. *J Protein Chem.* 1991;10:403-6.
830. Katz SA, Malvin RL, Lee J, Kim SH, Murray RD, Opsahl JA, Abraham PA. Analysis of active renin heterogeneity. *Proc Soc Exp Biol Med.* 1991;197:387-92.
831. Ishizuka Y, Shoda A, Yoshida S, Kawamura Y, Haraguchi K, Murakami K. Isolation and characterization of recombinant human prorenin in Chinese hamster ovary cells. *J Biochem (Tokyo).* 1991;109:30-5.
832. Campbell DJ, Valentijn AJ, Berka JL. Production of rat renin fusion protein in Escherichia coli and the preparation of renin-specific antisera. *Mol Cell Endocrinol.* 1990;73:83-91.
833. Vlahos CJ, Walls JD, Berg DT, Grinnell BW. The purification and characterization of recombinant human renin expressed in the human kidney cell line 293. *Biochem Biophys Res Commun.* 1990;171:375-83.
834. Hatsuzawa K, Kim WS, Murakami K, Nakayama K. Purification of mouse Ren 2 prorenin produced in Chinese hamster ovary cells. *J Biochem (Tokyo).* 1990;107:854-7.
835. Evans DB, Cornette JC, Sawyer TK, Staples DJ, de Vaux AE, Sharma SK. Substrate specificity and inhibitor structure-activity relationships of recombinant human renin: implications in the in vivo evaluation of renin inhibitors. *Biotechnol Appl Biochem.* 1990;12:161-75.
836. Green DW, Aykent S, Gierse JK, Zupec ME. Substrate specificity of recombinant human renal renin: effect of histidine in the P2 subsite on pH dependence. *Biochemistry.* 1990;29:3126-33.
837. Carilli CT, Vigne JL, Wallace LC, Smith LM, Wong MA, Lewicki JA, Baxter JD. Characterization of recombinant human prorenin and renin. *Hypertension.* 1988;11:713-6.
838. Sharma SK, Evans DB, Tomich CS, Cornette JC, Ulrich RG. Folding and activation of recombinant human prorenin. *Biotechnol Appl Biochem.* 1987;9:181-93.

839. Poorman RA, Palermo DP, Post LE, Murakami K, Kinner JH, Smith CW, Reardon I, Heinrikson RL. Isolation and characterization of native human renin derived from Chinese hamster ovary cells. *Proteins*. 1986;1:139-45.
840. Imai T, Cho T, Takamatsu H, Hori H, Saito M, Masuda T, Hirose S, Murakami K. Synthesis and characterization of human prorenin in Escherichia coli. *J Biochem (Tokyo)*. 1986;100:425-32.
841. Weighous TF, Cornette JC, Sharma SK, Tarpley WG. Secretion of enzymatically active human renin from mammalian cells using an avian retroviral vector. *Gene*. 1986;45:121-9.
842. Shinagawa T, Do YS, Baxter J, Hsueh WA. Purification and characterization of human truncated prorenin. *Biochemistry*. 1992;31:2758-64.
843. Luque T, O'Reilly DR. Generation of baculovirus expression vectors. *Mol Biotechnol*. 1999;13:153-63.
844. Possee RD. Baculoviruses as expression vectors. *Curr Opin Biotechnol*. 1997;8:569-72.
845. Jarvis LJ, Kawar, Z. S., Hollister, J.R. Engineering N-glycosylation pathways in the baculovirus-insect cell system. *Current Opinion in Biotechnology*. 1998;9:528 - 533.
846. Vaughn JL, Goodwin RH, Tompkins GJ, McCawley P. The establishment of two cell lines from the insect Spodoptera frugiperda (Lepidoptera; Noctuidae). *In Vitro*. 1977;13:213-7.
847. Granados RR, Gouxun, L., Derkson, A.C.G., McKenna, K.A. A New Insect Cell Line from *Trichoplusia ni* (BTI-Tn-5B1-4) Susceptible to *Trichoplusia ni* Single Enveloped Nuclear Polyhedrosis Virus. *Journal of Invertebrate Pathology*. 1994;64:260-266.
848. Miltenburger HG, David P. Nuclear polyhedrosis virus replication in permanent cell lines of the cabbage moth (Mamestra brassicae L.). *Naturwissenschaften*. 1976;63:197-8.
849. Wickham TJ, Davis T, Granados RR, Shuler ML, Wood HA. Screening of insect cell lines for the production of recombinant proteins and infectious virus in the baculovirus expression system. *Biotechnol Prog*. 1992;8:391-6.
850. Jarvis DL, Finn EE. Modifying the insect cell N-glycosylation pathway with immediate early baculovirus expression vectors. *Nat Biotechnol*. 1996;14:1288-92.
851. Altmann F, Staudacher E, Wilson IB, Marz L. Insect cells as hosts for the expression of recombinant glycoproteins. *Glycoconj J*. 1999;16:109-23.
852. Snow BE, Betts L, Mangion J, Sondek J, Siderovski DP. Fidelity of G protein beta-subunit association by the G protein gamma-subunit-like domains of RGS6, RGS7, and RGS11. *Proc Natl Acad Sci U S A*. 1999;96:6489-94.
853. Sharma SK, Evans DB, Vosters AF, McQuade TJ, Tarpley WG. Metal affinity chromatography of recombinant HIV-1 reverse transcriptase

containing a human renin cleavable metal binding domain. *Biotechnol Appl Biochem.* 1991;14:69-81.
854. Smith MC, Furman TC, Ingolia TD, Pidgeon C. Chelating peptide-immobilized metal ion affinity chromatography. A new concept in affinity chromatography for recombinant proteins. *J Biol Chem.* 1988;263:7211-5.
855. Porath J, Carlsson J, Olsson I, Belfrage G. Metal chelate affinity chromatography, a new approach to protein fractionation. *Nature.* 1975;258:598-9.
856. Vosters AF, Evans DB, Tarpley WG, Sharma SK. On the engineering of rDNA proteins for purification by immobilized metal affinity chromatography: applications to alternating histidine-containing chimeric proteins from recombinant Escherichia coli. *Protein Expr Purif.* 1992;3:18-26.
857. Liu Q, Li MZ, Leibham D, Cortez D, Elledge SJ. The univector plasmid-fusion system, a method for rapid construction of recombinant DNA without restriction enzymes. *Curr Biol.* 1998;8:1300-9.
858. Shuman S. Novel approach to molecular cloning and polynucleotide synthesis using vaccinia DNA topoisomerase. *J Biol Chem.* 1994;269:32678-84.
859. Abremski KE, Hoess RH. Evidence for a second conserved arginine residue in the integrase family of recombination proteins. *Protein Eng.* 1992;5:87-91.
860. Abremski K, Hoess R, Sternberg N. Studies on the properties of P1 site-specific recombination: evidence for topologically unlinked products following recombination. *Cell.* 1983;32:1301-11.
861. Abremski K, Hoess R. Bacteriophage P1 site-specific recombination. Purification and properties of the Cre recombinase protein. *J Biol Chem.* 1984;259:1509-14.
862. Kitts PA, Possee RD. A method for producing recombinant baculovirus expression vectors at high frequency. *Biotechniques.* 1993;14:810-7.
863. O'Reilly DRM, L.K. Luckow, V.A. *Baculovirus Expression Vectors: A Laboratory Manual.*: W.H Freeman and Company, New York, N.Y.; 1992.
864. Liebman JM, LaSala D, Wang W, Steed PM. When less is more: enhanced baculovirus production of recombinant proteins at very low multiplicities of infection. *Biotechniques.* 1999;26:36-8, 40, 42.
865. Li Y, Beitle RR. Protein purification via aqueous two-phase extraction (ATPE) and immobilized metal affinity chromatography. Effectiveness of salt addition to enhance selectivity and yield of GFPuv. *Biotechnol Prog.* 2002;18:1054-9.
866. Chen HM, Ho CW, Liu JW, Lin KY, Wang YT, Lu CH, Liu HL. Production, IMAC purification, and molecular modeling of N-carbamoyl-D-amino acid amidohydrolase C-terminally fused with a six-his peptide. *Biotechnol Prog.* 2003;19:864-73.

867. Choe WS, Clemmitt RH, Chase HA, Middelberg AP. Comparison of histidine-tag capture chemistries for purification following chemical extraction. *J Chromatogr A*. 2002;953:111-21.
868. Phan TC, Nowak KJ, Akkari PA, Zheng MH, Xu J. Expression of caltrin in the baculovirus system and its purification in high yield and purity by cobalt (II) affinity chromatography. *Protein Expr Purif*. 2003;29:284-90.
869. *Ion Exchange Chromatography: Principles and Methods*: Pharmacia Biotech.
870. Fiore C, Trezeguet V, Roux P, Le Saux A, Noel F, Schwimmer C, Arlot D, Dianoux AC, Lauquin GJ, Brandolin G. Purification of histidine-tagged mitochondrial ADP/ATP carrier: influence of the conformational states of the C-terminal region. *Protein Expr Purif*. 2000;19:57-65.
871. Goel A, Colcher D, Koo JS, Booth BJ, Pavlinkova G, Batra SK. Relative position of the hexahistidine tag effects binding properties of a tumor-associated single-chain Fv construct. *Biochim Biophys Acta*. 2000;1523:13-20.
872. Admiraal PJ, van Kesteren CA, Danser AH, Derkx FH, Sluiter W, Schalekamp MA. Uptake and proteolytic activation of prorenin by cultured human endothelial cells. *J Hypertens*. 1999;17:621-9.
873. Lauritzen C, Pedersen J, Madsen MT, Justesen J, Martensen PM, Dahl SW. Active recombinant rat dipeptidyl aminopeptidase I (cathepsin C) produced using the baculovirus expression system. *Protein Expr Purif*. 1998;14:434-42.
874. Bozon V, Remy JJ, Pajot-Augy E, Couture L, Biache G, Severini M, Salesse R. Influence of promoter and signal peptide on the expression and secretion of recombinant porcine LH extracellular domain in baculovirus/lepidopteran cells or the caterpillar system. *J Mol Endocrinol*. 1995;14:277-84.
875. Sisk WP, Bradley JD, Leipold RJ, Stoltzfus AM, Ponce de Leon M, Hilf M, Peng C, Cohen GH, Eisenberg RJ. High-level expression and purification of secreted forms of herpes simplex virus type 1 glycoprotein gD synthesized by baculovirus-infected insect cells. *J Virol*. 1994;68:766-75.
876. Krol BJ, Murad S, Walker LC, Marshall MK, Clark WL, Pinnell SR, Yeowell HN. The expression of a functional, secreted human lysyl hydroxylase in a baculovirus system. *J Invest Dermatol*. 1996;106:11-6.
877. Congote LF, Li Q. Accurate processing and secretion in the baculovirus expression system of an erythroid-cell-stimulating factor consisting of a chimaera of insulin-like growth factor II and an insect insulin-like peptide. *Biochem J*. 1994;299 (Pt 1):101-7.
878. Sprules T, Green N, Featherstone M, Gehring K. Nickel-induced oligomerization of proteins containing 10-histidine tags. *Biotechniques*. 1998;25:20-2.
879. Hemdan ES, Zhao YJ, Sulkowski E, Porath J. Surface topography of histidine residues: a facile probe by immobilized metal ion affinity chromatography. *Proc Natl Acad Sci U S A*. 1989;86:1811-5.

880. Gaberc-Porekar V, Menart V, Jevsevar S, Vidensek A, Stalc A. Histidines in affinity tags and surface clusters for immobilized metal-ion affinity chromatography of trimeric tumor necrosis factor alpha. *J Chromatogr A*. 1999;852:117-28.
881. Mohanty AK, Wiener MC. Membrane protein expression and production: effects of polyhistidine tag length and position. *Protein Expr Purif*. 2004;33:311-25.
882. Frohlich ED. State of the Art lecture. Risk mechanisms in hypertensive heart disease. *Hypertension*. 1999;34:782-9.
883. Rodriguez-Iturbe B, Zhan C-D, Quiroz Y, Sindhu RK, Vaziri ND. Antioxidant-Rich Diet Relieves Hypertension and Reduces Renal Immune Infiltration in Spontaneously Hypertensive Rats. *Hypertension*. 2003;41:341-346.
884. De Lima JJ, Xue H, Coburn L, Andoh TF, McCarron DA, Bennett WM, Roullet JB. Effects of FK506 in rat and human resistance arteries. *Kidney Int*. 1999;55:1518-27.
885. Oitzinger W, Hofer-Warbinek R, Schmid JA, Koshelnick Y, Binder BR, de Martin R. Adenovirus-mediated expression of a mutant I{kappa}B kinase 2 inhibits the response of endothelial cells to inflammatory stimuli. *Blood*. 2001;97:1611-1617.
886. Jobin C, Panja A, Hellerbrand C, Iimuro Y, Didonato J, Brenner DA, Sartor RB. Inhibition of Proinflammatory Molecule Production by Adenovirus-Mediated Expression of a Nuclear Factor {kappa}B Super-Repressor in Human Intestinal Epithelial Cells. *J Immunol*. 1998;160:410-418.
887. Zuckerbraun BS, McCloskey CA, Mahidhara RS, Kim PK, Taylor BS, Tzeng E. Overexpression of mutated IkappaBalpha inhibits vascular smooth muscle cell proliferation and intimal hyperplasia formation. *J Vasc Surg*. 2003;38:812-9.
888. Mottram PL, Murray-Segal LJ, Han W, Maguire J, Stein-Oakley A, Mandel TE. Long-term survival of segmental pancreas isografts in NOD/Lt mice treated with anti-CD4 and anti-CD8 monoclonal antibodies. *Diabetes*. 1998;47:1399-405.
889. Danser AH. Local renin-angiotensin systems. *Mol Cell Biochem*. 1996;157:211-6.
890. Danser AH, Saris JJ, Schuijt MP, van Kats JP. Is there a local renin-angiotensin system in the heart? *Cardiovasc Res*. 1999;44:252-65.
891. Danser AH, van Kats JP, Verdouw PD, Schalekamp MA. Evidence for the existence of a functional cardiac renin-angiotensin system in humans. *Circulation*. 1997;96:3795-6.
892. Park JY, Lee J, Cho BY, Chae CB. Different bioactivities of human thyrotropin receptors with different signal peptides. *Mol Cell Endocrinol*. 1999;147:133-42.

893. Li Y, Luo L, Thomas DY, Kang CY. Control of expression, glycosylation, and secretion of HIV-1 gp120 by homologous and heterologous signal sequences. *Virology*. 1994;204:266-78.
894. Terpe K. Overview of tag protein fusions: from molecular and biochemical fundamentals to commercial systems. *Appl Microbiol Biotechnol*. 2003;60:523-33.
895. Spirin AS, Baranov VI, Ryabova LA, Ovodov SY, Alakhov YB. A continuous cell-free translation system capable of producing polypeptides in high yield. *Science*. 1988;242:1162-4.
896. Jermutus L, Ryabova LA, Pluckthun A. Recent advances in producing and selecting functional proteins by using cell-free translation. *Curr Opin Biotechnol*. 1998;9:534-48.
897. Mattingly JR, Jr., Yanez AJ, Martinez-Carrion M. The folding of nascent mitochondrial aspartate aminotransferase synthesized in a cell-free extract can be assisted by GroEL and GroES. *Arch Biochem Biophys*. 2000;382:113-22.
898. Frydman J, Hartl FU. Principles of chaperone-assisted protein folding: differences between in vitro and in vivo mechanisms. *Science*. 1996;272:1497-502.
899. Middleton RB, Bulleid NJ. Reconstitution of the folding pathway of collagen in a cell-free system: formation of correctly aligned and hydroxylated triple helices. *Biochem J*. 1993;296 (Pt 2):511-7.
900. Baneyx F. Recombinant protein expression in Escherichia coli. *Curr Opin Biotechnol*. 1999;10:411-21.
901. Schneider EL, Thomas JG, Bassuk JA, Sage EH, Baneyx F. Manipulating the aggregation and oxidation of human SPARC in the cytoplasm of Escherichia coli. *Nat Biotechnol*. 1997;15:581-5.
902. Prescott G, Silversides DW, Reudelhuber TL. Tissue activity of circulating prorenin. *Am J Hypertens*. 2002;15:280-5.
903. Wylie AA, Pulford DJ, McVie-Wylie AJ, Waterland RA, Evans HK, Chen YT, Nolan CM, Orton TC, Jirtle RL. Tissue-specific inactivation of murine M6P/IGF2R. *Am J Pathol*. 2003;162:321-8.
904. Inoue H, Noumi T, Nagata M, Murakami H, Kanazawa H. Targeted disruption of the gene encoding the proteolipid subunit of mouse vacuolar H(+)-ATPase leads to early embryonic lethality. *Biochim Biophys Acta*. 1999;1413:130-8.
905. Huang WY, Aramburu J, Douglas PS, Izumo S. Transgenic expression of green fluorescence protein can cause dilated cardiomyopathy. *Nat Med*. 2000;6:482-3.

Appendix 1

A1.1 Oligonucleotide Primers

A1.1.1 Primer and Probe Sequences used for Real Time PCR

Primers and probes for Real Time PCR were designed using Primer Express 1.5 software (Applied Biosystems) according to the optimal criteria specified by the manufacturer. The pan-renin assay was developed and optimised by Dr Matthew Sharp.

Table A1.1. Real-Time PCR Primers and Probes

Sequence (5'-3')	Comment
GCTGCTTTGGGCAGAAGATAGA	Rat BNP forward primer
ACAACCTCAGCCCGTCACA	Rat BNP reverse primer
GGTGCCCTCCACCAAGTG	Pan-Renin forward*
AGTGTCGGAGATACTCAGGAGACT	Pan-Renin reverse *
AGCCGCCTCTACCTTGCTTGTGGG	Pan-renin probe *

*amplification and detection of rat and mouse renin. A commercial 18S ribosomal RNA kit was used for amplification of 18S ribosomal RNA as an internal standard (Applied Biosystems).

A1.1.2 Mouse Ren2^{d}

The primers sequences used for amplifcation of ren2^{d} cDNA and incorporation of immuno-tags are provided in table A1.2. Primers used for sequencing recombinant clones are shown in table A1.3. Rcombinant baculoviral plaques were screened using primers given in table A1.4.

Table A1.2. Primers used for Recombinant Prorenin Amplification

Primer ID	Sequence (5'- 3')	Properties	Tm (°C)
JJM 55	gtcgaccagatggacaggaggagg	ren2 signal sequence only (1-24)*	69.6
JJM 361	ccatggcccagaagctgatatccgaggaggacctgaacaccttcagtctcccaa	ren1d/2 myc tag (69-84)*	89.2
JJM 362	gcgagggaggcgtaatctggaacatcgtatgggtag cgggccaaggcgaatc	ren1d/2 HAtag (1201-1217)*	90.3
JJM 363	ctagagggaggcgtaatctggaacatcgtatgggtag cgggccaaggcgaatc	ren1d/2HA-STOP (1201-1217)*	87.7

*sequence positions according to ren2 cDNA sequence (GenBank BC 011473, gi 15079272).

Underlining indicates immuno-tag sequence. Tm values were calculated according to Breslauer et al., 1986 assuming 50mM salt concentration and 50nM primer concentration.

Table A1.3.Sequencing primers for pUni and pBB contructs

ID	Sequence (5'-3')	Comments	Tm (°C)
JJM 56	caccccagaccttcaaagtc	ren2[d] forward (289-308)*	59.3
JJM 57	ctgatccgtagtggatggtg	ren2[d] reverse (459-430)*	58.7
JJM 58	cctggcagatcacacaatgaagg	ren2[d] forward (793-803)*	66.1
JJM 59	gcatgatcaacttcagggagc	ren2[d] reverse (924-904)*	61.9
PF	aaatgataaccatctcgc	polyhedrin forward primer (365 – 383)§	50.2
UniF	ctatcaacaggttgaa	puni forward primer (564-584)§	39.5

*sequence positions according to ren2[d] cDNA sequence (GenBank BC 011473, gi 15079272).

§ pUniV5HisTOPO vector sequence

Table A1.4. Primers for Recombinant Baculovirus Screening

ID	Sequence (5'-3')	Comments	Tm (°C)
JJM 396	tttactgttttcgtaacagttttg	baculovirus forward primer (-44 to -21)*	55.4
JJM 397	caacaacgcacagaatctagc	baculovirus reverse primer (+794 to 774)*	58.3

* nomenclature of O'Reilly (1992)[863]

Appendix 2

A2.1 Real Time PCR Data

A2.1.1 Determination of Standard Curves

Standard curves for each gene of interest (BNP, renin) and the internal standard (18S RNA) were determined as appropriate, for each PCR plate using pooled total RNA. The total concentration of RNA in the pooled standard was determined by spectrophotometry, and serial dilutions were performed to obtain samples for the standard curve. The threshold cycle (Ct) was determined for each dilution in quadruplicate (tables A2.1, A2.3 and A2.5), and plotted against the natural logarithm of the RNA concentration. Linear regression was performed to determine the gradient (m) and y-intercept (b) (figures A2.1, 2.2 and 2.3).

A2.1.2 Relative Quantification of BNP and 18S Expression

Expression levels of individual samples were determined in the manner described in Applied Biosystems User Bulletin 2, 1997, using the standard curve for each gene to calculate the log input amount of RNA (Ln[Input RNA]), based on the threshold cycle (Ct) value for each sample. The following equation was used:

Ln[Input RNA]=(Ct-b)/m

where b=y-intercept of the standard curve line, and m= gradient of standard curve line. Therefore the input amount of RNA was the exponent of (Ct-b)/m. This was calculated for each replicate individually, and then averaged to give the mean RNA quantity for that sample. Expression levels were normalised to 18S quantity, to allow for variation in sample loading. The units of quantity are the same as those used to construct the standard curve. Standard curves and tabulated calculations are given for all real time PCR experiments.

Table A2.1 Determination of Standard Curves for Rat BNP and 18S RNA

Quantity of RNA (ng)	ln (ng RNA)	BNP threshold cycle (Ct)	18S threshold cycle (Ct)
0.001	-6.908	35.51	32.17
		35.62	32.28
		35.44	32.55
		35.91	32.65
0.01	-4.605	31.48	29.00
		31.38	28.65
		31.71	28.43
		31.06	28.43
0.1	-2.303	27.22	23.94
		27.37	24.45
		27.31	24.43
		27.37	24.23
1	0	23.55	21.26
		24.06	21.21
		23.66	21.16
		23.98	21.39
10	2.303	20.10	18.19
		19.90	18.19
		19.66	18.10
		19.79	17.72

Figure A2.1 Amplification Plots for SYBR Green BNP Real Time PCR Assay

a) b)

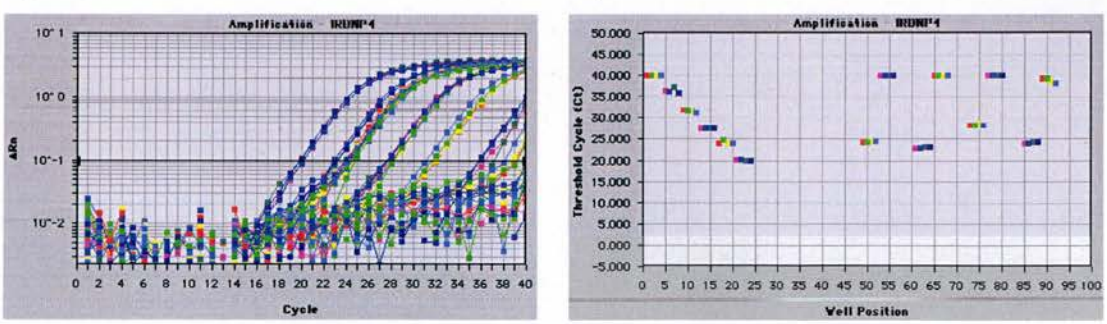

Typical amplification plots for BNP. a) Fluorescence (ΔRn) vs amplification cycle. b) Threshold cycle vs well position (sample): standard curve for BNP: wells 0 – 24, unknown samples including controls: wells 48 – 92.

Figure A2.2 Standard Curves for Rat BNP and 18S RNA

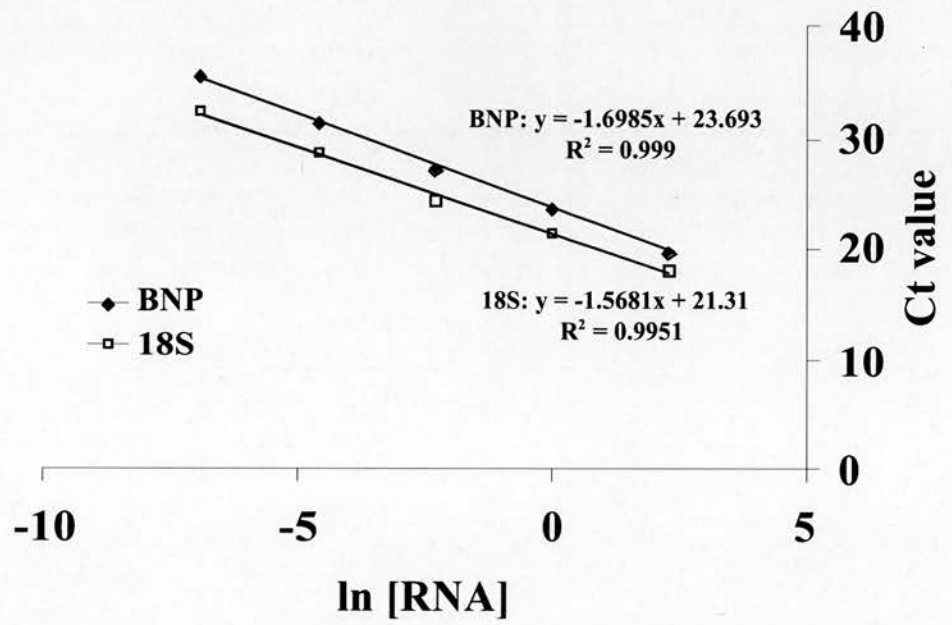

Standard curve for rat BNP and 18S amplification from left ventricular total RNA. BNP was detected using SYBR green dye, whilst 18S amplification was detected using VIC labelled probe. Data was plotted using Microsoft Excel 2001, and linear regression applied using the analysis package. The coefficient of correlation was automatically calculated by the software.

Table A2.2 Real Time PCR Data for Left Ventricular BNP and 18S RNA: TGRcyp1a1ren2 Induction and Regression Experiment

Animal	Assay	Ct	ln [Input RNA]	Input RNA (ng)	Av input RNA	Normalised to 18S
F344 Controls: 6 weeks Induction						
I1	BNP	24.20	-0.274	0.760	0.760	**0.593**
		24.11	-0.223	0.800		
		24.21	-0.280	0.757		
		24.28	-0.320	0.726		
	18S	21.23	0.046	1.047	1.283	
		20.52	0.500	1.648		
		21.10	0.129	1.138		
		20.89	0.263	1.361		
I2	BNP	23.42	-0.456	0.634	0.584	**0.672**
		23.24	-0.333	0.716		
		23.60	-0.579	0.561		
		24.01	-0.858	0.423		
	18S	22.52	-0.124	0.883	0.869	
		22.56	-0.150	0.860		
		22.45	-0.078	0.925		
		22.66	-0.216	0.806		
I3	BNP	24.34	-0.381	0.683	0.712	**0.757**
		24.22	-0.310	0.733		
		24.34	-0.381	0.683		
		24.19	-0.293	0.746		
	18S	21.55	-0.153	0.858	0.940	
		21.68	-0.236	0.790		
		21.17	0.089	1.093		
		21.28	0.019	1.019		
I4	BNP	23.93	-0.392	0.676	0.636	**0.749**
		24.15	-0.536	0.589		
		24.04	-0.461	0.631		
		23.99	-0.430	0.630		
	18S	22.07	-0.169	0.845	0.850	
		22.07	-0.169	0.845		
		22.17	-0.233	0.792		
		21.94	-0.086	0.918		
I5	BNP	24.03	-0.044	0.957	0.923	**0.565**
		23.91	-0.037	1.037		
		24.31	-0.193	0.824		
		24.21	-0.136	0.873		
	18S	20.17	0.780	2.180	2.199	
		20.32	0.685	1.984		
		20.04	0.862	2.367		
		20.11	0.817	2.264		

Table A2.2 continued

Animal	Assay	Ct	ln [Input RNA]	Input RNA (ng)	Av input RNA	Normalised to 18S
TGR: 6weeks Induction						
3453	BNP	23.02	0.548	1.730	1.671	**1.294**
		22.90	0.617	1.853		
		23.24	0.421	1.524		
		23.18	0.456	1.580		
	18S	21.26	0.155	1.168	1.292	
		21.08	0.206	1.228		
		20.44	0.294	1.342		
		20.84	0.357	1.429		
3612	BNP	22.67	0.055	1.057	1.269	**0.834**
		22.38	0.254	1.288		
		22.36	0.267	1.305		
		22.23	0.355	1.426		
	18S	21.74	0.390	1.477	1.521	
		21.85	0.318	1.374		
		21.52	0.535	1.708		
		21.69	0.423	1.527		
3615	BNP	23.74	-0.273	0.761	0.807	**0.340**
		23.46	-0.097	0.908		
		23.73	-0.266	0.766		
		23.68	-0.235	0.791		
	18S	20.56	0.797	2.220	2.353	
		20.44	0.874	2.397		
		20.39	0.906	2.475		
		20.49	0.842	2.322		
3610	BNP	23.09	0.356	1.428	1.644	**0.931**
		22.88	0.476	1.609		
		22.62	0.476	1.865		
		22.81	0.515	1.674		
	18S	20.94	0.231	1.260	1.762	
		20.40	0.376	1.778		
		20.32	0.627	1.872		
		20.10	0.768	2.155		
3455	BNP	22.21	0.873	2.394	2.230	**1.475**
		22.34	0.797	2.218		
		22.39	0.767	2.154		
		22.39	0.767	2.154		
	18S	20.98	0.214	1.234	1.512	
		20.85	0.293	1.341		
		20.48	0.529	1.700		
		20.41	0.574	1.775		

Table A2.2 continued

Animal	Assay	Ct	ln [Input RNA]	Input RNA (ng)	Av input RNA	Normalised to 18S
TGR: 6weeks Regression						
2563	BNP	24.02	-0.448	0.639	0.613	**0.316**
		24.02	-0.448	0.639		
		24.04	-0.461	0.631		
		24.27	-0.605	0.546		
	18S	20.85	0.612	1.844	1.938	
		20.70	0.708	2.030		
		20.77	0.663	1.941		
		20.77	0.663	1.941		
2564	BNP	23.78	-0.051	0.950	0.905	**0.302**
		23.73	-0.022	0.978		
		24.03	-0.198	0.820		
		23.93	-0.140	0.870		
	18S	19.56	1.116	3.053	2.996	
		19.59	1.097	2.995		
		19.65	1.059	2.882		
		19.56	1.116	3.053		
2565	BNP	24.37	-0.227	0.797	0.743	**0.339**
		24.38	-0.233	0.792		
		24.66	-0.394	0.674		
		24.54	-0.325	0.722		
	18S	20.17	0.780	2.181	2.199	
		20.32	0.685	1.984		
		20.04	0.861	2.367		
		20.11	0.817	2.265		
2924	BNP	23.53	0.106	1.112	0.956	**0.228**
		23.82	-0.059	0.943		
		23.95	-0.132	0.876		
		23.92	-0.115	0.981		
	18S	18.96	1.496	4.464	4.184	
		18.98	1.483	4.407		
		19.31	1.272	3.570		
		19.02	1.458	4.296		

Table A2.2 continued

Animal	Assay	Ct	ln [Input RNA]	Input RNA (ng)	Av input RNA	Normalised to 18S
F344 control: 6weeks Regression						
R1	BNP	23.06	0.372	1.452	1.414	**0.543**
		23.15	0.320	1.377		
		23.04	0.384	1.469		
		23.17	0.308	1.361		
	18S	20.02	0.823	2.277	2.602	
		19.69	1.033	2.810		
		19.75	0.995	2.704		
		19.80	0.963	2.619		
R2	BNP	22.23	0.355	1.426	1.306	**0.396**
		22.18	0.389	1.475		
		22.40	0.239	1.270		
		22.68	0.048	1.050		
	18S	20.23	1.385	4.000	3.293	
		20.44	1.247	3.479		
		20.81	0.996	2.708		
		20.67	1.095	2.990		
R3	BNP	28.03	-2.330	0.097	0.090	**0.310**
		28.61	-2.405	0.090		
		28.29	-2.180	0.838		
		28.19	-2.423	0.888		
	18S	23.82	-1.522	0.218	0.291	
		23.81	-1.516	0.220		
		22.96	-0.980	0.375		
		23.07	-1.050	0.350		
R4	BNP	23.03	0.390	1.477	1.336	**0.548**
		23.16	0.316	1.372		
		23.23	0.277	1.319		
		23.13	0.163	1.177		
	18S	20.12	0.755	2.128	2.438	
		19.83	0.940	2.361		
		19.79	0.966	2.627		

Table A2.3 Real Time PCR Standard Curves for Rat BNP and 18S RNA: FK506 Study

Quantity of RNA (ng)	ln (ng RNA)	BNP threshold cycle (Ct)	18S threshold cycle (Ct)
0.01	-4.605	35.67	27.07
		36.12	27.07
		35.44	27.08
0.1	-2.303	31.41	23.58
		31.60	23.66
		31.60	23.50
1	0	27.76	19.98
		27.96	20.00
		27.11	20.60
10	2.303	23.93	17.82
		24.18	17.41
		24.03	17.32
30	3.401	22.42	16.28
		22.32	16.18
		22.22	16.19

Figure A2.3 Standard Curves for Rat BNP and 18S: FK506 Study

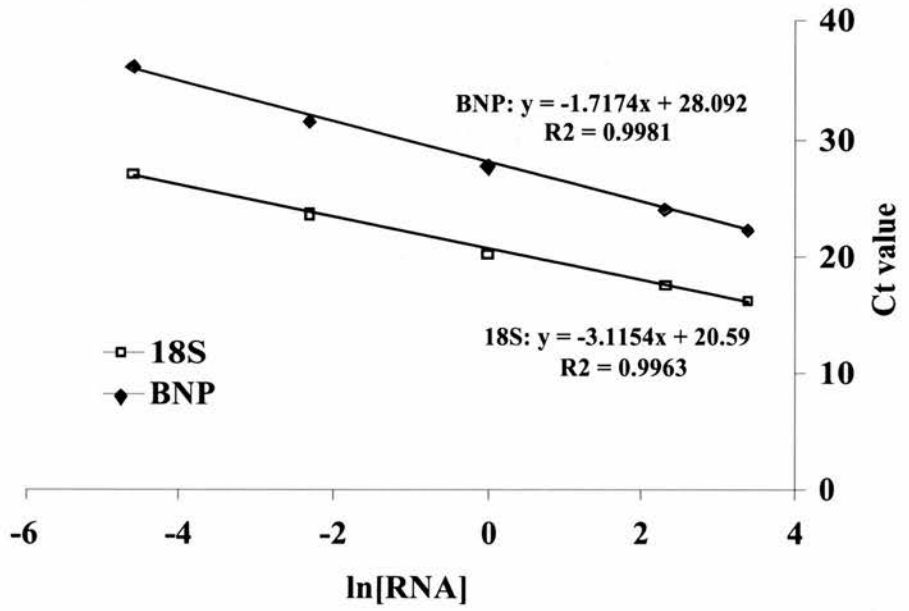

Standard curves for rat BNP and 18S amplification from left ventricular total RNA. Methods were as described in figure A2.1

Table A2.4 Real Time PCR Data for Rat BNP and 18S RNA: FK506 Study

Animal	Assay	Ct	ln [Input RNA]	Input RNA (ng)	Av input RNA	Normalised to 18S
TGRcyp1a1ren2: Water treated						
4116	BNP	24.77	2.022	7.559	7.009	**0.754**
		24.96	1.913	6.776		
		24.92	1.936	6.933		
	18S	17.44	2.180	8.668	9.398	
		17.27	2.282	9.799		
		17.28	2.275	9.728		
4117	BNP	25.16	1.612	5.016	4.502	**0.675**
		25.42	1.458	4.297		
		25.46	1.434	4.197		
	18S	17.71	1.995	7.351	6.670	
		17.94	1.828	6.214		
		17.98	1.863	6.445		
4118	BNP	25.09	1.776	5.227	4.862	**0.707**
		25.36	1.654	4.453		
		25.26	1.553	4.726		
	18S	17.72	1.966	7.140	6.800	
		17.65	2.017	7.514		
		18.02	1.746	5.714		
4119	BNP	26.48	0.939	2.556	3.959	**0.548**
		25.51	1.503	1.377		
		25.39	1.573	1.469		
	18S	17.92	1.973	7.195	7.227	
		17.81	2.052	7.804		
		18.02	1.900	6.682		
F344						
4	BNP	26.09	1.060	2.857	2.718	**0.523**
		26.28	0.947	2.579		
		26.21	0.989	2.689		
	18S	18.08	1.702	5.188	5.193	
		18.21	1.607	4.990		
		18.18	1.629	5.101		
8	BNP	27.97	0.181	1.198	1.195	**0.310**
		27.87	0.238	1.269		
		28.09	0.112	1.118		
	18S	18.54	1.366	3.921	3.858	
		18.62	1.309	3.702		
		18.53	1.374	3.950		

Table A2.4 (continued)

Animal	Assay	Ct	ln [Input RNA]	Input RNA (ng)	Av input RNA	Normalised to 18S
F344 (continued)						
3	BNP	26.44	1.061	2.890	2.650	**0.368**
		26.78	0.866	2.377		
		26.57	0.987	2.682		
	18S	17.70	1.972	7.186	7.208	
		17.75	1.936	6.932		
		17.64	2.015	7.504		
9	BNP	26.65	0.728	2.071	1.868	**0.276**
		27.00	0.520	1.682		
		27.01	0.514	1.672		
	18S	17.85	1.871	6.492	6.558	
		17.87	1.856	6.400		
		17.79	1.914	6.783		
TGRcyp1a1ren2: FK506 treated						
4052	BNP	26.14	1.234	3.435	2.959	**0.529**
		26.52	1.015	2.760		
		26.57	0.987	2.682		
	18S	18.10	1.684	5.386	5.599	
		18.03	1.734	5.664		
		18.01	1.749	5.748		
4053	BNP	25.75	1.292	3.639	3.781	**0.598**
		25.47	1.262	3.533		
		26.65	1.428	4.172		
	18S	17.71	1.973	7.192	5.319	
		17.99	1.768	5.861		
		17.98	1.776	5.904		
4054	BNP	24.60	1.945	6.992	5.490	**0.873**
		25.25	1.559	4.754		
		25.26	1.553	4.726		
	18S	17.91	1.827	6.214	6.291	
		17.86	1.863	6.445		
		17.91	1.827	6.214		
4055	BNP	27.16	0.543	1.721	1.644	**0.388**
		27.21	0.514	1.671		
		27.35	0.432	1.540		
	18S	18.52	1.530	4.618	4.240	
		18.61	1.463	4.321		
		18.79	1.330	3.782		

Table A2.5 Determination of Standard Curves for Rat Renin and 18S RNA

Quantity of RNA (ng)	ln (ng RNA)	BNP threshold cycle (Ct)	18S threshold cycle (Ct)
0.12	-2.120	30.55	35,28
		30.37	36.68
		29.92	-
0.6	-0.510	28.11	33.87
		28.55	33.27
		27.09	-
3	-1.099	25.43	30.53
		25.17	28.75
		25.66	29.10
15	2.708	23.15	27.31
		23.01	26.92
		23.12	28.39
75	4.317	21.11	25.44
		21.07	25.33
		21.25	-

- : failed reaction

Figure A2.4 Standard Curves for Renin and 18S RNA

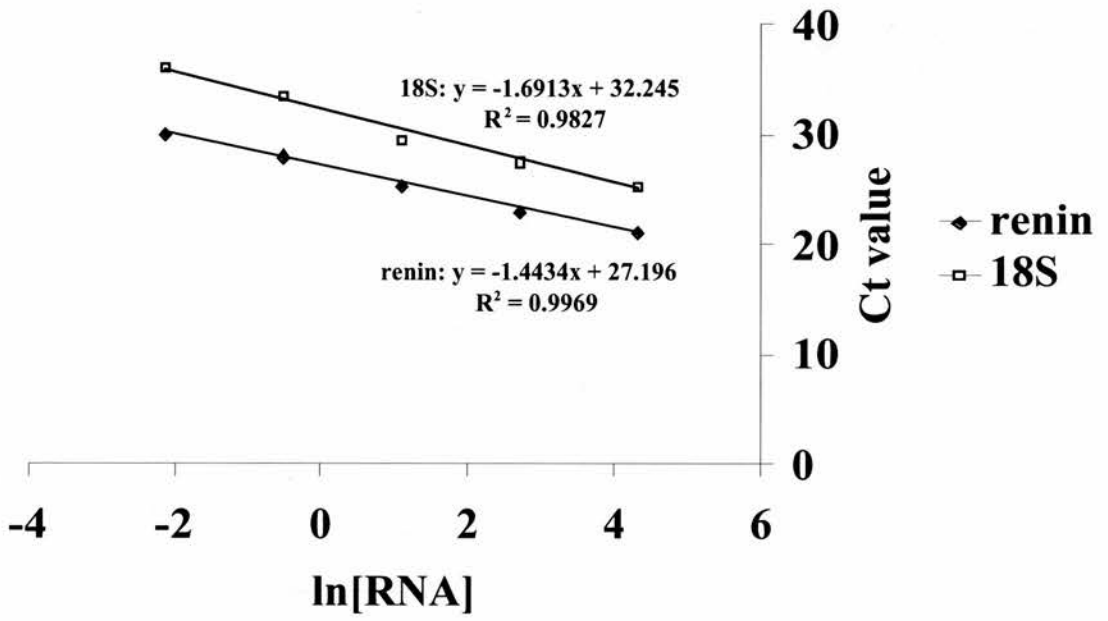

Standard curve for renin and 18S amplification from hepatic total RNA. Renin was detected using Fam labelled probe, whilst 18S amplification was detected using VIC labelled probe. Data was plotted using Microsoft Excel 2001, and linear regression applied using the analysis package. The coefficient of correlation was automatically calculated by the software.

Table A2.6 Real Time PCR Data for Rat Renin and 18S RNA: FK506 Study

Animal	Assay	Ct	ln [Input RNA]	Input RNA (ng)	Av input RNA	Normalised to 18S
TGRcyp1a1ren2: FK506 treated						
4049	renin	23.13	2.824	16.838	16.03	**1.051**
		23.06	2.872	17.676		
		23.44	2.608	13.576		
	18S	28.30	2.333	10.304	15.240	
		27.33	2.906	17.133		
		27.44	2.841	21.576		
4052	renin	24.32	1.997	7.369	7.208	**0.51**
		24.52	1.858	6.413		
		24.31	2.050	7.844		
	18S	27.97	2.528	12.524	14.376	
		28.41	2.267	9.655		
		27.10	3.042	20.948		
4053	renin	27.72	-0.364	0.695	0.869	**1.169**
		27.36	-0.114	0.892		
		27.17	0.018	1.018		
	18S	33.68	-0.848	0.428	0.743	
		31.71	0.316	1.372		
		33.68	-0.848	0.428		
TGRcyp1a1ren2: water treated						
4115	renin	26.10	0.761	2.141	2.400	**0.066**
		25.99	0.878	2.311		
		25.74	1.011	2.749		
	18S	27.05	3.072	21.576	36.236	
		26.29	3.521	33.816		
		25.52	3.976	53.317		
4116	renin	26.97	0.157	1.170	1.281	**0.058**
		26.72	0.331	1.392		
		26.84	0.247	1.280		
	18S	27.59	2.752	15.679	22.063	
		26.85	3.190	24.284		
		26.72	3.266	26.225		
4117	renin	25.05	1.490	4.438	4.225	**0.073**
		25.24	1.358	3.890		
		25.08	1.469	4.368		
	18S	25.94	3.728	41.592	57.509	
		24.92	4.331	76.019		
		25.47	4.006	54.915		

0.004 0.000

Table A2.6 (continued)

Animal	Assay	Ct	ln [Input RNA]	Input RNA (ng)	
					67.173
F344: FK506 treated					
					0.001 0.000
1	renin	38.48	-7.836	0.000	
		35.92	-6.058	0.002	
		36.50	-6.461	0.002	
	18S	25.55	3.958	52.378	
		25.66	3.893	49.080	
		25.66	3.893	49.080	
					69.772
3	renin	36.31	-6.329	0.002	
		35.85	-6.010	0.002	
		34.52	-5.086	0.006	
	18S	23.85	4.964	143.113	
		24.30	4.698	105.680	
		24.47	4.597	99.191	
					0.000 0.000
7	renin	36.03	-6.135	0.002	
		36.11	-6.190	0.002	
		40.00	-8.892	0.001	
	18S	26.18	3.586	36.089	
		26.29	3.521	33.817	
		27.15	3.012	20.338	
					31.678
F344: water treated					
2	renin	36.77	-6.649	0.001	
		34.07	-4.774	0.008	
		34.07	-6.072	0.002	
	18S	25.08	42.36	69.157	
		25.20	4.165	64.421	
		25.11	4.219	67.942	
6	renin	35.52	-5.781	0.003	
		38.05	-7.538	0.001	
		40.00	-8.892	0.000	
	18S	24.20	4.757	116.36	
		25.92	3.740	42.086	
		25.65	3.900	49.371	
8	renin	40.00	-8.892	0.000	
		38.36	-7.753	0.000	
		40.00	-8.892	0.000	
	18S	27.18	2.994	19.980	
		25.82	3.800	44.650	
		26.47	3.415	30.403	